Refinery ready bio-petroleum via novel catalytic hydrothermal processing of microalgae

Thomas François Robin

Submitted in accordance with the requirements for the degree of
Doctor of Philosophy

The University of Leeds

School of Chemical and Process Engineering (SCAPE)

Energy Research Institute

April 2015

The candidate confirms that the work submitted is his own and that appropriate credit has been given where reference has been made to the work of others.

The Figure 2-5 has been removed by the author of this thesis for copyright reasons page 22

Acknowledgements

First of all, I would like to thank my supervisor Andy Ross to let me doing this PhD and I am very grateful for his help and for his guidance. I am grateful to the EPRSC to fund this project. I would like to thank my co supervisor Jenny Jones, Amanda Lea-Langton and Alan Williams. I would like to give a special thanks to Simon Lloyd for his help in the labs and his valuable advice. This research has been carried out by a team which has included Surjit Singh, Patrick Biller, Philippa Usher, Ramzi Cherad, Leilani Darvell, Antonio Salituro, Gaurav Nahar, Ugochinyere Ekpo, Kelechi Anyikude and other PhD or staff from the University of Leeds.

I also thank Adrian Cunliff, Sara Dora, Susanne Patel, Timothy Hunter, and Nicole Hondow for helping me to analyse some samples. I am grateful to Heather Strachan, Sheilagh Ogden and David Haynes for their help for administrative tasks. I would like to thank Jenny Brady, Simon Phillips who gave me support during the PhD.

Finally, I thank my parents, my family and my friends who have given me support over these years.

Abstract

Hydrothermal liquefaction of microalgae is recognised as a favourable route to produce renewable fuel from high moisture feedstocks such as microalgae. However, there are still some uncertainties regarding the fate of nitrogen and the best approach to reduce the level of nitrogen in the bio-crude oil.

The aim of this study is to gain a better understanding of the main degradation route of carbohydrates, lipids and proteins and use this to predict the behaviour of microalgae. To reach this goal, different model compounds were selected including vegetable oils containing different degrees of saturation, proteins and carbohydrates (sugars and polysaccharides). The results from the model and study were compared with four different microalgae; stressed and non-stressed strains of *P. ellipsoidea, Chlorella v.* and *Spirulina*. Mixtures were prepared using the same model compounds to simulate the composition of microalgae. Reaction variables such as temperature (250, 300 and 350 °C), and influence of additives such as organic acids were investigated.

As the temperature increases, the nitrogen in the bio-crude decreases in general from 250 to 300 °C; in contrast the ammonium compound concentration in the process water increases with temperature. Carbohydrates enhance the formation of carbonaceous residues. Protein and lipids enhance the formation of amides. The protein and carbohydrates enhanced the formation of “heavy molecular weight” materials. A higher yield of 52.9 wt.% of bio-crude containing 1.5 wt.% of nitrogen was achieved with the stressed *P. ellipsoidea* at 300 °C. The addition of organic acids affected the molecular weight distribution of the bio-crude but had little effect on the heteroatom content.

In a parallel study, the influence of metal doped HZSM-5 on liquefaction behaviour was carried out. Different metal salts were incorporated into HZSM-5 to study the effect on reducing the nitrogen content of the bio-crude. MoZSM-5 was selective in producing aromatics from sunflower oil. In general, NiZSM-5 enhanced the deoxygenation of the bio-crude, but, lower effect on the nitrogen content.

Table of Contents

Conference poster and presentation

- Poster presentation, Leeds (England) December 2014, Showcase 2014

Subject: *The production of a petroleum-like from microalgae in hot compressed water*

- Poster presentation Sheffield (England) August 2014 Algal Biotechnology Sheffield Symposium

Subject: *Fate of Nitrogen during hydrothermal processing of microalgae, a model compound approach*

- Poster presentation, Manchester (England) March 2014, Bioenergy 2014 Conference

Subject: *The fate of nitrogen during the hydrothermal liquefaction of proteins and microalgae*

- Flash presentation and poster in London (England) Novembre 2013 Sustainable Chemicals from Microalgae

Subject: *The fate of unsaturated fatty acids during hydrothermal liquefaction of microalgae*

- Oral presentation in Newcastle (England) August 2013 Northern Postgraduate Chemical Engineering Conference 2013

Subject: *Catalytic hydrothermal processing of different vegetable oils using HZSM5*

- Oral presentation in Lund (Sweden) July 2013 catalysis for renewable source: fuel, energy, chemicals

Subject: *Catalytic hydrothermal processing of vegetable oils using metal exchanged zeolite*

List of Tables

List of Figures

Abbreviation

AAS: atomic absorption spectroscopy

ar: as received

amu: Atomic mass unit

asn: asparagine

BET : Brunauer–Emmett–Teller

CHNS : carbon, hydrogen, nitrogen sulphur analysis

CV: coefficient of variance

daf: dry ash free

db: dry basis

DKP: diketopiperazine

EDX: Energy-dispersive X-ray

FAME: Fatty acid methyl ester

FT-IR: Fourier transform infrared

GC: gas chromatography

GC-MS: gas chromatography mass spectrometer

GPC: gel permeation chromatography

gnu: glutamine

IC: ionic chromatography

ICP-OES: Inductively coupled plasma- optical emission spectroscopy

haadf: high-angle annular dark field

HHV: Higher heating value

HPLC: high pressure liquid chromatography

HTL: hydrothermal liquefaction

HTC: hydrothermal carbonisation

HTG: hydrothermal gasification

M: mol/L

MJ: mega joule

ppm: parts per million (in this thesis ppm means mg/L)

STA: simultaneous thermal analysers

STEM: scanning transmission electronic microscope

TGA: thermo gravimetric analysis

TOC: total organic carbon

TCD: thermal conductivity detector

vol.%: volume %

wt.%: weight %

XRD: x-ray diffraction

Chapter 1 Introduction and objectives

1.1 Introduction

The discovery of low carbon sustainable fuels is considered a major priority for modern society in order to tackle climate change and to find an alternative to fossil oil. Microalgae are seen as a strong candidate to displace fossil fuel. Indeed, these microorganisms produce more lipids and have the highest growth rate compared to arable plants (for example palm and rapeseed oils). Additionally, microalgae are able to fix the carbon dioxide via the photosynthesis process and use this technology to sequester carbon from coal power plants flue gas for example .

Transesterification of the lipids extracted from the microalgae was initially developed to produce biodiesel. However, a high amount of energy was required to dry the biomass and waste was produced as the non-lipids fraction was not used. Hydrothermal liquefaction is an alternative method to convert the whole microalgae into a bio-crude oil which requires no drying prior to processing of the feedstock. A schematic of the potential integration of algal cultivation and hydrothermal liquefaction is described Figure 1-1.

This technique involves reactions in subcritical water from 250 to 350 °C and a pressure from 50 to 170 bar. Higher bio-crude yield can be obtained from hydrothermal liquefaction compared to the initial lipid content of the feedstock. Another advantage of this process is that the aqueous phase is enriched in ammonium and phosphate cations and can be recycled in order to grow more microalgae [2]. Although, some major advances have been made over the last ten years, there is still a need to improve the quality of the bio-crude and in particular reduce the heteroatom content (nitrogen and oxygen). These heteroatoms could cause formation of environmentally undesirable NO_x from fuel bound nitrogen during combustion and complicate refinery operations during catalytic upgrading. Also fuel oxygen decreases the energy content of the bio-crude.

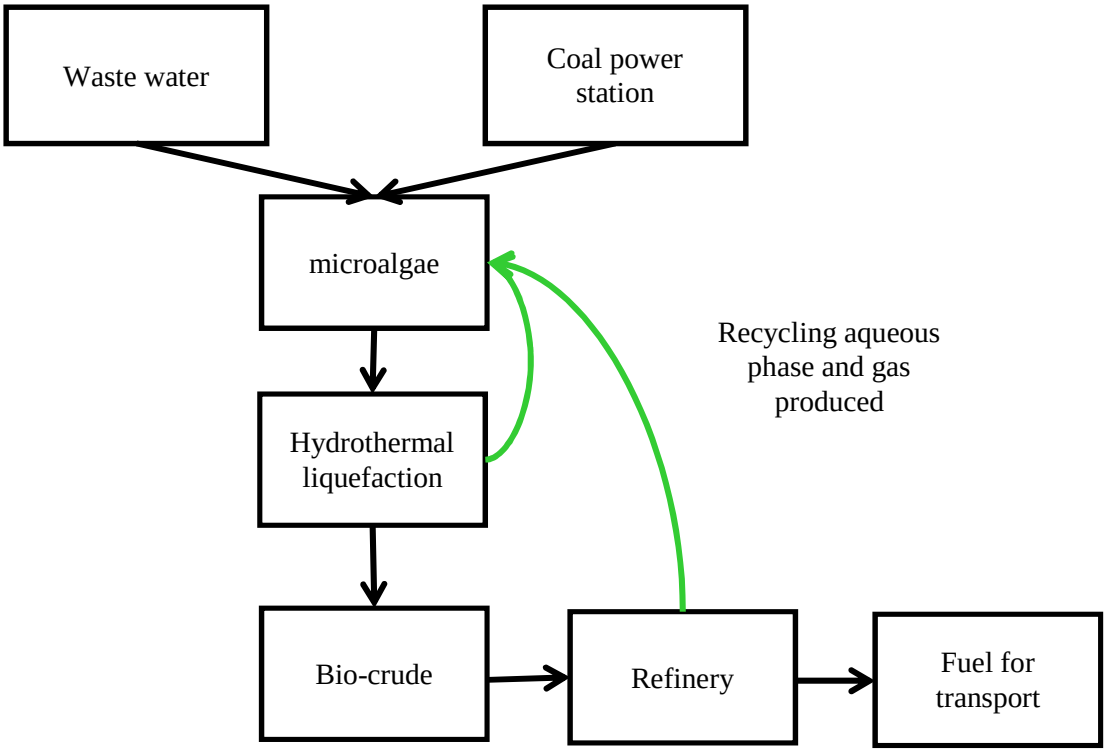

Figure 1-1: Diagram of the overall process

1.2 Aims and objectives

The purpose of this project is to produce refinery ready bio-petroleum by hydrothermal liquefaction of microalgae. The research is focused towards developing a better understanding of the fate of nitrogen. Catalysts including HZSM-5 doped with different metals were selected to investigate their influence on reducing the level of nitrogen and oxygen in the oil and to increase the fraction of hydrocarbons. Furthermore, model compounds (proteins, lipids and carbohydrates) were used in order to provide a better understanding of their degradation in subcritical water from 250 to 350 °C. Four different strains of microalgae with different compositions (*Chlorella vulgaris*, *Spirulina* and *Pseudochoricystis ellipsoidea* (stressed and non-stressed strain)) were compared to the processing of model compounds. The PhD thesis is divided into six result chapters where experiments carried out with each model components are detailed. **Chapter 2** includes the literature review, **Chapter 3** includes the general methodology; **Chapter 4** contains the analysis of the stability of process catalyst under hydrothermal condition; **Chapter 5** describes the processing of different lipids; **Chapter 6** includes the results regarding the processing of different carbohydrates; **Chapter 7** contains the results concerning the processing of proteins; **Chapter 8** includes the results of the processing of microalgae, **Chapter 9** describes

the experiments of the mixture of different model compounds and **Chapter 10** is the conclusion.

- The first main goal was to develop a clear understanding of the degradation route of each model compounds and microalgae under hydrothermal liquefaction. The study is focussed more on understanding the formation of nitrogen compounds in the bio-crude and in the aqueous phase. The formation of high molecular weight compounds was investigated in particular during the processing of lipids.
- The second goal was to investigate the hydrothermal stability of HZSM-5 in subcritical condition. The effect of different doped metals on HZSM-5 is investigated on the processing of different model compounds and microalgae.
- The effect of *in-situ* hydrogen donor compounds such as formic acid was studied to determine the influence on the bio-crude oil quality and product distribution.
- The other aim was to study the effect of each component (protein, lipid and carbohydrate) on the formation of the bio-crude and their interactions with each other. The processing of four microalgae with different composition was investigated in parallel.

1.3 Description of each chapters

In **Chapter 2**, the literature review includes the current advances in the research into hydrothermal liquefaction of microalgae and describes the advantages compared to first and second generation biofuels and the use of different conditions to cultivate microalgae. This includes recent progress towards improving bio-crude yields and quality in particularly lowering the amount of oxygen and nitrogen in the bio-crude. Previous studies using heterogeneous catalysts are reviewed in this section. Studies carried out concerning the upgrading of biomass in pyrolysis and hydrothermal processing are included. The use of microalgae producing high value chemicals and the life cycle assessment are briefly discussed. The different chemical reactions that occurred during hydrothermal liquefaction are also reviewed to understand the different pathways during the hydrothermal liquefaction (HTL).

In **Chapter 3**, the methodologies used for hydrothermal liquefaction is presented. A description of the reactor facilities, variables and operation are included.

The methods for the characterisation of the bio-crude oil, aqueous phase and the residue are described. A brief description of the theory of the instrumentation is also included.

In **Chapter 4**, the stability of different zeolites HZSM-5 doped with metal (molybdenum, copper, iron and nickel) is investigated at 350 °C. The activity and the regeneration of HZSM-5 during the processing of sunflower oil is studied. The objective of this section is to demonstrate the tolerance of the catalyst under subcritical conditions and the reuse of the catalyst. The stability of catalysts was measured using X-ray, transmission electronic microscope (TEM), BET (Brunauer–Emmett–Teller) techniques. Further, the metal leaching was measured by ICP (induced coupled plasma).

In **Chapter 5**, different vegetable oils (sunflower, linseed, jatropha, soya bean and palm oils) are processed at different temperatures (250, 300 and 350 °C). The influence of degree of saturation of fatty acids is investigated by use of different model fatty acids (oleic, linoleic and linolenic acids). The effect of HZSM-5 doped zeolite was also investigated in water and in formic acid for the decarboxylation of fatty acids. The other aim was to elucidate a degradation pathway of the lipids during liquefaction. Lipids were transesterified in order to quantify the different fatty acids and analysed by gas chromatography mass spectrometry (GC-MS). Gel permeation chromatography was used to measure the molecular weight of the products. Thermogravimetric analysis (TGA) of bio-crude oil provides information on the boiling point distribution of the oils. The elemental analysis determines the carbon and hydrogen contents (C and H wt.%). The total organic carbon (TOC) provides the carbon fraction within the aqueous phase.

In **Chapter 6**, the hydrothermal liquefaction of different carbohydrates (starch, glucose, alginic acid and mannitol) was investigated at 250, 300 and 350 °C. The purpose of the chapter was to study the degradation of carbohydrates at different temperatures, and the influence of additives such as formic acid and potassium hydroxide (KOH). The formation of chars was investigated using thermogravimetric and elemental analysis. Starch, glucose, mannitol and alginic acid were processed with HZSM-5.

In **Chapter 7**, the hydrothermal liquefaction of proteins (soya and hemps) and asparagine acids are processed at different temperatures (250, 300 and 350 °C) in

water and in formic acid at 350 °C. The purpose of this chapter is to investigate the degradation of proteins. For this, the ammonium compound concentration in the aqueous phase was used to determine the nitrogen balance. The elemental analysis measured the nitrogen content in the bio-crude oil. Subsequently, at 350 °C experiments were performed with the metal doped catalyst (HZSM-5) in water and formic acid. These experiments were conducted in order to investigate the influence of these conditions on the fate of nitrogen and other parameters. The bio-crude oil was combusted and the gas released was analysed by mass spectrometry, the emission of nitric oxide provides insight into the molecular weight distribution of nitrogen in the bio-crude oil.

In **Chapter 8**, different microalgae and cyanobacteria such as stressed and non-stressed strains of *P. ellipsoidea, Chlorella v.* and *Spirulina*) are processed. The same conditions to **Chapter 7** are applied in this chapter. The results are combined and compared with previous chapters using different model compounds in order to explain the behaviour of microalgae with different compositions. A global degradation route for the macromolecules in microalgae has been elucidated.

In **Chapter 9**, an investigation of hydrothermal behaviour of different binary mixtures is carried out to study the interaction between proteins, carbohydrates, and lipids (two vegetable oils: sunflower and linseed oils). Subsequently, the results are compared to the processing of each model compound. In addition, ternary mixtures are also prepared with similar composition to microalgae such as *Chlorella* and the stressed *P. ellipsoidea* in order to have a better comprehension towards the general interaction of each element combined and the results will be compared to the real microalgae. Similar techniques are performed in **Chapter 9** than with **Chapter 7**.

In **Chapter 10**, a summary of the different chapters is included and an overall conclusion of the research project. The future work and the feasibility of the use of hydrothermal liquefaction of microalgae are discussed.

Chapter 2 Literature review

2.1 Production of fuels from biomass

2.1.1 Current status of technology

Mankind has used biomass (especially wood as charcoal) as a source of energy for thousands of years. Nevertheless, humans had really started to efficiently master the use of biomass energy since the first industrial revolution in the eighteenth century. However after the Second World War, petroleum oil became one of the predominant sources of fuels within the transport sector. The high availability and low price triggered the rapid expansion and development of western countries over the last 60 years. After 1973, with the first petroleum crisis, the price of crude oil began to rise, inducing research in alternative fuels to be launched [3]. However, at the beginning of the 2000's, research regarding renewable energy has been considered a priority as there is clear evidence carbon dioxide produced from the combustion of petroleum oil is associated with climate change and global warning.

According to IPCC data, the atmospheric concentration of carbon dioxide has risen from 200 ppm at the beginning of the twentieth century to 400 ppm in 2015 [4]. Research communities have anticipated a decrease in the carbon dioxide uptake within the ocean. Therefore, this has induced a modification to the climate explaining the rise in carbon dioxide levels within the atmosphere [5]. The International Energy Agency (IEA) has predicted in their latest forecast that by 2050 the world emission of greenhouse gases will still increase, ranging between 41 Gt and 55 Gt (best case prediction model), with an increase in temperature of 6 °C [6]. The reduction of carbon dioxide emissions within the next fifty years will be made difficult by the rapid economic growth of China and India. By 2050, these two countries will represent at least 41 % of the total carbon dioxide emissions or a combined total consumption of approximately 2000 million tonnes of oils [6]. Therefore, the shift to renewable energy and biofuels is imperative in order to meet the different targets set out by the climate summits of Kyoto (1997) and Copenhagen (2009) recommending that countries need to reduce their emission of carbon dioxide by half.

Renewable energy is widespread to produce electricity from the sun (solar panel), water power (hydraulic with dam) and wind power. For example, Denmark aims in the following years to produce 50 % of its total electricity consumption by wind power and by 2050, 100 % of its electricity capacity generated from renewables [7]. In the transport sector, the usage of biofuels seems currently to be the better alternative even though some other technologies are available such as electric cars or hydrogen (still in development). Little is known about the environmental impact regarding the production of lithium batteries [8].

Within the European Union (EU), directive (229/28/EC) states that the EU members must use at least 20 % their total energy with renewable energy and 10 % of biofuels in the transport sector by 2020 [9]. The United Kingdom is committed to reducing its carbon dioxide emission by 80 % of the levels produced in 1990. Now a percentage of fossil fuels should come from sustainable sources which represents 450,000 litres of biofuel a year blended into normal fuel [10, 11]. The IEA has predicted by 2050 the use of biomass and waste as a source of energy will surpass fossil oil (164 EJ compared to 110 EJ) [6].

2.1.2 Biofuels

2.1.2.1 First generation

Biofuels could offer an alternative to fossil fuel and lower the carbon dioxide emissions as the carbon of biofuels produced during combustion was already part of the carbon cycle and thereby does not increase the amount of carbon dioxide in the atmosphere. Biofuels are divided into three categories depending on the progress of research, and the sources. The first generation of biofuels includes the production of biodiesel from vegetable oils, and bioethanol from the fermentation of corn starch and sugar cane. Nevertheless, the concept of biodiesel was not a novelty as in 1892 Rodolf Diesel designed one of the first engines working with peanut oil [12].

- Biodiesel

Vegetable oils contain lipids in the form of triglycerides which are made of three fatty acids (long chain carboxylic acid) attached to a glycerol molecule. Table 2-1 lists examples of fatty acids and their origin in nature. The presence of double bonds in the chain referred to as unsaturated fatty acids, changes the chemical and physical properties of the compounds. For example, stearic acid (no double bond) has

a melting point of 70 °C, whereas oleic acid (1 double bond) is liquid at 14 °C [13]. Vegetable oils can be extracted from edible plants (sunflower, rapeseed or palm oil) and non-edible (jatropha oil) by mechanical processes. Palm oil yields the highest amount of lipids amongst terrestrial plants with 5,000 kg oil/ha compared to jatropha with 1590 kg oil/ha [14].

Table 2-1: Example of different fatty acids and their origin [13].

Common Name	IUPAC name	Number of carbon and double bonds	Principal source
Caprylic acid	Octanoic acid	C8:0	
Capric acid	Decanoic acid	C10:0	
Lauric acid	Dodecanoid acid	C12:0	Coconut oil
Myristic acid	Tetradecanoic acid	C14:0	Coconut, tallow oils
Myristoleic acid	9-tetradecenoic acid	C14:1	Palm or cottonseed, lard oils
Palmitic acid	Hexadecanoic acid	C16	
Palmitoleic acid	(Z)-9-hexadecenoic acid	C16:1	
Stearic acid	Octadecanoic acid	C18:0	Lard, tallow oils
Oleic acid	(Z)-9-octadecenoic acid	C18:1	Rapeseed, peanut, jatropha oils
Linoleic acid	cis,cis-9,12-octadecadienoic acid	C18:2	Sunflower oil
Arachidic acid	Icosanoic acid	C20:0	

Raw vegetable oils, for example rapeseed oil, possess poor thermal properties because of its high kinematic viscosity of 33 m^2/s [13]. In order to have similar properties to current fuel, oils need to be transformed. Biodiesels are fatty acids methyl esters (FAME) produced from the reaction of triglycerides and methanol (called transesterification) using catalysts (Figure 2-1). Table 2-2 illustrates the difference in the physical properties between the raw rapeseed oil, FAME and diesel.

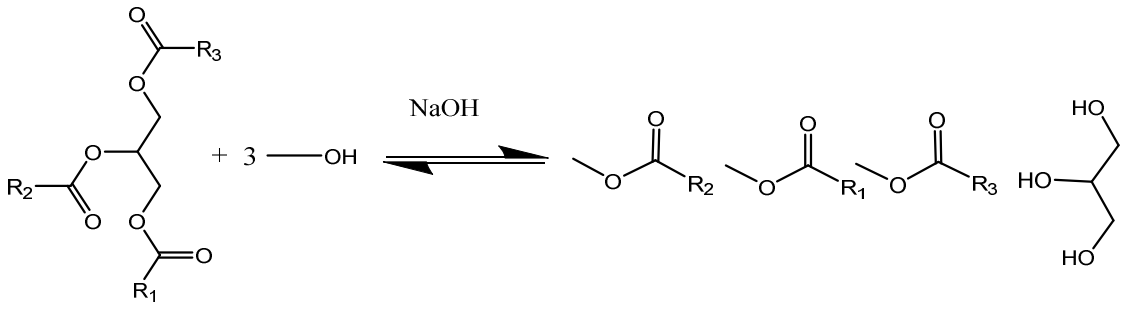

Figure 2-1: Transesterification reaction of triglyceride (Reaction 2-1)

Table 2-2: Comparison of properties between crude vegetable oils and FAME and diesel [15]

Characteristics	Rapeseed oils	Rapeseed methyl ester	Diesel
Specific gravity	0.9	0.9	0.8
Viscosity at 40 °C (m^2/s)	33.0	4.0	3.0
Cloud point (°C)	-21.0	-3.0	-23.0
Cetane number	32.0	48.0	49.0
Heating value (MJ/kg)	40.2	37.7	45.4

There are several techniques in order to produce FAME, the most common are as follows: alkali (NaOH) or acidic (H_2SO_4) catalysts [16, 17], heterogeneous catalyst such as TiO_2 [18], microwave [19] and at high temperature under subcritical methanol [20]. Biodiesel is now sold in petrol stations in a blended form as B5, B10 and B20 (5 to 20 vol.%). Special engines are required to use pure biodiesel. The production of biodiesel soared in the last twenty years reaching 140 barrels/day in 2012 but remained insignificant compared to the production of crude oil (90,026 barrels/day) for the same year [21].

Glycerol is produced as waste and separated from the FAME by distillation. In order to have a stable fuel, the majority of the fatty acids should be saturated, as unsaturated could undergo oxidation and form dimers [22]. Even though the use of biodiesel allows the emission of carbon dioxide to be reduced; the cultivation of these seeds, in particular sunflower oil or rapeseed, requires a large amount of fertilisers which enhances the eutrophication phenomena. Moreover, the emission of nitrous

oxide (N_2O), a powerful greenhouse gas with an impact 298 times greater than carbon dioxide is boosted [23, 24]. When biodiesel was combusted, emissions of NO_x and particulate matter compared to diesel combustion was measured [25]. The other drawback is ethical: debates concerning the impact of biofuels on the rise of the price of food especially for sunflower, rapeseed corn or sugarcane for the production of bioethanol. The production of biofuels occupied 1 % of the world arable land to produce 1 % of the world fuel demand [26]. Developing countries would have the most impact on their economy caused by the rise in price of first necessity products (flour, vegetable oils). Jatropha oil, a non-edible oil, could be used in place of the aforementioned crops, although the crop would still require fertilisers. Furthermore, the high demand would enhance deforestation, as already observed in Malaysia for the production of palm oil. In order to meet half of the fuel demand in the USA, 77 % of the total area used for growing crops would be required to produce the requisite yield of jatropha oil (oil yield of 1892 L/ha) [1].

- Bioethanol from starch

Bioethanol could be a potential candidate to replace gasoline. Fermentation of starch is the common route to synthesise this fuel. Corn starch and sugarcane are the most widespread feedstock. Ethanol is readily produced from the hydrolysis of *Saccharomyces* yeasts [27]. The chemical equation (Reaction 2-2) shown below summarises the fermentation of glucose under anaerobic conditions:

$$C_6H_{12}O_6 \rightarrow 2C_2H_5OH + 2CO_2 \quad \text{(Reaction 2-2)}$$

Starch material would need a treatment prior to fermentation in order to hydrolyse into glucose. A chemical reaction facilitates the breakdown of the cell wall with acidic or alkali media, and enzymes such as α-glucoamylase and α-amylase participate in the depolymerisation of the starch chain [28]. Brazil has been using bioethanol as a blend or pure fuel for at least the last 30 years. Its annual production of ethanol from sucrose represents approximately 17 billion litres. The United States reached this level of production in 2006 from the processing of corn starch [27]. The blends which are currently available are E5, E15, E85; the latter necessitates a special type of engine because of corrosion problems. Ethanol has a higher octane number (108) compared to isooctane or gasoline (100), also it has a larger flammability limit which allowing for an easier compression ratio [29].

The production of ethanol from first generation crops leads to the same drawbacks as with the biodiesel: eutrophication, increase of the nitrous oxide (N_2O) emissions, and erosion of soils, etc [30]. The further disadvantage for this fuel is the problem of corrosion (fuel tank) and carburet for the miscibility of water [31]. Although not straight forward, the first generation fuels are easily produced and economically viable. Alternative sources of biomass should be investigated for the production of sustainable and ethical fuels.

2.1.2.2 Second generation of biofuels

- Bioethanol from lignocellulose

Currently, research focuses predominantly on producing ethanol from waste biomasses (lignocellulose) such as wheat straw, bagasse or wood belonging to the second generation of biofuels. However, the actual technologies available for first generation fuels are not suitable for the production of ethanol from lignocelluloses as they contain more complex structures such as cellulose, and lignin. Figure 2-2 represents the chemical structure of cellulose.

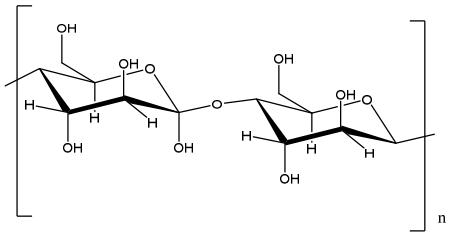

Figure 2-2: Cellulose structure

Each year, 3-5 tonnes per hectares of waste cereal straw is produced in the United States which could yield a production of ethanol between 350 to 1600 L/ha/year depending on the method of conversion [32, 33].

Several pre-treatment steps are necessary to produce bioethanol from the conversion of lignocellulose into cellulose and subsequently into simple sugars such as glucose which can be fermented into ethanol. Although, cellulose could be hydrolysed using different types of microorganisms such as bacteria or fungi, this process is slow and inefficient. The first step would involve the removal of lignin or any impurities contained within the cellulose. The most widespread technique is to use alkali or acidic salts, for example dilute sulphuric acid at 160 °C under reflux [34]. At the last stage, 85 % of bioethanol could be produced, even though the acidity of the

solution could hinder the activity of the yeasts [27]. Pre-treating cellulose using the steam explosion method has given encouraging results in terms of enzymatic efficiency in the final step [35]. The remaining methods include ozonolysis [36], ammonia fibre explosion [37], and supercritical CO_2 [38].

These methods are not currently commercially viable as they include multiple steps involving onerous techniques which are necessary to produce ethanol. The production of bioethanol from lignocellulose will have a better impact compared to the first generation with lower emissions of greenhouse gases (depending on the method used) and lower eutrophication, depending on the source of lignocellulose [39].

- Thermo-chemical processing of lignocelluloses

Lignocelluloses (or biomass) could be converted into different products and fuels or gas commonly called biomass-to-liquid (BTL) using thermo-chemical processes (Figure 2-3) which involved thermal conditions such as pyrolysis, combustion, liquefaction and gasification. The grey represents where an oil is obtained and the red a gas.

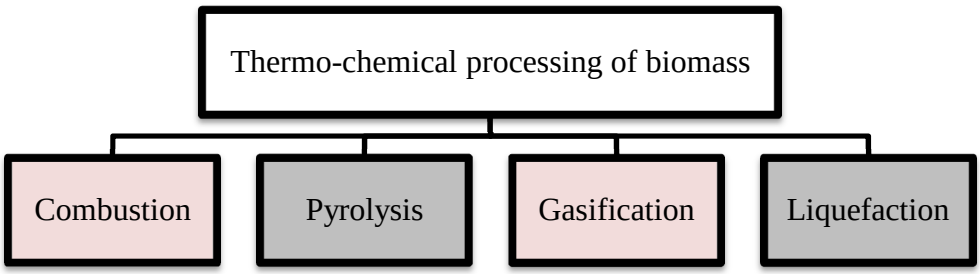

Figure 2-3: Diagram of the different process

Combustion involves the processing of biomass at high temperature in the presence of oxygen. The purpose is to generate heat, for direct use, or to raise stream for electricity production.

Gasification refers to the formation of gas, usually syngas, hydrogen and carbon monoxide (CO and H_2), at high temperatures in the presence of air above 1000 °C with or without a catalyst [40]. The first application was to produce hydrogen via the water gas shift reaction (Reaction 2-3) in the chemical equation.

$$CO + H_2O \rightarrow H_2 + CO_2 \text{ (Reaction 2-3)}$$

A development on this is the Fisher Tropsch process which converts the syngas into hydrocarbons or green diesel using iron or cobalt catalysts, although catalysts are susceptible to poisoning from the biomass [41]. The composition of the oil, for example the chain length, depend on the conditions used during the reaction, for example the reaction time [42]. This technology still faces several challenges. Gasification pilot plants already exist, for example, the fluidised reactor in Austria in Güssing which is a fluidised bed gasification plant producing 8 MW_{th} [14, 43].

Pyrolysis involves the conversion of dried biomass into a bio-oil or bio-char in the absence of air. At lower temperatures, char is produced; a greater yield of oil is obtained at higher temperatures. The composition of the bio-oil is dependent on the pyrolysis heating rate, reaction time and temperature. Slow pyrolysis is conducted at temperatures between 270 and 680 °C with a slow heating rate and timespan from 45 to 550 seconds with larger size particles. Fast pyrolysis takes place between 580 to 970 °C in less than ten seconds with particle sizes of 1 mm. Flash pyrolysis requires temperatures above 1000 °C in less than one second and a particle size of 0.2 mm [44]. In the absence of a catalyst, the typical pyrolytic oil, with a yield of 60 % contains a high fraction of oxygenated compounds and has poor thermal properties. Compounds from the pyrolysis of lignocellulose are: aliphatic alcohols/aldehydes, furanoids, pyranoids, benzenoids [29].

Second generation biofuels (lignocellulose and wood) face similar challenges to that of vegetable oils, as previously discussed. Nevertheless, this is a different route compared to first generation biofuels in the production of green diesel by hydrotreatment under pyrolysis conditions. A comparable diesel composition has been achieved [45].

Liquefaction involves the process of compressing a feedstock into a liquid at high pressure in order to obtain an oil in the presence of hydrogen. This technology was used several years ago to liquefy coal into fuels [46]. Currently, hydrothermal liquefaction is more commonly applied to the processing of wet biomass feedstock (refer to section 2.2).

Although, some promising results have been achieved, however it is noted that a new generation of biofuels could rapidly overtake first and second generation biofuels. This is due to second generation biofuels presently not being an economically viable option because of the high investment costs.

2.1.2.3 Third generation of biofuels

Third generation biofuel production is based on the extraction of microorganisms (fungi, microalgae or yeasts) [47]. Microalgae offer an encouraging potential which in the future could be a viable alternative to fossil fuel.

2.1.3 Microalgae

2.1.3.1 Generalities

Microalgae are one of the Earth oldest living microorganisms. They are an attractive feedstock for the production of a biofuel in comparison to terrestrial plants due to the following factors:

- Not enter in competition with the food crops and therefore do not use arable land.
- Ability to grow in fresh, salty or brackish water.
- Strains of microalgae are present in the major part of ecosystems.
- Their growth rate allows them to be harvested several times a year, in contrast to other plants.

These organisms are composed of lipids, proteins and carbohydrates; Table 2-3 illustrates the lipids and proteins compositions for the most common strains of microalgae. The variation between the different strains is dependent on their environmental conditions and nutrient availability [47].

Table 2-3: Composition of oils from different strains of microalgae

Biomass	Lipids (wt.%)	Proteins (wt.%)	reference
Chlorella pr.	14.6	52.6	[23]
Chlorella v.	25.0	55.0	[48]
Nannochloropsis sp.	28.0	52.0	[49]
Spirulina	5.0	65.0	[48]
Scenedesmus	12.0	50-55	[50]
Chlorella py.	2.0	57.0	[50]
Dunaliella s.	6.0	57.0	[50]
Synechococcus sp.	11.0	63.0	[50]

According to Chisti et al. [1], the algae lipid content has potential of reaching 80 wt.% on a dried basis (db). 136,900 L/ha of oil from microalgae containing 30 wt.% lipids could be achieved in comparison the palm oil production yield production is 5950 L/ha/year. Approximately 3 % of the total landmass for the United States would be required in order to produce half of the country's annual consumption.

The second advantage in using microalgae is that they had the highest photosynthesis efficiency compared to terrestrial plants, in other words, microalgae are able to covert approximately 7 % of the total solar energy arriving on the surface of the Earth (170 W/m^2). In contrast, switch grass (a fast growing terrestrial plant) could only convert 0.5 % (1 W/m^2) of the irradiation in normal latitude [51]. It was estimated by Zhu et al. [52] that with 3 % photosynthesis efficiency, it would require from 0.4 to 0.7 % of the total surface area of the planet to produce enough biomass to meet global energy demand [53]. Via the photosynthesis process (Reaction 2-4), microalgae could be a solution for carbon dioxide mitigation to transform into glucose as in the chemical equation:

$$6\ CO_2 + 6\ H_2O + \text{light} \rightarrow C_6H_{12}O_6 + 6\ O_2 \quad \text{(Reaction 2-4)}$$

On a dry basis, one kilogram of microalgae is able to sequester 1.8 kg of carbon dioxide [54]. As the carbon dioxide in the ambient air limits the development for microalgae, Chisti et al. [55] suggested using the flue gas emission from coal combustion power plants as a sequestration solution, reducing the cost of biofuel production. However, it must be noted that some acidic flue gas species such as NO_x and sulphur dioxide (SO_2) could be toxic for the growth of microalgae. *Chlorella v.* has the highest carbon dioxide fixation rate [55].

2.1.3.2 Cultivation

Three different growth conditions are possible for microalgae: phototrophic (autotrophic), mixotrophic and heterotrophic. Under phototrophic conditions, microalgae utilise carbon dioxide as a carbon source via photosynthesis. In contrast under heterotrophic conditions the microorganisms use organic compounds (glucose or glycerol) as the source of carbon.

Microalgae can be grown in a dark environment and use other sources of carbon for their metabolism. In this case, the lipid accumulation was found to be more rapid and reproducible compared to the phototropic condition for example *Chlorella v, Chlorella sa., Chlorella pr., Chlorella so.,* could accumulate four times more lipids

than under autotropic conditions [56]. Espinosa Gonzalez et al. [57] succeeded in growing *Chlorella p.* using dairy waste or whey protein; a maximum biomass of 9 g/L was achieved with 42 wt.% of lipids. However, only a limited amount of strains could be grown within these conditions. Another disadvantage is that the microalgae are dependent on the concentration of carbon fed.

Nitrogen as ammonia (NH_3) and phosphorus as phosphate (PO_4^{3-}) are the most common inorganic nutrients for the autotrophic organism. However calcium or magnesium salts are also needed; an empirical formula would give $CO_{0.48}H_{1.83}N_{0.11}P_{0.01}$ of total nutrients [58]. To lower the production costs, waste water from industry or domestic houses could be used and it would not be necessary to add nutrients. Domestic waste water contains enough nutrients to produce 77.6 million kg/day [59]. Cyanobacteria develop well in streams from agricultural waste water (rich in carbohydrate and proteins) [60]. By starving the microalgae strain of nitrogen nutrients, the microalgae will become stressed in response producing more lipids despite a slower growth rate [61]. Microalgae could even be used to remove toxic metal such as mercury from waste streams by bio-sorption [62]. Nevertheless, the growth of some microalgae (*Chlorella*) could be inhibited by some metal ions such as copper (with a concentration of 240 ppm) and nickel [63].

There are several reactors where microalgae could be cultivated either in open space (ponds, lagoons, raceways ponds) or in photobioreactors.

- The open ponds are the most common low cost technique to grow algae on a large scale. The microalgae slurry is circulated by the way of a paddlewheel in a close and shallow pond (less than 0.3 m). Baffles are present to regulate the flow. This technology is currently in use for strains such as *Chlorella*, *Spirulina* or *Dunaliella.* Waste water could be fed into this reactor. In addition, ponds are more efficient where the photosynthesis is higher, as in southern Spain and in Texas. Water is continuously supplied and harvesting occurs at constant intervals. Open raceway is an economic process and with low maintenance. The inconvenience is that contamination by external sources is frequent, thus multi-culture of different strains is easier to achieve [64].
- Photobioreactors (PBR) are more efficient and sophisticated than open pond in order to avoid contamination. They can be described as an array of small diameter tubes transparent in order to let the light penetrate efficiently. There are two

categories: the flat-plate PBRs and the tubular PBRs. Tubes are arranged in a north to south direction to enable the optimum exposure to the sun, which has allowed achieving 47 g/m^2/day of dried biomass [65]. The flat plated bioreactor has a large surface area which results in a low accumulation of oxygen. The microalgae are circulated via the pump (mechanical or air lifted). Degassing was found to be important, as oxygen could damage or inhibit their growth [64]. Carbon dioxide from flue gas has been injected more efficiently in PBR than in open ponds. However the optimum level should be 1.7 g CO_2/g of biomass in order not to raise the pH level. The PBR has yielded a higher production of microalgae; for example with *Nannochloropsis* the harvesting yield was 20 to 40 g/m^2/day in a tubular reactor [66].

PBR require complex materials which increase their cost to £51.8/kg for a 3 m^3 tubular photobioreactor. It was estimated that the cost could drop to £9.9/kg of dry biomass if the production exceeds 200 tonnes/year [55]. The cost would fall five times lower, if raceway ponds were used, to £0.15/kg [67].

Different techniques of harvesting microalgae such as flocculation, centrifugation, filtration, flotation and electrophoresis have been considered. The flocculation method involves adding some metal salts such as ferric chloride to allow the biomass to aggregate and settle down by sedimentation; the problem in using this method is the feedstock could not be treated under anaerobic digestion. Flotation processes separate the biomass in relation to their density, and this is only suitable on a small scale. Electrophoresis sends an electric discharge into the broth to induce coagulation and subsequently sedimentation. Centrifugation is an expensive technique. The method of harvesting depends on the strain of microalgae to be cultivated; for example for *Botryococcos b*. dispersed air flotation is the most suitable, whereas with cyanobacteria as *Spirulina* a simple microscreening is only necessary from the filamentous shape [1, 68]. Yet, the most suitable and economic method is by filtration or gravimetric sedimentation [69].

2.1.3.3 Extraction of lipids and chemicals

As reported earlier, microalgae have the potential to accumulate more lipids than terrestrial plants. In order to carry out lipid extraction, drying steps are necessary to increase the yield. There are two possible routes either by mechanical (cell disruption) or chemical treatments. Figure 2-4 shows the products which can be extracted from microalgae.

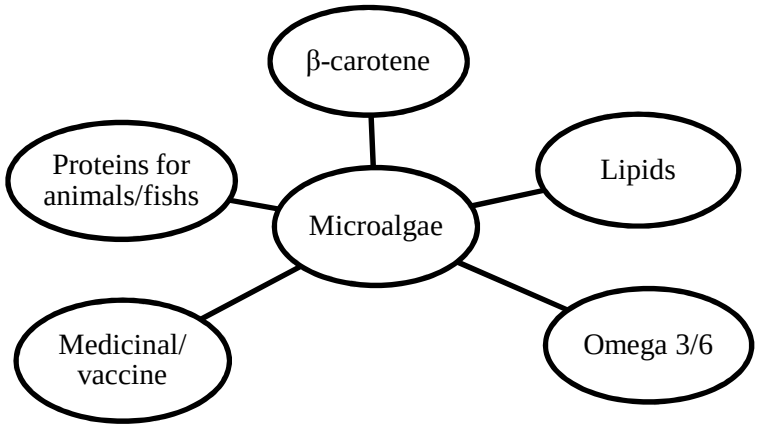

Figure 2-4: The use of microalgae

- In 1959, Bligh and Dyer were the first to develop a chemical extraction method by soxhlet using chloroform and methanol with a 3:1 ratio [70]. This technique has been widely used; however it does not meet the green chemistry principles because of high flammability and toxicity of the solvents. Ionic liquid is a more environmentally friendly technique as the solvent can be regenerated at the end. Compared to normal solvent extraction the total lipid yield was improved from 12 to 19 wt.% with ionic liquid [71].
- Supercritical carbon dioxide seems to be the most efficient technique as it allows a 100 % recovery of the lipids from the microalgae [72]. Once extracted, the same procedure of transesterification used for the vegetable oils is performed producing a microalgal oil with a 90 to 100 % conversion [73]. *In-situ* esterification avoids extracting or even drying the microalgae by carrying out the esterification reaction with the whole biomass. Ultrasonic or microwave methods are investigated, the second enhanced the lipids recovery and the production of ester with catalyst [74, 75]. Levine et al. [76] demonstrated the efficiency of the transesterification with supercritical ethanol to produce fatty ethanol ester with 100 % of biodiesel and 66 % of ester at 325 °C for *Chlorella*.

The disadvantages of the extraction and the production of FAME is that only lipids are used and the remaining part of the microalgae is considered as waste; more energy or oil could be produced when the entire microalgae is processed.

- Extraction of other chemicals

Not only lipids can be extracted from microalgae but high value compounds such as omega-3 and 6; β-carotene and astaxantin. Food and pharmaceutical companies have a huge interest in these compounds. Omega-3 such as eicosapentanoic acid (EPA) 20:5, and decosahexaenoic acid (DHA) 22:6 have proven to be efficient in the treatment of some diseases, for example with asthma or heart problems. *Phaeodactylum* contain a high level of these fatty acids [77]. Chlorophyll a and b from Chlorella could be used to help recovery from ulcers and application within the cosmetic industry [78]. *Dunaliella* is well recognised to produce β-carotene used as a food supplement because of its antioxidant propriety. For example, the revenue from β-carotene could to £559/kg; in 2006 the industry had generated approximately £511 million of benefit by selling carotenes. *Haematococcus* sp. contains the highest level of astaxantin, it is fed to salmons to give their pinkish texture and the cost of this product was £1518/kg [79].

Microalgae have other potential applications. Recently, the research group in San Diego has designed a stem cell from microalgae to produce a vaccine against malaria or to fight against cancer [80]. Whole algae, for example *Spirulina*, are used as a food supplement, and some other strains are fed to livestock or fish farms. *Hypnea cer.* is used to feed shrimps [78]. In order to make the production of biofuels profitable, most companies in microalgae now sell these products in parallel, as with Solazyme. Chisti et al. [67] estimated that to compete with fossil oil the cost of production of microalgae should be approximately £0.15/kg. The large array of applications makes microalgae very challenging.

2.1.4 Conversion of microalgae to energy and fuels

Microalgae have been processed via different routes, biological and thermochemical conditions, producing either a bio-gas, bio-oils or other products.

- Some microalgae strains are able to hydrolyse water to produce hydrogen; for example, using the energy of the sun a marine strain *Chlamydomonas r.* is found to hydrolyse water into hydrogen under anaerobic conditions [81].
- Anaerobic digestion of biomass produces methane by microorganisms at 35 °C in a digester in the absence of air. Residues from lipids extraction could also be treated under this condition. The processing of a seaweed, *Ulva*, produces 180 ppm of methane [82]. In comparison to sludge, the conversion of microalgae was quite

slow as the bacteria could be poisoned by the ammonia from the proteins; in order to obtain a 500 kW bio-methane plant it would be necessary to have 10,000 tons of microalgae [83]. These technologies are not efficient as they require a long time to produce gas and a large amount of feedstock.

- Bioethanol could also be obtained from the algal strains with a high carbohydrate content which could be an alternative from the first generation of biofuels (corn and sugarcane). The fermentation of marine green alga, *Chlorococcum l.* has also been investigated with a conversion of 25 % [84]. However, macroalgae *Saccharomy ces.* gives better results as higher carbohydrate content is present [78].

- Thermochemical processing of dried microalgae

Thermal processing techniques give a low yield and require challenging conditions. Consequently, the research in to thermochemical processing is less advanced. Milne et al. [85] were the first group which carried out the pyrolysis of a microalgae with catalyst obtaining challenging results. Miao et al. [86] pyrolysed *Chlorella pro.* at 500 °C. A yield of 17.5 wt.% of bio-oils was obtained with a high production of chars. The heating value of the pyrolysis oil was approximately 29 MJ/kg contrary to pyrolysis wood oil which has an energetic value of 17 MJ/kg. In another study, the same authors pyrolysed the same algae grown under heterotrophic conditions, a larger yield of 57.9 wt.% was achieved with a calorific content of 41 MJ/kg, even though the bio-oil had a large amount of polar compounds, 20-25 wt.% oxygen [86, 87]. Slow pyrolysis reduced the formation of bio-char. The inconvenience of this technique is that high amount of energy is required to heat the reactor to 500 °C and furthermore to dry the microalgae, which contains initially 80 wt.% of moisture. Due to the presence of oxygenated compound, the resultant bio-oil was unstable and corrosive.

Direct combustion and gasification have been carried out on dried microalgae to either produce heat or syngas, however the efficiency is compared to other biomass and coal. In order to pyrolyse microalgae, a significant heat input is initially required for drying, as the moisture content can be up to 80 wt.% [88]. Therefore, it would be more convenient and efficient to process the wet biomass directly, using a technique known as hydrothermal processing.

2.2 Hydrothermal processing

Hydrothermal processing consists of processing biomass in hot compressed water above 200 °C where the water is first liquid (subcritical), and subsequently after 375 °C in a supercritical state. As the temperature increases, the properties change, such that different results can be achieved. Hydrothermal processing is divided into three regions, depending on the pressure, as presented in This image has been removed by the author of this thesis for copyright reasons

Figure 2-5:

- Hydrothermal carbonisation (HTC) from 170 to 250 °C where biomass is transformed into bio-chars.
- Hydrothermal liquefaction (HTL) from 250 to 370 °C where the production of bio-crude oils is maximal.
- Hydrothermal gasification (HTG) above 370 °C where gas phase is the main outcome from the processing.

In comparison to dried pyrolysis, liquefaction and gasification, hydrothermal processing takes place at lower temperatures which allows saving some heating energy. Furthermore, water is a green solvent, highly available compared to chemical solvents.

Hydrothermal processing was historically used in the early 1980's to treat hazardous waste or sludge under supercritical oxidation (SCWO), this process has been industrialised [89]. During the same decade, the company, Shell, started to perform research on the hydrothermal liquefaction of biomass [90]. The research group in Pittsburgh carried out research on the liquefaction of wood and coal in water and other solvents [91].

The aim of hydrothermal processing is to replicate the natural formation of crude oil, natural gas and coal. Crude oil was formed over millions of years trapped in pressurised cavities from the decay of microorganisms (zooplankton or phytoplankton) [92]. Ideally, hydrothermal liquefaction could bring a green alternative to petroleum depletion when this system is optimised. It is noted that hydrothermal conditions are present in the bottom of the ocean within hydrothermal vents [93]. Bio-crude oil is viscous with a high energy content ranging from 30 to 40 MJ/kg. The oil

composition is a complex mixture of oxygenated and aliphatic compounds. Bio-crude derived from microalgae, may further contain cyclic nitrogen compounds.

This image has been removed by the author of this thesis for copyright reasons

Figure 2-5: Phase diagram of water with hydrothermal processing regions diagram from Peterson et al. [94]

Subcritical water is a more advantageous medium to work with as at high temperature; the water has different chemical and physical properties.

- The water density decreases from 1000 at room temperature to approximately 650 kg/m^3 at 350 °C. This temperature change lowers the polarity of water or dipole moment from 78 F/m at room temperature to 14 F/m at 350 °C and 20 bar, above the supercritical point water forms a single gaseous phase [95]. Likewise water would have proprieties similar to acetone at this temperature and be able to dissolve polar molecules such as triglycerides. Khuwijitjaru et al. [96] demonstrated that the solubility of fatty acids increased with the temperature and in relation to the carbon chain length. Benzene is miscible in water at 300 °C and 170 bar [94].
- In the temperature region between 200 to 350 °C, the ion product or the dissociation constant defined in Equation 2-1 is at its maximum of 10^{-11}. At these temperatures the concentration of hydroxyls and protons is increased improving the hydrolysis of macromolecules and avoiding the need for additional inorganic acids [97].

$$K_w = [H_3O^+] \text{ x } [OH^-] \quad \textbf{Equation 2-1}$$

- The solubility of salts is lowered before the supercritical point and induced reactor plugging. For example, sodium sulphate (Na_2SO_4) precipitates at a lower temperature compared to sodium chloride (NaCl) [98]. This problem of precipitation could be exacerbated during the processing of microalgae grown in salt water. Corrosion of the reactor could be an issue depending on the biomass processed.

However, a suitable material for a reactor such as inconel 625 has demonstrated to robust under subcritical water [2].

2.2.1 Chemical degradation under hydrothermal liquefaction

The main chemical pathways involve proton reactions with radical reactions being dominant at temperatures higher than 375 °C. Physical and chemical properties could be tuned in relation to the water loading. Three major steps are found to occur during the hydrothermal liquefaction of biomass according to Toor et al. [2]:

- Depolymerisation of the biomass
- Decomposition of the monomer by cleavage or dehydration
- Recombination of some molecules.

During the first stage, macromolecules such as carbohydrates, proteins and lipids are hydrolysed. At higher temperature, these molecules are broken down further and recombined to form “heavy molecular weight” materials.

Subcritical water is able to undergo a range of chemical reactions without the need of a catalyst. The increase of the dissociation constant enhances the concentration of proton and hydroxyl species. The hydrolysis of organic compounds for example alcohols, ester, ether and amines are readily carried out at temperatures between 200 and 300 °C [97]. This is important as the majority of macromolecules in the biomass form polymers; for example amino acids are bonded together with amide group to form the peptide chains.

Ester hydrolysis at 350 °C is fast occurring, where 96 % of ethyl acetate is hydrolysed within 170 seconds to ethanol and acetic acid in the absence of a catalyst [99]. The hydrolysis of amides for example N-methylacetamide occurs between 200 to 400 °C and decomposes into acetic acid and methyl amine, although the hydrolysis kinetics are faster at a pH < 3 and > 10 [100].

The hydration of alcohols such as ter-butanol (ternary alcohols) to yield methyl propene occurs in less than 60 seconds due to a higher water dissociation rate between 250 to 350 °C. The addition of sulphuric acid is recommended to hydrate primary or secondary alcohols such as butanol to butene with a pH ranging from 2-3 [101].

Condensation reactions occur commonly in subcritical water including Friedel–Crafts alkylation, aldol and Claisen condensation. Friedel Craft involves the addition of an alcohol or acyls group into an aryl cycle (with an electron withdrawing

group). This reaction is considered to be common in the liquefaction of biomass as phenol and alcohol (as tert butanol) are commonly present in the water phase [102]. The aldol reaction involves the condensation reaction of two aldehydes as acetaldehydes and the Claisen reaction consists of the condensation between two esters (Figure 2-6). These reactions necessitate the addition of basic catalysts. For example in hot compressed water, the conversion of butyraldehyde into 2-ethyl-2-hexanal was carried out at 250 °C with a yield 40 % [103].

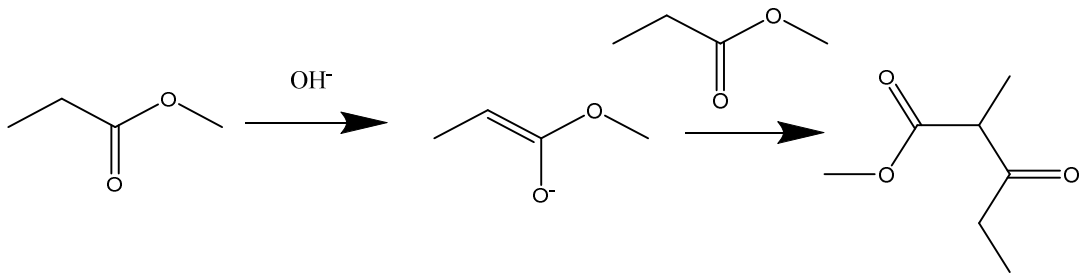

Figure 2-6: Example of Claisen reaction condensation between two ethyl acetate (reaction 2-5) [103]

The reverse reaction of the aldol condensation also occurs, splitting into two aldehydes, this is observed during the hydrolysis of glucose to glycolaldehyde [104].

Sub or supercritical is an interesting media to carry out the Diels-Alder reaction as at high pressure; the polarity of the water decreases, thus apolar molecules are soluble, and the reaction is able to take place at room temperature. Furthermore, compressed water is found to be more selective for certain isomers (endo or exo ratio) in comparison to standard temperature and pressure. Figure 2-7 shows a typical reaction of Diels-Alder between a diene and a dienophile. This reaction could take place in the presence of unsaturated fatty acids such as oleic and linoleic acids [105].

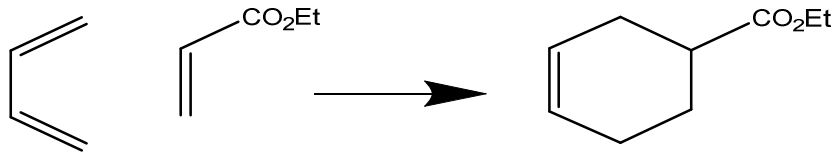

Figure 2-7: Diels-Alder reaction (Reaction 2-6)

Rearrangements could also take place under these conditions, such as the delocalisation of the double bonds from the migration of the protons (1,8) leading to cyclisation. The other rearrangement observed is the Beckman reaction; it is widely used during the production of nylon 6 with the synthesis of caprolactam [106].

Oxidation and reduction reactions could be carried out in subcritical water using a catalyst. However, it is noted that different mechanisms take place after the critical point, involving radical reactions [105].

Therefore, there are many advantages of working with subcritical temperatures, as the properties of the solvent rely on the operating conditions (temperature and pressure). Water can be used as catalyst for the hydrolysis in the solvation of a reactant in particular with the Diels-Alder reaction. The water can have an impact on the kinetic of a reaction. The large variety of compounds present in bio-crude can be explained by the different reactions possible in subcritical water. One purpose of this present study is to reduce the oxygen and nitrogen content in the bio-crude. The dehydration and hydrolysis reactions of macromolecules occurring within these conditions maybe are a potential solution. Nevertheless the historical studies indicate that the oxygen and nitrogen contents are still significant. Therefore, it is observed that further investigations need to be performed.

A large variety of biomass has been investigated under hydrothermal liquefaction, such as woods [91, 107], lignocelluloses [108], vegetable oils [109, 110], and protein [111, 112]. For instance, most of carbohydrates (cellulose, starch, hemicelluloses) underwent a rapid hydrolysis under subcritical conditions to degrade in the aqueous or gaseous phase [2]. Degradation of other feedstocks (lipids, carbohydrates or proteins) are further detailed within this present study (refer to **Chapter 5, 6** and **7**).

As previously discussed, microalgae, because of it high productivity, and large amounts of lipids, are more suitable for hydrothermal liquefaction processing. Hence, it is why more detailed research has been conducted in this in comparison to other biomass. The next section includes research on hydrothermal carbonisation and gasification.

2.2.2 Hydrothermal carbonisation (HTC) of microalgae

This process involves the formation of bio-chars at temperatures below 250 °C and a low pressure (not greater than 20 bar). The objective of this method is to synthesise bio-coal with a low environmental impact for the production of an absorbent and carbon dioxide sequestration. Bio-chars are produced from simple carbohydrates (glucose, xylose). At lower temperatures, these compounds (hexoses) are degraded into hydroxymethyl-furfural and subsequently into a carbon material.

Chars obtained previously possess a lower surface area. Furthermore, the shape of pores can be modified in the presence of different additives, such as silica [113].

Heilmann et al. [114] investigated the HTC with different strains of microalgae. A 62 wt.% carbon recovery was achieved in less than one hour at 190 °C. Higher energy content was present from the bio-char of *chlorella r.* when compared to natural coal or from lignocellulose materials. The char from microalgae contained more than 5 wt.% of nitrogen which could lead to the production of NO_x emissions during combustion. High value compounds could be extracted from the aqueous phase, such as sugars and organic acids, produced during the carbonisation of *Spirulina*. The mass yield was superior at 175 °C with half of the energy recovery compared to 215 °C [115]. During the HTC reaction, lipids were absorbed into the chars and they could be retrieved by organic solvents [116]. Du et al. [117] produced bio-chars from *Chlorella* at low temperature and recycled the nutrient from the waste water to cultivate the same strain. When microalgae were mixed with glucose, the fixation of nitrogen was enhanced [118].

Hydrothermal carbonisation has received less interest than gasification and liquefaction as it is a novel technique, and for the moment, the product has low economic impacts.

2.2.3 Hydrothermal liquefaction (HTL) of microalgae

The attention in hydrothermal liquefaction of microalgae was triggered by early research carried out in Japan (Tsubaka) during the 1990's. The first detailed publication was released by Dote in 1994 investigating the liquefaction of *Botryococcus b.* in the presence of sodium carbonate (5 wt.%) at 300 °C. A 64 wt.% yield was reported, which is superior than the lipid content (50 wt.%). Further, a similar energy content to petroleum crude oil was measured at 42 MJ/kg with low nitrogen and oxygen content. However, it was observed that not all the algae had been processed, only the extracted oil [119, 120]. Furthermore, the strain of *Botryococcus* was not easy to cultivate with a high yield [121]. One year later, Minowa et al. [48] carried out the hydrothermal liquefaction of *Dunaliella t,* a microalga with higher protein content, obtaining a maximum yield of 42.0 wt.% with a 5 wt.% loading sodium carbonate. The energy content obtained was 37 MJ/kg, and approximately 7 wt.% of nitrogen within the bio-crude oil. The energy consumption rate (ECR) was calculated at a ratio of 0.34 implying that the energy balance was positive. From these

studies Sawayama et al. [54] investigated that the *Botryococcus* strain in large scale could be used for carbon dioxide mitigation, with the conversion of this gas approximating to 1.5 10^5 ton/year, in the space of 8400 hectares. Again the difficulty of cultivation of this microalgae was not taken into account [122].

Yang et al. [123] selected a microalga strain *Microcystis v.* produced during eutrophication in lakes. The reaction was carried out in 5 wt.% sodium carbonate loading, as previously producing a good yield of 39.5 wt.% at 340 °C for 30 minutes. With one hour a slightly lower yield was achieved (37.8 wt.%). The composition of the bio-crude oil included a high oxygen and nitrogen contents (approximately 6 wt.%).

Since the late 2000's, there has been a remarkable interest in hydrothermal liquefaction. Zou et al. [124] carried out the liquefaction of *Dunaliella t* using different conditions with ethylene glycol and 3 vol.% sulphuric acid instead of water, to producing a 23 wt.% yield at 170 °C. The bio-crude oil produced had some acidic properties. A low yield of 25.8 wt.% compared to the study of Minowa [48] was achieved by Shuping et al. [125] processing *Dunaliella t* cake with the same concentration of sodium carbonate at 360 °C for 50 minutes. A high oxygen content was measured in the bio-crude oil, it was elucidated that temperature influenced the increase the bio-crude yield. The change in concentration of sodium carbonate was reported to have no impact on the yield.

The advantage of hydrothermal liquefaction is the selection of the strain is not dependant on the lipid content in contrast to the lipid extraction. Thus Yu et al. [126] investigated the processing of *chlorella py.* with 0.1 wt.% of lipids at 280 °C with a 20 wt.% loading. A maximum bio-crude yield of 34.0 wt.% was obtained with a reaction time of 120 minutes. An increase of bio-crude yield was observed with an increase the temperature (200 to 300 °C) and reaction time. Brown et al. [127] measured similar trends selecting *Nannochloropsis* with the highest yield obtained at 350 °C of 43.0 wt.%. A higher temperature, gasification was favoured compared to the liquefaction. The maximum content of nitrogen was measured at 300 °C with 4.3 wt.%. A comparison was investigated by Vardon et al. [128] between a normal (with 13 wt.% of lipids) and defatted strain of *Scenedesmus* and *Spirulina (*approximately 5 wt.%). Lipids enhanced the bio-crude oil yield with 45.0 wt.% instead of 36.0 wt.% for the defatted strain and 31 wt.% for *Spirulina*. Furthermore, the nitrogen content was

higher with the defatted microalgae (7.8 wt.%) compared to the original (6.5 wt.%). Ross et al. [129] investigated the effect of alkali salts and organic acids on the bio-crude yield and compositions at two different temperatures, 300 and 350 °C, on two strains *Chlorella* and *Spirulina*. Compared to the studies described above, lower yields were achieved. Biller et al. [112] examined the fate of nitrogen by processing different biomasses and model compounds with different nitrogen content. These included *Chlorella, Nannochloropsis Porphyridium* and *Spirulina* .for microalgae, albumin and soya proteins, and two acids (asparagine and glutamine acids). It was established with combining the results of the processing of the microalgae and model compounds, that lipids had the highest impact on the bio-crude yield, compared to proteins and carbohydrates. Materials with a high protein content gave high aqueous phase yield and the opposite for the biomass with high lipids.

Vardon et al. [130] demonstrated that bio-crude achieved from *Spirulina* was superior (32.6 wt.%) compared to the processing of swine manure and sludge, although the nitrogen was higher with oil from the microalgae. The simulated distillation showed that the main fraction of the bio-crude oil was present in the vacuum gas oil. Greater bio-crude of 39.9 wt.% and energy content of 35.3 MJ/kg was reported by Jena et al. [131] in a larger reactor size (1.8 litres) and with a loading of 20 wt.% of biomass. Increasing the temperature from 200 to 380 °C enhanced the deoxygenation however the level of nitrogen progressed from 5.5 to 6.5 wt.%, while the nitrogen was progressively reduced from 6.4 to 0.4 wt.% in the solid residue. Toor et al. [132] achieved a maximum yield of 46.0 wt.% with *Nannochloropsis* s. carried in a 400 ml reactor and 40.0 MJ/kg of heating content.

In a complete investigation of the hydrothermal degradation of *Desmodesmus sp.* operating under different parameters (temperature and reaction time), the maximum bio-crude oil of 49.7 wt.% was achieved at 375 °C with a holding time of five minutes. For one hour the yield decreased slightly to 47.9 wt.%, yet with a high concentration of nitrogen. The residue degraded at different temperatures was analysed via scanning electron microscopy (SEM); from 175 to 200 °C no major change in the cell structure was observed, above 200 °C the microalgae started to form clusters together, and at 250 °C, the cell wall strength was completely degraded [133]. This statement was emphasised by the study of López Barreiro et al. [134] where different strains of microalgae in the form of a paste (*Scenedesmus o., Phaeodactylum,*

Nannochloropsis g., Scenedesmus a., Tetraselmis s., Chlorella v., Porphyridium p., Dunaliella) were processed at extreme temperatures (250 and 375 °C) with a short reaction time (five minutes). A relationship between the cell wall strength and the yield and temperature is elucidated. Indeed, *Dunaliella*, at low temperature (250 °C), with a low cell wall strength yields 44.8 wt.% of bio-crude oils in contrast to *Scenedesmus o.* (17.5 wt.%) which have a resistant cell structure. At higher temperatures, this parameter did not affect the yield. The maximum yield was achieved with *Scenedesmus a.*, with 58.0 wt.% even though the strain containing high carbohydrate content give low bio-crude oil.

Valdez et al. [135] produced a complete study of the liquefaction of *Nannochloropsis*, as did Garcia Alba et al. [133] except that the kinetics were investigated in detail. At low temperature and short time the microalga is converted into products found mainly in the aqueous phase. As the temperature increased to 400 °C, the oxygen content in the fraction of heavy crude oil decreased, and nitrogen content was mostly converted to ammonium compound. 80.0 % of the total energy was contained in the bio-crude oil [135]. The same author elucidated that the primary pathway with a short time was the degradation from the solid biomass into aqueous products, light and heavy crude oil. Higher activation energy is required for the conversion of the aqueous phase or the heavy oil into the gaseous phase. A model prediction is deduced suggesting that the main degradation or yield occur within the first twenty minutes and subsequently levelled out at most temperatures. This model was relatively close to the literature results [136]. Torri et al. [137] suggested a general route for the degradation of microalgae of each element present in the microalgae (proteins, carbohydrates and lipids), basing the result on the pyro-probe studies. Proteins depolymerise by forming cycles which are reduced with times and temperatures to obtain diketopiperazines; the reaction with proteins and carbohydrates forms “heavy molecular weight” compounds called melanoidin.

In order to achieve higher bio-crude yield with superior quality, pre-treatment is proposed as an alternative. Miao et al. [138] were the first to propose this solution for the processing of *Chlorella s.* grown heterotrophically. During the first step, the alga was treated at 160 °C where the carbohydrates and high value chemicals were recovered and the remaining residues were processed at 240 °C for 20 minutes with a maximum yield of 32.0 wt.%; the denitrogenation is also more efficient. The

sequential process is more energy efficient than the direct liquefaction. Furthermore, the concentration of fatty acids increased in the bio-crude from the two steps, and had the advantage that the energy input was reduced from 15.0 MJ/kg of bio-crude oils [138, 139]. This method is also carried out to extract proteins and chemicals from *Scenedesmus sp*. at 240 °C for 10 seconds to recover 60.0 wt.% of the total nitrogen in the water [140].

Microwave was selected as a technique to extract valuable chemicals and lipids from three strains *Nannochloropsis o, Chlorogloeopsis f and P. ellipsoidea* [141]. Cheng et al. [142] carried out in situ transesterification of *Nannochloropsis o* in a microwave and subsequently processed the remaining residue at 300 °C and finally combined the bio-crude oils with FAME. In this way, 40 wt.% of bio-crude oil is obtained, and the amount of nitrogen was lower; it also avoided the formation of amides.

Biller et al. [143] used the processed water produced during hydrothermal liquefaction at 300 and 350 °C to cultivate *Chlorella v., Scenedesmus d, Spirulina p,* and *Chlorogloeopsis f.*. The liquefaction yielded 47.0 wt.% as maximum bio-crude oil. A dilution higher than 400 times is necessary to have a similar culture growth using a normal media. In order to accelerate the culture growth of *Desmodesmus,* Alba-Garcia et al. [144] added supplementary nutrients to the diluted aqueous phase from HTL. In a different aspect, Chen et al. [145] processed a mixed microalgal strain which treated waste water, the maximum bio-crude oil was achieved at 300 °C with 49.0 wt.% of oil. The nitrogen content was recovered in the aqueous phase and subsequently recycled in the cultivation process. Recently, the same authors performed a co-processed liquefaction with swine manure and mixture of algae (75 wt.% of manure with 25 wt.% of microalgae), and a bio-crude oil yield of 35.7 wt.% was achieved [146].

The optimum yield of 82.4 wt.% was reported recently by Li et al. [147] from the processing of a modified strain *Chlorella sp.* (Y) at 220 °C with a 25 wt.% loading and a reaction time of 90 minutes in a stirred reactor. In addition, the oil contained 20 wt.% of hydrocarbons. *Nannochloropsis* with low lipids also yielded encouraging results with 50.5 wt.% with the same condition.

In parallel, the processing of seaweeds has been studied, although lower bio-crude yields are achieved. For example, Zhou et al. [148] carried out the liquefaction of the macroalgae *Enteromorpha p*. and produced 23.0 wt.% of bio-crude oil at 300 °C using 5 wt.% of sodium carbonate for 30 minutes. The inconvenience of this feedstock was the high level of ash, approximately 30.0 wt.%. Anastasaki and Ross [149] operated different reaction parameters during the liquefaction of *Laminaria s.*, the optimum temperature was at 350 °C for 15 minutes to achieve lower yield (19.3 wt.%) compared to Zhou et al. [148] *Sargassum*, a marine alga, was liquefied at different temperatures by Li et al. [150]. The maximum bio-crude oil yield of 32.0 wt.% was achieved at 340 °C for 15 minutes. Recently, Neveux et al. [151] screened different strains of macroalgae from fresh water and marine origin. Fresh water algae yielded more bio-crude oil (*Oedogonium* 26.2 wt.%) as they originally contain less ash (less than 20 %) compared to seaweed (from 20 to 30.0 wt.%). Nevertheless, producing bio-crude oil from this biomass could not be viable as the yield compared to microalgae was inferior and the quality of the oil was low in energy (approximately 30.0 MJ/kg) with a high concentration of salts in the aqueous phase.

To conclude, since the first publication of Dote et al. [119], an extensive amount of research has been carried out for 20 years. Table 2-4 summarises the main bio-crude oil yields obtained by the studies which had the most impact. *Chlorella*, *Spirulina*, *Nannochloropsis* and *Dunaliella* are strains which are most commonly used with low production price and these microalgae are used in the food industry. The selection of the strains depend on the wall strength structure [134]; likewise lipids content play an important role. The highest yield achieved so far is 82.4 wt.% from a strain containing initially 60 wt.% of lipids [147]. New pre-treatment has been carried out using microwave or two sequential steps in order to extract chemicals at low temperatures and process the biomass more readily. The kinetic studies suggest that the reaction time should be less than 20 minutes in low temperatures (200-330 °C) [136]. Faeth et al. [152] developed a novel method to rapidly process microalgae doing fast liquefaction in less than five minutes at high temperature reaching 600 °C, although important energy is required to heat the reactor in a short time; this gave a bio-crude oil of 66 wt.%. In general a high biomass loading of more than 15 wt.% is recommended to enhance the bio-crude oil yield [131]. In most of the cases, the nitrogen content in the bio-crude oil was 2 to 8 wt.%. In comparison the proportion of total nitrogen in the aqueous phase was approximately 60-80 wt.%. Elliott et al. [153]

were the first researchers in developing a semi continuous reactor using two steps. During the first step, the biomass is hydrolysed under subcritical water and subsequently the oil is upgraded as fuel under pyrolysis with the hydrodeoxygenation process. The system could process 35 wt.% of biomass. This represented one of the ultimate steps before the scale up of the hydrothermal liquefaction and a potential commercialisation.

2.2.4 The addition of organic and inorganic salts

As mentioned in the previous section, some hydrothermal liquefaction has been carried out with the addition of organic acids (formic acid, acetic acid), and other salts (sodium carbonate). It should be pointed out that sodium carbonate and formic acid are referred to as catalysts; however these compounds decompose during the reaction into hydrogen or carbon dioxide. Alkali and acids, such as sodium hydroxide and sulphuric acid, for example, are homogeneous catalysts, and the initial and the final concentration should be identical. Salts are added in order to improve the quality of the bio-crude oil.

During the early stage of the research on hydrothermal liquefaction, sodium carbonate was commonly added with 5 wt.% loading [48, 119, 123]. At low temperatures from 250 to 300 °C, sodium carbonate enhances the formation of oil and the deoxygenation, for an experiment time of one hour [48]. Yang et al. [123] suggested that this salt had a greater effect at 300 °C with a reaction time of 30 minutes compared to the experiment at 340 °C for one hour. The same observation was found with the deoxygenation. Ross et al. [129] illustrated that sodium carbonate compared to other salts was more efficient for the processing of *Chlorella* and *Spirulina* for the production and also for the deoxygenation of oil, while clear behaviour of the removal of nitrogen content was found in this study. Biller et al. [112] reported that at 350 °C the deoxygenation and denitrogenation was favoured with *Chlorella* and *Spirulina* and for soya protein. This alkali salt also reduces the formation of residues during the processing of carbohydrates. The formation of amides was not observed under this solution. Jena et al. [154] obtained a bio-crude yield of 51.6 wt.% during the processing of *Spirulina* containing a low amount of nitrogen (5.4 wt.%). Sodium carbonate helps to promote deoxygenation and the formation of bio-crude at low temperature however the side effect was that with high

amount of lipids, soap was formed. The impact is not fully understood during hydrothermal liquefaction.

The purpose of formic acid is to produce *in-situ* hydrogen. This acid has been demonstrated to have a rapid decomposition (less than two minutes) under subcritical water either via decarboxylation to produce carbon dioxide and hydrogen or decarbonylation with carbon monoxide and water. The solvent water has an influence in stabilising the transition state. Above 253 bar and relatively high concentration (0.01 mol/L), the production of hydrogen was predominant [155]. Ross et al. [129] were the first researchers to investigate the effect of formic acid on the liquefaction. It is elucidated that this organic acid improves the viscosity (flow properties) and diminish the boiling point range; in addition, gas formation is enhanced. Nevertheless, no effects on the nitrogen and oxygen contents were observed and lower bio-crude yield was produced [129]. Biller et al. [112] found that formic acid enhanced the formation of the gaseous and residue phases. Duan et al. [156] added formic acid to produce *in-situ* hydrogen during the upgrading of algal oil in supercritical water. An increase in concentration of this organic acid enhanced the formation of bio-crude oil to 70 wt% and increased gaseous yield. Furthermore, the level of coke was reduced. A mild reduction of nitrogen in the oil was observed with high concentration of formic acid.

Acetic acid was also selected by Ross et al. [129], but had minor impact during the liquefaction. Potassium hydroxide (KOH) was used by the same authors without giving significant changes compared to sodium carbonate. In another study from Anastasakis and Ross [149], the variation of different concentration of potassium hydroxide was investigated and as the concentration increased the production of bio-crude oil decreased to favour the aqueous phase.

Jena et al. [154] investigated the effect of NiO and $Ca_3(PO_4)_2$ powders on the liquefaction of *Spirulina*. These powders enhance the formation of the gaseous phase with lower bio-crude oil formation. Furthermore, the analysis of the oil indicated that nickel oxide enhanced the formation of aromatics.

The effect of alkali and organic salts needs to be investigated in more details to elucidate the effect during the hydrothermal liquefaction of microalgae. Some new acids such as oxalic acid should be tested under these conditions as interesting results were achieved with carbohydrates [157].

There has been some speculation as to whether oxalic acid could be a better hydrogen donor compared to formic acid. Indeed, particularly at temperatures below 300 °C, oxalic acid is less stable compared to formic and acetic acids. Furthermore, low acidic pH enhances the rate of decarboxylation of oxalic acid. This organic acid was found to decompose into formic acid as in Reaction 2-7:

$$H_2C_2O_4 \rightarrow H_2CO_2 + CO_2$$ Reaction 2-7 [158]

Oxalic acid is identified as an intermediate during the decomposition of glucose to formic acid in the presence of oxygenated water (H_2O_2) at a lower temperature (150 °C) [159]. The only application for *in-situ* hydrogen from oxalic acid was carried out by Izhar [160] for the denitrogenation in pyrolysis conditions.

Table 2-4: Yields of different strains of microalgae

Authors	Algae used	Homogeneous or hydrogen donors	Oil conversion
Dote et al. [119]	*Botryococcus b.,*	Na_2CO_3 (5%)	64.0 wt.% at 300 °C, 57.0 % without catalyst
Minowa et al. [48]	*Dunaliella t.*	Na_2CO_3	37.0 wt.%
Yang et al. [123]	*Microcystis v.*	Na_2CO_3 (5%)	33.0 wt.%
Zou et al. [124]	*Dunaliella t.*	Na_2CO_3	25.8 wt.%
Yu et al. [126]	*Chlorella py*		39.0 wt.% 280 °C (120 minutes)
Vardon et al. [130]	*Scenedesmus*		22.7 and 21.3 wt.% deffated (300 °C)
Brown et al. [127]	*Nannochloropsis sp.*		43.0 wt.% at 350 °C
Jena et al. [131]	*Spirulina*		40.0 wt.% 350 °C
Garcia Alba et al. [133]	*Desmodesmus sp*		49.7 wt.% 5 minutes at 375 °C

Authors	Algae used	Homogeneous or hydrogen donors	Oil conversion
Ross et al. [129]	*Chlorella v.*	KOH, NaOH	For KOH 9.0 wt.% *Spirulina* and 13.6 wt.% for *Chlorella*
	Spirulina	CH_3COOH	
		HCOOH	With formic acid 19.5wt.% and acetic acid 15.7
Biller et al. [112]	*Chlorella v., Nannochloropsis occulata Porphyridium c.*	Na_2CO_3	*Spirulina* 17-18.0 wt.% with catalyst (formic acid or Na_2CO_3)
	Spirulina.	HCOOH	
Valdez et al. [135]	*Nannochloropsis sp.*		46.0 wt.% 300 °C 15 minutes
Miao et al. [138]	*Chlorella so.*		31.0 wt.% two steps preatment 2steps
López Barreiro et al. [134]	*Scenedesmus o., Phaeodactylum, Nannochloropsis g., Scenedesmus a., Tetraselmis s., Chlorella v., Porphyridium p.,*		*Scenedesmus* 58.1 wt.% 375 °C *Dunaliella* 44.8 wt.% 250 °C
Chen et al. [145]	Waste water culture algae		49.0 wt.% (300 °C)

2.2.5 Hydrothermal gasification (HTG) of microalgae

Hydrothermal gasification is an interesting technique as different gas compositions can be achieved in relation to the catalysts and the temperature selected. Compared to dry gasification, lower temperatures are used from 400 to 700 °C and a pressure range between 250 to 300 bar under supercritical water.

At the first stage of the research on this topic, researchers were more interested in producing methane (CH_4). Elliot and Antal first conducted the early research in to the processing of wastes or slurries [161]. Minowa and Sawayama [162] investigated gasification at 400 °C with a high loading (15 g) of catalyst (Ni/Al_2O_3). These conditions favour the formation of methane (35 vol.%) and carbon dioxide (49 vol.%). They also suggested recycling the aqueous phase, which contains a significant ammonia content for the cultivation of *Chlorella*. The SunChem project developed by the Paul Scherrer Institute in Switzerland followed the same initiative to gasify *Spirulina* or *Phaeodactylum t.* with ruthenium and carbon or zirconia supports (Ru/C, Ru/ZrO_2) [63]. Their objectives were to design a semi continuous reactor. Ru/C with a 2.5 wt.% loading at 400 °C for five hours achieved a 100 % carbon conversion with the formation of carbon dioxide (49 vol.%) and methane (41 vol.%). Ru/ZrO_2 enhanced the formation of hydrogen to approximately 20 vol.% in one hour. The inconvenience of this process is metal leaching from the catalysts (for example nickel or copper) which could be poisonous to the development of the microalgae when the aqueous phase is recycled; also sulphur poisoning of the catalyst was an issue [63, 163]. The complete gasification involves loading the reactor with a higher proportion of catalyst compared to the feedstock which is not economically viable.

Some authors were more interested in producing hydrogen. Brown et al. [127] carried out the hydrothermal gasification and liquefaction of *Nannochloropsis* from 200 to 500 °C without a catalyst. As the temperature increased, the formation of bio-crude decreased, in contrast to the gaseous phase. 39 vol.% of hydrogen was produced at 400 °C. Chakinala et al. [164] obtained a full gas conversion or gas efficiency of *Chlorella* at 700 °C with Ru/TiO_2 with a high proportion of hydrogen. Guan et al. [165] elucidated that the reaction time favoured the formation of hydrogen and methane whereas the loading of microalgae tended to reduce the concentration of these gases. An increase in the water loading enhanced the gaseous phase carbon yield. The addition of sodium hydroxide improves the concentration of hydrogen and

reduces the formation of tars [166]. The hydrothermal gasification of seaweed gave a good yield; for example 16 g of hydrogen per kg of macroalgae was obtained by Schumacher et al. [167] despite the high ash or carbohydrate content. Cherad et al. [168] proposed a new route to gasify the aqueous phase produced via the liquefaction of microalgae into hydrogen for upgrading the bio-crude oils and increasing the quality of bio-crude.

In order to achieve full gaseous conversion, it has been found that high loading of catalysts is necessary, which makes the scale up of this process difficult and expensive.

2.3 Catalytic upgrading

A catalyst is a chemical compound which helps to reduce the activation energy during a particular reaction. During the processing of biomass, the selection of catalysts should satisfy the following criteria:

- Robustness: the catalyst should be stable to harsh conditions, for example in hydrothermal liquefaction at high temperature and pressure. It should have good mechanical resistance (a high surface area and good metal dispersion and a low leaching), and be resistant to poisoning from the heterogeneous atoms (nitrogen, sulphur) from the biomass.
- Selectivity: in relation to the desired products, the catalyst should have adequate properties (pore size, chemical functions, for instance acidic or basic, oxidant or reductant).
- Activity: heterogeneous catalyst should give consistent results after several regeneration cycles.

In the case of upgrading biomass, the catalyst should be designed to be selective for deoxygenation and denitrogenation. In other words, it should be able to yield a good hydrolysis rate of ester and carboxylic group and subsequently be able to cleave the C-O bonding in the carbohydrates and lipids and the C-N bonding for proteins [169]. Zeolites represent good candidates to convert biomass into a high energetic fuel as this type of material is widely used in industry. Their chemical properties can be tuned without difficulty.

2.3.1 Introduction to zeolites

Zeolites are composed of networks of aluminium and silica oxides forming a microporous or mesoporous complex framework. The incorporation of other elements such as phosphorus or gallium is possible. Natural zeolites, for example modernites, occur naturally during volcano eruptions. They have different usages including detergents, ion exchange for water purification, catalysts for petrochemical industry [170].

The coordination of the bonding of silica oxide to alumina induces the presence of two different acidic sites, the Brønsted acid site is created by the Si-(OH)-Al bridge, and the Lewis acid site by the aluminium atom (weak acidic site) [171]. Zeolite X and Y belong to the faujasite family; ZSM-5 and silicatite are MFI

(Mordenite Framework Inverted). Synthetic alumina silicate zeolites are classified in relation to the pore size and also depending of the ratio on silica over alumina Si/Al:

- Low Si/Al ratio up to 1.5: zeolite A and X
- Between to 2 to 5: modernite, Y, omega, clinoptilolite
- High Si/Al from 10 to 100: HZSM-5, beta β, natural erionite, MCM-41

The zeolites A and X contain the largest amount of alumina. These classes of zeolites are used as detergents especially in laundry powder to remove stains from clothes. The high silica zeolites or molecular sieves are used to absorb organic molecules [172].

Aluminophosphate zeolites are widely used as molecular sieves. These zeolites are divided into two classes: the first group contains VPI-5 which has large pore sizes and an 18 membered ring structure. The other class includes the silico aluminophosphate commonly names SAPO, for example SAPO-34 which has an average pore size of 0.4 nm. These catalysts are reputed to have good hydrothermal stability [173-175].

Fluid catalytic cracking (FCC) was developed by the petroleum industry to crack down and isomerise heavy crude oil to smaller light fuel fractions. Zeolites, including Y, β, USI or HZSM-5, are commonly used because of their high Brønsted acidity. For instance, zeolite Y has a narrow pore size of 0.8 nm which allows only long straight alkane chains to diffuse inside the pore whereas branched alkanes could not go through the pore. The inconvenience of FCC catalysts is the significant production of coke and for example HZSM-5 can be deactivated rapidly. This is the reason why this process is carried out with a fluidised bed reactor, where zeolites can be constantly regenerated in a combustion chamber [176].

Because of these interesting properties, the investigation of processing biomass with selected micro and meso porous zeolites has been significant, especially for experiments carried out under pyrolysis conditions.

Zeolites can also be used as an alternative compared to the homogeneous catalyst during the transesterification process, for example with ETS-10 (a titanosilicate catalyst type) a 80 % conversion of FAME was obtained with a mild temperature 60 °C [177]. Side reactions such as saponification are likely to take place with mesoporous catalysts. The addition of different salts change the propriety of the

catalyst, for example lanthanum enhanced the Brønsted acidity of beta zeolite and improve the conversion of FAME [178]. The research community has selected zeolites for the production of green diesel from triglycerides by cracking. Idem et al. [179] processed canola oil with HZSM-5 producing principally aromatics and gaseous compounds. MCM-41 doped with a mixture of cobalt and molybdenum (Co/Mo) showed good conversion of vegetable oils into hydrocarbons [180]. Twaiq et al. [181] converted palm oil in a continuous reactor with different zeolite (HZSM-5, USY and β). USY and β was more selective for producing diesel range fuel, while with HZSM-5 more gasoline-like fuel was obtained. Nevertheless, the yield of aromatics could be reduced by doping with potassium.

Hydrodeoxygenation has been widely studied; this technique consists of producing hydrocarbons by hydrogenation at high temperature. Several companies such as Neste oil develop this process at large scale to produce green diesel. An added advantage is that unsaturation of the vegetable oil could be reduced to improve the fuel quality. HZSM-5 and other zeolites were selected for this reaction, combined with doped metals which were oxygen labile such as molybdenum, cobalt, cerium and activated towards carbonate functional groups. Furthermore, these metals are more efficient if they were combined with noble metals such as palladium, platinum or rhodium, which has the function to hydrogenise biomass [182, 183].

The hydrolysis of carbohydrates including starch and cellulose is possible but is a complex process using zeolites. HZSM-5 and USY with ruthenium converts cellulose into glucose and subsequently short alcohols at 160 °C in the presence of hydrogen [184]. French et al. [81] pyrolysed aspen wood selecting HZSM-5 doped with different metals such as bismuth, cerium, cobalt, iron, copper, nickel and gallium (Bi, Ce, Co, Fe, Cu, Ni, Ga) at 500 °C. The incorporation of these metals helps to reduce the oxygen content of the oil. Nickel enhances the formation of hydrocarbons, although when good activity is obtained the level of coke produced was significant.

Milne et al. [85] were the first researchers to process an unknown oil from algae with HZSM-5 achieving a good deoxygenation. Peng et al. [185] converted, in high hydrogen pressure (40 bar), an algal oil in dodecane as solvent selecting HZSM-5 and Hβ doped with nanoclusters of nickel. As the ratio of Si/Al increased from 45 to 200, the selectivity for alkanes reached up to 93 %. With low Si/Al ratio, cracking to light fraction was enhanced. The full hydrogenation of the double bonds was

achieved. Du et al. [186] compared the pyrolysis of *Chlorella* and three different model compounds (egg protein, canola oil and cellulose) with HZSM-5. Cellulose produced the highest amount of aromatic compounds such as naphthalene. *Chlorella* pyrolysis yielded 16 wt.% of aromatics (toluene, xylene and furfural) also 3-methyl-indole. The proteins degrade into phenol and indole which the canola oil yielded benzene, toluene and xylene Thangalazhy Gopakumar et al. [187] carried out the pyrolysis of *Chlorella* with HZSM-5 obtaining a bio-oil yield of 52.4 wt.%.

The inconvenience of pyrolysis is that a large amount of coke is produced with HZSM-5 and products are mainly aromatics and gases. An oil produced with the main boiling range in the kerosene would be more favourable. Doped metals-HZSM-5 such as copper, nickel or molybdenum enhances and changes the chemical properties of this zeolite and by producing different products. It would be interesting to test some of them and to investigate their activities and hydrothermal stabilities.

2.3.2 Hydrothermal liquefaction using HZSM-5 or other zeolites

Ravenelle et al. [188] assessed the stability of two zeolites, Y and HZSM-5, in hot compressed water (low temperature 150-250 °C and pressure 5 bar). The authors illustrated that HZSM-5 was more robust in these conditions and that the de-alumilation was low in contrast to the modification of the silica groups. Mo et al. [189] investigated the stability of HZSM-5 in supercritical water at 500 °C. No major structure and crystallinity change was observed. Furthermore, a good conversion into hydrocarbons was achieved from palmitic acid after several regeneration cycles.

Duan et al. [190] and Yang et al. [191] investigated the activity of zeolite on the conversion of microalgae strains into a fuel. Yang et al. [191] selected Ni/REHY (the zeolite Y doped with rare earth group metal). The nickel group reduces the surface area of the catalyst as the metal blocked the pores even though a good deoxygenation was achieved at 200 °C from *Dunaliella s.*; the resulting oil had a heating content of 30.0 MJ/kg. Sinag et al. [192] observed that the processing of baby food (a mixture of carbohydrates and proteins) in the critical region with HZSM-5 yielded large amount of acetic acid and acetaldehyde in the aqueous phase.

Li et al. [189] upgraded, in supercritical water, a bio-crude produced from *Nannochloropsis* with a good conversion rate. Dodecane was successfully cracked into light compounds in sub and supercritical water by HZSM-5 [193]. Research is

still needed to be carried out to investigate the effect of HZSM-5 for the hydrothermal liquefaction of microalgae.

2.3.3 *In-situ* catalytic liquefaction of microalgae

The selection of a heterogeneous catalyst is more advantageous compared to homogeneous ones, as the catalyst can be recovered and used several times. The use of catalysts is to improve the deoxygenation and denitrogenation reaction of the bio-crude oil. The first study relating the catalytic processing of microalgae was reported by Hillen et al. [194] on *Botryococcus* oil using a CoMo catalyst at 440 °C in apolar solvent. The oil obtained was composed of 67.0 wt.% of petrol fraction. Matsui et al. [195] carried out the liquefaction of *Spirulina* under liquefaction in tetralin as a solvent at 350 °C with an iron catalyst ($Fe(CO)_5$-S). 60 wt.% of hexane soluble material was obtained. Working with water is more suitable as it was a green solvent (environmentally friendly) and highly available.

The publication of Duan and Savage (2011) was the first to mention the heterogeneous catalytic screening under subcritical water during the liquefaction of microalga *Nannochloropsis*. Catalysts such as Pd/C, Pt/C, Ru/C, Ni/SiO_2-Al_2O_3, CoMo/γ-Al_2O_3 (sulfided), and zeolite were selected for the screening in two conditions in helium and pressurised hydrogen. Most of the catalysts yielded a higher amount of bio-crude compared to the run without catalyst (obtaining 35.0 wt.%). Pd/C was the most efficient catalyst with a bio-yield of 55.0 wt.%. The lowest nitrogen content was detected with Ni/SiO_2-Al_2O_3 with 3.3 wt.%. Under hydrogen noble metals led the increase of the H/C ratio. The deoxygenation was more advanced with CoMo/γ-Al_2O_3 (sulfided) with approximately 8.5 wt.% of remaining oxygen content. In the case, the addition of hydrogen do not have a high impact on improving the propriety of the bio-crude [190].

Biller et al. [196] carried out comparable research with two microalgal strains (*Chlorella v.* and *Nannochloropsis o.*) and soya bean oils selecting a mixture of cobalt molybdenum, platinum and nickel (CoMo, Ni and Pt) supported on alumina catalysts. Lower bio-crude oil yield was achieved with the nickel catalyst as it promoted gasification. Platinum improved the bio-crude oil yield slightly to 38.9 wt.% with *Chlorella* in contrast to the run in water (35.8 wt.%). The results agreed with the trend observed by Duan and Savage regarding the deoxygenation. CoMo/γ-Al_2O_3, nickel and platinum had a mild effect on the denitrification [196]. Nevertheless, results with

these catalysts were not outstanding as the difference in product yields and properties with and without catalysts was not significant. Post catalytic hydrothermal liquefaction of microalgae has been attempted with HZSM-5 and Raney nickel in sub/supercritical ethanol. Experiments with this solvent could be carried out at lower temperatures below 300 °C, with higher bio-crude yield. For example with Raney nickel and hydrogen, 70.0 wt.% bio-crude oil yield was achieved. The low degree of denitrogenation was the drawback of this process [197].

2.3.4 Post catalytic upgrading

In an attempt to reduce the level of heteroatoms, Duan and Savage [198] proposed the upgrade of bio-crude oil from *Nannochloropsis sp.* under supercritical water conditions (Pt/C in pressurised hydrogen, reaction time two to three hours). The first results published were encouraging, producing an oil with a high energy content (43 MJ/kg), similar to a petroleum crude oil (42 MJ/kg). The nitrogen was reduced by half and the oxygen content from 6 to 4 wt.%. Hydrochloric acid and sodium hydroxide were used as an additive without influencing the composition of the bio-crude oil. In their second study, the upgrading with more catalysts such as Mo_2C, Pt/C and HZSM-5 was investigated with a longer reaction time. A high proportion of aromatics are produced above 430 °C especially with HZSM-5 and Pt/C with a long reaction time (four to six hours). The optimum parameter for the denitrogenation was at 530 °C using Pt/C for six hours, whereas complete deoxygenation was achieved using Mo_2C at 530 °C for two hours. The same catalyst promoted the formation of saturated hydrocarbons (42 %) presumably from fatty acids, at a lower temperature of 420 °C and six hours [199]. 20 wt.% of Pd/C loading was the best catalyst to obtain the maximum bio-crude oil. An 80 wt.% catalyst loading with a four hour reaction time yielded less bio-crude. The principal compounds detected were hydrocarbons from octane to dotriacontane with less than 2.0 wt.% of nitrogen content [200].

Duan et al. [156] upgraded for one hour at 400 °C a bio-crude oil with Pt/γ-Al_2O_3 produced from a different strain *Chlorella p.* The variation of catalyst loading enhanced the formation of gas by 15 wt.% with a 30 wt.% loading and subsequently reduced the bio-crude oil yield. In addition, the formation of coke was non-negligible at high temperatures. When the catalyst was recycled, after the third cycle the production of bio-crude oil increased while the nitrogen content decreased to 2.4 wt.% which was the lowest amount of this study. The change of water density (the increase

of water:oil) did not affect the amount of nitrogen in the oil. A complete catalytic screening was carried out by Bai et al. [147] who selected 5% Pt/C, 5% Pd/C, 5% Ru/C, 5% Pt/C (sulfided), Mo_2C, MoS_2, alumina, CoMo/γ-Al_2O_3 (sulfided), Ni/SiO_2–Al_2O_3, HZSM-5 processing of the same algae. Ru/C and Raney Nickel was more selective for the conversion of saturated hydrocarbons and aromatics from the original bio-crude oil. This explains why the combination of the two catalysts produced a non-viscous oil containing less than 2.0 wt.% of nitrogen and oxygen compared to other bio-crude oils. In addition, the heating content exceeds the petroleum value at 45.0 MJ/kg. Indeed, these catalysts have been demonstrated to deoxygenate fatty acids. The support alumina had a good deoxygenation of the oil.

Although research results carried out by Peigao Duan [156, 201] is promising, severe conditions are required within supercritical water, as well as expensive catalysts with high value metal such as ruthenium in order to obtain high quality oil. Therefore, the final cost of the algal fuel would rise, making it uncompetitive compared to fossil fuels. The non-catalytic run resulted in 40.0 wt.% of oil and during the catalyst processing approximately 77.0 wt.% was obtained. In order to produce the equivalent of one barrel of crude oil (138.8 kg), 460 kg of algae would be necessary.

2.4 Life cycle analysis

Life cycle analysis has been used to estimate potential yields of bio-crude from different technology approaches. Comparing the lipid extraction and the hydrothermal liquefaction, more biofuels were produced with the latter with 10,4000 m^3/year, compared to 91,300 m^3/year although the greenhouse gas emissions were lower with the lipid extraction. Delrue et al. [202] stated that the greenhouse emissions were dependant on the bio-crude yield. Furthermore, lipid extraction necessitated 1.8 more biomass feedstock compared to HTL which also has a surplus of energy of 9.2 MJ as no drying was required. It was calculated that when the bio-crude oil yield exceeded 40.0 wt.%, the emission of greenhouse gases would increase as the organic concentration in the water would be lessened and thus some extra energy needed to be added [203].

One of the challenges for the HTL process is the nitrogen removal, as the bio-crude oil contains at its best approximately 2-3 wt.% of nitrogen content. This is lost from the cycle, and in order to have enough nutrients some additional nitrogen

compounds should regularly be injected into the system. Denitrogenation is possible however a large amount of hydrogen is necessary. According to Franck et al. [203] compared to lipids extraction 5.2 times of ammonia and 1.5 times of phosphorus would be needed for the HTL process, which represents 3 m^3 ton of ammonia for 45.5 billion of m^3 of oil produced.

The production of fuels from microalgae via the hydrothermal liquefaction route could emit less greenhouse gases compared to the production of corn ethanol and conventional fuels such as gasoline and diesel [204]. Furthermore, the potential energy return on investment (EROI) could be 1 for the pilot scale production and approximately 3 for the full scale production which is approaching the EROI for gasoline which was 4. A sensitivity analysis for the pilot scale emphasised the supply of nutrients and fertilisers [204]. According to Liu et al. [205], the recycling of hydrothermal water could bring only 12.5 % of the necessary nutrients. The carbon dioxide supply was the other problematic factor as pointed out by Chisti et al. [55] and in order to be economically viable the production should be located near to a coal power plant. For the large scale, the bio-crude yield and the recovery of the energy could be more problematic. Fortier et al. [206] emphasised that in order to produce bio jet fuel, the production should be carried out in the facility of a waste water treatment plant, as the emission of greenhouse gases could be reduced by up to 76 % (to 35 kg CO_2/GJ) compared with the transport to the biomass to a special refinery. In general, nitrogen was found to play a major role in the production of biofuels with respect to the nutrients recycle and the emissions and the presence of nitrogen content in the bio-crude oils. Furthermore, LCA assumes that the bio-crude oil obtained has similar properties with regular fuels. At the present time, many upgrading steps are necessary to obtain ready use fuel. Therefore, in order to achieve the commercialisation of an algal fuel, many hours of research remain to be done in particular to reduce efficiently the nitrogen content in the bio-crude oil.

2.5 Conclusion

The depletion of fossil fuels and the accumulation of greenhouse gases underline the importance of finding new sustainable fuels. The production of biofuels from microalgae could offer an alternative, which reduces the amount of arable land required. Microalgae can be cultivated in non-arable land, require less water and fertilisers than crops also containing a high lipid content (superior to palm oil). Microalgae could be used as a solution for carbon dioxide mitigation and waste water recycling. The extraction of lipids involves prior drying of the biomass which consumes a large amount of energy. Hydrothermal liquefaction has been demonstrated as a better solution, as low lipid microalgae can yield large amounts of bio-crude. The other advantage is that the aqueous phase can be recycled to feed microalgae, thus potentially representing a closed loop system with no waste. The challenge is removing the nitrogen compounds still present within the bio-crude oils, and the harsh conditions required for removal. In theory the addition of 5.2 wt.% of ammonia would be required for each regeneration cycle due to the nitrogen losses within the bio-crude. This however, could be offset by the use of municipal waste water and other low cost nitrogen sources such as the flue gas from coal power plants.

Some progress has been observed in the reduction of the nitrogen within the bio-crude over the last 20 years. One solution could be to select microalgal strains grown in a stressed environment with a high lipid content and low protein content. The other option would be to upgrade, prior to liquefaction using microwave treatment, or post liquefaction under supercritical water using noble catalysts (Pd/C or Pt/C). Changing operating conditions (time, temperature, weight loading) has been extensively investigated and the best results were obtained with a reaction time below 15 minutes at a temperature between 250 to 350 °C. Even so, there are still some uncertainties concerning the fate of nitrogen and the production of nitrogen heterocycles in the bio-crude. Thus further work is needed to understand the degradation reactions of nitrogen compounds taking place during the hydrothermal liquefaction of microalgae. This would allow for the enhanced development of process strategies in achieving a better quality bio-crude oil with a lower nitrogen content.

HZSM-5 is an economical substitute to precious metal catalysts as it is widely used in the petrochemical industry. Furthermore, the upgrading of biomass (vegetable oils, lignocelluloses) under pyrolytic conditions has been studied widely using this

catalyst. Therefore, there is an interest in processing microalgae under hydrothermal liquefaction conditions in the presence of HZSM-5. Doping with different metals could change the selectivity of the catalysts and result in different bio-crude oil compositions. However, there are still some challenges on improving the stability of HZSM-5 and the reactivity of this catalyst with biomass under hydrothermal liquefaction. Finally, the hydrothermal bio-refinery of microalgae appears to be an encouraging solution to produce oil from an alternative bio-renewable source.

Chapter 3 Methodology

In this chapter, details of the procedure of the hydrothermal liquefaction are included first. Subsequently, a standard procedure describes how samples have been analysed and processed. In this chapter, general techniques which have been used throughout the project are listed; the others which are more specific to the individual chapter are described at the beginning of each chapter.

3.1 Hydrothermal processing of biomasses

3.1.1 Analysis of biomass

Both strains of microalga *Pseudochoricystis ellipsoidea* (stressed and non-stressed) were supplied by Denso Corporation. *Chlorella vulgaris* is obtained from a commercial source. Hemp and soya proteins are food supplements from the food shop Holland and Barrett; likewise for the strain of *Spirulina*. Asparagine was bought from Alfa Aesar. Sunflower, soya bean and palm oil are refined oils of food grade obtained from a local supermarket. Linseed oil was obtained from a local art supplier. Jatropha oil is unrefined. Oleic acid was purchased from Alfa, linoleic acid and linolenic acid from Sigma Aldrich.

3.1.2 Proximate analysis

Proximate analysis includes the determination of moisture, ash and volatile, they are been carried out according the European standard procedure for ash, moisture and volatile (CEN/TS 14775:2004, CEN/TS 15148:2005 and: CEN/TS 14774-1-3:2004).

Moisture is determined using a duplicate of 1 g at 105 °C for four hours. Ash of the biomass is calculated at 550 °C for three hours in the muffle furnace.

The weight % of ash was determined as follows in Equation 3-1:

$$\% \text{ ash} = \frac{m_2 - m_3}{m_2 - m_1} \times 100$$

Equation 3-1

Where m_1 is the weight of the empty crucible, m_2 is the weight with the biomass before ashing and m_3 is the mass of the crucible after the ashing. The

elemental analysis of the raw biomass is determined using the CHNS analyser and the formulas are found in section 3.1.4.3.

3.1.3 Liquefaction

Hydrothermal liquefaction experiments are carried out in a 77 ml unstirred stainless steel bomb reactor SS316 from Parr (USA) following methods described elsewhere [129, 196]. The diagram of the reactor is shown in Figure 3-1. The reactor has a bursting disk which released the pressure inside the reactor when the pressure reaches 200 bar. A graphite gasket is placed at the top of the reactor ensuring that the reactor is sealed. The temperature is measured by two thermocouples: one to control the temperature of the heater and the other the temperature inside the reactor. Only the temperature inside the reactor is recorded. (The pressure is measured thanks to the controller by a pressure sensor), a cooling part is placed before in order to protect the part from high temperature. A pressure gauge is also placed above the pressure valve. The reactor is also connected with air and nitrogen cylinders.

Experiments are prepared as illustrated in Figure 3-2 for the work-up as follows: 3 g (as received) of different biomasses (vegetable oils, vegetal proteins, amino acids, microalgae, carbohydrates (mono-sugar and poly-sugars) were introduced with or without 0.5 g of catalysts (in a stainless steel mesh basket) and diluted with 27 ml of solvent (deionised water or 1 vol.% formic acid); a mesh was introduced at the top of the reactor to avoid biomass escaping into the upper part of the reactor following which the reactor was flushed to remove air and filled with 2 bar of nitrogen and heated at temperatures from 250 to 350 °C with an average heating rate of 9 °C/min. The reaction was considered to have started when the temperature reached 249, 299 or 349 °C and lasted one hour. Finally, the reactor was allowed to cool down for about two-three hours in air. When the temperature was below 35 °C, the gas pressure and temperature were recorded and the gas was evacuated; this pressure was subtracted from the initial pressure 2 bar to calculate the wt.% gaseous mass balance as in the Equation 3-4.

After opening the reactor, the upper mesh and gaskets were washed with water and dichloromethane, subsequently the content of the reactor was poured into a 250 ml separating flask; successively 10 ml of water and 10 ml of dichloromethane were used to wash the reactor, it was repeated several times until solutions became clearer. When catalysts were used in the experiments, the aqueous phase was filtered prior to

being poured into the separating flask. In the last step, the upper part was washed with 20 ml of water and 10 ml of dichloromethane and flushed with nitrogen.

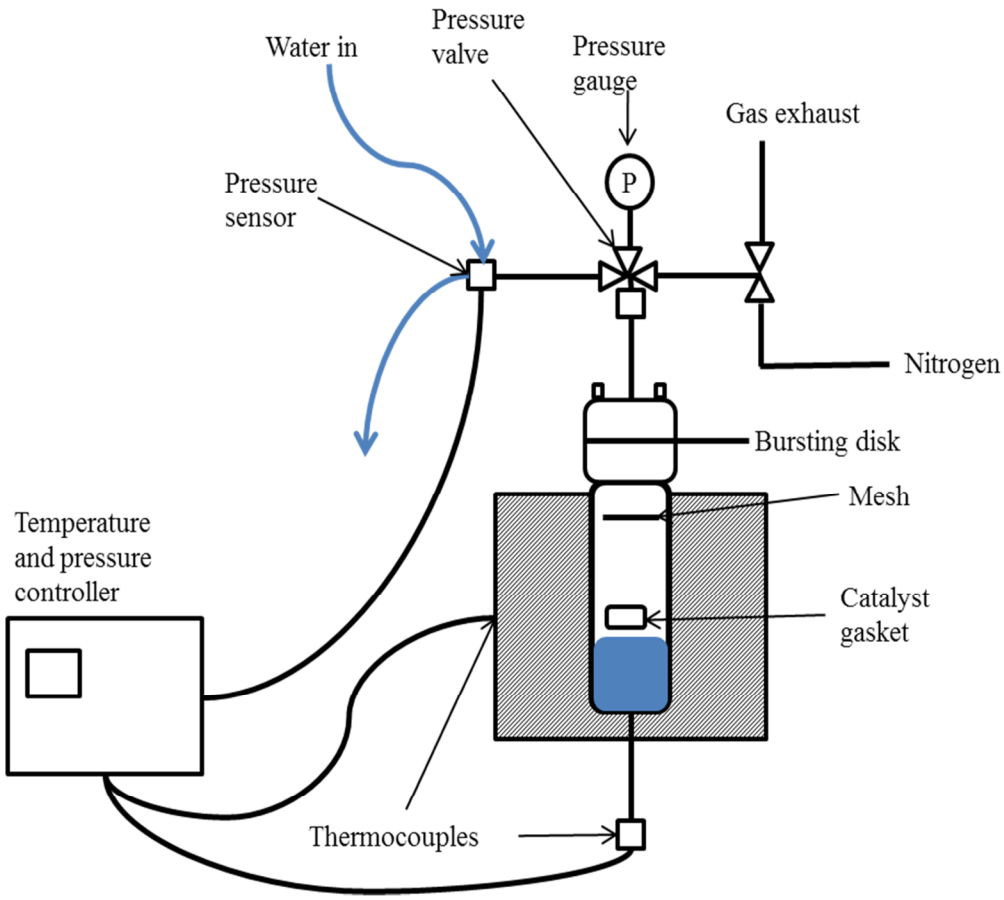

Figure 3-1: Schematics of the setting of the 77 ml Parr bomb reactor

Subsequently, the organic (the bottom part) and aqueous phase were mixed together and allowed to settle for a moment. The organic phase was separated and filtered (using a 9 cm PS (Phase Separator) filter) into a weighted beaker and left to evaporate. More dichloromethane, (approximately 10-20 ml), was added again into the aqueous phase and subsequently mixed and separated. Following the complete evaporation of dichloromethane, the resulting bio crude oil was weighed to calculate the mass yield. The aqueous phase was filtered with a Buchner filter using a 9 cm grade 5 filter paper, and the resulting solution was made up to 1 litre. Bio-crude yields (wt.%) are defined for two cases without the addition of salt as dried ash free basis in Equation 3-2 and with the addition of salt as dried ash basis Equation 3-3:

$$\% \text{ yield bio-crude (daf)} = \frac{\text{mass crude oil}}{\text{mass of biomass (daf) - \% ash \% - \% moisture}} \times 100$$

Equation 3-2

$$\% \text{ yield bio-crude (daf)} = \frac{\text{mass crude oil}}{\text{mass of biomass(daf) + mass inorganic salt}} \times 100$$

Equation 3-3

Determination of the gaseous fraction:

$$n_{\text{gas produced}} = \frac{P \times V}{R \times T}$$

Equation 3-4

P is the pressure when the reactor is cold in bar, V is the volume in m^3, R is the gas constant (8.314 J/mol.K), T is the temperature in Kelvin (T (K) = 273+ T(°C)).

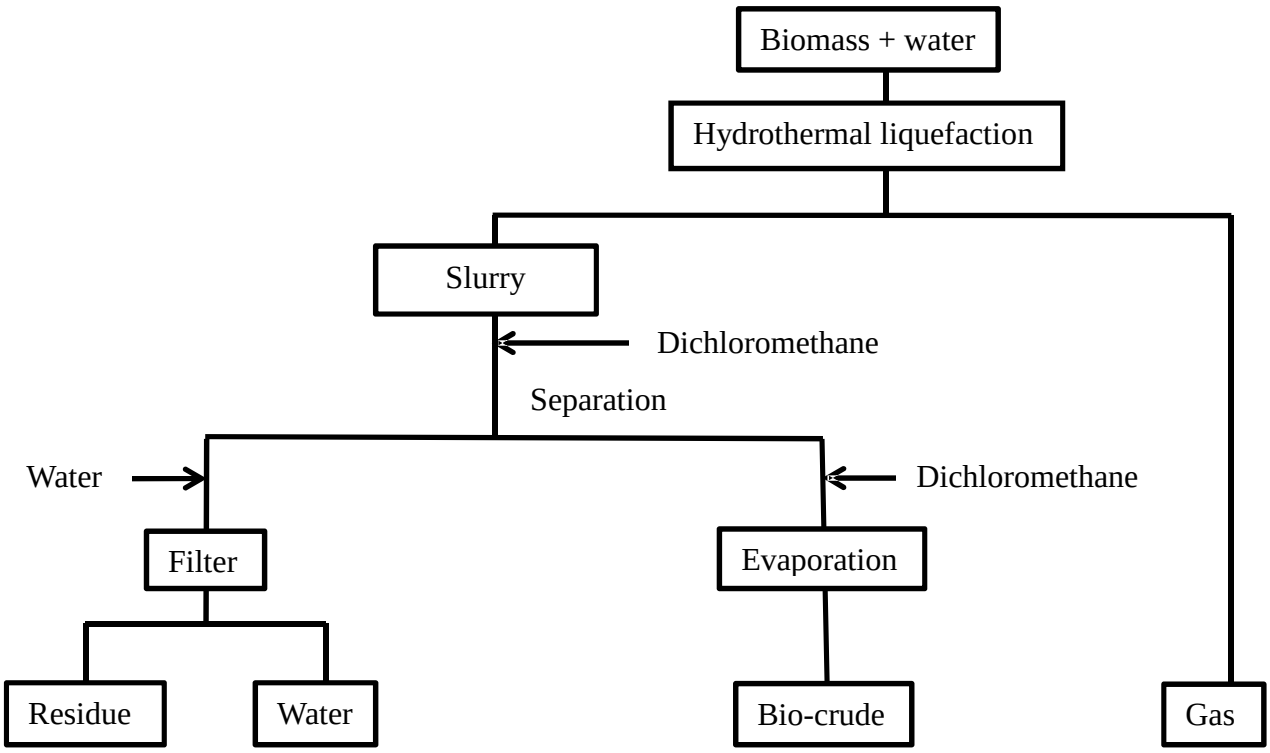

Figure 3-2: Schematic of the experimental procedure for hydrothermal liquefaction of biomass

Some experiments were carried out in duplicate to investigate the reproducibility. The coefficient of variance CV is used as the error measurement as in Equation 3-5 where σ is the standard deviation over the average $\overline{X}$ (x_2-x_1) between two repeat experiments.

$$\%CV = \frac{\sigma}{\bar{X}} \times 100$$

Equation 3-5

These are typically found to be in the range of 5-10 %, depending on the bio-crude yield.

There are several factors which could explain the variance such as the particle size of the sample, whether the sample is weighed accurately, or the homogeneity of the feed slurry before the experiment. To reduce these impacts, ground samples are used and the samples are measured accurately and subsequently mixed before carrying out the hydrothermal liquefaction. During the working up and separation process, loss of the samples could occur during transfer to different containers (from the separating flask to the beaker); during the evaporation some volatile compounds could also be evaporated with the dichloromethane. During the washing of the reactor, some samples could be difficult to remove or stuck on the wall of the reactor. Some water could be present in the bio-crude especially when high lipids content was used.

3.1.4 Analysis of liquefaction products (bio-crude oil)

Bio-crude oil is analysed using different techniques: gas chromatography mass spectrometry (GC-MS) for the identification of the molecules, elemental analysis for the determination of per cent carbon, hydrogen nitrogen and sulphur (CHNS), and gel permeation chromatography (GPC) for determining the size of the compounds. The diagram in Figure 3-3 illustrates the different techniques used to analyse the bio-crude. The GPC is performed under the supervision of a technician.

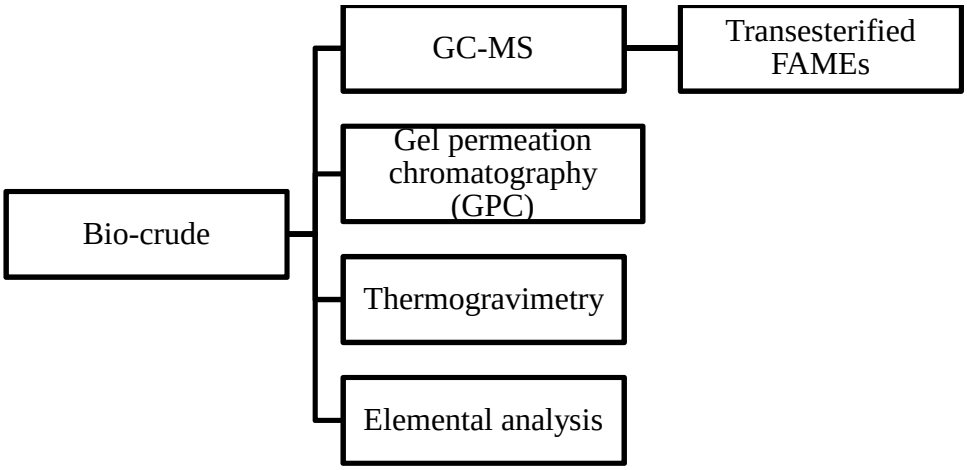

Figure 3-3: Schematics of the different techniques used to analyse the bio-crude

3.1.4.1 Gas Chromatography/Mass Spectroscopy (GC-MS)

3.1.4.1.1 Theory

Chromatography is a method which allows molecules to be separated from a complex mixture. This mixture is dissolved into a solvent or gas called the mobile phase. It subsequently passes or elutes through a column containing stationary phase and depending on the interaction between them molecules will be retained as a function of their physical (molecular weight) and chemical interaction (polarity). When this molecule reaches the detector, retention times can be measured. There are various sorts of chromatography involving different media: gas chromatography (GC), liquid chromatography with high pressure liquid chromatography (HPLC) or ion chromatography (IC) [207].

Gas chromatography, detailed in this section, allows volatile molecules to be separated, using a gas as a mobile phase. Organic molecules require heating in order to elute through the column, therefore, this is the reason why the compounds need to be stable at high temperatures. Once injected, the sample enters a heated injection part containing a liner retain any particulate and subsequently into a column. There are two classes of column:

- Packed columns are generally short (approximately 2-3 m) and filled with stationary phases such as silica or molecular sieves. They are usually used for gas analysis.
- Capillary columns are more common for the analysis of complex mixtures. The column consists of a long capillary to 60 meters in length. There are different type of stationary phases including WCOT (Wall Coated Open Tubular) where the stationary phase is a liquid; the SCOT (Support Coated Open Tubular) where the stationary phase is deposited on an inert support and the PLOT (Porous Layer Open Turbular) with a porous stationary phase [207].

The composition of the stationary phase depends on the nature of the analysed product. Polysiloxanes are used for separating apolar molecules. They consist of silicone chains where a carbon R group is added. The nature of the added R group affects the polarity of the column. They are suitable for hydrocarbons, aromatics, PCB etc. It was for this reason why it was the appropriate column for separating heterocyclic, fatty acids and some apolar molecules [207].

The column use in this study is the RTx 1701 which is semi polar with the following composition 14 % cyanopropyl-phenyl 86 % dimethyl polysiloxane. It is used to separate polar from apolar molecules. Therefore, it is suitable for a mixture of small hydrocarbons with some polar molecules such as alcohols aromatic heterocyclic.

Detectors are used to monitor and quantify components. They should be sensitive, give reproducible results and be robust. The most widespread detector for GC includes TCD (thermal conductivity detector) for gas analysis, FID (flame ionisation detector) for hydrocarbons and MS (mass spectrometer) for higher molecules [208].

Mass spectrometry is a common method to determine the molecular weight and therefore provide molecular information allowing compounds to be identified. In order to be analysed, the analyte compound is fragmented and bombarded by a high energy electron beam (19 eV). The collision induces the formation of charged specie M^+; as it is not stable the excited molecule fragment into smaller ions of different m/z ratios. The charged fragment ions are separated in a mass analyser and attracted into the detector. The detector plots the abundance of ions versus their mass/charged ratio [208]. Figure 3-4 includes the general schematic of the gas chromatography mass spectrometer [208].

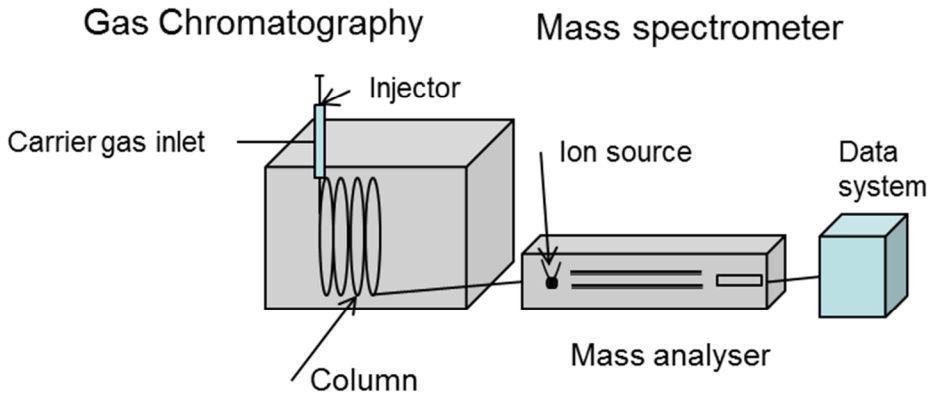

Figure 3-4: Schematics of the gas chromatography mass spectrometer drawn in power point

3.1.4.1.2 Preparation

About 10 vol.% of concentrated sample was dissolved into dichloromethane and was analysed into Agilent 5975B inert MSD GC-MS using the following program: 40 °C, hold time two minutes, ramped to 280 °C at 60 °C/min, hold time 10

minutes. The column head pressure was 30 psi at 40 °C, using the RTx 1701 60 m capillary column, 0.25 id, 0.25 µm film thickness with a split ratio 1:10.

3.1.4.2 Gel permeation chromatography (GPC)

3.1.4.2.1 Theory

High pressure liquid chromatography (HPLC) uses a liquid as a mobile phase. This technique is more suitable for separating non-volatile, highly polar molecules, and high molecular weight molecules. This technique is non-destructive thus it is possible to purify the solution. The mobile phase is delivered into a column containing a stationary phase thanks to a high pressure pump [207].

The choice of the eluent is crucial to achieve a good separation. It should solubilise the sample. The solvent used needs to have a low viscosity and must be compatible with the detector (if the detector is UV, the eluent needs to have a low absorbance in this region) [207].

The pump is one of the most important parts of HPLC as it injects the eluent into the column. Certain pumps can reach the pressure of 42 bar. They also regulate the flow rate. The injector allows the mixing of the sample and the mobile phase. It can be injected using a syringe or a loop injector. The injecting time should be short in order not to fluctuate the flow rate. The sample is loaded inside a loop with a syringe in the load mode; subsequently, for introducing it inside the column the valve is turned to inject. Compared to the GC, HPLC's columns are short (5-30 cm) with an internal diameter of 3-10 mm. The packing of the reverse phase is made of silica bound to functional groups with a wide range of polarity (octadecyl C_{18} for non-polar column and nitrile group for polar column). The column for normal phase chromatography are polar, a guard column is placed prior to this [207].

The type of separation used during this project is by gel permeation chromatography (GPC) and also called size exclusion chromatography (SEC). It separates molecules according to their size; they pass inside a porous stationary phase. Large molecules have short retention times compared to low molecular weight. It is commonly used for determining the size of the chain of proteins or polymers. Figure 3-5 illustrates a simple diagram of the size exclusion chromatography (GPC) [209].

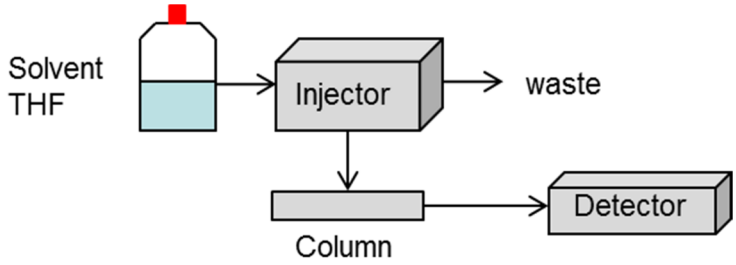

Figure 3-5: Schematic of the size exclusion chromatography

The average molecular weight Mn can be calculated using Equation 3-6 [208]:

$$M_n = \frac{W}{\sum N_i} = \frac{\sum (M_i N_i)}{\sum N_i}$$

Equation 3-6

w is the total weight of the polymer over the sum of all the molecules in the solution N_i.The weight average of the Molecular weight M_w was calculated as follows in Equation [209]:

$$M_w = \frac{\sum (M_i w_i)}{w}$$

Equation 3-7

M_i is the molecular weight of the polymer at i time, w_i is the weight at i time. The most common detector used is UV/visible, compared to fluorimetric detector which is more sensible for polycyclic aromatic hydrocarbons. SEC is commonly linked to a differential refractometor. This technique obeys the Fresnel law where the light is deviated between two hollow phases [209].

3.1.4.2.2 Preparation

For the GPC, about 50-70 mg of sample was dissolved into 1 ml of stabilised tetrahydofuran (THF) and analysed using a Perkin Elmer series 200 HPLC instrument fitted with a refractive index detector. The column used was a Varian PGEl 30 cm length with a diameter of 7.5 mm and a particle size of 100 Å, the flow rate of mobile phase was 1 ml/min in stabilised tetrahydrofuran (THF). The instrument was calibrated using different molecular weight polystyrene polymer standards (poly labs). The per cent fraction of different weight was determined by the integration of curve by the software Origin 8 at different molecular size ranges, the first fraction was integrated between 8.5 to 11 minutes (0 to 200 g/mol), the second fraction from 8 to

8.5 minutes (200 to 600 g/mol), third fraction from 7.5 to 8 minutes (600 to 1000 g/mol) and the last fraction 6 to 7.5 minutes (superior to 1000 g/mol).

3.1.4.3 Elemental analysis

Figure 3-6 shows the diagram of the elemental analyser. The sample is enclosed into a tin cap and introduced into the auto sampler. The capsule is subsequently transferred into a quartz tube where combustion takes place at 800 °C. The gas evolved pass through a catalyst bed made of copper which reduces NO_x to N_2. Water is collected in a trap containing magnesium perchlorate to measure per cent hydrogen. Sulphur gases are reduced using a vanadium catalyst. Gases are quantified and separated by passing the final gaseous products through a column and detected with a TCD detector [210].

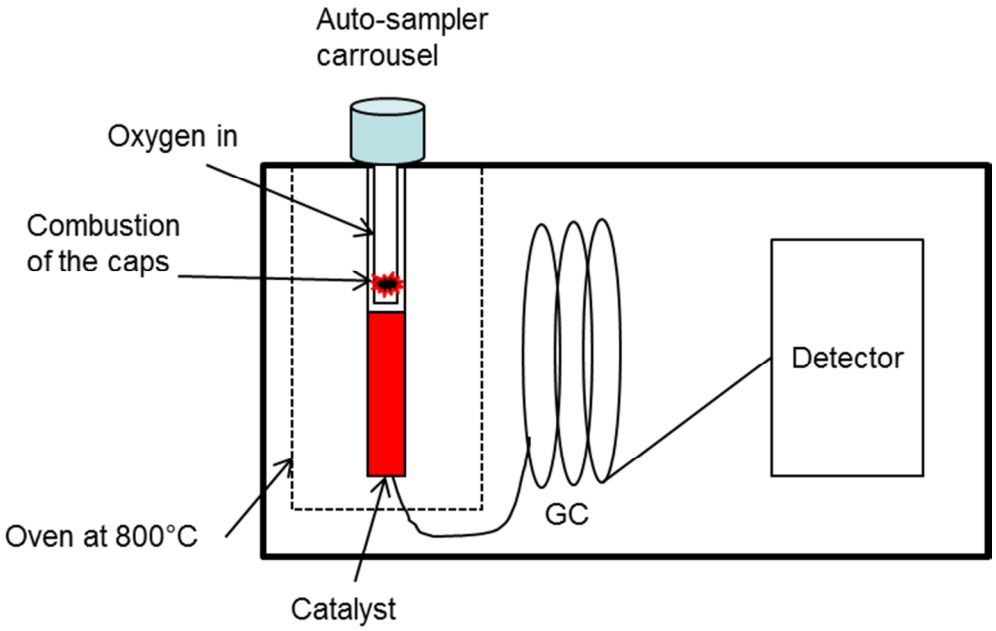

Figure 3-6: Schematics of the CHNS elemental analysis analyser.

3.1.4.3.1 Preparation

Elemental composition of raw biomass was measured using the CHNS analyser CE instrument Flash EA 1112r. 2-3 mg of sample was weighed accurately into tin caps with about 5 mg of vanadium pentoxide added and subsequently the caps were crushed. A set of four chemical standards were used to calibrate the instrument (for example 2,5-di(5-tert-butylbenzoxazol-2-Yl)-thiophene (BBOT), atropine, cysteine and methionine). Some reference materials are incorporated every 10-15 caps to check the reliability of the results. The type of reference materials depends on the

sort of biomass analysed for example when raw microalgae was measured oat meal and olive stone were selected whereas when the bio-crude and residue were used the reference materials were a lubricants and coal sample.

For the elemental analysis, CHNS of the bio-crude was determined using the CE instruments Flash EA 1112 series elemental analyser. Prior to analysis, samples were filtered with a 1-PS (9 cm) grade to remove any moisture and remaining residue. The viscous bio-crude was dissolved into 10 vol.% methanol/dichloromethane with a ratio of 1:4 and about 20 μl was injected into smooth walled tin capsules and allowed to evaporate. In the case of less viscous samples such as processed vegetable oils, a different preparation was carried out as follows: approximately 1.5 mg of oil was injected into a smooth wall tin capsule, 5 mg of chromosorb was added and capsules were crushed. Per cent oxygen was calculated by the difference from the carbon, hydrogen, nitrogen and sulphur.

The percentage of each element (wt.% C (carbon), wt.% H (hydrogen), wt.% N (nitrogen) wt.% S (sulphur)) in weight % is determined as the free moisture basis as follows in Equation 3-8 and the formula for calculating oxygen content as free dry basis in Equation 3-9:

$$\% \text{ Element(dry basis db)} = 100 \text{ x } \frac{\% \text{ element (CHNS)}}{100 - \% \text{ moisture}}$$

Equation 3-8

$$\% O_{db} = 100 - (\%C_{db} - \%N_{db} - \%S_{db} - \%H_{db})$$

Equation 3-9

HHV (higher heating value) energy content in MJ/kg is determined using the Dulong formula [211] in Equation 3-10:

$$HHV = 0.338 \text{ x } C + 1.428 \text{ x } \left(H - \frac{O}{8}\right) + 0.095 \text{ x } S$$

Equation 3-10

H/C and O/C is calculated in the Equation 3-11 and Equation 3-12 represents the energy recovery. Where the term in the equation implied $HHV_{bio\text{-}crude}$ $HHV_{raw\ sample}$ is the energy value determined by the Dulong formula above for the bio-crude and the raw sample respectively. wt.% H, C contents are determined by the CHNS analyser, wt.% O is determined by difference of CHN, M_{carbon} is the molar mass of carbon (12

g/mol), M_{oxygen} is the molar mass of oxygen (16 g/mol). $m_{bio\text{-}crude}$ and $m_{raw\ sample}$ is the dried mass of the bio-crude and the raw sample.

$$\frac{H}{C} = \frac{\%\ H}{\%\ C\ /M_{carbon}} \qquad \frac{O}{C} = \frac{\%\ O\ /M_{oxygen}}{\%\ C\ /M_{carbon}}$$

Equation 3-11

$$\%\ \text{Energy recovery} = \frac{HHV_{bio\text{-}crude}\ x\ m_{bio\text{-}crude}}{HHV_{raw\ sample}\ x\ m_{raw\ sample}}\ x\ 100$$

Equation 3-12

3.1.4.4 Thermogravimetry (TGA)

3.1.4.4.1 Principal

This method determines the weight change when a sample is heated between a temperature range in different environment (in nitrogen or in air). It is possible to observe a physical and chemical change from the sample. There are different ways to perform thermogravimetric analysis:

The differential thermal analysis (DTA) consisted of measuring the difference between the thermal behaviour of an inert reference material (alumina) and 10 mg of sample. The sample is heated by a furnace in which nitrogen or air is introduced. The difference measured by a thermocouple is plotted in relation to the temperature inside the cell. The sample is heated inside a fragile microbalance. The sample could be heated using an isothermal mode or using a defined heating rate. The constant change of weight is plotted as a function of temperature. When the sample is heating under nitrogen, pyrolysis occurs whereas with oxygen or air the sample is combusted [208].

Differential thermogravimetric analysis (DTG) is the same technique as previously described except that the graph is the derivative of the weight loss over the time $\Delta w/\Delta t$ against the temperature. Using inert gases such as nitrogen, it is possible to observe the volatile release profile [212].

3.1.4.5 Preparation

Less than 10 mg of sample was added in a pre-tared platinum pan; thermogravimetry was analysed with the TGA Q5000 analyser as follows: as a drying

process, the furnace was heated from room temperature to 105 °C at 10 °C/min and subsequently at 20 °C/min until 900 °C with nitrogen (flow rate of 50 ml/min): 900 °C was held for 15 minutes when the gas was switched to 20 % oxygen to combust the remaining char. Boiling point distribution or simulated distillation was carried out in nitrogen for the analysis of the processed lipids and detailed in **Chapter 5**.

3.1.5 Analysis of the aqueous phases

In this section, methods and instruments (total organic carbon, ion exchange chromatography, pH) used to analyse the aqueous phase are developed as shown in the Figure 3-7. The sample are filtered and diluted to a suitable concentration for ion exchange chromatograph and total nitrogen. The TOC, IC was carried out under supervision in a service laboratory. The ICP was carried out in different departments.

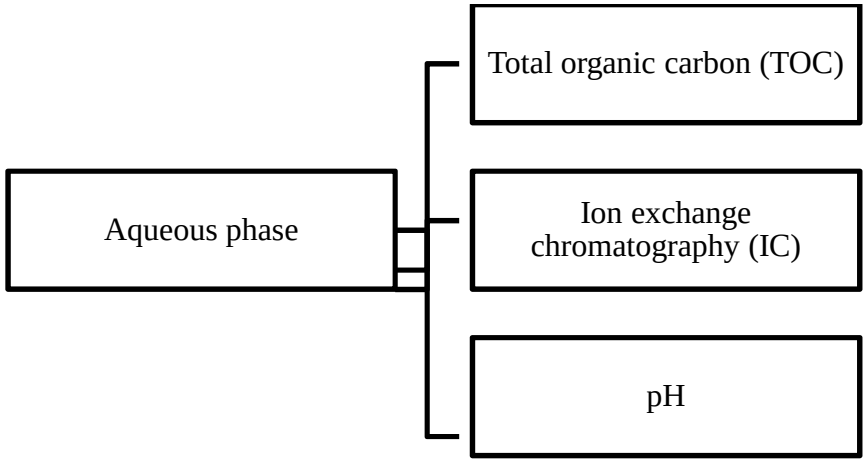

Figure 3-7: Schematics of the different techniques used to analyse the bio-crude

3.1.5.1 Total organic carbon

3.1.5.1.1 Principal

In aqueous solutions, there are two forms of carbon compounds: the inorganic carbon which is the carbon dioxide dissolved into the water and the organic carbon (organic molecules: alcohols, carboxylic acids…). Therefore the concentration of TOC (in ppm) is determined as in Equation 3-13:

$$[TOC] = [TC] + [IC]$$

Equation 3-13

The TOC and the inorganic carbon (IC) are generally measured and thus the organic carbon (TC) is calculated by subtraction. The NPOC or Non-Purgeable

Organic Carbon is a technique where only the TC is measured; the inorganic carbon is discarded by purging and acidifying the sample with a 2 M hydrochloric acid (HCl) solution. The total carbon is determined by oxidising the carbon into carbon dioxide (CO_2). There are various ways to achieve the oxidation:

- Combustion: the sample is heated under an excess of oxygen.
- Photooxydation: the UV break down the organic carbon.
- Catalytic oxidation: the carbon is oxidised by the help of catalysts (platinum or chromium oxide) [207].

3.1.5.1.2 Preparation

Once filtered, aqueous samples were analysed using several techniques including total organic carbon analyser (TOC) and ion chromatography (IC). Samples were diluted by 37. The analysis was performed using HACH TOC IL 550 analyser. In this project, only the total organic concentration was determined using the NPOC method where inorganic carbon was initially removed by automatically adding a concentrated acidic solution to remove any inorganic carbon.

3.1.5.2 Ion exchange Chromatography

3.1.5.2.1 Theory

The principal of ion chromatography is relatively similar to HPLC, instead of the separation by polarity the column separates the species in relation to the ionic interaction of chemical species with the column. Columns are composed in general of ionic long chain molecular weight resins with sulphate groups for example. The exchange in the cation column happens as follow where M^{x+} is the metal salt analysed and $xRSO_3^-H^+$ the mobile phase in (RQ-5) [207]:

$$xRSO_3^-H^+ + M^{x+} \rightarrow (RSO_3^-)_xM^{x+} + xH^+ \quad \text{(Reaction 3-1)}$$

The retention of the species depends on their size and their ionic strength with the column for instance potassium would have a longer retention time than sodium or lithium [207].

3.1.5.2.2 Preparation

Anions and cations were analysed by ionic chromatography from Dionex using a different column for cationic DX100 with IonPacCS12A column, methyl sulfonic

acid (0.2 M) mobile phase and anionic column using the column AS14A ionPac and the eluent Na_2CO_3/$NaHCO_3$ 8 mM/1 mM) and a flow rate of 1 ml/min. The main anions observed were acetate chloride, bromide, sulphate and phosphate and the main cations were sodium ammonium, potassium and calcium ions.

3.1.5.3 Other techniques

The pH was measured by a HACH pH meter (HQ 40d) and calibrating with three sets of standard with a pH of 4,7 and 10.

3.1.6 Analysis of solid residue

Solid residues were obtained from the filtration of the liquid and organic phase. In this study, elemental analysis was carried out in order to determine the wt.% C, wt.% H, wt.% N and wt.% S. and oxygen content by difference. Some chars were analysed by thermogravimetry as the same procedure for that of the bio-crude.

3.2 Catalyst

3.2.1 Preparation of metal doped HZSM-5

20 g of NH_4-ZSM5 was ion exchanged in one litre of a 0.05 M solution of different metal salts copper, iron, molybdenum and nickel (Cu (II), Fe (III), Mo (II), Ni (II)) under constant stirring at room temperature for 24 hours. For copper, and nickel acetate salts were used; for ammonium molybdate $(NH_4)_6Mo_7O_{24}$ $4H_2O$), subsequently zeolite was filtrated under vacuum and washed. The solid was dried in the oven at 110 °C overnight. Finally the doped zeolite was calcined in a tube furnace at 550 °C under a constant flow (50 ml/min) for five hours according to the method found in Long et al. [83].

HZSM-5 was prepared by calcination of NH_4-ZSM5 for three hours at 550 °C in a tube furnace under a constant air flow (50 ml/min). The method for the determination of silica and aluminium can be found in Chapter 4.

3.2.2 Hydrothermal stability of zeolites

0.5 g of catalysts was added with 27 ml of deionised water into the Parr reactor and heated to 350 °C for one hour. Once the reactor was cooled down to room temperature, the content was poured into a beaker and solids were recovered via vacuum filtration with a filter grade 5 (9 cm). The aqueous solution was made up to

250 ml and subsequently metals dissolved were analysed by ICP-OES and AAS to measure the % metal leachate. The catalysts were dried overnight at 105 °C.

3.2.3 Atomic absorption (AAS)

Atomic absorption spectroscopy (AAS) is a common technique used to determine metallic salts concentration in a solution. The measurement is carried out by exciting metallic ions in a flame and by measuring the absorbance under the resonance wavelength produced by a hollow cathode lamp. The sample is introduced into a nebuliser via a capillary tube to be passed into the flame as small droplets. The temperature of the flame could be tuned by the ratio of fuel/oxidant according to the element studied, for example with acetylene-air the temperature would be 2400 K (2127 °C) whereas with acetylene-nitrous oxide the temperature can reach 3400 K (3127 °C). Absorbance is determined by a detector which measured the difference between the absorbance from the flame and from the lamp. A monochromator with a narrow slot of 0.04 mm allows high resolution to be obtained [212].

Several chemical interferences might be encountered depending on the element; however, some solutions are available to reduce them:

- The formation of refractory compounds could be reduced by increasing the temperature of the flame, such as for aluminium.
- High concentration of ionisation in the flame could be suppressed by adding a saturated solution, for example 2000 ppm of potassium.
- Some elements such as zinc and sodium chloride have a close absorption wavelength of 213.9 nm. To correct this, a background correction would allow separating absorbance [208].

3.2.4 Inductively coupled plasma- optical emission spectroscopy (ICP-OES)

The inductive plasma (ICP) is a device used for determining metals inside plasma. The analysis was performed in another department in the school of geography (university of Leeds). It is composed of ionised gas forming an electrically neutral mixture. This plasma is created by three concentric silica tubes; three coils generated a high radio frequency current (40 MHz). The argon is passed into the burner chamber thanks to a quartz tube (15-30 mm). The magnetic field regulates the circulation of ions and electrons, and subsequently they collide with an argon atom. This process generates more electrons creating an avalanche effect. The sample is introduced into

the flame thanks to a nebuliser at a low flow rate. The temperature of the plasma is enough to excite most elements of the periodic table. The matrix effect is quite low. Measurements take place at the hottest point of the flame [212].

The only interference was that molybdenum and magnesium have close absorbance, an overlap is also observed for zinc and chromium.

Light is diffracted thanks to grating and was measured by a photo cathode detector. Less interference occurs because the temperature of the flame is higher 7000 K (6727 °C) [212].

The preparation of the sample for AAS and ICP is detailed in **Chapter 4**. AAS was used for the metal content from the digested zeolite samples and the ICP-OES was used to measure the leachate from the processed water during the stability tests.

3.2.5 Brunauer-Emmett-Teller (BET) Physisorption

The BET technique is the measurement of adsorption of an inert gas (nitrogen argon, carbon dioxide, etc) on a surface of a material. The diagram measured is called isotherm with the absorption (unit of volume, ml/g) in ordinate versus the P/P_0 (unit of pressure) with the equation 3-12, analysis was carried out at 77 K (-196 °C). As surfaces of catalysts or materials are irregular, the isotherm (produced by number of layers) measured will depend on the size and shape of the pores. Pores are separated, according to the IUPAC (International Union of Pure and Applied Chemistry), into three categories from 0.3 to 2 nm for the micropores, 2 nm to 50 nm for mesopores and above 50 nm for macropores [213].

The type I isotherm is more characteristic for microporous materials where monolayers are formed with chemisorption (formation of different bond between the gas and the material) for example with graphite. The type II and III isotherms are typical of macroporous solids where multilayers are produced. The type IV and V isotherms are usually observed for mesoporous materials, they have a particular behaviour, where because of the shape of the pores, condensation could occur creating a desorption loop on the isotherm called hysteresis [213]. Figure 3-8 shows the different shape of curves for the gas adsorption for different materials.

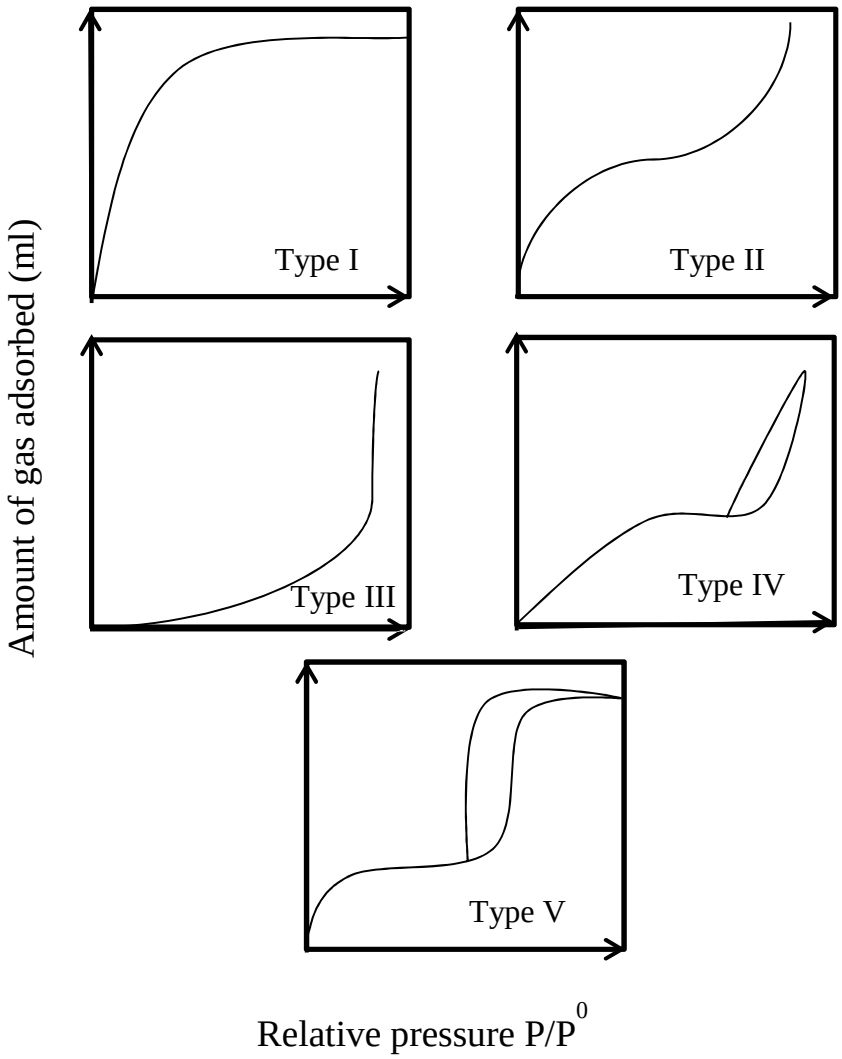

Figure 3-8: Different shape of isotherm curves of adsorption in relation to the pore size [213].

To extract the data and determine the surface area, the method of isotherms of Brumauer, Emmet and Teller should be used in Equation 3-14 [213].

$$\frac{P}{V(P_0-P)} = \frac{1}{V_m C} + \frac{C-1}{V_m C} \times \frac{P}{P_0}$$

Equation 3-14

P is the gas pressure (Pa, Pascal), V is the volume adsorb (m^3); V_m corresponds to the volume adsorb for a monolayer, C is a constant, and $P_R = P/P_0$ is the reduced pressure.

To obtain a linear plot from the previous formula it should be rearranged as in Equation 3-15 as linearized BET and the surface area is given in Equation 3-16:

$$\frac{P_R}{V(1-P_R)} = \frac{1}{V_m C} + \frac{C-1}{V_m C} \times P_R$$

Equation 3-15

$$S_{BET} = \frac{V_M}{22.414} N_a x S_m$$

Equation 3-16

V_m is the volume of the monolayer, S_m is the area occupied one molecule of nitrogen (16.2 $Å^2$ at -196 °C) , 22.4 M (L/mol) is the standard molar volume for a gas and N_a is the Avogadro's number [170].

3.2.6 X-Ray Diffraction (XRD)

The X-ray diffraction method determines the crystallinity of material by emitting through a beam some X-ray wavelength to the crystal; they are diffracted or deviated in relation to the morphology and position of the atom network in the materials. Bragg's law is used to measure the diffracted angle as in the equation in Equation 3-17 [213].

$$n \lambda = 2 d_{(hkl)} \sin 2\Theta$$

Equation 3-17

Where λ is the wavelength measured, 2θ is the incident angle, d is the distance from the different lattice and the orientation indicated by the Miller indices *hkl.* [213]

Zeolites are complex materials. They had different composition of silica and alumina therefore the interpretation of XRD spectrum is quite complex. Reference zeolites are collected on an online data base created by the Structure Commission of the International Zeolite Association (IZA-SC). Ion exchanged moities have an impact on the intensity of spectrum [170].

The intensity of the reference spectrum could be used for calculating the crystallinity of the sample as in Equation 3-18 [170]:

$$\text{Xray crystallinity} = \frac{\text{Intensity of peak sample}}{\text{Intensity of peak standard}} \text{ x } 100$$

Equation 3-18

3.2.6.1 Physical characterisation

The XRD measurements are performed with a BRUKER-binary V3 machine and used to determine the crystallinity. 0.125 g of used or fresh zeolites was mixed with 0.375 g of corundum Al_2O_3 (reference materials) and measured from 20 to 45° with an increment step of 0.01.

3.3 Conclusion

This chapter briefly described the different instruments used during this project. The resulting bio-crude was analysed by GC-MS, elemental analysis, gel permeation chromatography and the aqueous phase by total organic carbon analyser, ionic chromatography. This section also describes the preparation and the analysis of the catalyst.

Chapter 4 Hydrothermal behaviour of catalysts

Throughout this first results chapter, catalysts (ion metal doped HZSM-5) have been characterised by various analytical techniques (BET, XRD, TGA). Subsequently, these catalysts have been treated under hydrothermal conditions at 350 °C. Reactions with sunflower oil have been carried out four times with the plain HZSM-5 and with a regeneration step after each tests in order to study the activity of the catalyst. The amount of coke deposed and the surface areas of the catalysts have been measured.

4.1 Introduction

Originally developed by MOBIL (a chemical company), HZSM-5 is one of the most common zeolites. This catalyst is used widely in the petrochemical industry; due to its high acidity which allows heavy crude to break down into lighter fractions. This propriety is explained by the presence of Brønsted and Lewis acidic sites in the framework of the catalyst [170]. The other advantage is their high selectivity due to micropores and the ability to separate isomers, for example xylene [214]. The main drawbacks of this material are that under cracking of crude oils, high amounts of coke are produced at high temperature, consequently blocking the acidic sites and subsequently in presence of steam, structural changes were observed [215].

Steam conditions enhance the deoxygenation of short oxygenated molecules (e.g. alcohols, and aldehydes…), the most famous technique is called methanol to olefins (MTO). In the presence of steam, there is a change in the zeolite, whereby migration of aluminium occurs out of the framework forming AlO^{+} species which decrease of the acidity of the materials [216-218]. Nevertheless, even with a low acidity, the formation of olefins is enhanced and the formation of aromatics or cokes is reduced. Sano et al. [219] remarked that the zeolite could regain its initial acidic proprieties by processing under reflux in concentrated hydrochloric acid (HCl) at 80 °C for one hour, which allowed the reinsertion of non-framework aluminium.

Metals are incorporated into the framework in order to improve the stability of zeolite and tune the reactivity of the zeolite. Gayubo et al. [220] illustrated that doping HZSM-5 with nickel by the wet impregnation method (from 0.5 to 3 wt.% loading) enhanced the stability and the performance during the production of hydrocarbons

from bioethanol, reducing as well the formation of coke. Molybdenum was impregnated with the same method and demonstrated a stable behaviour under steam conditions. Furthermore, MoZSM-5 was shown to convert methane into aromatics in the process called “de-hydroaromatisation” due to their high acidic sites [221, 222].

Metal doped HZSM-5 can be prepared with other techniques such as ion exchange. For example, CuZSM-5 (Cu^{+}) and FeZSM-5 (Fe^{2+}) are used in car exhausts catalytic converters to convert NO_x and ammonia to nitrogen [83, 223]. The aim in this study was to investigate whether these catalysts have the same properties and stability under subcritical hydrothermal conditions.

Upgrading of different sources of biomass or compounds such as carbohydrates or woods [81], lipids [179] and microalgae [187] has been investigated with HZSM-5 under pyrolysis conditions. The problem is the energy penalty required in order to dry and subsequently processes the feedstock. Thereby, hydrothermal liquefaction is a more appropriate method to undertake. Yang et al. [189] and Duan et al. [190, 191] already used zeolite to process microalgae at 350 °C.

Ravenelle et al. [188] demonstrated the robustness of HZSM-5 in hot compressed water (from 150 to 200 °C) with a low loss of crystallinity compared to HY (the acidic Y zeolite). Recently, Mo et al. [189] investigated the stability of HZSM-5 under supercritical conditions and their reactivity with palmitic acid. A mild change in the structure regarding the silica bonding was observed at 400 °C. Otherwise, this catalyst appeared robust after several regeneration cycles with a consistent activity to produce hydrocarbons. The regeneration involved the oxidation of the catalyst to remove any coke deposits. However, no studies detail the stability of HZSM-5 at lower temperatures, as water has different properties to that 400 °C.

The purpose of this chapter is first to characterise HZSM-5 by itself and subsequently the metal doped zeolites by different methods (the ion exchange and wet impregnation); subsequently their stabilities are investigated under subcritical water (350 °C). The changes of physical or chemical properties are observed using techniques such as x-ray crystallography, surface area (BET) and by transmission electronic microscopy (TEM). Moreover, the robustness of HZSM-5 is studied by carrying out four regeneration experiments and testing with sunflower as a feedstock. After these analyses it could be deduced if subcritical water has an impact on the

structure of zeolites. Additionally it is investigated if the metals have an impact in improving the stability of HZSM5.

4.2 Methodology

4.2.1 Preparation of HZSM-5 metal doped

The preparation method for ion exchanging of HZSM-5 (molybdenum, copper, iron and chromium) is discussed in the methodology chapter.

For the preparation of the impregnated sample of molybdenum (5 wt.%), 0.9 g of ammonium molybdate tetrahydrate ($(NH_4)_6Mo_7O_{24}$ $4H_2O$) was dissolved into 1.5 ml of water (pore of the HZSM-5 is 0.15 ml/g) and poured in 10 g of HZSM-5. The slurry was crushed, mixed well and finally dried overnight (more than 12 hours) at 105 °C. The final step was the calcination of the solid at 550 °C for four hours under a constant flow of air at 50 ml/min.

The preparation of the kaolin-HZSM-5 pellet was carried out as follows: 2.1 g of kaolin clay and 1.0 g binder polyvinyl alcohol (PVA) with a molecular weight of 88,000 g/mol were mixed in 20 ml of water for 30 minutes. Subsequently, 22 ml of concentrated hydrochloric acid (HCl) (35 vol.%) was carefully added drop-wise for one hour under stirring, forming a foam. Subsequently, a suspension of 2 g of HZSM-5 in 20 ml of water was added into the slurry under constant mixing for 30 minutes. The water was evaporated on a hot plate for six hours and the residue was further dried in an oven overnight. The solid was calcined at 500 °C for one hour, once it had cooled down. The solid was washed in 45 ml of water and 0.094 g of ammonium chloride (NH_4Cl) to remove any trace of sodium. The mixture was stirred under a mild heating at 60 °C for 30 minutes. The residue was retrieved by filtration and subsequently calcined at 550 °C for three hours.

4.2.2 Characterisation of the unprocessed catalyst

Detailed procedures for the analysis of the metal content (silica, aluminium and the different metals) are incorporated in this section.

4.2.2.1 Silica and aluminium determination

In a nickel crucible, around 1.5 g of sodium hydroxide (NaOH) was fused above a burner flame. After cooling, 0.05 g of the sample were weighed and added and the crucible was placed in the flame again for approximately five minutes at the

dull of the flame. When the crucible was cold, 20 ml of water was added and placed in the water bath for 60 minutes. The content of the crucible was precisely transferred into an 800 ml beaker containing 400 ml of water and 25 ml of hydrochloric acid (HCl) (diluted 5.8 M solution) and finally made up to 1 litre in a volumetric flask.

Silica is measured using a colorimetric method. In each 100 ml volumetric flask, 10 ml of the solution previously prepared, 10 ml of the standard (30 ppm of silica) and 10 ml of water for the blank were added. Subsequently 1.5 ml of ammonium molybdate ($(NH_4)_6Mo_7O_{24}$) was poured in to each flask, the solution was mixed and allowed to rest for 10 minutes. 4 ml of a solution of tartaric acid was added followed immediately by 1 ml of a reducing agent. Measurements were carried out using a UV/visible spectrometer at 650 nm with a glass cuvette.

For aluminium determination, 0.2 g of sample was weighed accurately into a 60 ml polyethylene beaker. Subsequently, 2 ml of water was initially added to the beaker before carefully adding 10 ml of hydrofluoric acid (HF) (handled in the fume cupboard). The beaker was heated in a water bath to dryness following which, 10 ml of water was added and the contents completely transferred into a nickel crucible by washing with water to avoid any losses. The water was evaporated in a sand bath. When, the crucible was dry, 2 g of potassium hydroxide (KOH) was weighed and added to the crucible which was further heated over the flame for at least five minutes. Once, the crucible was cold, 20 ml of water was added and heated in a water bath for 30 minutes. The content was finally transferred into a 250 ml volumetric flask together with a 25 ml solution of potassium at 1000 ppm. Aluminium ion was measured by AAS using an oxidant mixture of acetylene and nitrous oxide because it forms refractory compounds. Five standard solutions were prepared from 10 ppm to 50 ppm of aluminium ion made up from a certificated 1000 ppm aluminium solution. The Equation 4-1 is used for the determination of silica by UV/visible at 650 nm:

$$\% SiO_2 = \frac{A_1 \times C \times V_1 \times V_3 \times d}{A_2 \times w \times 10^4 \times V_2}$$

Equation 4-1

Where A_1 is the absorbance of the sample; A_2 the absorbance of the standard, C the concentration of standard (ppm or mg/L); V_1 is the volume of the standard (ml); V_2 is the volume or aliquot of the original sample (ml), w is the weight and d is the

dilution factor. The Equation 4-2 is used for the determination of % of aluminium or % of metal loading:

$$\% X = \frac{c \times V \times d}{w \times 10^4}$$

Equation 4-2

4.2.2.2 Determination of the metal inside the zeolite

The metal content was determined according to the following method: 0.2 g of sample was weighed accurately into a 60 ml polyethylene (PE) beaker. Subsequently, 2 ml of water was first added to the beaker before carefully adding 10ml of hydrofluoric acid (HF). The beaker was heated to dryness in a water bath. 10 ml of concentrated hydrochloric acid (HCl) is added for 10 minutes afterwards, 30 ml of water was subsequently added carefully and the solution was transferred into a 400 ml pyrex beaker and heated on a sand heater plate until dry. 3 ml of 1:1 sulphuric acid (H_2SO_4) (diluted by 2) was added to the dried residue, beakers were covered with a clock glass and left heating until constant fumes were appearing for more than five minutes. Once cooled down 50 ml of deionised water was added and heated for 30 minutes at around 100 °C. Finally, solutions were transferred into 250 ml volumetric flasks. 10 ppm standard solution for each metals studied were made up and an auto diluter prepared successively five solutions. For the analysis of molybdenum by AAS, solution of 1000 ppm of aluminium is added as suppressant and the gas used was acetylene/NO flame for the aluminium determination.

4.2.3 Other techniques

Transmission electronic microscope (TEM) is conducted using a FEI Tecnai F20 field emission gun (FEG)-TEM operated at 200 kV and equipped with a Gatan Orius SC600A CCD camera and an Oxford Instruments 80mm X-Max SDD detector. TEM samples were prepared by dispersing powders in isopropanol, with a drop placed on a holey carbon coated copper grid (Agar Scientific).

4.2.4 Stability and regeneration of the catalyst

For the regeneration experiment, 3 g of sunflower oil, 0.5 g of catalyst in compressed pellet form and 27 ml of water were added into the reactor and heated to 350 °C for one hour. Pellets were prepared by using a press and bringing a pressure of one ton following which the HZSM5 was crushed to have a size of 100-80 mesh.

HZSM5 was recycled four times. The first experiment was performed five times, for the second cycle, three experiments were carried out, subsequently two and for the last cycle only one. After each run the reactor was cleaned according to the procedure in **Chapter 3**, the organic phase was separated from the aqueous phase; the catalyst was separated from the aqueous phase by filtration, dried and recycled. Results relating to the weight mass balance, the coke content and the BET surface area are included in this chapter.

The determination of coking during the recycling step was carried out using the Netzsch STA (simultaneous thermal analysers), according to the method found in the paper of Ortega et al. [224]. During the first step, any impurities were removed by pyrolysing approximately 20 mg of samples in a constant flow of helium at 100 ml/min with a heating rate of 10 °C/min and holding at 500 °C for 30 minutes. This step was also used to age the coke. In the second step, combustion was performed, the amount of coke was measured from 300 to 550 °C with a heating rate of 10 °C/min in a gaseous mixture of 12.5 vol.% O_2/He, and this temperature is held for 30 minutes. Combustion gases were determined using an on line FT-IR. The spectrometer was previously calibrated using $CaCO_3$. The wavelength measured of carbon dioxide (CO_2) is 2362 cm^{-1} and for carbon monoxide (CO) 2175 cm^{-1} and water (H_2O) 3400 cm^{-1}.The concentration of carbon dioxide, carbon monoxide and water are calculated in order to know the H/C of the coke. The equation deduced from the calibration for the water in Equation 4-3 where x is the mass of water and y the absorbance. The equation for carbon monoxide is in Equation 4-4 and carbon dioxide is in Equation 4-5.

$$y = 0.6363x + 0.2291$$ **Equation 4-3**

$$y = 0.2147x + 0.2703$$ **Equation 4-4**

$$y = 3.4127x + 4.4405$$ **Equation 4-5**

4.3 The stability of HZSM5 under subcritical condition

4.3.1 Unprocessed sample

HZSM-5 is produced by the calcination of NH_4-ZSM-5. Hydrofluoric acid is used to discard the silica, and sulphuric acid to obtain sulphate metal salts which are

ionised in a flame. Potassium is added in order to avoid interferences and so that aluminium does not form the refractory materials (Al_2O_3) in the AAS's flame. This technique is carried out in duplicate and using Feldspar potash as a reference material. From the Equation 4-2, the amount of aluminium calculated is 4.9 % (with a coefficient of variance of 9.6 %), while 82.2 wt.% for the silica (with 2.1 % coefficient of variance). The % difference between the experimental value and from the reference clay is 6.9 % for the silica. $nSiO_2/nAl_2O_3$ (Si/Al) ratio is calculated by the Equation 4-6 giving a value of 28.8.

$$\frac{nSiO_2}{nAl_2O_3} = \frac{n_{alumina}/M_{alumina}}{n_{silica}/M_{silica}}$$

Equation 4-6

A low ratio (<30) indicated that the zeolite is acidic with a high number of Brønsted sites, whereas higher ratios, up to 280, exhibit more amphoteric behaviour with a large proportion of silica.

The following percentage composition is found for the ion exchanged metal: FeZSM-5 0.3 wt.%, CuZSM-5 1.25 wt.%, NiZSM-5 0.12 wt.% MoZSM-5 0.14 wt.%. These values are lower than the ones obtained by the same conditions used by Long et al. [83] with 1.59, 0.85 and 4.30 wt.% for iron, nickel and copper respectively. For the impregnated molybdenum sample, 4.5 wt.% of metal was measured which is higher than the ion exchanged samples. There is an efficient impregnation with the majority of molybdenum retained in the pores.

These metals are probably present as oxide form. Thus, the method of ion exchange is the most efficient with copper. The loading of metal probably depends on the size of the element to enter through the pore. STEM images of FeZSM-5 and MoZSM-5 with EDX and Annular dark-field imaging (haadf) are included in Figure 4-1 and Figure 4-2. Figure 4-3 illustrates HZSM-5 with a zoom of 20 nm. The copper found in the EDX scan was from the grid. It was difficult to obtain clear pictures with this material because after a few minutes, the structure was starting to deteriorate. Haadf is a technique that indicates the heavy molecular weight atoms with a brighter colour.

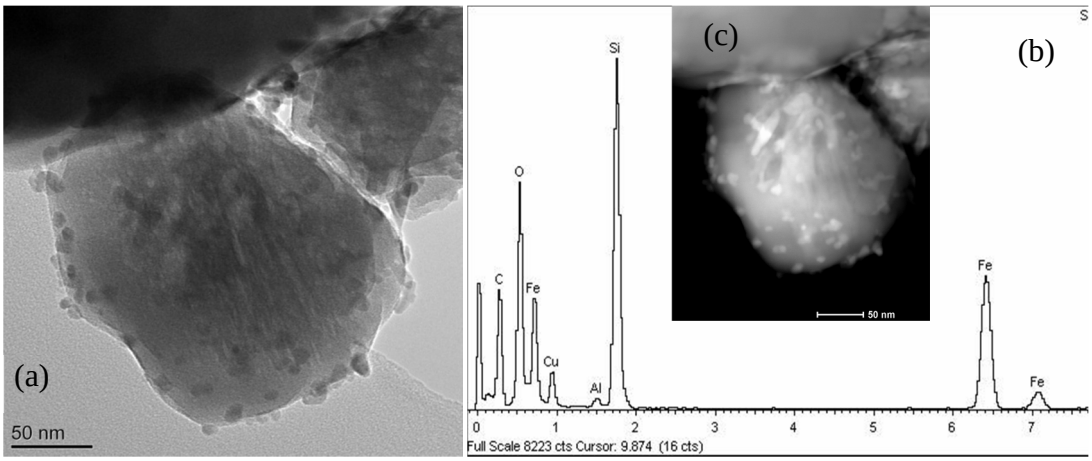

Figure 4-1: (a) STEM analysis of FeZSM-5 with (c) analysis of the haadf (high-angle annular dark-field) (b) EDX

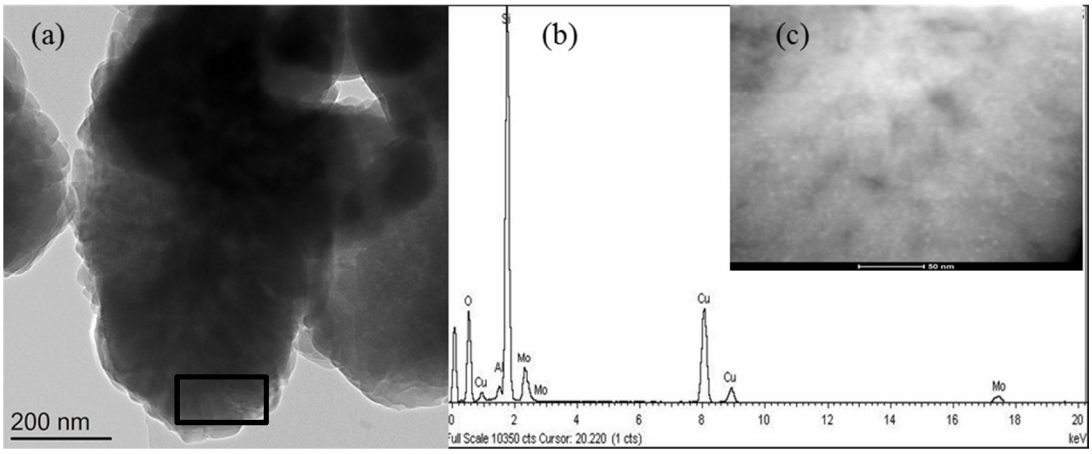

Figure 4-2: (a) STEM using the haadf (high-angle annular dark-field) zoomed from the picture (a) (c) methods and the EDX (b) to confirm the position of Mo

Figure 4-1 suggests that iron formed clusters on the edge of the particle with a size of approximately 16 nm, the presence of iron is confirmed by EDX although this technique does not allowed the quantification of metals. Figure 4-2 proposes that molybdenum is located inside the pores as observed with the image (c) forming a little dot of approximately 1 nm. Nickel (STEM not shown) probably forms a thin layer as the EDX identifies nickel without seeing any difference to Figure 4-3. This picture shows a good lattice network with a size of 1.6 nm for the unprocessed HZSM-5. The circle indicates where the lattice measurement is taken.

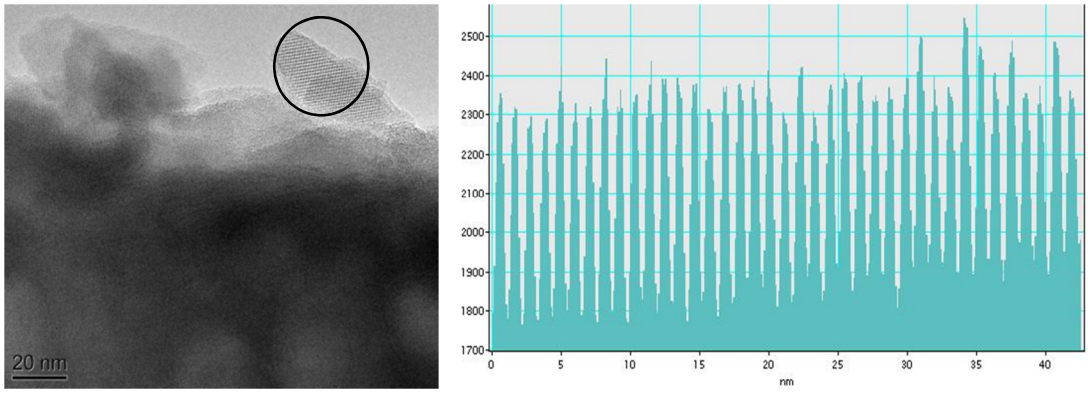

Figure 4-3: STEM of the unprocessed HZSM-5 and the lattice interstice

4.3.2 Stability test

The method of subcritical water liquefaction involves harsh conditions with high pressure between 140 and 150 bar at 350 °C. Therefore, catalysts should be robust under these circumstances.

Metal leachates from the reactor are measured by ICP-OES, a blank experiment is carried out and the main cations detected are iron, calcium and nickel with a concentration of 1.1, 1.0 and 2.7 ppm respectively. Ideally some insert should have been used to avoid the corrosion of the reactor or influence of the wall.

Generally, the de-alumination is low with approximately 0.2 wt.% leaching of the HZSM-5. As said earlier, migration of aluminium was possible out of the framework [217]. The loss of silica is more significant with approximately 20.0 wt.%. This result is in accordance with the one obtained by Ravenelle et al. [188] where the hydrolysis of the siloxane bond (Si-O-Si) was enhanced under hot compressed water (150-200 °C), this phenomena does have an impact on the reactivity for HZSM-5 as will be discussed later. The leaching of the doped metal at 350 °C is high with 6.2 wt.% for FeZSM-5, 7.9 wt.% for CuZSM-5, 10.0 wt.% with NiZSM-5 and 34.0 wt.% with MoZSM-5. These results are counter-intuitive with the TEM analysis, as iron is located outside the particle which is more subject to sintering, while molybdenum is found in the pores. Yet, these leachate ions could have a catalytic impact during the liquefaction of biomass. For MoZSM-5 between the impregnated and ion-exchanged samples, a similar value is measured (35.0 wt.%). Molybdenum might have reacted with the silica leachate as the aqueous phase is blue after the stability test.

The loss of aluminium and silica are lower with the doped metal especially with FeZSM-5 and MoZSM-5 with 11.2 and 7.2 wt.% of leachate of silicon. Thus, these metals could have an impact on the strength of the silica framework. The STEM imaging for the samples treated under subcritical water at 350 °C suggests that the lattice interstice widens to 2.3 nm. With the processed MoZSM-5, the EDX shows no indication of the presence of molybdenum but the sample is degraded under the beam for a long time and it is difficult to be certain. Agglomeration of iron is observed in some concentrated part, whereas elsewhere no iron has been detected. Some traces of nickel are detected for the processed sample although the size is too small to be seen by stem haadf.

In future, doped metal HZSM-5 could be doped with phosphorus (from phosphoric acid) to enhance the stability of the metal and also their performance [225].

4.3.3 Effect of the surface area and pore sizes

The BET method determines the surface area by absorption of nitrogen at 77 K. Figure 4-4 shows an example of BET isotherm with the unprocessed HZSM-5. The loop shape curve indicated the pores of this material are bottle neck types (with a narrow end); this process is called hysteresis [213]. The pore size of HZSM-5 is located in majority in the microporous region below 1.8 Å (radius) calculated by the HK (Horváth-Kawazoe) method.

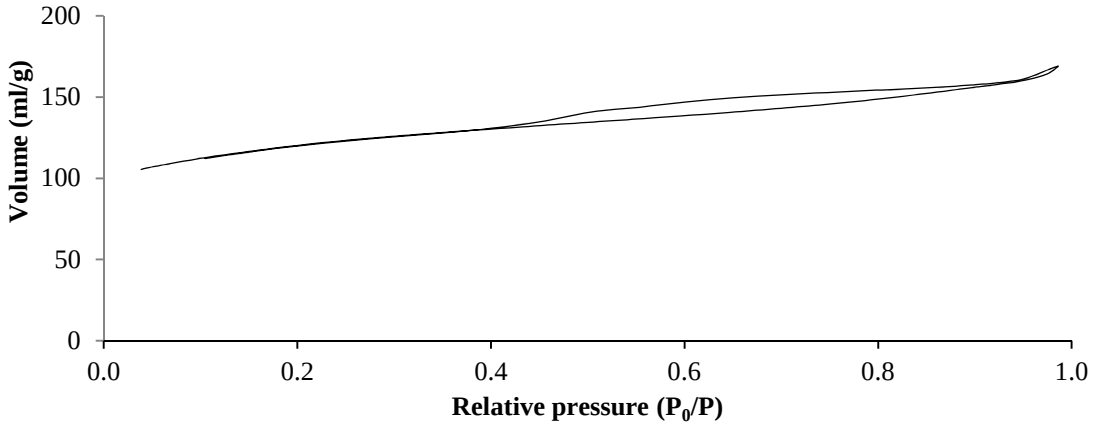

Figure 4-4: BET isotherm of HZSM-5

Table 4-1 compares the surface area (m^2/g) and the cumulative pore volume (ml/g) of the fresh and the used metal doped HZSM-5. The BJH (Barrett, Joynet and Halenda) method allowed the calculation of the cumulative volume in the micro and

mesoporous. This method predicts the pressure when condensation happens inside the cylindrical pore, subsequently pore size is determined by the Kevin equation. t-plot was also a method used commonly to determine the pore size.

Table 4-1: BET values calculated for fresh and used doped HZSM-5; pore volume and desorption calculated by the BJH methods

Catalysts	Surface area (m^2/g)	Cumulative Pore volume (ml/g)	Surface area after hydrothermal run (m^2/g)	Cumulative hydrothermal Pore volume (ml/g)
HZSM-5	382	0.09	141	0.05
CuZSM-5	384	0.09	285	0.05
FeZSM-5	399	0.09	52	0.03
MoZSM-5 ion-exchanged	435	0.1	250	0.07
NiZSM-5	370	0.1	219	0.1
MoZSM-5 impregnated	321	0.1	184	0.1
kaolin pellet HZSM-5	174	0.09	200	0.4

During the hydrothermal treatment using HZSM-5, the pore size remains unchanged i.e 1.8 Å. The volume of the micropores (t-plot) is 0.17 ml/g and the mesoporous is 0.05 ml/g. The difference between the fresh and doped samples is probably caused by the metal blocking the pores. Copper increase the cumulative pore volume compared to HZSM-5. Impregnated HZSM-5 has a lower surface area than HZSM-5 doped by ion exchange. In the literature, a surface area of 324 m^2/g was measured which was lower than the value during this study [179]. A surface area of 334 m^2/g and a pore volume of 0.11 ml/g was determined by Gayubo et al. [220] for impregnated HZSM-5 with nickel (0.5 wt.%). The surface area of the pellet was lower compared to the pure material as the binder (the clay kaolin) had a very low surface area of approximately 15 m^2/g.

Under subcritical condition, abrasion of the catalyst was observed with the loss of surface area. Indeed, a 25 % of loss was calculated between the fresh and the used sample at 350 °C. The reduction was more significant with FeZSM-5 with 87 % of loss (between the two values). Pieterse et al. [226] established that under steam, iron enhanced the migration of aluminium from the framework and reduced the dispersion of the metal, the same phenomena might result in the loss of surface area. The

observation in the STEM confirmed that iron formed cluster during this condition. Ravenelle et al. [188] determined that no change in pore volume was noticeable in the microporous and mesoporous under hot compressed water (150-200 °C).

For the majority of samples, with the exception of the kaolin pellet HZSM-5, a decrease of cumulative pore volume (mesopores) is apparent probably caused by the destruction of pores during the elevated pressure. Nevertheless, the BJH desorption profile indicates that new pores have been created in the region of 20-30 Å for HZSM-5 and CuZSM-5, from 80 to 110 Å for FeZSM-5 and in the region of 120 Å for MoZSM-5. Interestingly, the surface area of the kaolin-pellet increases the surface area to 200 m^2/g which implies that the binder and the clay enhance the stability toward abrasion. Moreover, the pore volume is larger than the fresh catalyst.

To conclude, subcritical water has an impact on the physical aspect of HZSM-5, yet binder could enhance the stability of the catalyst. Unfortunately, no time is available to undertake the experiment with metal doped pellets, since only wet impregnation could be used as HZSM-5 was already calcined.

4.3.4 Crystallinity of HZSM-5

HZSM-5 has high crystallinity as explained earlier and as represented in the Figure 4-5 (reference spectrum). The spectrum displays the complexity of the material which makes the interpretation difficult. The metal loading was too small to observe a peak on the XRD spectrum.

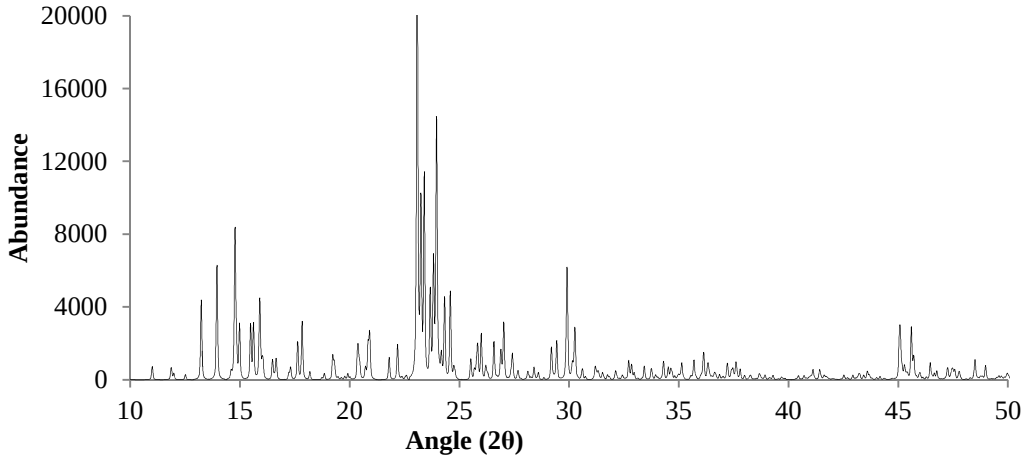

Figure 4-5: Reference spectrum for HZSM-5 from the Structure Commission of the International Zeolite Association (IZA-SC)

In the order to determine the crystallinity and be able to compare the fresh and the processed sample, HZSM-5 is mixed with a standard solution of alumina corundum with a ratio of 3:1 of reference. Indeed, intensity depends on different parameters such as the moisture and the presence of amorphous material; with the mixture this parameter is reduced. The sum of the intensity between 20 to 25° is chosen as this peak is influenced by the Si/Al [227] and 35 to 40° for the alumina as represented in the spectrum of Figure 4-6. Crystallinity is estimated using Equation 4-7 where the ratio of the fresh sample with the used was taken, I is the increment of the measurement. The results are included in Table 4-2.

$$\% \text{ crystallinity} = \frac{\frac{\sum \text{Intenstity fresh}[20\text{-}25] \text{ x I}}{\sum \text{intensity fresh}[35\text{-}40]}}{\frac{\sum \text{Intenstity htl}[20\text{-}25] \text{ x I}}{\sum \text{intensity htl}[35\text{-}40]}}$$

Equation 4-7

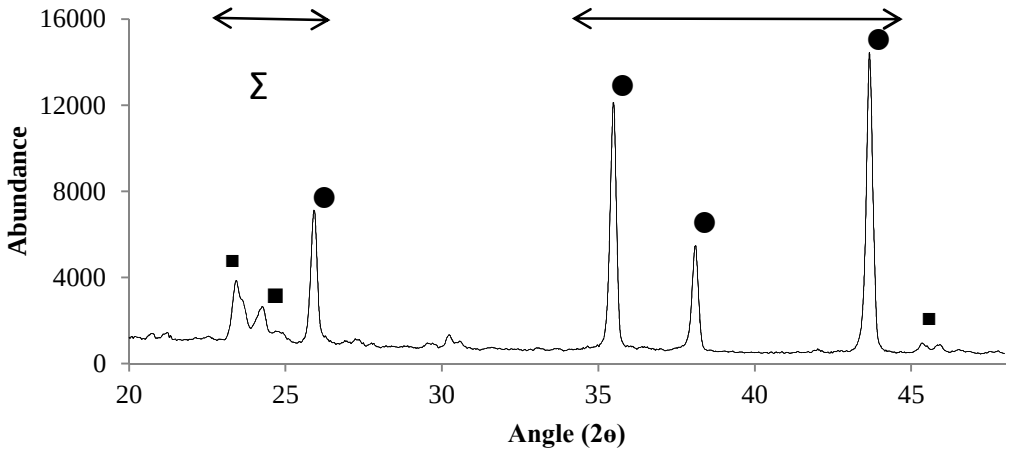

Figure 4-6: XRD spectrum of the mixture 25 % of HZSM-5 and 75 % of Al_2O_3 corundum where ▪ represents signals of HZSM5 and ● signals of Al_2O_3 corundum

Table 4-2: Peak area ratio of mixture 25 % HZSM-5- 75% γAl_2O_3 for the determination of the % of crystallinity

	HZSM-5	FeZSM-5	MoZSM-5 exchanged	CuZSM-5	NiZSM-5	MoZSM-5 impregnated
% Crystallinity compared to the fresh catalyst	75.5	77.4	86.2	72.4	79.2	75.6

Doped metal with the exception of CuZSM-5 enhanced the percentage of the crystallinity after the stability test compared to the plain HZSM-5. Yet, molybdenum prepare with ion-exchange had the highest effect compared to the other samples. Generally, impregnated samples have a lower crystallinity with respectively 75.6 for molybdenum compared to ion-exchange metal doped HZSM-5. Even though, FeZSM-5 has a low surface area, its crystallinity is higher to HZSM-5. Copper contains slightly more amorphous material than HZSM-5 however, no explanation is found.

Figure 4-7 represents the x-ray spectrum overlay between the fresh and the sample treated sample in subcritical water for the kaolin-pellet HZSM-5. The main difference with the used sample is the presence of new peak at approximately 12° and the intensity is larger between two regions of 21-25° and 35-40°. The change in intensity could be caused by the presence of moisture and amorphous material (explaining why previously zeolite was mixed with a reference material). This pellet is mixed with kaolin clay which was an amorphous material.

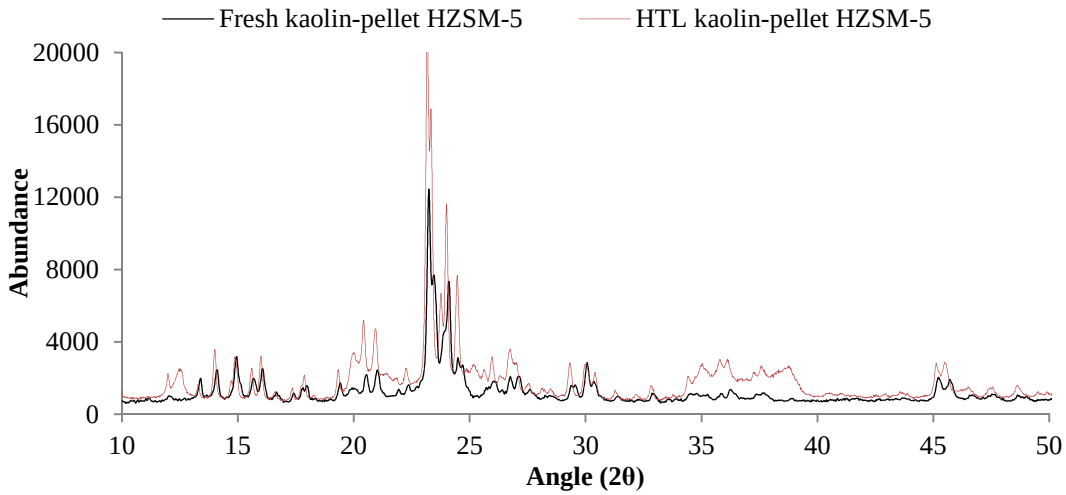

Figure 4-7: Overlay of the fresh and used pellet 40-40 kaolin-HZSM-5

Mo et al. [189] remarked how two new peaks appeared after two regeneration tests under supercritical water with no effect though on the activity as these peaks disappeared after calcination. No change of structure was noticed under low temperature [188].

To summarise, although the metal loading achieved via ion exchange is low and that the leaching is something not negligible, these metals have an impact on enhancing the crystallinity or for some the surface area. Impregnated doped metals with a high loading do not have an effect on the physical propriety of HZSM-5. The next step was to test this catalyst with real biomass.

4.3.5 Regeneration cycles

The hydrothermal liquefaction of sunflower oil is investigated with the metal doped HZSM-5 by ion exchange (HZSM-5, MoZSM-5, FeZSM-5, NiZSM-5 and CuZSM-5); results are presented in details in **Chapter 5**. Basically, some metals did have impacts on the selectivity regarding the degradation of the bio-crude and the formation of aromatic compounds for MoZSM-5. The mass of bio-crude for the pellet made with 40 wt.% of kaolin was about 86 wt.% (similar to processing of sunflower oil without catalyst). The impregnated MoZSM-5 give a higher mass bio-crude yield with 75 wt.% compared to the ion exchanged MoZSM-5 with 60 wt.%. Thereby, the aspect and the preparation of the catalyst have an impact on the bio-crude yield.

The regeneration and the stability of pellet HZSM-5 (compressed pellet) is investigated in this section. The analysis was focused on the production of coke rather than the propriety of the bio-crude. Table 4-3 includes the bio-crude yield measured after the HTL reaction with a coefficient of variance of 4.6 % and the wt.% of coke which is calculated from the thermogravimetric curve, weight loss (from 300 to 900 °C) in Figure 4-8. During this process according to the detail in the study from Ortega et al. [224], the first stage heated the catalyst to 500 °C under high flow of helium to age the coke and subsequently the coke was combusted from 300 to 900 °C.

Table 4-3: % Yield of the hydrothermal processing of sunflower oil at 350 °C for one hour in a 77 ml bomb reactor recycling HZSM5 four times

experiment	Bio-crude yield (wt.%)	Coke formed (wt.%)
HTL of sunflower with pellet HZSM5 cycle1	82.4	2.6
HTL of sunflower with pellet HZSM5 cycle2	92.0	3.9
HTL of sunflower with pellet HZSM5 cycle3	84.5	4.2
HTL of sunflower with pellet HZSM5 cycle4	91.5	3.4

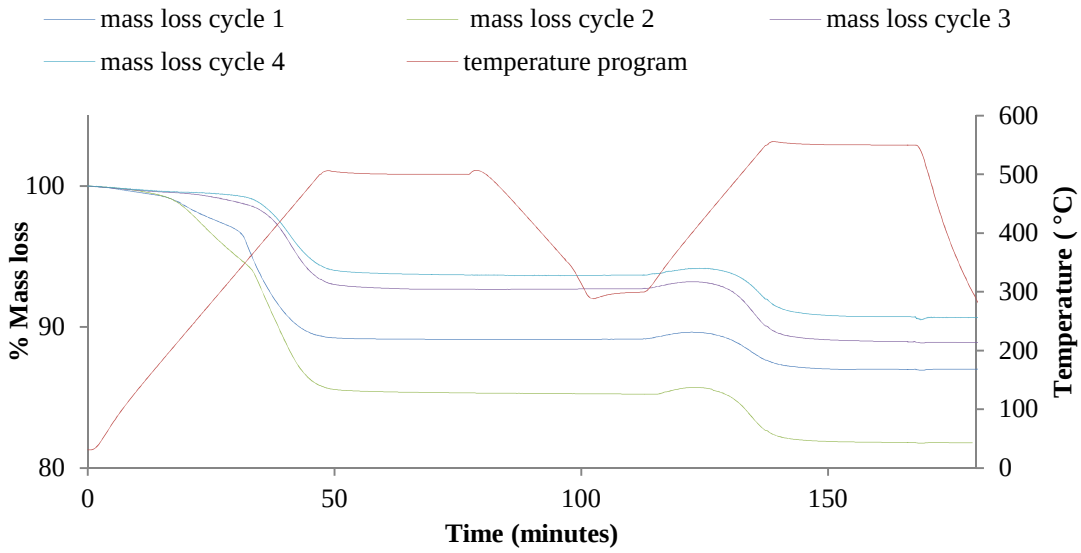

Figure 4-8: Temperature profile and weight loss curve for the catalyst after the four regeneration test

The initial size of the pellet was approximately 1 mm of diameter, yet after each experiments, the size of the particles was reduced due to the abrasion; this is the reason that cycle 1 is carried out six times, in order to have sufficient catalyst (0.5 g) for the last cycle. The bio-crude yield increases from the step one to two and subsequently the bio-crude yield is levelled out with cycle three (regarding the error margin) and cycle four. Yet the yield is higher than with the powder HZSM-5 with 68.0 wt.% (experiment presented in the next chapter) indicating that the cracking is less efficient with compressed pellet as the surface area of contact was higher with the powder. In other word, lipids could not access the acidic site. The coke content increases throughout cycle 1 to 3 and decreases for the last regeneration 4. Between each stage, the catalyst is dried but not calcined. Compared to pyrolysis the formation of coke is up to 6 wt.%, whereas under subcritical condition the coking was lower [228]. The gas emission is analysed by the FT-IR where absorption of the carbon monoxide and dioxide and the water are detected during the combustion stage. Thanks to a calibration, the mass is calculated and presented in Table 4-4 and Equation 4-8 is used to calculate the H/C ratio. n_{H2O} represents the molar amount of water calculated from the infrared spectrum, n_{CO} and n_{CO2} is also determined from the absorbance of carbon monoxide and dioxide. % C is the represents the total carbon content for both gases.

$$\frac{H}{C} = \frac{\frac{\%\ H\ in\ water\ x\ n_{H_20}}{2}}{\frac{(n_{CO}+n_{CO_2})\ x\ \%\ C}{12}}$$

Equation 4-8

Table 4-4: Mass of water, carbon monoxide and dioxide determined by the FT-IR and the H/C ratio for a sample of mass of approximately 20 mg

	Pellet cycle1	Pellet cycle2	Pellet cycle 3
Mass of water (mg)	4.5	7.7	7.4
Mass of carbon dioxide (mg)	17.6	47.9	44.0
Mass of carbon monoxide (mg)	1.0	1.8	1.9
Wt.% Carbon	40.3	43.3	43.1
Wt.% Hydrogen	2.3	1.5	1.5
H/C ratio	1.1	1.5	0.7

The H/C ratio of the coke increased for the first cycle to the second and is reduced for the third regeneration cycle. Previous study proposed that the reduction of the H/C ratio was caused by the de-alumination and the increase of formation of coke. Moreover, a low H/C ratio indicates the presence of aromatics in the coke [228]. Thus, HZSM-5 started to degrade after the third cycle. Figure 4-9 shows the emission of methane, carbon dioxide during the different steps of the analysis. During the first step with pyrolysis, a large amount of methane is produced implying that even with the washing with dichloromethane, some aliphatic compounds are trapped inside the structure of HZSM-5. Subsequently, during the combustion stage mainly carbon monoxide and dioxide are formed.

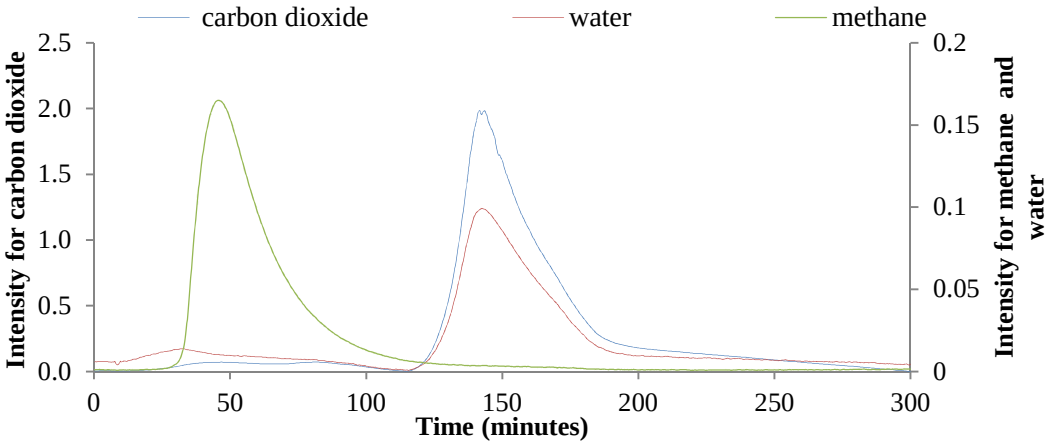

Figure 4-9: Emission of methane, water and carbon dioxide in function of time

Figure 4-10 represents the plot of the number of experiments against the surface area (m^2/g) during the regeneration cycle. A reduction of the surface area is caused by the abrasion of the pellet and the saturation of the pores by coke is observed. The surface area levels out between the cycles three and four.

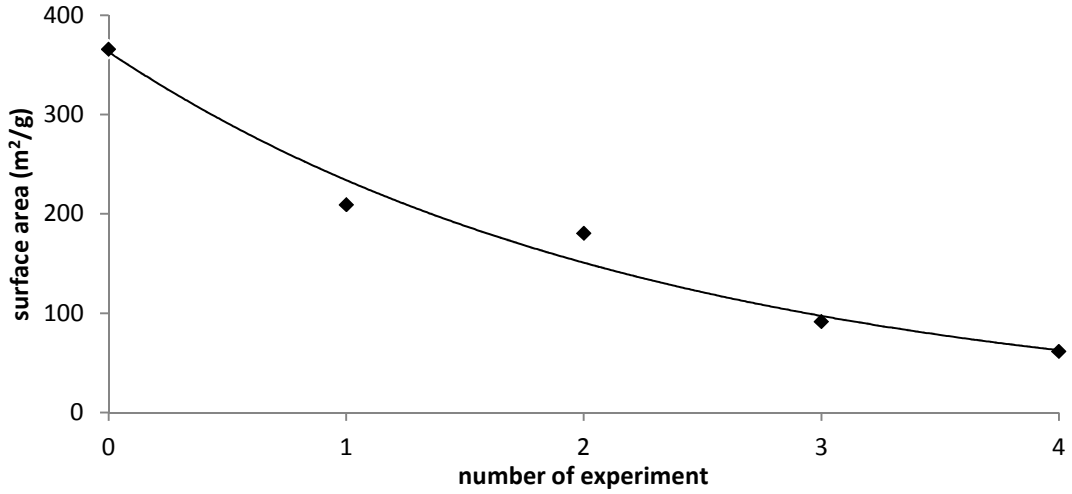

Figure 4-10: Plot of the number of experience against the surface area explaining the regeneration of HZSM5 HTL sunflower oil

Despite some physical change during the regeneration experiment no major change is observed in the bio-crude yield. Thus, HZSM-5 is stable during the recycling process. Unfortunately, no time is available to carry out the same types of experiments with the other catalysts. The stability of the pellet (kaolin-HZSM-5) should be investigated as it showed good resistance to abrasion and also the ion exchanged catalysts. In the next chapter for hydroprocessing of vegetable oils,

carbohydrates, proteins and microalgae, the catalysts are be used as powders for the reason that more surface contact was available compared to pellet. Even though, impregnated metal doped catalysts have a larger metal doped than ion exchanged, the latter show a higher stability and these catalysts are selected during the processing of the different biomass.

4.4 Conclusion

To conclude, the condition during subcritical water did have some influences on the physical (abrasion) and less on the chemical structure of HZSM-5. The leaching of silica in general was higher than aluminium. Less leaching occurred for nickel compared to molybdenum. The STEM imaging showed no change in the structure after the stability test, except that the metals were difficult to observe compared to the fresh catalyst. The doped metal HZSM-5 had some impact on enhancing the stability for example molybdenum with HZSM-5 improved crystallinity, and copper improved the surface area. Nevertheless, FeZSM-5 was subjected to high abrasion in hydrothermal condition. Finally, ion exchange HZSM-5 seemed to be more stable than the impregnated catalysts. HZSM-5 was processed with sunflower oil four times. It was found that the coke amount increased after each test and that the surface area decreased as well. In the next chapter, the processing of different vegetable oils and fatty acids was carried out and the effect on the bio-crude from the processing of sunflower oil with different metal doped is discussed more in detail.

Chapter 5 Hydrothermal liquefaction of lipids with and without HZSM-5

This chapter includes results from the liquefaction reactions of different vegetable oils (sunflower, soya, linseed, jatropha and palm oil) at different temperatures (250, 300, 350 °C) for one hour. Unsaturated fatty acids (oleic, linoleic and linolenic acid) have been processed at 350 °C. Synthetic mixtures have been prepared from model fatty acids with similar compositions to sunflower, linseed and jatropha. HTL experiments have also been undertaken with the different metal doped HZSM-5 (nickel, iron, copper, and molybdenum) in water and formic acid at 350 °C.

5.1 Introduction

Lipids are a major constituent produced by vegetal and microalgae as triglycerides and used to store energy. For this reason, triglycerides are commonly extracted and converted by esterification to produce biofuels such as fatty acids methyl esters [229]. Microalgae can potentially contain up to 60 dry weight per cent of lipids and in theory they are able to produce up to 136,900 L/ha compared to palm oil 5,950 L/ha [64].

Watanabe et al. [230] studied the reactivity of stearic acid in supercritical water for 30 minutes and showed that the conversion into alkenes was low. By adding sodium and potassium hydroxide, the concentration of alkane C_{16} was more prevalent. Linoleic acid is more reactive than oleic and stearic acids particularly above 300 °C, emphasising that the degree of saturation has an impact on the reactivity of the fatty acid in subcritical water [231]. Holliday et al. [109] demonstrated that 97 % of the triglycerides from soya bean and linseed oils are hydrolysed below 300 °C with a water density of 0.7 ml/g. Similar results were reported for the hydrolysis of soya bean oil in a continuous reactor by King et al. [110].

Final upgrading of the fatty acids can be performed using catalytic upgrading. HZSM-5 has been demonstrated to be a reliable catalyst under pyrolysis conditions yielding aromatic and alkane compounds [179, 232]. Peng et al. [185] used NiZSM-5 with and without hydrogen to upgrade a microalgal oil; a good conversion of fatty acids into alkane was achieved with 60 wt.% yield of octadecane at 260 °C and 40 bar

of hydrogen. Mo et al. [189] have recently proven that HZSM-5 could convert 99 % of palmitic acid at 400 °C and could be regenerated without any structural change. Thereby, HZSM-5 was selected as a catalyst for cracking the vegetable oils; furthermore the addition of metals into the structure of the zeolite improved its activity toward the reduction of triglycerides and fatty acids.

The aim of this chapter is first to use vegetable oils (sunflower, soya bean, linseed, jatropha and palm oils) and a series of model compound studies using fatty acids to study the effect of temperature on the composition of the unsaturated fatty acids and the hydrolysis of triglycerides. Subsequently, the addition HZSM-5 with different doped metals is investigated to verify the effect on sunflower oil for cracking and isomerisation. Microalgae can contain high levels of unsaturated fatty acids and it is unclear how the degree of saturation influences the reaction pathways and product quality. The main aim of this chapter is to understand the fate of lipids from microalgae during the hydrothermal liquefaction process.

5.2 Methodologies

In this chapter, some specific analyses for the lipids are carried out and thus are described here such as the quantification of fatty acids methyl ethers following esterification.

5.2.1 Quantification of fatty acids

Fatty acids methyl ethers (FAME) analysis is used to quantify the fatty acid composition of the raw vegetable oils and is performed as follows: 0.2 g of oil was mixed with 3 ml of methanol and one drop of sulphuric acid (96 vol.%) and heated to 60 °C for one hour. Once cooled, 2 ml of water and 2 ml of pentane were added to the solution and mixed. The pentane phase was separated and placed in a pre-weighed vessel and the pentane solvent was allowed to evaporate. The resulting FAME (approximately 3-5 mg) was dissolved in dichloromethane (1 ml) and analysed by GC-MS (Agilent 5975B inert GC-MSD). The GC-MS was calibrated using FAME standards (100 mg FAME Mix C8-C24 obtained from Supelco); the calibration equations are found in Table 5-1, and the samples were diluted 1000 times. Separation of the products was achieved using an RTx 1701 using the same program described in **Chapter 3**. FAME content is expressed in g/kg of oil from the Equation 5-1 using the equation $y= ax + b$, y is the integration of the GC-MS graph, a is the gradient, and b is

the intercept when y = 0 from the standard divided by the ratio of the m_{FAME} mass of sample in mg, to $V_{dichloromethane}$ the volume of dichloromethane (ml).

Table 5-1: Equation calculated by a set of standard from 100 mg FAME Mix C8-C24 obtained from Supelco

Fatty acids	Calibration equation
Hexadecanoic acid, methyl ester	y = 357,335x – 4,000,000
8,11-octadecadienoic acid, methyl ester	y = 355,939x – 2,000,000
Octadecanoic acid, methyl ester	y = 400,760x – 3,000,000
9,12,15-octadecatrienoic acid, methyl ester	y = 345,005x – 4,000,000
Docosanoic acid, methyl ester	y = 123,456,204.90x - 2,860,853.50
Octanoic acid, methyl ester	y = 73,582,151.00x - 122,212,450.00
Decanoic acid, methyl ester	y = 77,391,063.00x - 47,568,276.33
Dodecanoic acid, methyl ester	y = 81,484,220.90x - 13,970,313.50
Methyl-tetradecanoate	y = 88,060,167.40x - 1,122,292.50
8-octadecenoic acid, methyl ester	y = 228756x+168511
Eicosanoic acid, methyl ester	y = 115,771,350.60x - 1,067,620.00

$$\text{Concentration FAME} = \frac{\left(\frac{((y) \pm (b))}{(a)}\right)}{(m_{FAME})/(V_{dichloromethane})}$$

Equation 5-1

5.2.2 Other techniques

The boiling range of the bio-crude oils is estimated using thermogravimetric analysis (TGA) using a TA instrument (Q5000IR). A fraction of the oil, less than 10 mg, was heated from 40 to 900 °C at a heating rate of 10 °C/min under nitrogen (50 ml/min). The boiling curve was divided into five distinct boiling fractions; (i) the gasoline fraction (< 170 °C) also named gasoline range, (ii) the kerosene fraction or diesel range (170 to 250 °C), (iii) the diesel fraction (250-350 °C), (iv) the vacuum diesel fuel fraction (350-400 °C) and (v) residue (> 400 °C).

The carbon balances in the bio-crude and in the aqueous phase are calculated as follows in Equation 5-2. The carbon in the bio-crude oil is calculated similarly using the elemental value. [TOC] is the concentration of the organic carbon in ppm

(mg/L), $m_{intial\ biomass}$ is the mass of the dried biomass ash free, % $C_{raw\ sample}$ is the per cent carbon measured by the elemental analyser of the raw vegetable oil and % $C_{raw\ sample}$ is the per cent carbon measured by the elemental analyser of the bio-crude oil % $C_{\ bio\text{-}crude\ (CHNS)}$ and $m_{bio\text{-}crude}$ is the mass of the bio-crude obtained.

$$\%\ C_{aqueous\ phase} = \frac{[TOC] / 1000}{m_{\ raw\ sample} \times \%\ C_{raw\ sample}}$$

Equation 5-2

$$\%\ C_{bio\text{-}crude} = \frac{\%\ C_{\ bio\text{-}crude\ (CHNS)} \times m_{\ bio\text{-}crude}}{m_{\ raw\ sample} \times \%\ C_{raw\ sample}}$$

Equation 5-3

5.3 Chemical composition of the raw vegetable oils

Table 5-2 includes the per cent FAME and the amount of triglyceride and free fatty acids of the raw vegetable oils: sunflower, linseed, soya, jatropha and palm oil. Some mixtures have been prepared using different concentrations of stearic acid (C18:0), oleic acid (C18:1), linoleic acid (C18:2) and linolenic acid (C18:3) as a comparison of linseed, sunflower and jatropha oils. An average coefficient of variance of approximately 7.5 % is calculated. The elemental analysis of raw vegetable oils was performed as explaining in **Chapter 3**. The % normalised fatty acids is calculated by the ration of the concentration over the total sum of all the fatty acids.

Table 5-2: Chemical composition of the raw vegetable oils and mixtures

	Elemental analysis				Normalised % Composition Fatty acids						% Size range	
	C wt.%	H wt.%	O wt.%	HHV (MJ/kg)	C16:0	C18:0	C18:1	C18:2	C18:3	Total polyunsaturated	Triglycerides	Free fatty acids
Sunflower oil	72.9	11.1	16.0	37.6	14.6	13.8	27.3	43.7	-	43.7	93.8	2.0
Linseed oil	72.8	11.3	16.0	37.9	6.9	8.2	16.7	11.7	56.0	67.7	96.0	1.5
Soya bean oil	75.5	12.6	11.9	41.4	11.0	5.3	32.7	45.5	5.4	50.9	90.5	2.5
Jatropha oil	76.5	12.4	11.1	41.5	12.3	15.8	39.5	32.4	-	32.4	73.1	11.6
Palm oil	77.4	12.2	10.3	41.8	39.3	9.6	39.9	11.3	-	11.3	82.4	5.3
Synthetic linseed	81.5	12.3	6.3	43.2	-	4.0	12.5	8.3	75.0	83.3	-	-
Synthetic sunflower	70.9	11.6	17.4	41.7	-	6.0	26.7	67.0	-	67.0	-	-
Synthetic jatropha	75.8	12.0	12.2	40.7	-	33.3	33.3	33.3	-	33.3	-	-
Oleic acid	76.5	12.1	11.3	41.8	-	-	-	-	-	-	-	-
Linoleic acid	77.1	11.5	11.4	41.1	-	-	-	-	-	-	-	-
Linolenic acid	77.6	10.9	11.5	40.4	-	-	-	-	-	-	-	-

From Table 5-2, linseed oil contains mainly linolenic acid with approximately 56.0 % whereas sunflower and soya bean oils contain mainly linoleic acid with approximately 43.7 and 45.5 %. For Jatropha and palm oil, the main fatty acid is oleic acid although palm oil also contains high level of palmitic acid; this is the reason why a paste forms at room temperature. The fatty acids for each plant depend on the factors such as growth conditions of the species. In a dry climate, plants such as sunflower oil produce more unsaturated fatty acids [233]. According to Thomas et al. [13], the typical composition of linseed oil is: oleic acid 18-26 %; linoleic 14-20 % and linolenic 51-56 %; comparing this with the values obtained in this study, the amounts of oleic, linoleic and linolenic acids are relatively close to these ranges. Sunflower, soya bean and linseed oils are initially refined as they contain mainly triglycerides (up to 90 %) whereas jatropha and palm oil are crude oils and as such contained higher levels of free fatty acids (11.6 and 5.3 %). These values have been determined using GPC by integrating the peaks but it was also possible to measure by potassium hydroxide titration with 10.3 wt.% and 3 wt.% for the same oils. However, titration requires a large amount of samples whereas with GPC only approximately 70 mg is necessary and other materials could also be detected; as for jatropha oil some free glycerol and other compounds are identified with a molecular weight around 120 g/mol. Soya bean oil, palm and jatropha oils contain the highest energy content. Sunflower and linseed oils contain the largest oxygen content compared to the other vegetable oils. The elemental composition of the synthetic mixtures is determined by the average of value from the model oleic, linoleic and linolenic acids. The synthetic linseed contains higher carbon content compared to the original oil.

Figure 5-1 lists the chemical formula and the elemental composition of the three model fatty acids used. The isomer of linolenic acid used in this study is (Z,Z,Z)-9,12,15-octadecatrienoic acid or the α-linolenic acid also call ALA, this fatty acid is part of the omega 3 well known dietary nutrition and is mainly found in linseed oil, and canola oil.

The isomer of linoleic is the 9-*cis*,12-*cis*-linoleic acid and *cis*-9,*cis*-12-octadecadienoic acid. It is mainly found in sunflower oil or poppy seed [13]. Most fatty acid configurations found in vegetable oils are *cis*-form.

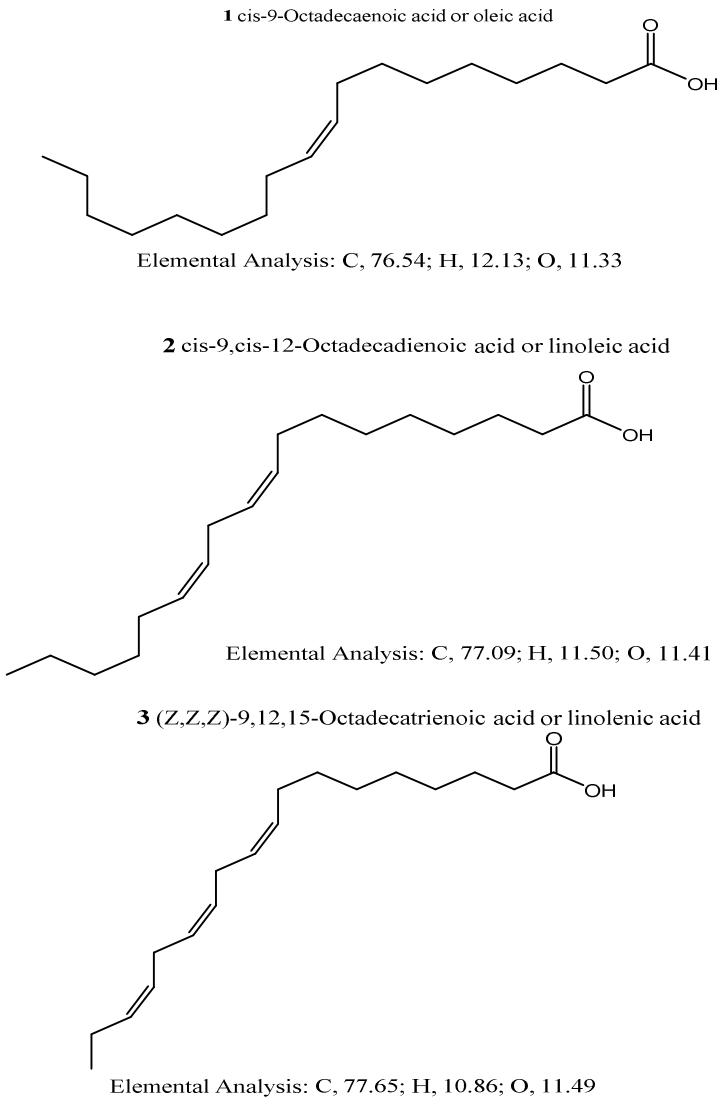

Figure 5-1: Chemical structure for oleic, linoleic and linolenic acids

5.4 Effect of HTL temperature on oil compositions for the different vegetable oils

5.4.1.1 Mass balance yield

Table 5-3 includes the percentage bio-crude oils mass yield for sunflower, linseed, soya, jatropha and palm (equation in **Chapter 3**) for all the experimental runs carried out with vegetable oils. The typical experimental error or coefficient of variance for these values is approximately 3-4 %. The bio-crude oil is shown as received as it is assumed that the original vegetable oils do not contain ash and moisture.

Table 5-3: Mass bio-crude oils yield, for the processing of different vegetable oils at different temperature

Reaction conditions	Bio-crude yield wt.%
Sunflower oil	
250 °C	74.0
300 °C	87.0
350 °C	86.0
Linseed oil	
250 °C	91.0
300 °C	99.0
350 °C	93.0
Soya bean oil	
250 °C	91.0
300 °C	99.0
350 °C	93.0
Jatropha oil	
250 °C	89.0
300 °C	89.0
350 °C	93.0
Palm oil	
250 °C	89.0
300 °C	88.0
350 °C	90.0
HTL oleic acid	97.0
HTL linoleic acid	92.0
HTL linolenic acid	93.0
HTL synthetic sunflower	86.0
HTL synthetic linseed	86.0
HTL synthetic jatropha	73.0

As vegetable oils are liquid, it is not surprising at the end to recover high yield of bio-crude oils. In this chapter, only the bio-crude oil is presented here although in the following chapters the mass balances of the different phases (bio-crude oil, gas, residue and aqueous phases) are included. In theory, if the hydrolysis of 3.0 g of triglycerides with a molecular weight of 883 g/mol is predicted to yield 92.0 wt.% of bio-crude (about 2.7 g) with three fatty acids (molecular weight of 280 g/mol each);

the remaining phase would be glycerol 8 wt.% soluble into the aqueous phase. This accounts for the loss in yields from the different oils.

At 250 and 300 °C, no gas production is observed as the initial and final pressures are equalled, whereas at 350 °C one bar of gas is released. Pressures, at 250, 300 and 350 °C, are 38, 82 and 161 bar respectively. It would be likely if the gas composition had been analysed, it would mainly be carbon dioxide [94], a product of decarboxylation. C_{16} and C_{18} fatty acid chains start to be soluble above 230 °C with 10^{-3} mol/kg of H_2O [96].

For most of the vegetable oils, the maximal bio-crude yield is achieved at 300 °C. For jatropha and palm oil, the difference between each temperature is rather low. The appearance of the processed oil from jatropha and palm oils is different from the other vegetable oils (brownish-liquid oil) resulting in a white-solid, suggesting that it contains mainly saturated fatty acids which are not liquid at room temperature.

After the HTL reaction, most of the model fatty acids are been recovered, the results are consistent with those obtained by Shin et al. [231] with 99 wt.% for oleic acid and 87 wt.% for linoleic acid. An identical mass yield is obtained between the HTL run of sunflower and synthetic mixtures; for the two other mixtures the mass yield is lower compared to the use of vegetable oils.

5.4.1.2 GPC analysis

Figure 5-2 contains the per cent of integrated fraction between a set retention time representing different molecular weight ranges as follows: “heavy molecular weight” (≥ 1000 g/mol), oligomers (between 1000 to 600 g/mol), free fatty acid or “long chain” (600-200 g/mol) and low molecular weight (≤ 200 g/mol). The average coefficient of variance of this analysis is approximately 5 %. It is observed that the initial molecular weight of triglyceride is above 1000 g/mol whereas the theoretical molecular weight of sunflower oil is 886 g/mol. The difference is caused by a shift in the retention time. In addition, The GPC does not allow distinguishing between fatty acids and long chain alkanes because of their close molecular weight. However, it is an efficient technique to give an estimation of the different molecular size range.

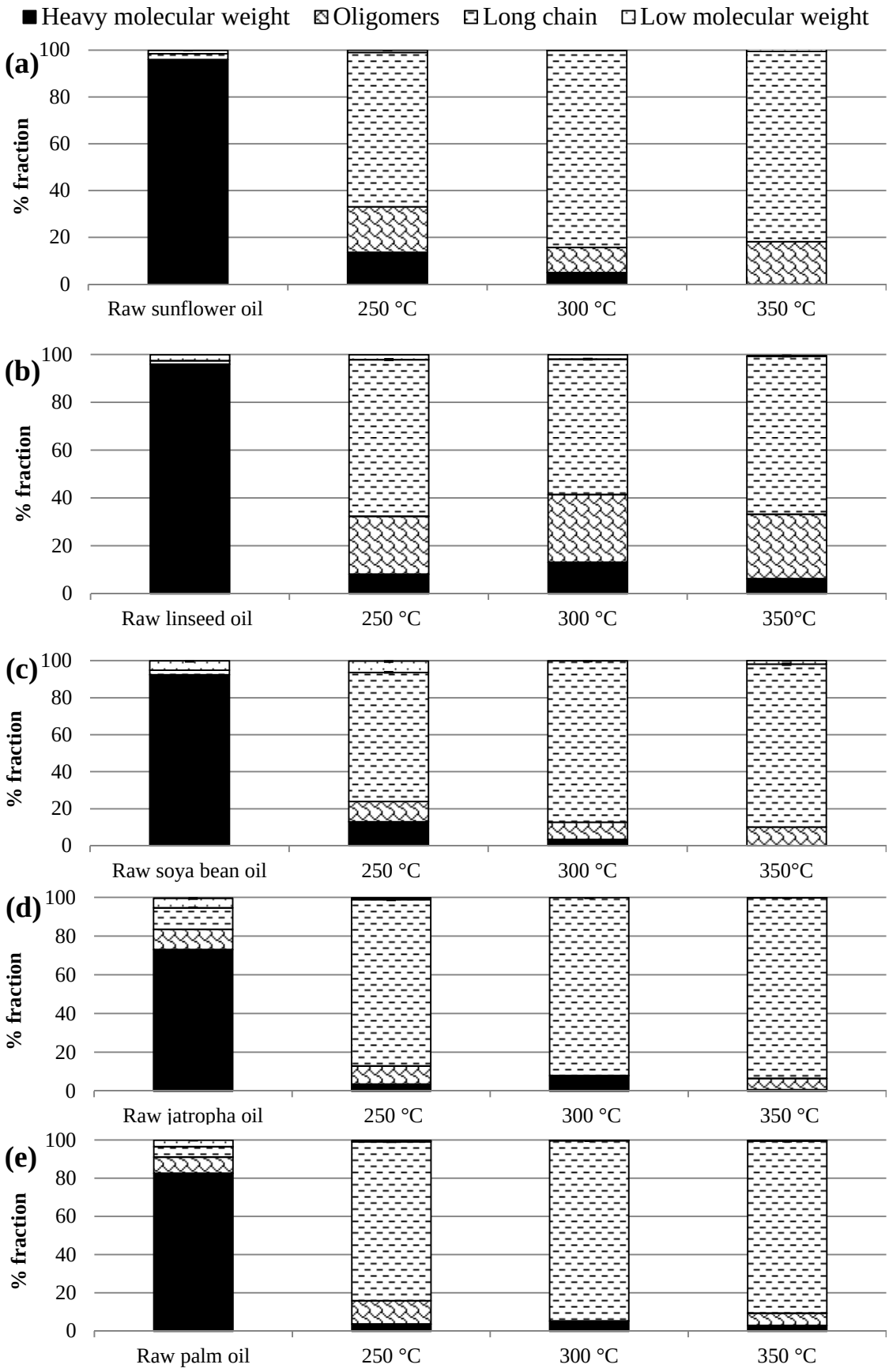

Figure 5-2: Different different molecular weight fractions for (a) sunflower, (b) linseed, (c) soyabean, (d) jatropha (e) palm oils at different temperatures.

The GPC results with the raw jatropha and palm oils (Figure 5-2 (c), (d)) are slightly different compared to the other vegetable oils as explained previously. These oils are unrefined which explained why the fraction of triglycerides is lower.

The GPC results at 250 °C (Figure 5-2) show that a large fraction of vegetable oils are been hydrolysed into lower molecular weight materials compared to the raw vegetable oils. At this temperature, some oligomers are observed which could be assigned as diglycerides. It has been demonstrated that above 300 °C, the hydrolysis of triglyceride are complete [110]. The hydrolysis of corn oil started at 200 °C and was complete at 280 °C under subcritical water [234]. Holiday et al. [109] observed a 97 % conversion of vegetable oil into fatty acid between 260-280 °C for less than 20 minutes. Alenezi et al. [235] obtained a 90 % hydrolysis of sunflower oil using a continuous reactor at 330 °C for 12 minutes. It was concluded that the time and temperature were affected the conversion.

The GPC result above 300 °C, some cross linking reactions could take place [236]. This is particular noticeable for linseed oil (Figure 5-2 (c)) which contained high amounts of polyunsaturated fatty acids, explaining the large fraction of oligomers materials. A decrease of the “heavy molecular weight” materials in relation to the temperature is observed for sunflower and soya bean oils.

The GPC result at 350 °C, the bio-crude of processed of jatropha and palm oils contain in majority “long chain” materials or fatty acids (higher to 90 %) as these vegetable oils have lower amount of polyunsaturated oils. More “heavy molecular weight” materials for palm oil are found in comparison to jatropha oil. The formation of crossed linked could be more significant at 350 °C as the oligomers materials increase for sunflower oil between 300 to 350 °C.

Figure 5-3 shows the different molecular weight fractions for unprocessed fatty acids and processed at 350 °C and the different mixtures.

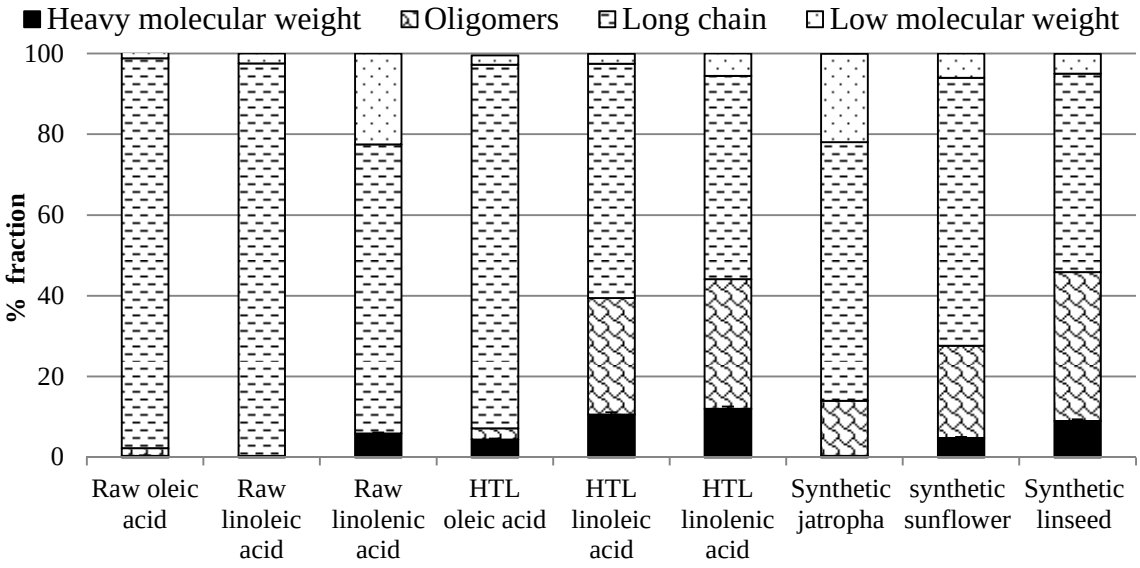

Figure 5-3: Molecular weight fraction determined by GPC of the different model compounds and mixtures

For the raw linolenic acid, the reason why some "heavy molecular weight" materials are found prior to the experiment is because fatty acid is unstable and easily oxidised by air or even by the mobile phase tetrahydrofuran (THF). It is possible that some epoxidation reaction between each chain might have occurred forming dimers or heavy molecular weight material [237, 238]. Nevertheless, it is only affected processed linolenic acid.

It is observed that the oligomers and "heavy molecular weight" materials increase in relation to the unsaturated number of double bonds as the oligomers fraction was 28 % and 32 % for linoleic and linolenic acids. The "heavy molecular weight" materials produce from oleic acid is relatively scarce, indicating its stability as mentioned previously. Furthermore, it demonstrates that linolenic acid is not stable at 350 °C as almost half of the initial fatty acids are converted into "heavy molecular weight" materials forming dimers or larger polymers [236].

The GPC of the synthetic mixture matches with the experiment of the corresponding vegetable oils especially with sunflower and linseed oil. The amount of oligomers for the synthetic linseed compared to the processing of linolenic acid suggesting that some cross linking occurs [236]. The synthetic sunflower oil contains less oligomer than linoleic acid which probably means that the other fatty acids could reduce the formation of dimers.

In general, there is an overall decrease of the “heavy molecular weight” materials with temperature suggesting a hydrolysis of the triglycerides. Nevertheless, when the concentration of polyunsaturated fatty acids for example with linseed oil are significant, crossed-linked materials are being formed.

5.4.1.3 Composition of FAME

Figure 5-4 represents the concentration in g/kg of different fatty acids palmitic or hexadecanoic acid (C16:0); stearic or octadecanoic acid (C18:0); oleic acid (C18:1); linoleic acid (C18:2) and linolenic acid (C18:3), for (a) sunflower oil, (b) linseed oil, (c) soya bean oil, (d) jatropha oil and (e) palm oil, the concentration was calculated as in section 5.1.1 and the coefficient of variance for the analysis is approximately 6-8 %.

The FAME results (Figure 5-4 (b), ((c)) for linseed and soya bean oils show the instability of linolenic acid, the concentration in the case of linseed oil decreases from 500 g/kg with the raw materials to almost zero at 350 °C. Holidays et al. [109] explained that as the temperature approaches 270 °C linolenic acid *cis cis, cis* can be isomerised into different configurations as *trans, cis, cis*. The processing of the model linolenic acid alone shows the presence of some oleic acid (160 g/kg) and linoleic acid (approximately 560 g/kg) and also 11,14-octadecadienoic acid. Some FAME with cyclic groups are also detected such as methyl 9-(o-propylphenyl)-nonanoate, and the methyl-2-octylcyclopropene-1-heptanoate. It confirms that some internal cyclisation happens [239].

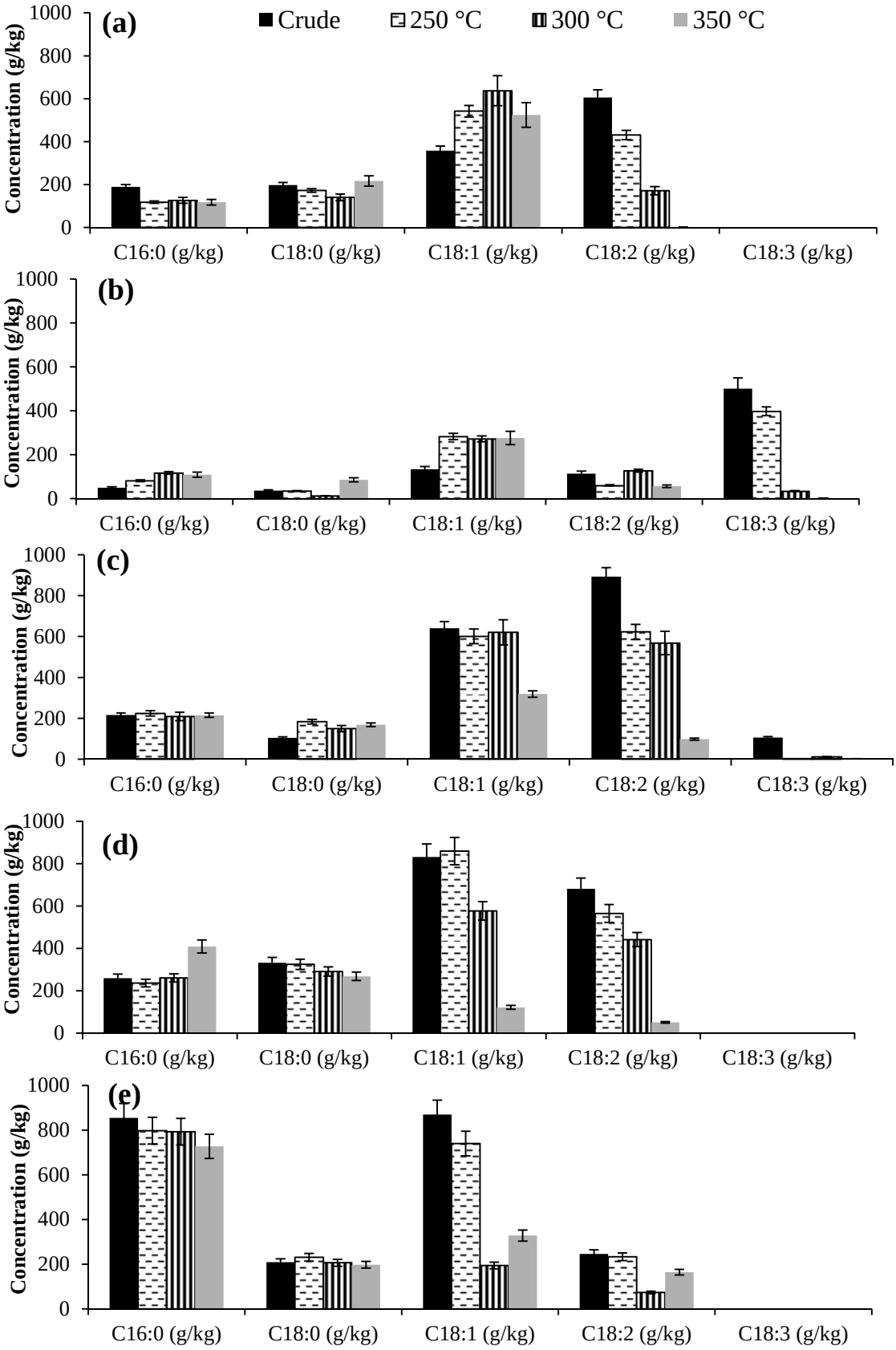

Figure 5-4: Normalised fatty acid distribution of oils following hydrothermal liquefaction at different temperatures without catalyst for (a) sunflower oil, (b) linseed oil, (c) soya bean oil, (d) jatropha oil and (e) palm oil

The FAME results for sunflower, soya bean and jatropha oils (Figure 5-4 (a), (c), (d)) indicate a decrease of the concentration of linoleic acid between 250 to 350 °C. Li et al. [236] illustrated that at low temperature the linoleic acid (9,12 *cis, cis*) underwent a conjugation to 10,12 *cis*. Most of the configurations of the unsaturated fatty acids are *cis*-form. King et al. [110] clarified that during the hydrolysis of soya bean oil in a continuous reactor that linoleic and linolenic acids underwent *trans*-isomerisation or by the conjugation of the double bonds. Only 11 % (peak ratio) of linoleic acid has been recovered after the processing at 350 °C of the model compound. Delocalisation and conjugation of the double bonds from the initial linoleic acid are identified by the NIST library with 8,11-octadecadienoic acid, 11,14-octadecadienoic acid, 6,9-octadecadienoic acid; however, these compounds could not be quantified because there were not present in the standard solution. Also some aldehydes are present with the Z,Z-10,12-hexadecadienal, indicating that linoleic acid can be reduced.

There is no clear relation of the concentration of oleic acid with the temperature. Nevertheless, the concentration of oleic acid decreases with jatropha and palm oil which could be explained by the formation intra-cyclisation between oleic and linoleic acids [236]. Another justification could be explained by the isomerisation of oleic acid caused by the delocalisation of the double bonds. Shin et al. [231] explained that some 9-(E) isomer could also be formed. In the method selected for this project and the column do not allow us to distinguish and separate the two isomers and so this why is the peak areas are more important. 66 % of oleic acid has been recovered after the processing of the pure fatty acid at 350 °C (the initial concentration is 5692 g/kg to 3740 g/kg).

The FAME results (Figure 5-4 (e)) for palm oil show mainly palmitic acid and stearic acid. During hydrothermal liquefaction, these two fatty acids are relatively stable with a low change in concentration. Shin et al. [231] did not detect any degradation of the stearic acid below 370 °C.

Figure 5-5 represents the diagrams of the synthetic mixtures of linseed, sunflower and jatropha.

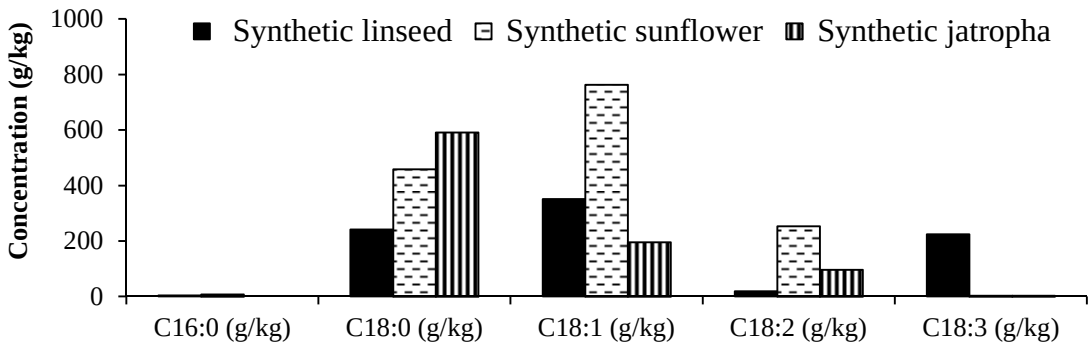

Figure 5-5: FAME analysis of the mixtures

As with the sunflower and linseed oil, the most abundant fatty acid is oleic acid with respectively 51 and 41 %. The amount of linolenic acid is higher compared to the real linseed oil. For jatropha oil, the concentration of stearic acid has doubled compared to the initial composition with 60 %. In general, it is deduced that polyunsaturated fatty acids (linoleic and linolenic acids) are unstable in subcritical water compared to stearic and palmitic acids.

5.4.1.4 Elemental analysis

Table 5-4 lists the elemental analysis CHO, and heating value calculated using the Dulong equation (HHV). Samples were prepared as duplicates with a coefficient of variance of 2.5 %.

Table 5-4: Elemental analyis, as received, of the different oils at different temperatures for the processing of 5 vegetable oils

	C wt.%	H wt.%	O wt.%	HHV (MJ/kg)	H/C	O/C	% Energy recovery
Sunflower oil							
250 °C	77.1	12.0	10.9	41.3	1.9	0.1	81.6
300 °C	78.0	11.43	10.6	40.8	1.8	0.1	94.0
350 °C	76.8	11.49	11.7	40.3	1.8	0.1	92.3
Linseed oil							
250 °C	77.8	10.7	11.5	39.5	1.6	0.1	94.3
300 °C	74.67	10.42	14.91	37.46	1.7	0.2	97.4
350 °C	75.2	10.3	14.5	37.5	1.6	0.1	92.2
Soya bean oil							
250 °C	79.8	11.6	8.5	42.1	1.8	0.1	91.7
300 °C	79.9	11.4	8.7	41.8	1.7	0.1	96.4
350°C	79.0	11.2	9.7	41.0	1.7	0.1	97.2
Jatropha oil							
250 °C	78.3	11.4	10.3	40.9	1.7	0.1	87.6
300 °C	69.2	11.1	19.7	35.7	1.9	0.2	76.8
350 °C	68.3	12.6	21.7	37.2	2.2	0.2	89.0
Palm oil							
250 °C	73.1	11.9	14.9	39.1	2.0	0.2	91.9
300 °C	73.2	11.0	15.9	37.6	1.8	0.2	61.7
350 °C	72.0	11.6	16.4	38.0	1.9	0.2	82.6
HTL oleic acid	77.9	12.5	9.6	42.5	1.9	0.1	99.9
HTL linoleic acid	77.1	8.3	14.6	35.3	1.3	0.1	80.3
HTL linolenic acid	71.7	10.2	18.1	35.6	1.7	0.2	83.2
Synthetic sunflower	80.0	10.0	10.0	39.5	1.5	0.1	78.7
Synthetic linseed	75.4	11.1	13.5	38.9	1.8	0.1	80.3
Synthetic jatropha	78.26	12.26	9.48	42.3	1.9	0.1	75.8

The CHNS result shows a reduction of oxygen content between the raw and processed samples. For most of the processed vegetable oils, as the temperature increases from 250 to 350 °C, the oxygen content increases. This might emphasise the reduction in molecular weight from the conversion of triglyceride to fatty acids or aldehydes or alcohol chains.

For linseed oil, the hydrogen content decreases from 250 to 350 °C. For jatropha oil, the hydrogen content is higher at 350 °C compared to the unprocessed sample. The carbon content decreases more particularly for the same vegetable oil. Comparing the HTL sample of linseed and sunflower oils, an energy content (HHV) is calculated with the latter suggesting that sunflower oil would be more suitable to be used as fuel. In general, the energy content (HHV) is higher at 250 °C. There is a sight change in the elemental compositions for the model fatty acids. For example for linoleic acid, the decrease of the hydrogen content shows that there could have been more double bonds in the resulting product.

The carbon content in jatropha oil is higher than its synthetic mixture which is correlated with the previous section where it is found that the concentration of stearic acid is doubled. Taking into account the error, the synthetic linseed and sunflower oils are similar to the respective vegetable oils. The oleic acid retains all the energy in the oil. Previous lipid analyses under hydrothermal liquefaction do not include elemental analysis therefore it is difficult to draw a conclusion.

5.4.2 Carbon mass balance

Table 5-5 includes the carbon mass balance in the aqueous and bio-crude; the carbon in the gaseous phase is calculated by difference from the two others. For the TOC, several measurements are obtained using the instrument until the repeatability was below 1 % and displays an average value. The TOC concentration values in the table are multiplied by the dilution factor (37) because the solution is made up to 1 litre.

Table 5-5: TOC concentration in ppm and the carbon mass balance of the aqueous phase, the carbon in the bio-crude oils and in the gas

	TOC (ppm)	% C aqueous	% C bio-crude	% C gas
		Sunflower oil		
250 °C	1922	1.9	78.5	19.6
300 °C	3993	4.8	92.7	2.5
350 °C	1329	1.5	90.7	7.8
		Linseed oil		
250 °C	2263	2.6	96.7	0.7
300 °C	2407	2.9	101.1	-4.0
350 °C	2356	2.8	96.3	0.9
		Soya bean oil		
250 °C	2263	2.6	95.3	2.1
300 °C	2407	2.9	101.0	-3.9
350 °C	2356	2.8	102.7	-5.5
		Jatropha oil		
250 °C	4267	4.9	92.0	3.1
300 °C	3593	4.1	81.7	14.2
350 °C	1404	2.2	89.6	8.2
		Palm oil		
250 °C	4441	5.1	94.2	0.7
300 °C	2385	2.8	65.9	31.3
350 °C	785	0.9	85.8	13.3
HTL oleic acid	496	0.6	99.1	0.3
HTL linoleic acid	230	0.3	92.7	7.0
HTL linolenic acid	256	0.3	86.3	13.4
Synthetic sunflower	1618	1.8	88.7	8.0
Synthetic linseed	2315	3.3	79.7	18.0
Synthetic jatropha	2089	2.3	80.5	16.9

The majority of the carbon fraction is measured in the bio-crude oil for vegetable oils and model fatty acids as high bio-crude oil yields are obtained over 80 wt.%. For linseed and soya bean oils, the carbon fraction, in the bio-crude, is over 100 %, which could be caused by the presence of remaining dichloromethane or some absorbed water.

The highest TOC concentration is obtained at 300 °C for sunflower, linseed and soya bean oils. For the experiment with jatropha and palm oils, there is a clear trend indicating the decrease of the carbon fraction in the aqueous fraction. Carbon

fraction, in the aqueous phase, can be found as glycerol because of its high solubility (≥500 g/L) [240]. Some aqueous samples are analysed by ionic chromatography and some acetate anions are detected for example with sunflower oil at 350 °C with a concentration of 6290 ppm; although, the level of most the sample is below the calibration range. It may indicate that mild cracking occurred to form carboxylic acid compounds. Watanabe et al. [230] claimed without given proof that acetic acid could be one product of the decarboxylation of stearic acid at 400 °C. The aqueous phase from the model fatty acid contains a low amount of carbon fraction indicating that the formation of low molecular carboxylic acid is low. The combination of fatty acids enhances slightly the formation of the lower fraction (or soluble compound carbon in the water) with higher the TOC concentration for the mixtures.

In summary, from this section, the following conclusions could be drawn:

- Triglycerides from vegetable oils during the HTL are mainly degraded as bio-crude with little production of gas and residues. A slight increase of bio-crude occurs with increasing temperatures.
- Sunflower, palm and jatropha oils are mainly hydrolysed to fatty acids. In contrast to linseed and soya bean oil, where a larger fraction to oligomers is formed caused by the formation of cross-linked compounds.
- The concentration of linoleic and linolenic acids decreases with temperature for most of vegetable oils as they are converted as oligomers. In addition, inter-cyclisation is observed with the formation of methyl-9-(o-propylphenyl)-nonanoate.
- The results with the synthetic mixtures and the fatty acids results in similar trends with the vegetable oils.
- From 250 to 350 °C, the oxygen content calculated from the elemental analysis, generally increases. The carbon content of the bio-crude is higher than initial vegetable oils explained by the hydrolysis of the triglycerides into fatty acids.

5.5 Influence of metal doped HZSM-5 catalysts on oil composition in water and in formic acid

In this section, the effect of the catalyst on the conversion of the vegetable oils to lighter fraction is investigated.

5.5.1.1 Mass balance yield

Table 5-6 contains the weight per cent bio-crude yield. With catalyst the coefficient of variance felt between 2-3 %.

Table 5-6: Mass balance yield of the bio-crude oil used to calculate the carbon mass balance for the experiment of the catalytic screening of sunflower oil

Reaction conditions	Bio-crude yield wt.%
Water	
No catalyst	86.0
HZSM-5	68.0
MoZSM-5	60.0
FeZSM-5	58.0
NiZSM-5	55.0
CuZSM-5	73.0
HTL oleic HZSM-5	53.0
Formic acid	
No catalyst	89.0
HZSM-5	55.6
MoZSM-5	68.0
FeZSM-5	70.0
CuZSM-5	65.0
NiZSM-5	77.0
HTL oleic acid	73.9

Bio-crude yields without catalysts are commonly above 85 wt.% whereas in the presence of HZSM-5 it is reduced to about 60 wt.% indicating that some cracking has occurred. Lower yields are obtained with NiZSM-5 and FeZSM-5 with 55 and 57 wt.%. After the experiment, 3 bar of gases is obtained with NiZSM-5 which suggests that some gasification reaction might have occurred as nickel is known to promote gasification [63]. For the other catalysts, the typical pressure obtained is 4 bar which is

higher than without any catalysts. Unfortunately, the gas analysis could not be carried out for these experiments thus it is not possible to determine the wt.% gas accurately.

Reactions were also carried out in 1 vol.% formic acid using the same catalyst in order to investigate the effect on the hydrogenation or producing *in-situ* hydrogen to reduce the unsaturated fatty acids in the oil. The pressure after the experiment is higher than in water alone (approximately 5-6 bar) indicating that formic acid is decomposing into hydrogen and carbon dioxide during the reaction. Without any biomass, 4 bar is obtained at 17 °C after the reaction. Yu et al. [155] measured that at 358 °C with a residence time of 15.2 seconds after the processing of formic acid was 32 vol.% of hydrogen, 42 vol.% of carbon dioxide and 1.4 vol.% of carbon monoxide. Compared with the run in water and in formic acid, the bio-crude yield is in the latter which could indicate that the cracking is lower in formic acid.

5.5.1.2 Characterisation of the bio-crude oils by GPC, GC-MS and TGA

In this section, some further analyses are carried out in order to demonstrate the activity of the catalyst using the gel permeation chromatography, the thermogravimetric analysis and the gas chromatography mass spectrometry. These techniques allow the investigation of the light fraction.

5.5.1.2.1 GPC analysis

Figure 5-6 represents the GPC fraction of the different molecular size during the catalytic screening in water (a) and in formic acid (b).

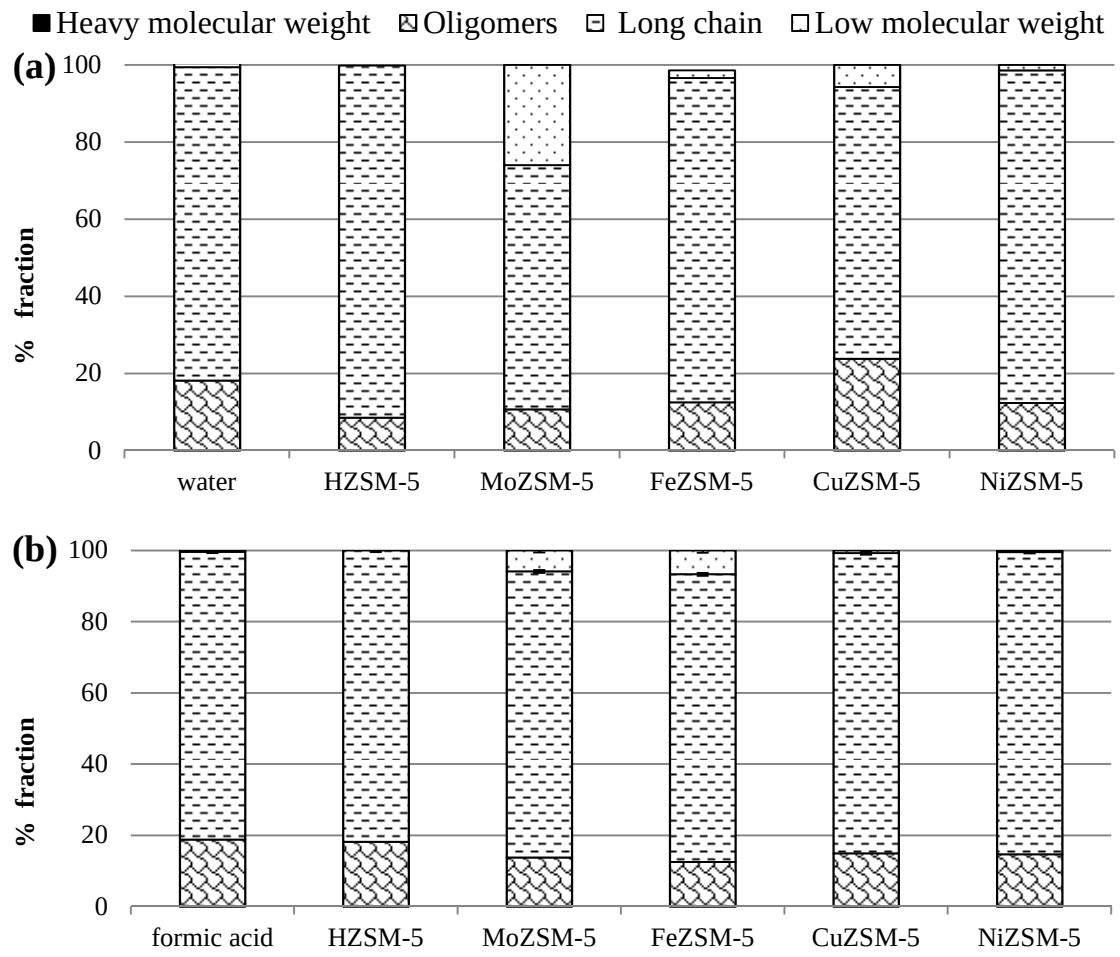

Figure 5-6: Diagrams representing the different molecular weight fraction of the catalytic screening of vegetable oils in water (a) and (b) in formic acid at 350 °C

From this Figure 5-6 (a), HZSM-5 contains in majority "long chain" materials and the lowest fraction of oligomers materials compared to the other catalysts. MoZSM-5 contains the highest fraction of lower molecular weight materials which could include aliphatic hydrocarbons and aromatic compounds. The fraction of oligomers is more significant with CuZSM-5. It is possible that this catalyst enhances the formation of oligomers.

From Figure 5-6 (b), for the run in formic acid, it illustrates that the overall difference between each fraction is low and the main fraction is the fatty acid. In comparison to the run without catalyst or with formic acid, there is low fluctuation with both showing around 18 % of oligomers. MoZSM-5 and FeZSM-5 are the only samples to contain low molecular weight materials. It is likely that some heavy waxes or "heavy molecular weight" materials could have been formed. FeZSM-5 and

MoZSM-5 contain the least fraction of oligomer materials. On the whole, the average molecular weight of the bio-crudes falls within 300-400 g/mol.

The GPC analysis of the processing of oleic acid in water, formic acid and with HZSM-5 is shown Figure 5-7. The molecular weight profile is similar compared the run in water and formic acid. For the processing of oleic acid and HZSM-5, a new peak (shoulder) appears at 8.5 minutes suggesting the presence of lower molecular weight material compared to oleic acid, although this technique could not confirm that some of oleic acid has been decarboxylised. A Similar shoulder-shape is observed in the GPC profile during the screening of sunflower oil with HZSM-5.

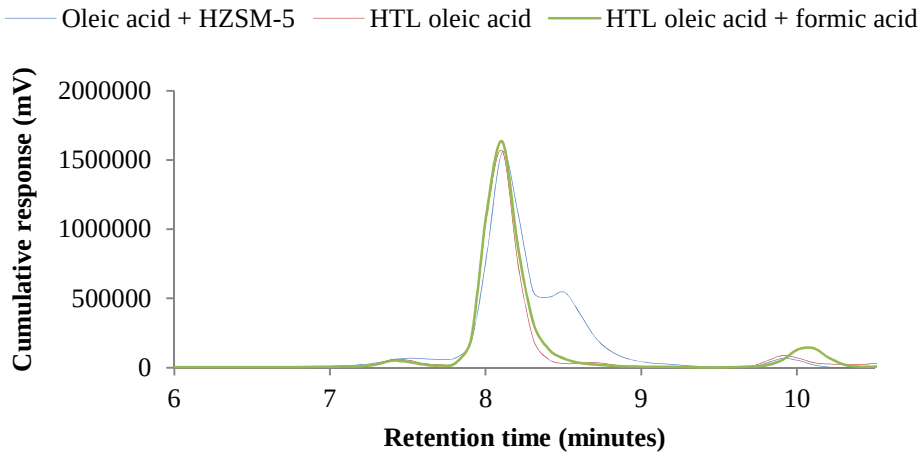

Figure 5-7: GPC overlay of the three chromatograms of oleic at 350 °C oleic acid with HZSM-5 or formic acid at the same temperature

5.5.1.2.2 Simulated distillation

Table 5-7 displays the different % derivative curve from the thermo-analysis of the different oils from sunflower oil using the catalytic screening. The different fractions used is based on the literature [241]. The value below 100 °C is removed as it is assumed that it is residual water and dichloromethane.

Table 5-7: The wt.% of the different distillation range for the catalytic screening of sunflower in water

	Gasoline-like ≤ 170 °C	**Kerosene-like 170-250 °C**	**Diesel-like 250-350 °C**	**Fuel oil-like 350-400 °C**	**Residue ≥ 400 °C**
Raw sunflower oil	0.0	2.9	37.7	14.2	45.2
		Water			
No catalyst	1.9	62.8	26.8	1.6	6.9
HZSM-5	8.8	81.0	7.0	0.6	2.6
MoZSM-5	16.1	71.1	9.0	0.6	3.2
FeZSM-5	3.6	23.9	61.5	3.6	7.3
CuZSM-5	14.6	73.8	8.8	1.4	1.4
NiZSM-5	21.0	69.1	7.6	1.2	1.2
		Formic acid			
No catalyst	7.7	68.7	18.1	1.6	3.9
HZSM-5	6.6	71.7	14.1	1.6	5.9
MoZSM-5	7.0	61.0	27.9	2.1	2.1
FeZSM-5	15.6	73.8	8.0	1.3	1.3
CuZSM-5	17.3	70.8	8.1	1.9	1.9
NiZSM-5	16.2	69.0	10.8	2.0	2.0

Initially, the boiling curve from the raw sunflower oil contains mostly high temperature boiling compounds whereas for the run without catalyst the boiling range is found in the diesel and kerosene range. Using different arrays of metal inside the HZSM-5 have an impact on the boiling curve of the different bio-crude. With HZSM-5, most of the fractions are kerosene-like with 81 wt.%. The curve using MoZSM-5 suggests the presence of 16.1 wt.% of gasoline-like fraction. The gasoline-like fraction is more significant with NiZSM-5 with approximately 21 wt.%. It emphasises that these catalysts enhance the cracking of sunflower oil. The diesel-like range is enhanced by FeZSM-5 with 61.5 wt.%. The run with no catalyst 26.7 wt.% of diesel-like range is produced and is explained by the presence of oligomers.

More diesel-like range and kerosene-like with formic acid are measured for most of the catalysts especially with MoZSM-5. NiZSM-5 in water contained more gasoline-like ranges compared to the HTL run in formic acid. The analysis of the bio-crude oils using GPC and the TGA do not match however since GPC shows that only MoZSM-5 and FeZSM-5 contain low molecular weight materials. This anomaly is difficult to explain although it could be due to interactions between molecules and the stationary phase over estimating the molecular weight of the fractions during GPC.

5.5.1.2.3 GC-MS analysis

GC-MS is only capable of measuring the material which is volatile and has a boiling point below approximately 300-400 °C. In other words, only the gasoline, diesel and kerosene range could be analysed. With doped metal HZSM-5 catalysts however this accounts for 70 % of compounds. The column and the method were previously identified by Biller et al. [196] and Ross et al. [129] as the most suitable parameter for bio-crude oils analysis. Figure 5-8 contains three different chromatograms: (a) is the run without any catalysts, chromatograms with (b) MoZSM-5 and (c) with HZSM-5. Table 5-8 lists the main compounds identified in the bio-crude.

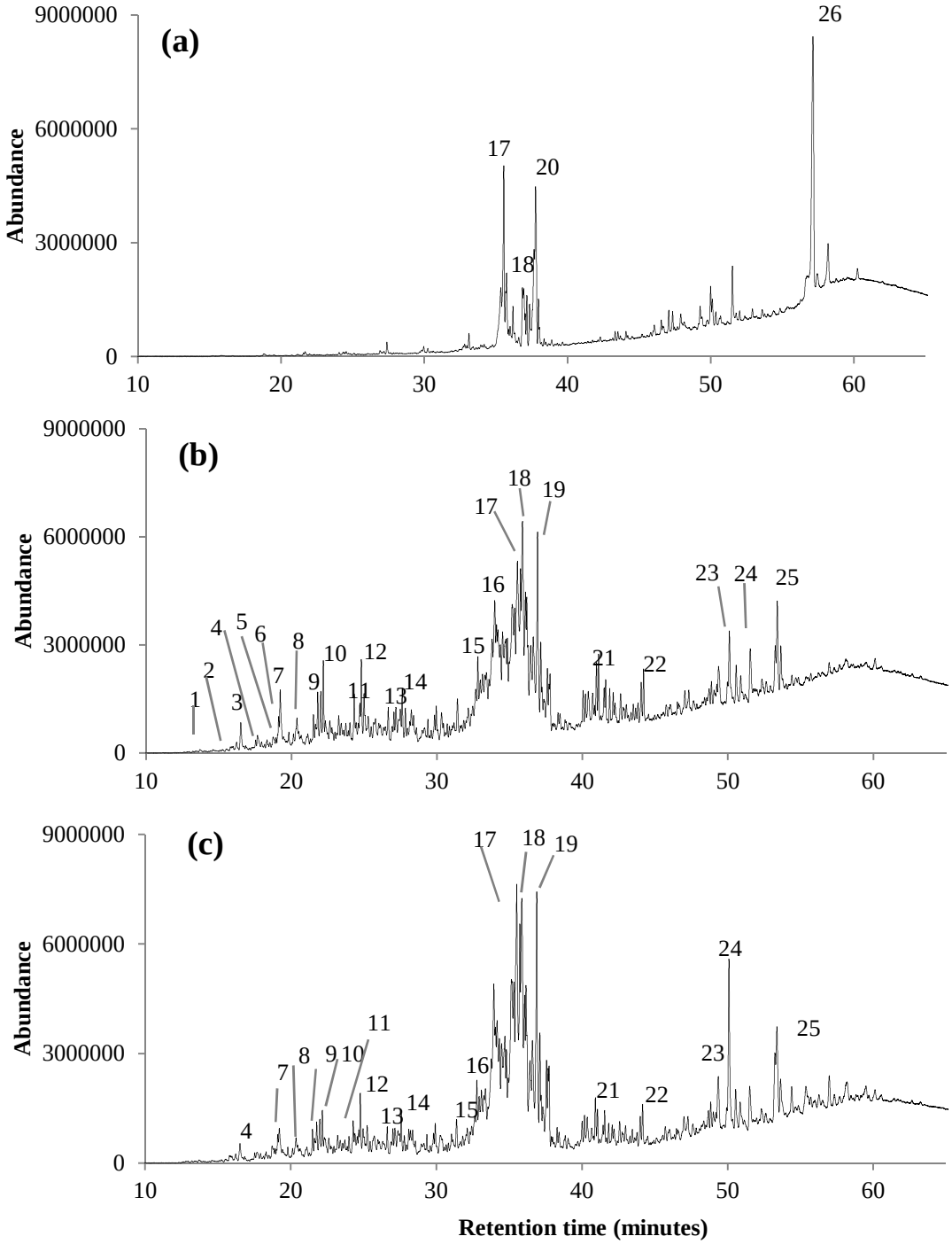

Figure 5-8: GC-MS chromatograms of oil from hydrothermal processing of sunflower oil at 350 °C in (a) water alone without a catalyst, (b) in the presence of MoZSM-5 catalyst and (c) in the presence of the HZSM-5

Table 5-8: Identification of compounds from previous chromatograms

Number	Retention time (minutes)	Compounds
1	12.8	o-xylene
2	14.7	3-ethyl-2-pentene
3	16.5	decene
4	17.4	1-ethyl-2-methyl benzene
5	18.2	3-undecene
6	19.0	4-undecene
7	19.2	1-methyl-3-propyl-benzene
8	19.8	decahydronaphthalene
9	21.8	dodecene
10	22.2	1,3-ethyl-dimethyl-benzene
11	24.3	1-methyl-butyl-benzene
12	25.8	1,4-methyl-2-(2-methyl-propyl)-benzene
13	26.6	1-methyl-2-methylenecyclohexane
14	27.1	1-methyl-3-hexyl-benzene
15	32.8	2,6-dimethyl-naphthalene
16	34.6	tridecanol
17	35.5	3-heptadecene
18	35.8	8-heptadecene
19	36.9	1,6-dimethyl-cyclohexane
20	37.0	Z,Z-10,12-hexadecadienal
21	40.9	1,2 dimethyl-cyclohexene
22	44.0	1,2,3-tetrahydro naphthalene
23	50.0	cyclohexyl
24	51.5	oleic acid
25	53.4	fluoranthene
26	57.0	Z,Z-9,12-octadecadienoic acid

The numerated peaks are identified by the NIST library with highest probability. Chromatograms could be divided into three portions: the first section from 10 to 30 minutes contained the short alkenes (C_5-C_{12}), aromatics and some oxygenated compounds such as alcohols and ketones; the second section with C_{16}-C_{17} alkenes or

aldehydes chains and the remaining section with C_{18} chain with fatty acids. The chemical structures of some molecules are included in Figure 5-9.

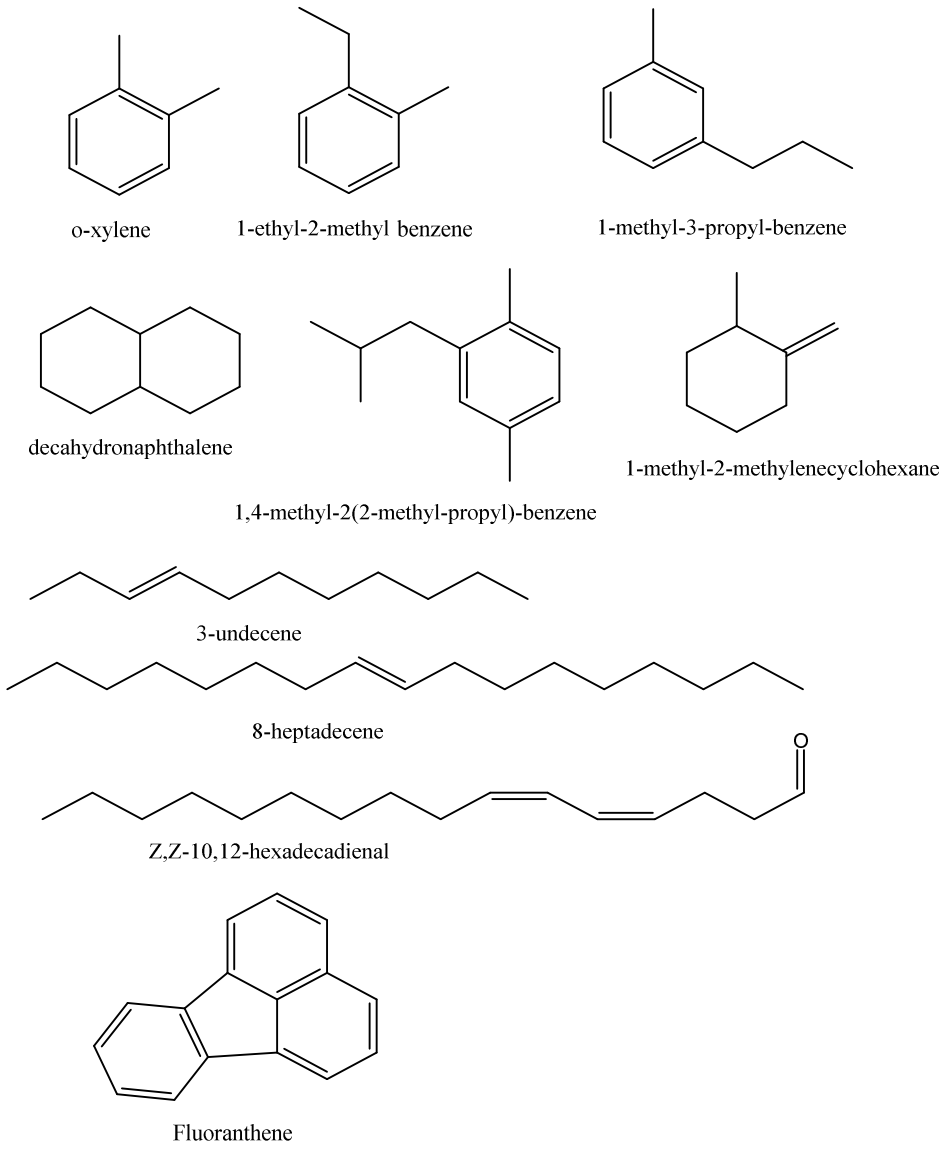

Figure 5-9: Chemical structures of some molecules identified in GC-MS

An attempt to improve the quality of the chromatogram is engaged in order to change the temperature program in order to improve the peak resolution however with some minor changes for example between 30 and 40 minutes the poor resolution could be explained by close molecular/polarity structure and the column is not able to separate these materials further. Furthermore, the signal after 50 minutes is caused by fatty acids which are poorly retained by the column.

The first chromatogram (a) shows that in the absence of catalysts, some fatty acids are cracked into aliphatic compounds such as heptadecene in agreement with

previous results by the TGA and the GPC analysis. The Z,Z-10,12-hexadecedienal found at 37 minutes has been identified by Li et al. [236] as a key compound in the reduction of linoleic acid but also for the possible formation of aromatics afterwards. For the aliphatic chains, more alkenes rather than alkanes are identified, Watanabe et al. [230] also identified alkenes as one of the major products from the decarboxylation of stearic acid under supercritical water and using basic catalyst such as CeO_2 or ZrO_2.

More aromatics compounds such as the 1,3-ethyl-dimethyl-benzene; 1-methyl-butyl-benzene; 1,4-methyl-2-(2-methyl-propyl)-benzene are identified with MoZSM-5. It explains why with GPC a fraction of 18 % of low molecular weight materials is observed. Less aromatic compounds are identified with HZSM-5 with rather more short alkenes, suggesting that molybdenum improves the selectivity toward the formation of aromatic compounds.

The chromatograms displayed in Figure 5-10 compare the bio-crude for the run with (a) in formic acid, (b) HZSM-5 in formic acid and (c) MoZSM-5 in formic acid.

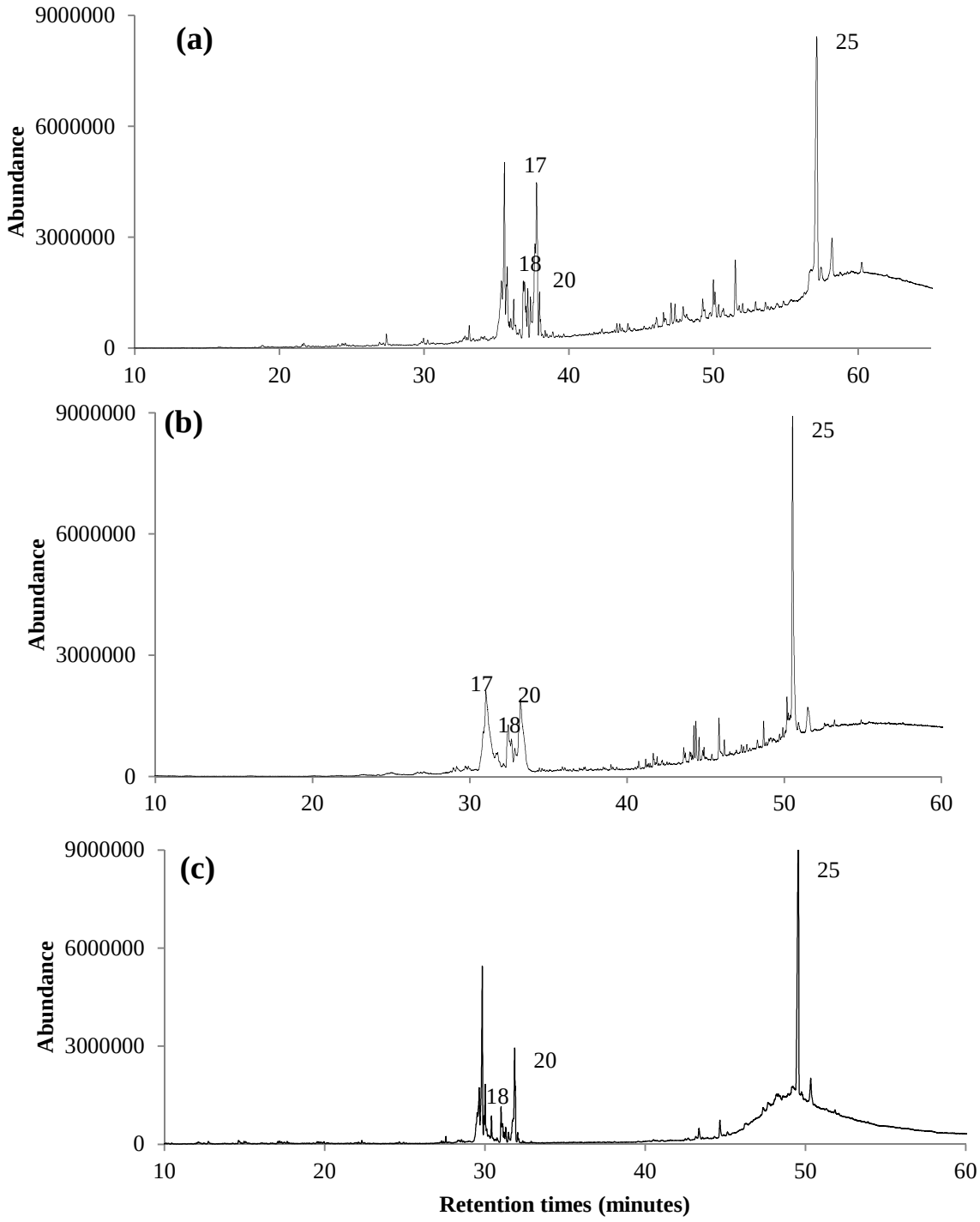

Figure 5-10: GC-MS chromatograms of the different samples as (a) run in formic acid (b) run of sunflower oil with HZSM-5 and (c) with MoZSM-5 in formic acid

Similar chromatograms are observed when using catalysts and formic acid. Lower aromatic compounds were produced compared to the GC-MS chromatograms with water. It is likely that formic acid hindered catalytic activity. Peak intensity is higher with the Z-Z-hexadecadienal, it would suggest that aldehydes is more stable

under this solution, it is the reason why Diels-Alder reaction could not take place. More alkenes are also observed compared to the experiment in water.

5.5.1.2.4 Composition of FAME analysis

The concentration of the different fatty acids after the hydrothermal reaction with the catalytic screening was shown in the Figure 5-11. A coefficient of variance of 11 % was calculated.

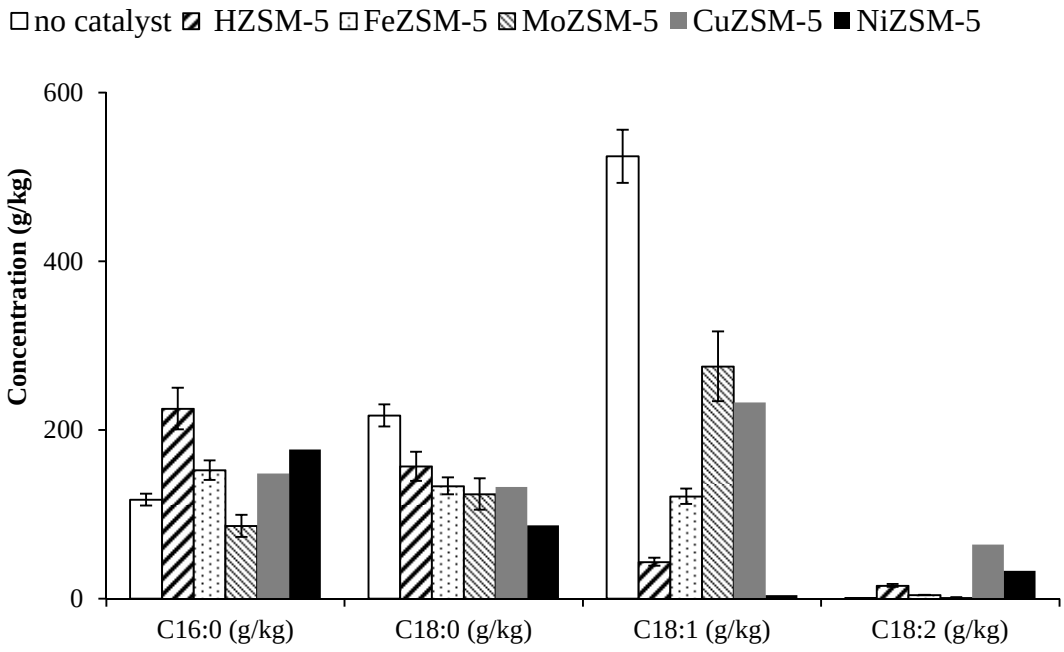

Figure 5-11: FAME composition of the different metal doped ZSM-5 processing with sunflower oil at 350 °C in water

The presence of catalysts increases the non-FAME content as it is observed in the previous section however this could not be quantified. The analysis of FAME indicates that the oleic acid concentration is reduced by HZSM-5. FeZSM-5, CuZSM-5 and MoZSM-5 have less impact on reducing oleic acid compared to the other catalysts. A slight decrease of stearic acid is observed for most of the catalyst yet it is more pronounced compared to the other fatty acids. The palmitic acid concentration fluctuates more which could be explained by a poor reproducibility of the peak. No oleic acid is detected with NiZSM-5.

In order to emphasise that HZSM-5 has an impact on the isomerisation of the fatty acid, oleic acid only is processed at 350 °C with HZSM-5. The initial

concentration of oleic acid is 5692.0 g/kg, without catalyst the concentration is 3780.5 g/kg and with HZSM-5 is only 446 g/kg. The MS library has identified that the oleic acid could be reduced as 7-octadecenoic acid and 15-octadecenoic acid. The fraction of other molecules is also important with some alkenes 3 or 8-heptadecene however these compounds could not be quantified.

Figure 5-12 includes the FAME composition using different metal doped catalyst in formic acid.

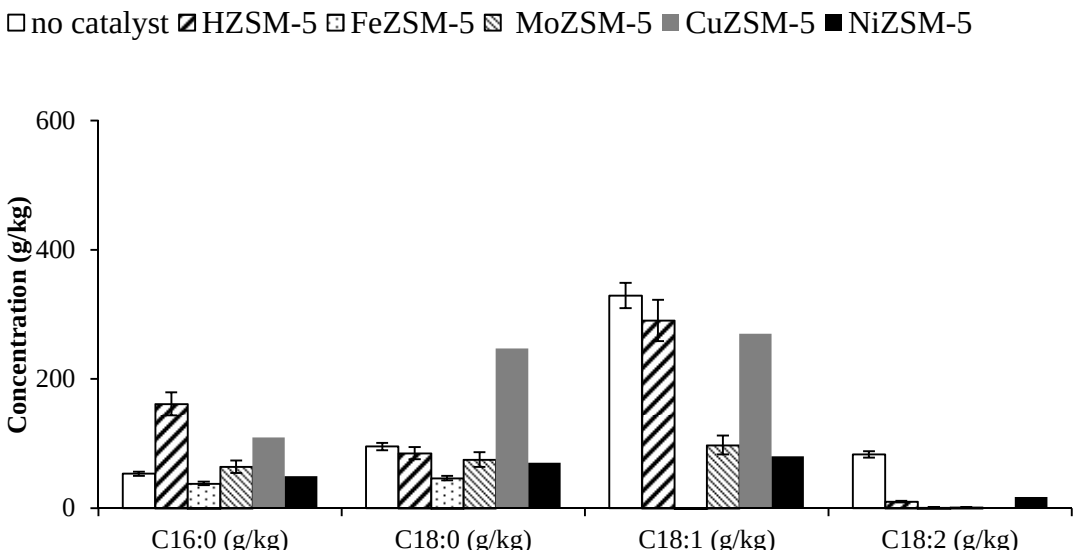

Figure 5-12: FAME composition of the different metal doped ZSM-5 processing with sunflower oil at 350°C in formic acid

Replacing water with formic acid in combination with FeZSM-5, MoZSM-5 also reduce the oleic acid concentration, although, there is no evidence that oleic acid is hydrogenated to stearic acid as the concentration is not increased. On the whole, the overall concentrations are much lower than without catalyst. The concentration of linoleic acid is less significant compared that without any catalysts.

One experiment with oleic acid in 1 vol.% formic acid was carried out. The FAME analysis shows different isomers of oleic acid are detected including the 7-octadecenoic acid and the 8-octadecenoic acid. The concentration of the 9-Z is 510 g/kg whereas the raw is 5692 g/kg. No stearic acid (octadecanoic acid) is detected implying that the gas produced from the decomposition of formic acid does not hydrogenate the double bond but induces the conjugation of the double bond. Some traces of E-14-hexadecenal and 2-(3H)-furanone-dihydro-5-tetradecyl are also observed; the last compound are detected by Fu et al. [242].

5.5.1.2.5 Elemental analysis

The elemental analysis of the bio-crude oils with the metal doped and sunflower oil is found in Table 5-9.

Table 5-9: Elemental composition as received of the oils using the different catalysts in water

	C wt.%	H wt.%	O wt.%	HHV (MJ/kg)	H/C	O/C	% Energy recovery
Water							
No catalyst	76.8	11.49	11.7	40.3	1.8	0.1	92.3
HZSM-5	80.4	11.9	7.7	42.8	1.8	0.1	72.0
MoZSM-5	80.0	11.6	8.4	42.1	1.7	0.1	67.1
FeZSM-5	75.5	11.4	13.1	39.5	1.8	0.1	65.4
CuZSM-5	74.4	11.6	13.9	39.3	1.9	0.1	76.1
NiZSM-5	77.2	11.7	11.1	40.8	1.8	0.1	50.0
Oleic HZSM-5	78.3	12.3	9.5	43.2	1.9	0.1	55.9
Formic acid							
No catalyst	74.2	11.9	14.0	39.5	1.9	0.1	44.6
HZSM-5	76.3	12.0	11.7	40.8	1.9	0.1	60.3
MoZSM-5	75.9	11.8	12.3	40.3	1.9	0.1	73.1
FeZSM-5	78.0	12.1	9.9	41.9	1.9	0.1	78.0
CuZSM-5	69.4	10.8	19.8	35.4	1.9	0.2	81.0
NiZSM-5	74.8	11.6	13.6	39.4	1.9	0.1	75.0
HTL oleic acid	72.2	12.0	15.8	43.0	2.0	0.2	76.0

For the run in water, the result illustrates that the addition of HZSM-5 and metal doped HZSM-5 help to reduce oxygen content in the bio-crude oils. It is more significant with HZSM-5, MoZSM-5 with respectively 7.7 and 8.8 wt.% of oxygen content. In addition, the carbon content for HZSM-5 and MoZSM-5 is the highest, in this way, a high heating content is calculated which is similar to the petroleum oil with 42-44 MJ/kg [243]. Higher oxygen content with CuZSM-5 is detected compared to the reaction at 350 °C indicating that an oxidation might have occurred. It was also possible that these samples contain more residual water. Yet the decarboxylation is less pronounced compared to the result published by Mo et al. [189] because more catalysts and higher temperature with supercritical conditions are used.

For the runs in formic acid, HZSM-5 and MoZSM-5 have an oxygen content slightly higher indicating that the deoxygenation is less significant in this solution. The lowest oxygen content is calculated for FeZSM-5, moreover it has an high energy content with 41.9 MJ/kg. It points out that catalysts are less active in formic acid compared to water. Less products from the secondary cracking is found for example with aromatic compounds enhancing only the primary cracking product with heptadecene and Z,Z-hexadecadienal and fatty acids [215]. Formic acid has the highest energy recovery compared to the run carried out in water. The hydrogen content for the oleic acid processed in formic acid is slightly lower compared to the run in water (12.5 wt.%). Higher hydrogen content implies that the double bond is hydrogenated, for instance the hydrogen content of stearic acid is 13.3 wt.%. It explained why no stearic acid is observed during the FAME analysis.

The amount of hydrogen formed during the decomposition of formic acid is not sufficient to hydrogenate double bonds as they are more stable in hydrothermal conditions. Noble metals are necessary to improve this reaction. In the case most of formic acid is converted into hydrogen and carbon monoxide; 27 mol of hydrogen would be necessary to hydrolyse a triglyceride containing 5 double bonds. The use of 1 vol.% formic acid or 0.26 M only 2 mM could be produced [155].

5.5.1.3 Carbon mass balance

Table 5-10 shows the TOC concentration and the carbon mass balance in the aqueous phase, bio-crude and gaseous phases for the catalytic screening in water and in formic acid.

Table 5-10: TOC concentration in ppm and the carbon mass balance of the aqueous phase, the carbon in the bio-crude oils and in the gas

	TOC (ppm)	% C aqueous	% C bio-crude	% C gas
		Water		
No catalyst	1329	1.5	90.7	7.8
HZSM-5	925	1.3	69.8	28.9
MoZSM-5	958	1.3	65.8	32.9
FeZSM-5	1852	1.9	64.4	33.7
NiZSM-5	1251	2.1	48.8	49.1
CuZSM-5	2369	3.7	74.3	22.0
Oleic HZSM-5	2185	2.6	54.5	42.9
		Formic acid		
No catalyst	2619	3.9	43.1	53.0
HZSM-5	1080	1.5	58.2	40.3
MoZSM-5	3602	5.5	71.1	23.4
FeZSM-5	4979	7.2	78.6	14.2
CuZSM-5	9475	13.6	73.4	13.0
NiZSM-5	4949	7.5	81.9	10.5
HTL oleic acid	1480	0.6	70.1	29.3

For the run in water, HZSM-5 and MoZSM-5 reduce the level of organic carbon in the aqueous phase with respectively 925 and 958 ppm. The opposite trend is found with CuZSM-5 with higher bio-crude oils and TOC concentration. It could suggest that these catalysts were less active for cracking sunflower oils. The pH range of most of the processed water with vegetable oils is including within the 3-4 pH range. This means that most of the compounds, in the aqueous phase are acidic species. As expected half the carbon is converted in the gaseous phase selecting NiZSM-5.

For the run in formic acid, except for HZSM-5, the concentration of organic acids in the aqueous phase are more significant, in particular with CuZSM-5 with 9475 ppm. The high concentration gives a negative value for the gaseous phase; it is possible that the bio-crude contains some water and gave higher yield. It could also explain why a lower mass of bio-crude oils is found with the catalyst. It is likely that formic acid enhances the formation of soap thus fatty acid became more soluble in the aqueous acid but also some residual formic acid is present and increased the TOC

value. A blank experiment was carried out with formic acid at 350 °C and it was found that the concentration was 1472 ppm. Generally, the amount of carbon in the bio-crude oil is higher in the formic acid compared to water.

To summarise, the following conclusions could be drawn from this section

- NiZSM-5 and MoZSM-5 are the most reactive towards sunflower oil with the formation of the highest fraction of gasoline. HZSM-5 and MoZSM-5 have the lower level of oxygen in the bio-crude.
- HZSM-5 enhances the isomerisation of oleic acid and with some extent the reduction of size
- FeZSM-5 enhanced the formation of diesel-like fraction measured by the simulated distillation.
- MoZSM-5 increases the formation of aromatics. Compared than the runs without catalyst, the zeolite increases slightly the formation of alkenes.
- HZSM-5 has a lower reactivity in formic acid compared than in water.
- Formic acid enhances the delocalisation of the double bond of oleic acid and increased the % carbon in the aqueous phase.

5.6 Discussion of the degradation of lipids

There are several factors which can be drawn from most of the experiments without catalysts carried out with the different vegetable oils. Figure 5-13 shows the reaction from a triglyceride to a diglycerides where R represents C_{18} chains. Figure 5-14 contains the chemical pathways of the possible degradation of vegetable oils including oleic, linoleic and linolenic acids.

1) The hydrolysis of most of the vegetable oils (sunflower, linseed, jatropha, soya bean and palm oils) is completed around 300 °C. In previous literature, the hydrolysis of triglyceride to diglyceride and free fatty acids involved a first kinetic order [233]. The hydrolysis occurs in three steps where for each reaction, a fatty acid is released resulting in three fatty acids and one molecule of glycerol. The equilibrium of the full hydrolysis is reached in 2.5 hours in 225 °C whereas at 280 °C the hydrolysis can be achieved in 30 minutes [244].

2) As the level of polyunsaturated fatty acid such as linoleic and linolenic acids increase, the fraction of oligomers and “heavy molecular weight” materials is more significant. Furthermore, delocalisation of the double bonds is observed with the FAME analysis. Unfortunately the different isomers could not be quantified with this technique.

3) As delocalisation occurred, it is possible that the fatty acids undergo internal cyclisation as suggested Li et al. [236] and in depth by Dobson et al. [236, 239]. Two types of cycles have been identified with the GC-MS, a benzene aromatic ring from the carbon position 10 and 15 and another C_{18} fatty acid with a propyl cycle. The benzene ring might be formed by a 1,5 hydrogen shift involving a radical mechanism [245]. Dobson et al. [105, 246] identified only the formation of fatty acids containing non-aromatic cycles. These products are usually predicted during the heating in air. In hot compressed water, most of the mechanism involves protons however; as the temperature increased towards 350 °C a radical reaction may also be likely, therefore a hydrogen shift could have happened.

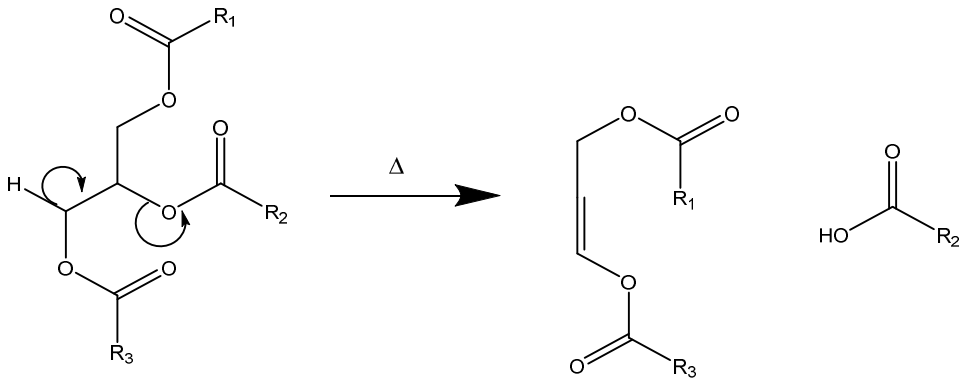

Figure 5-13: Proposed mechanism for the formation of diglycerides (Reaction 5-1) [215]

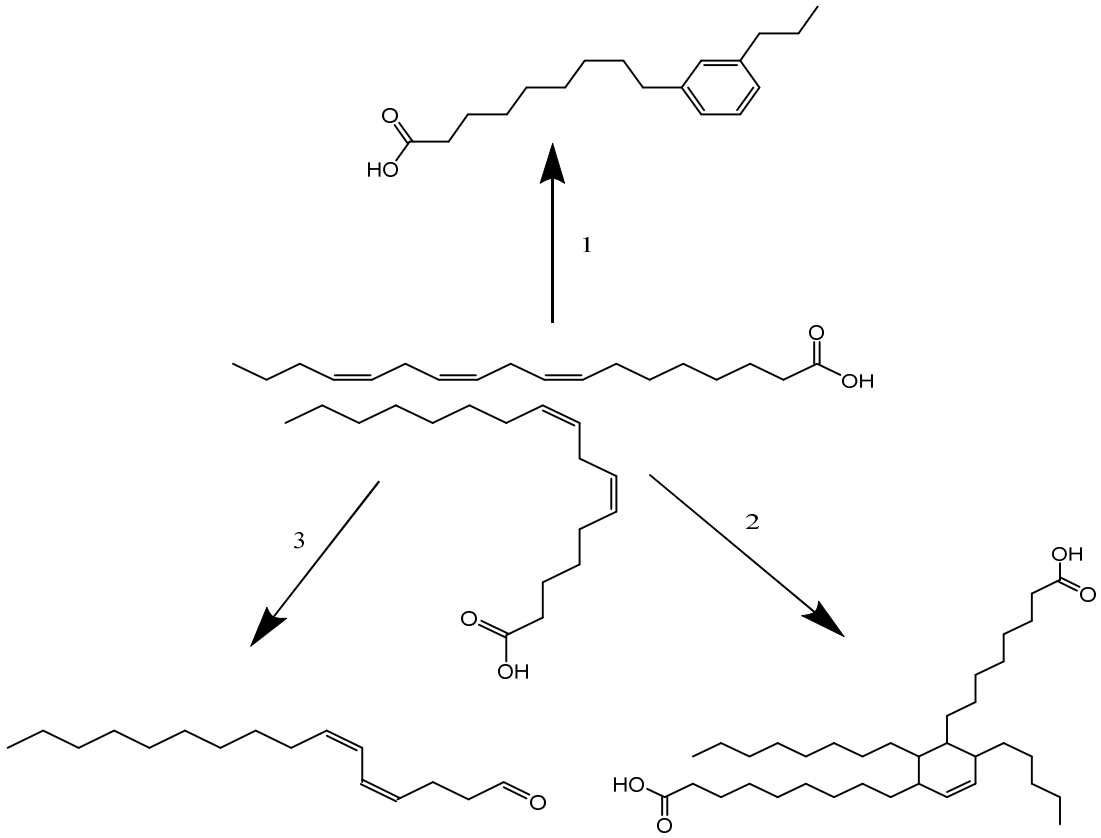

Figure 5-14: Proposed main mechanism step for the degradation of lipids in subcritical water where 1= Inter-cyclisation of linolenic acid 2= Intra-cyclisation via Diels-Alder between oleic and linoleic 3= Deoxygenation of linoleic acid

The formation of dimers could be possible by Diels-Alder, where the reaction of the cross linking consisted of the formation of a “bridge” between each chain forming a polymer. Moreover, it is possible with high concentration of unsaturated fatty acids that the samples are oxidised and form dimers (peroxy) [22]. It is why it is most suitable to produce biodiesel using saturated or hydrogenated fatty acids because they are more stable. The long storage and the long heating and cooling stages could induce the formation of epoxy chain (bonding) and increase the molecular weight of

the bio-crude oils. Without catalyst, linoleic acid can be reduced into aldehydes for example the Z,Z-10,12-hexadecadienal from the conjugated linoleic acid.

The formation of “heavy molecular weight” and oligomer materials is problematic if the bio-crude is used as a fuel as these compounds have a low burning capacity as was observed during the boiling curve of linseed oil. Li et al. [236] claimed that the addition of saturated $ZnCl_2$ at high temperature at 700 °C reduced the amount of cross linking compounds but it was not relevant to use such high temperature. An experiment with linseed oil was performed at 350 °C using $ZnCl_2$ (0.1 M) although no effect has been observed on the reduction of the molecular size fraction.

The result shows that HZSM-5 is more active with sunflower oil compared to the other vegetable oils. As seen in the previous chapter, HZSM-5 has nanopores approximately 3.6 Å, whereas the size of a model triglyceride here triolein (a triglyceride with C_9 chain) with a size of 6.3 by 4.03 Å could not enter in the pore. Therefore, only fatty acids are small enough to go through the pore and undergo cracking with the Brønsted site or Lewis [232]. Zeolites are involved in β cracking; under pyrolitic environment and high temperature above 400 °C, the high acidity of HZSM-5 favours the production of aromatic compounds, short olefins propene, butene which form via the Diels-Alder reaction. The drawback is the formation of coke which blocked the pore and deactivated the catalyst [179, 216].

Molybdenum (Mo) is more selective for the production of aromatic compounds compared to the other catalyst as this metal with HZSM-5 is used to produce benzene from methane at high temperature [221]. The majority of the aromatics found in the bio-crude oils are bi or tri substituted as ortho (1,2) or metha (1,3) configuration. Kubatova et al. [179] suggested that aromatics could also be produced by internal cyclisation. HZSM-5 has a strong Brønsted and Lewis acidic sites which allows the conversion of straight fatty acids. Doped metal has an impact on the coordination and absorption of the carboxylic group in order to decarboxylase and hydrolyse using the aluminium site inside afterwards [247]. Even with a small loading the different metals seem to have an effect within the error range. From the TGA analysis, it is observed that iron is more selective to produce diesel-like material; it is surprised that it is not identified using the GPC method. However, it should be pointed out that aromatic and alkene compounds do not represent a majority of the

total compounds contained in the bio-crude oil, even though, with sunflower oil, the GPC, GC-MS and TGA analysis indicate that the gasoline fraction is more abundant compared with other vegetable oils.

Mo et al. [189] obtained full conversion of palmitic acid with the production of long alkane chain and benzene, toluene and xylene (BTX). Nevertheless, this reaction was carried out at 380 °C for 180 minutes and the catalyst loading was 1:1 with the sample, at these conditions the water is in supercritical state [189]. Thus, the properties are quite different and in this study only the loading is less 1:6, the reason is because in industry a small amount of catalysts are usually preferred and also with a lower temperature. One experiment is undertaken using palmitic acid however it failed as at room temperature the fatty acid is insoluble in the water and it formed as crust which blocked the reactor. Vardon et al. [248] proposed a novel system where unsaturated fatty acids were hydrogenated by hydrogen produced in-situ from glycerol and Pt/C at 300 °C; this would avoid using high pressure hydrogen, generally 40 bar, which is a hazardous process.

5.7 Implications for the hydrothermal liquefaction of microalgae

The overall goal of this study is to have a better understanding of the fate of the lipids during the hydrothermal liquefaction of microalgae as they are a major constituent in the composition. Table 5-11 lists some examples of composition of fatty acids for five microalgae from the publication of Volkman et al. [249].

Table 5-11: Examples of composition for different microalgae from Volkman et al. [249]

Fatty acids	*Spirulina*	*Chlorella*	*Dunaliella*	*Nannochlopsis*	*Skeletonema*
Total lipids wt.%	7.0	9.0	22.0	28.0	13.0
polyunsaturated C16	0	0	25.2	19.5	13.1
C16:1	7.8	18.7	2.9	11.3	30.5
C16:0	52.6	25.1	14.7	20.1	16.5
polyunsaturated C18	28	16.1	51	32.1	2.8
C18:1	0	25.3	2.3	5.3	1.5
C18:0	8.3	5.6	0.4	1.1	0.8
Others	3.4	9.2	28.7	30.1	47.9

Some microalgae contain more mono or saturated fatty acids which would not affect the molecular weight. *Dunaliella t.* and *Nannochloropsis* contain more polyunsaturated fatty acid thus it would be expected to see “heavy molecular compounds” materials in the bio-crude oils.

Microalgae could also contain from 10 to 50 wt.% of phospholipids. Changi et al. [250] investigated the hydrothermal degradation of 1,2-dioleoyl-sn-glycero-3-phosphocholine (phospholipids). The hydrolysis into oleic acid, phosphoric acid and choline occurred readily. Free fatty acids may catalyse the hydrolysis of other macromolecules from microalgae.

Zou et al. [124] processed *Dunaliella t.* under sub to supercritical water where a yield of 38 wt.% at 360 °C was achieved; although there is no study concerning this lipids composition and the formation of oligomers. However, there are different elements such as proteins and carbohydrates which also favoured the formation of “heavy molecular weight” material; they will be discussed in more detail in the next chapters. The presence of nitrogen as ammonium compound with lipid could be a problem since long chain amide is formed.

5.8 Conclusion

To conclude, it was deduced that hydrolysis of most triglycerides took place below 300 °C. The gel permeation chromatography showed that the main molecular fraction range was mainly fatty acids for sunflower, jatropha and palm oils. The large concentration of linoleic or linolenic acids with linseed oil enhanced the fraction of oligomers and “heavy molecular weight” materials in the bio-crude oil. It was suggested from result in the literature that polyunsaturated fatty acids underwent cross linking or oligomerisation reactions. As temperature increased, the concentration of linoleic and linolenic concentrations decreased. The results with model compounds were consistent with the vegetable oils. Oleic acid was more stable under hydrothermal conditions. Without catalyst a low amount of linoleic acid was reduced into aldehyde Z,Z-10,12-hexadecadienal. Delocalisation of the double bonds allowed the Diels-Alder reaction to take place. There was evidence of internal cyclisation with the identification of methyl 9-(o-propylphenyl)-nonanoate. Using catalyst, HZSM-5 had some impact on isomerisation of some fatty acids such as oleic acid, MoZSM-5 was slightly more selective for the production of aromatic, FeZSM-5 increased the amount of diesel-like fraction measured by the boiling curve. The catalysts with formic acid were less effective than in water and there was no evidence that the hydrogen produced in-situ hydrolysed the unsaturation of fatty acids.

Finally, for microalgae it could be problematic especially when the strain contains high amounts of polyunsaturated fatty acids as for example *Dunaliella*. In the next chapter another element carbohydrate will be studied in order to investigate its impact on the hydrothermal liquefaction of microalgae.

Chapter 6 The effect of HZSM-5 on the hydrothermal liquefaction of carbohydrates

This chapter presents and explains the results for the hydrothermal liquefaction of carbohydrates. Starch, glucose, alginic acid and mannitol have been chosen as model compounds. Experiments have been carried out at different temperatures in water (250, 300 and 350 °C) and at 350 °C in an organic acid (formic acid), alkali salt potassium hydroxide (KOH) and using heterogeneous catalyst HZSM-5 in water and formic acid.

6.1 Introduction

Carbohydrates including saccharides are a class of compounds synthesised by plants or animals which were used as fuels by organisms; they consist of polymers chains referred to as polysaccharides with some sugar units or monosaccharaides additionally oligosaccharides and disaccharides can be found. In chemical contexts, they are composed of carbon chains or cycles with an empirical of unit of $C_m(H_2O)_n$, most commonly C_5 cycles of fructose and C_6 of glucose for example are the most abundant. Cellulose and starch are both polysaccharides with glucose units but different structures, the cellulose forms a robust and linear layer because of the way in which it bonds β (1→4) in opposition to the starch which form a α (1→4) with a twisted and branched structure. Cellulose is scarcely found in microalgae. The composition and the amount of carbohydrates are dependent upon factors such as growth conditions, the time of the harvests. Glucose is the most common sugar in microalgae for example for *Dunaliella t.* with 85 wt.% of the total carbohydrate [251]. However, the total fraction of carbohydrates for the microalgae grown under autotrophic conditions is less than 15 wt.% [252]. Alginic (alginate) acid is one of the major constituents of the cell wall for brown seaweed, the polymer consists of two sugar. It is widely used in the food or pharmaceutical industry as an excipient in the form of a gel or a paste [253]. Mannitol is the linear version of mannose (cycle). *Phaeodactylum t.* contains 45 wt.% of mannose [251]. Mannitol is extracted in subcritical water from olive waste [254].

The behaviour of carbohydrates has been widely studied in hot compressed water (subcritical water) and in particular the hydrolysis of polysaccharides such as

cellulose and starch to produce glucose or organic acids [94, 255]. The hydrolysis of starch has been studied by Nagamori et al. [256] at low temperatures from 180 to 240 °C. A 64 wt.% yield of glucose was obtained after 10 minutes, which subsequently decreased with a rise in concentration of the products maltose, fructose and 5-hydroxymethylfurfural (5-HMF) with longer reaction times. In another study, it was shown that the molecular weight decreased in function of time (from 0 to 10 minutes) indicating the conversion of starch into monosaccharides or aldehydes [257]. Above 300 °C, the conversion of glucose was fast 90 % was converted in less than 3 seconds [258]. Similar trends were found with sodium salt of alginic acid with a fast hydrolysis to monomers above 200 °C [259].

The aim of this chapter is to gain a clearer understanding of the degradation of several carbohydrates (starch, mannitol, alginic acid and glucose) at different temperatures under acid or alkali conditions in hot compressed water. Furthermore, experiments with HZSM-5 in water and formic acid at 350 °C were performed to study the impact on the conversion of the starch, glucose, alginic acid and mannitol. It is proposed that these results will provide a deeper understanding of the significance of carbohydrates have in the formation of microalgae derived bio-crude oil. Potassium hydroxide was used in this chapter, because previous studies reported good results in alkali solution for the processing of carbohydrates [260].

6.2 Methodologies

In this chapter, the analysis techniques used in **Chapter 3** are repeated. The residue and gaseous carbon mass balance used in the section 6.4.4 where calculated according to the Equation 6-1 where % $C_{residue}$ is the weight per cent carbon of the residue or chars measured by CHNS, $m_{residue}$ is the mass of the residue in gram, $m_{raw\ sample}$ is the mass of the initial sample and $\%C_{raw\ sample}$ is the per cent carbon of the raw biomass and the carbon remaining Equation 6-2.

$$Carbon_{residue} = \frac{\%\ C_{residue}\ x\ m_{residue}}{m_{raw\ sample}\ x\ \%\ C_{raw\ sample}}$$

Equation 6-1

$$\%\ C_{remaining(gaseous)} = 100 - \%\ C_{aqueous\ phase} - \%C_{bio\text{-}crude} - \%C_{residue}$$

Equation 6-2

6.3 Chemical compositions

Table 6-1 includes the elemental composition on a dried basis with weight % carbon, % hydrogen and % oxygen, higher heating value (HHV) determined from the Dulong formula (**Chapter 3**) and the H/C ratio of the different sugars glucose, starch, alginic acid and mannitol.

Table 6-1: Elemental analysis o of the raw carbohydrates with glucose, starch, alginic acid and mannitol

	C wt.%	**H wt.%**	**O wt.%**	**HHV (MJ/kg)**	**H/C**
Glucose	40.0	6.7	53.3	13.5	2.0
Starch	38.5	6.4	55.0	12.3	2.0
Alginic acid	38.6	5.2	55.4	10.7	1.6
Mannitol	39.7	8.1	51.9	15.7	2.4

Glucose and mannitol are monosaccharides whereas starch and alginic acid are polysaccharides. The chemical formula of glucose is $C_6H_{12}O_6$ with cycle structure and mannitol $C_6H_{14}O_6$ with a linear structure Most of the carbohydrates used in this study contained high oxygen content, explaining their lower heating values. Alginic acid has a more complex structure of starch and cellulose as D-mannuronic acid and L-guluronic. These acids are the main constituent of the polymers. Therefore, it would require a high energy input to process these compounds. Figure 6-1 includes the chemical structure of glucose, mannitol, starch and alginic acid.

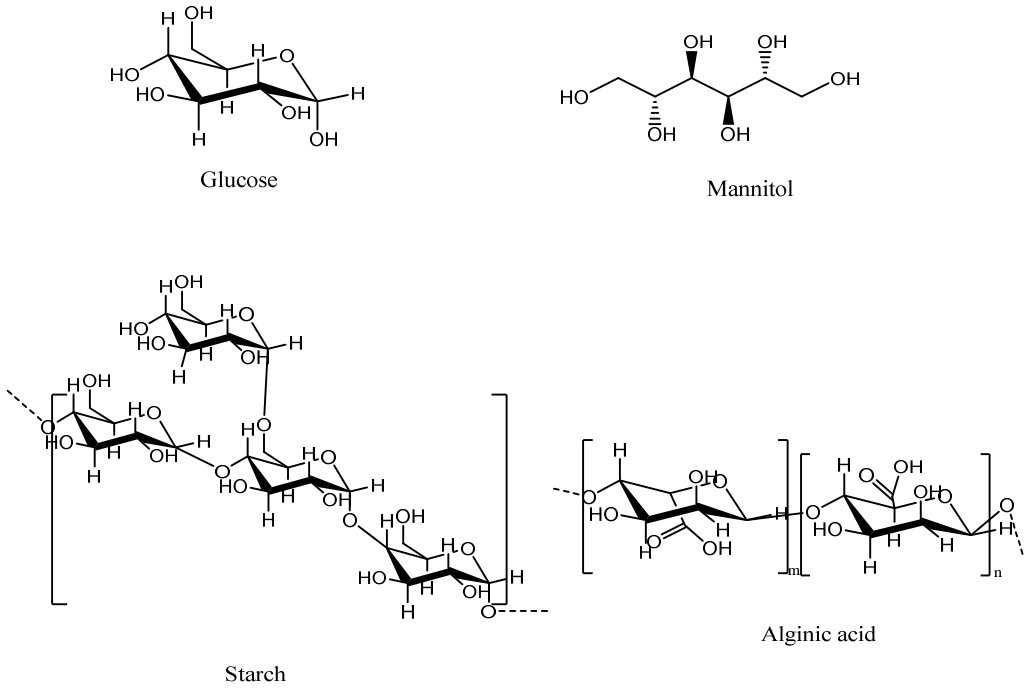

Figure 6-1: Chemical composition of the carbohydrate used

6.4 Effect of HTL temperature on oil composition

6.4.1 Mass balance yield

The products degraded via hydrothermal liquefaction are distributed into the oil, residue or chars, liquid and gaseous phases. Figure 6-2 represents the diagram for the mass yield of the different phase after the processing of starch with the bio-crude mass yield, the mass yield of the residue, the gaseous mass yield and the aqueous mass yield. The overall average coefficient of variance is 10 % determined from replicate the experiments. The coefficient of variance is higher than normal this is due to the difficulty in recovering the residue from the bottom of the reactor.

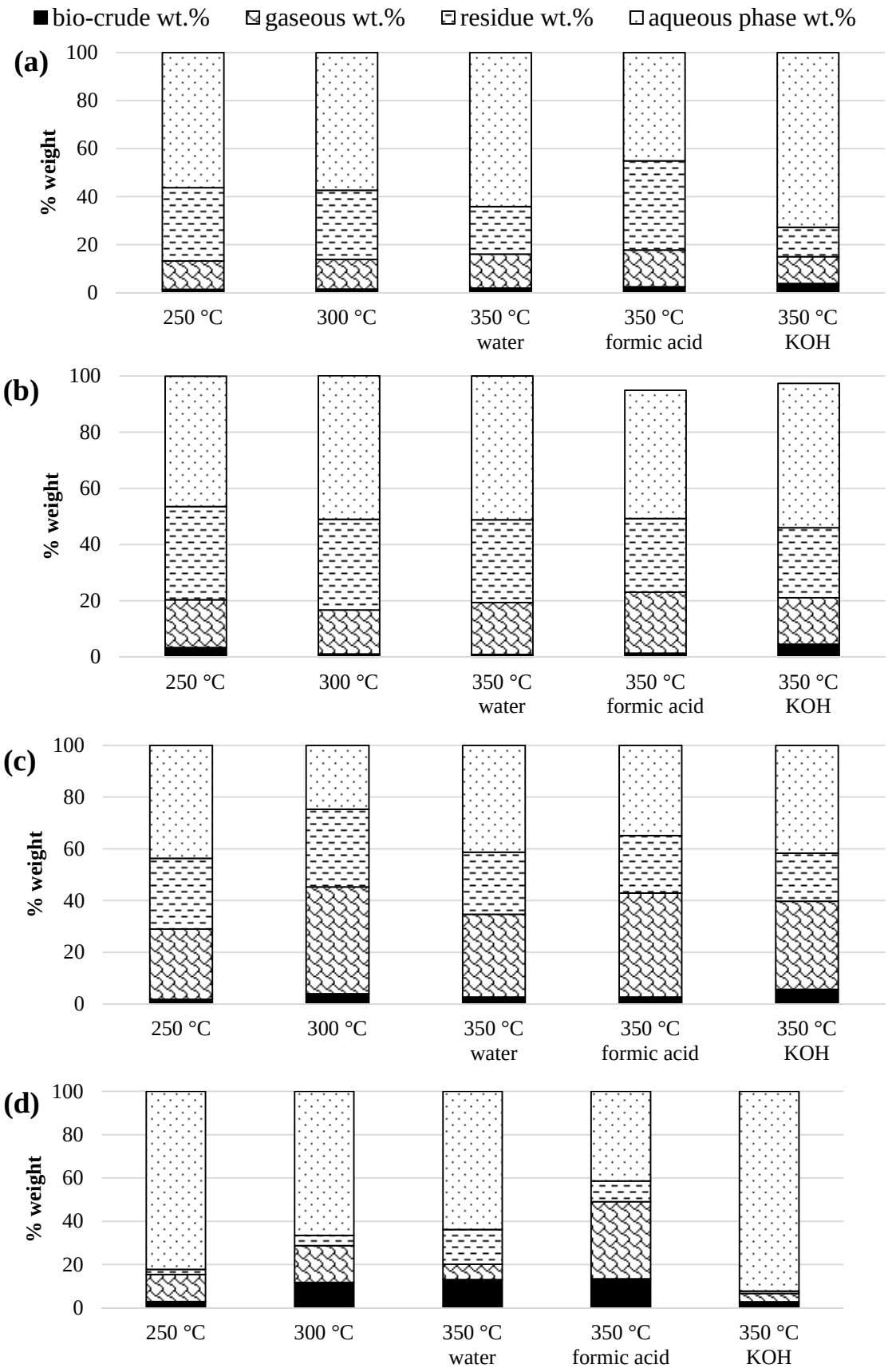

Figure 6-2: Diagram of the mass balance for the processing from 250 to 350 °C in water, formic acid and KOH (a) starch, (b) glucose, (c) alginic acid (d) mannitol.

For the processing of starch, glucose and alginic acid (Figure 6-2 (a), (b), (c)), the production of bio-crude yield is almost negligible at less than 5 wt.%. Carbohydrates are recognised for forming a lower amount of bio-crude oil or tar [261]. Mannitol (Figure 6-2 (d)) produces a higher yield of bio-crude which increases from 5 to 13 wt.% in relation to the temperature. Different values are obtained as mannitol has a linear structure instead of cyclic for example with glucose. Biller et al. [112] reported that the hydrothermal liquefaction of starch and glucose at 350 °C produced less of 10 wt.% of bio-crude.

Carbohydrates in subcritical water form higher residue yield. Overall, the gaseous and aqueous phase yields increase, whereas the residue (char) yield decreases when the temperature increases. For mannitol, less gaseous and residue yields are obtained implying that most of the degraded compounds are in the aqueous phase. The formation of high residue is probably caused by the slow heating rate of more than 9 °C/min.

For alginic acid, higher gaseous yield is obtained at 300 °C. There is some suggestion that the gas is produced from secondary cracking as no gas was detected after 200 seconds by Srkol et al. [261]. Carbon dioxide, with approximately 44 vol.%, was the major constituent of the gas measured from the degradation of starch for two hours at 350 °C observed by Williams et al. [262]. Promdej et al. [263] observed for glucose that the weight per cent of gaseous yield increased in relation to the temperature.

Aida et al. [264] remarked that as the residence time and the pressure increased the conversion of the glucose was higher, it was why at 350 °C the degradation was more rapid. Aida et al. [259] illustrated that the depolymerisation of sodium alginic was faster above 200 °C yielding high residue and gaseous yields.

For most of the carbohydrates, the addition of formic acid increases the formation of the gaseous and residue yields. Biller et al. [112] observed an increase of gas and residue in formic acid from the processing of starch at 350 °C. Potassium hydroxide improves slightly the formation of bio-crude compared to the reaction in water. Nevertheless, for mannitol, potassium hydroxide increases the yield of the aqueous phases compared to the other phases with a lower bio-crude yield.

6.4.2 Analysis of the bio-crude oils of carbohydrates

6.4.2.1 GPC analysis

Figure 6-3 contains the different fractions measured by integration of the chromatograms of bio-crude oil produced by (a) starch, (b) glucose, (c) alginic acid and (d) mannitol from the gel permeation chromatography (GPC).

The GPC analysis for the different carbohydrates, (Figure 6-3), show that as temperature increases from 250 to 350 °C, the average molecular weight decreases towards 200 g/mol signifying that most of the compounds could be composed of phenolic or furfural in nature. For the alginic acid, (Figure 6-3 (c)), “heavy molecular weight” and oligomers materials are higher at 300 °C to the other temperature. Formic acid and potassium hydroxide increase the formation of compounds of “heavy molecular weight” materials. This result would suggest that in these solutions, the polymerisation is enhanced.

Nagamori et al. [256] detected a move in the molecular weight composition from “heavy molecular weight” materials to monosaccharaides as the starch was heated from 180 to 240 °C, the same trend was observed when increasing the reaction time. Miyazawa et al. [257] confirmed that the average molecular weight decreased as a function of time when using a semi batch reactor.

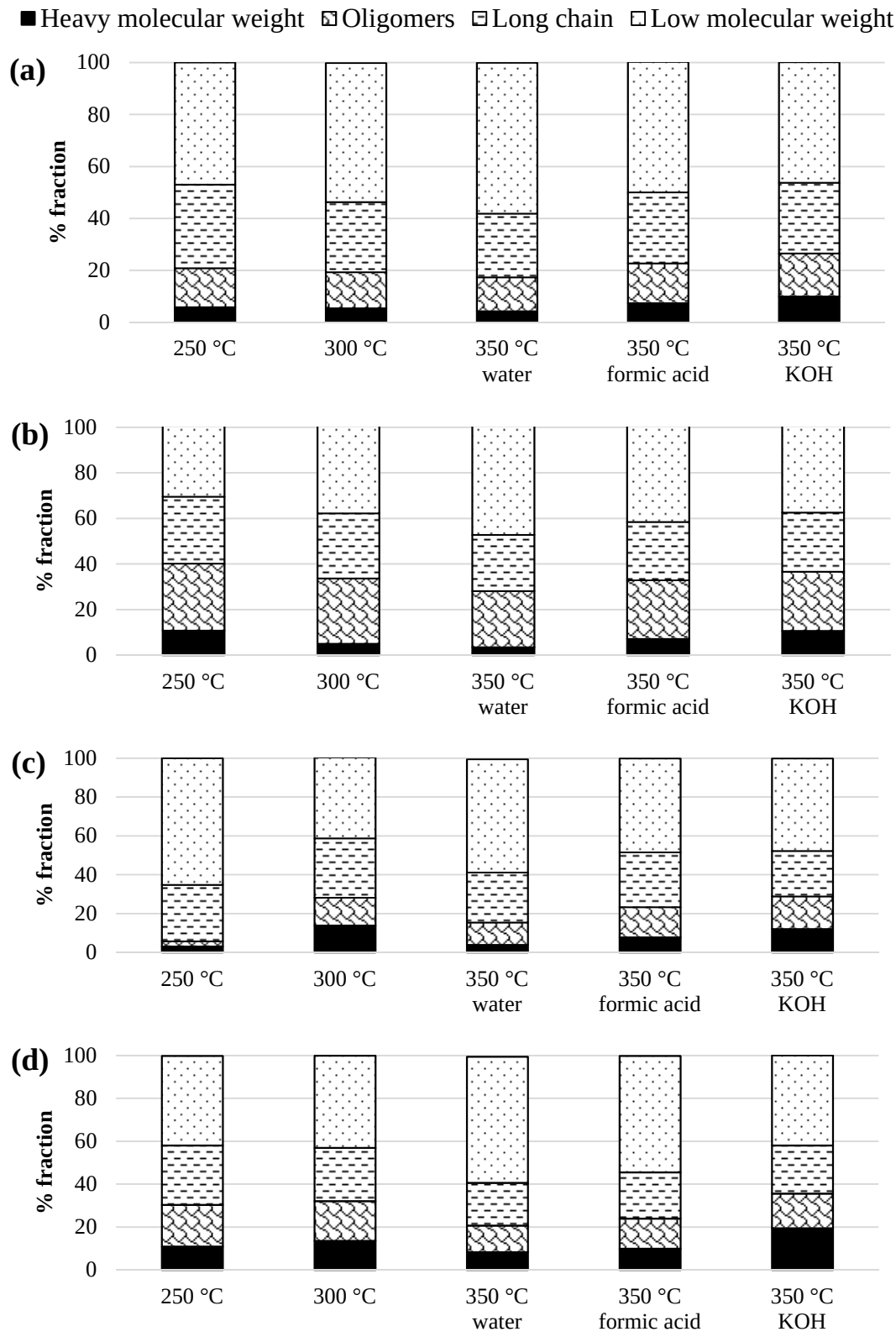

Figure 6-3: Diagram representing the different fraction determined by GPC analysis for the processing of mannitol from 250 to 350 °C in water, formic acid and KOH Where (a) corresponds to starch, (b) glucose, (c) alginic acid and (d) mannitol.

6.4.2.2 GC-MS analysis

Low intensity mass chromatograms are obtained on the whole for the processing bio-crude oil. Examples of some chromatograms are included in the shown in Appendix 3, section 3.1 page A-9, page 325. There are several reasons for that: the first is that the quantity of oils is not enough to produce good chromatograms; the second is that the polarity of compounds is not suitable with column used. Yet, the GPC results imply that at least 50 % compounds in the bio-crude oil has a molecular weight lower to 200 g/mol which should be detected with the program used. The peak at 32 minutes is assigned to butylated hydroxytoluene. There are limited mentions of the composition of the bio-crude oil in the literature as most of the compounds were soluble in the water phase. Figure 6-4 and Table 6-2 includes the chemical structures of some molecules identified in the bio-crude of model carbohydrates.

Table 6-2: Peaks identification in the GC-MS

Number	Retention time (minutes)	Compounds
1	18.0	3-methyl-pentan-one
2	19.0	3,4-dimethyl-pentan-one
3	21.8	phenyl-undecen-1-ol
4	22.4	naphathalendione
5	26.0	2,3-dihydro 1H-inden-1-one
6	27.1	1,2,3,4-tetrahydro-1,5,7-trimethyl-naphthalene
7	28.0	5-methyl-2-(1-methylethyl)-2-cyclohexen-1-one
8	33.8	1-(3-hydroxyphenyl)-ethanone

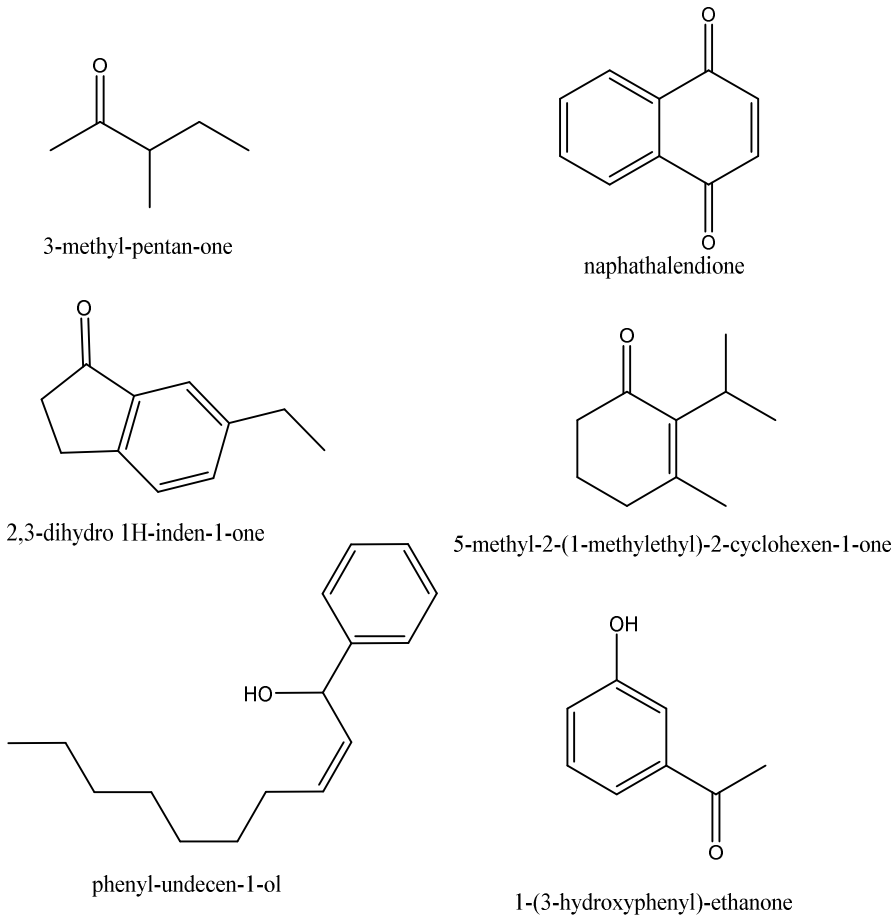

Figure 6-4: The chemical structure of some compounds identified during the processing of carbohydrates

The majority of molecules identified in the bio-crude oil from the processing of carbohydrates contain oxygen and cyclic functional groups. 1,4:3,6-dianhydromannitol (rt = 25.3 min) is identified for the mannitol experiments, this compound is formed by internal cyclisation of the mannitol. For alginic acid, 1-(3-hydroxyphenyl)-ethanone is the most abundant compounds. 2,3-dihydro-1H-inden-1-one is identified in the chromatogram of the bio-crude from mannitol and glucose. Ketones such as cyclohexanone, indenone or ethanone were among compounds detected by Biller et al. [112] in the bio-crude oil. No difference in the bio-crude oils composition is observed between the processing of glucose and starch. The presence of oxygenated compounds in bio-crude oils treated of glucose and starch under subcritical water was demonstrated by Williams et al. [262] using the infrared technique assigning typical functional group (OH, ketone or aldehydes).

6.4.2.3 Elemental analysis

Elemental composition of the bio-crude oil from starch is included in Table 6-3. Samples are prepared in duplicate and the average value was presented. The percentage energy recovery equation and the Dulong equation are found in **Chapter 3**. It is assumed that no moisture was present in the oil therefore the values were dry as basis.

Table 6-3: Elemental analysis as received of the bio-crude oil for starch, glucose, alginic acid and mannitol and heating value, and % energy recovery for the processing of chars in water, formic acid and KOH

	C wt.%	H wt.%	O wt.%	HHV (MJ/kg)	H/C	O/C	% Energy recovery
			Starch				
250 °C	69.4	6.2	23.8	28.1	1.1	0.3	3.2
300 °C	63.9	3.8	32.1	21.3	0.7	0.4	2.7
350 °C water	76.1	4.4	19.0	28.6	0.7	0.2	4.7
formic acid	66.4	3.6	30.0	22.3	0.7	0.3	4.1
potassium hydroxide	68.9	3.0	27.8	22.6	0.5	0.3	8.3
			Glucose				
250 °C	62.9	3.6	33.5	20.4	0.7	0.4	5.1
300 °C	67.1	3.5	29.4	22.4	0.6	0.3	1.8
350 °C water	68.7	3.4	27.9	23.1	0.6	0.3	1.5
formic acid	63.8	3.2	33.1	20.2	0.6	0.4	1.8
potassium hydroxide	74.2	3.2	22.6	25.7	0.5	0.2	8.5
			Alginic acid				
250 °C	63.3	2.9	33.7	19.6	0.5	0.4	2.7
300 °C	55.8	3.2	41	16.1	0.7	0.6	4.7
350 °C water	69.1	3.4	27.5	23.3	0.6	0.3	4.7
formic acid	62.9	2.9	34.3	19.2	0.6	0.4	3.5
potassium hydroxide	71.0	6.5	22.5	29.3	1.1	0.3	15.6
			Mannitol				
250 °C	64.3	3.4	31.9	21	0.6	0.4	4
300 °C	62.1	2.9	35.1	18.9	0.6	0.4	14.1
350 °C water	65.3	3.1	31.6	20.8	0.6	0.4	17.3
formic acid	78.2	3.3	18.5	27.8	0.5	0.2	21.6
potassium hydroxide	61.8	6.0	32.2	23.7	1.2	0.3	3.8

Compared to the raw and processed carbohydrates, the oxygen content of the processed samples decreases suggesting hydrolysis of the raw material. The oxygen

content for starch, alginic acid is higher for 300 °C. For glucose, there is some evidence that the carbon content increases with temperature, which reduces the oxygen content from 250 to 350 °C. Biller et al. [112] measured 20 wt.% of oxygen content from the bio-crude of starch. A lower oxygen content (18.1 wt.%) was measured for the processing of glucose.

The oxygen content is increased with the addition of formic acid for starch, glucose and alginic acid compared to the water runs. For mannitol, the oxygen content is almost reduced by half. For mannitol the bio-crude yield is more significant, a higher energy recovery is obtained which increases from 250 to 350 °C. For the other carbohydrates, because of the low bio-crude yield, the energy is not contained in the bio-crude. Potassium hydroxide enhances the energy recovery and energy content for glucose, starch and alginic acid.

6.4.3 Analysis of the residue

The elemental composition of the char from the HTL of starch is included in Table 6-4. The typical coefficient of variance was approximately 2-3 %. The results were shown as dried basis. At 250 °C for mannitol, no enough residue samples were available to perform the measurement.

Table 6-4: Elemental analysis of the chars and heating value, and % energy recovery for the processing of starch in water, formic acid and KOH

	C wt.%	H wt%	O wt.%	HHV (MJ/kg)	H/C	O/C	% Energy recovery
Starch							
250 °C	70.3	4.7	25.0	26.0	0.8	0.3	64.3
300 °C	72.0	4.7	23.4	26.8	0.8	0.2	62.5
350 °C water	75.0	4.6	20.5	28.2	0.7	0.2	45.1
formic acid	74.9	4.6	20.5	28.3	0	0.2	84.6
potassium hydroxide	76.3	5.8	17.9	30.8	0.9	0.2	42.0
Glucose							
250 °C	66.9	2.1	31.0	20.1	0.7	0.3	56.8
300 °C	71.9	4.8	23.2	27.1	0.8	0.2	64.6
350 °C water	74.9	4.9	20.2	28.7	0.8	0.2	62.6
formic acid	79.4	5.2	15.4	31.5	0.8	0.1	61.2
potassium hydroxide	75.5	4.5	20.0	28.4	0.7	0.2	31.4
Alginic acid							
250 °C	71.9	4.8	23.2	27.1	0.8	0.2	69.6
300 °C	73.7	2.2	24.1	23.7	0.8	0.2	58.3
350 °C water	75.6	4.8	19.6	28.9	0.8	0.2	64.9
formic acid	76.7	4.9	18.4	29.7	0.8	0.2	68.6
potassium hydroxide	74.3	5.3	20.4	29.1	0.9	0.2	48.0
Mannitol							
250 °C	-	-	-	-	-	-	-
300 °C	74.3	5.3	20.4	29.1	0.9	0.2	9.0
350 °C water	79.8	5.9	14.3	32.8	0.9	0.1	14.6
formic acid	75.5	5.6	18.9	30.1	0.9	0.2	17.3
potassium hydroxide	67.1	4.1	28.8	23.4	0.7	0.3	1.5

From the CHNS analysis of starch and glucose, as the temperature increases from 250 to 350 °C, the carbon content and the heating value increases for example with glucose from 20.1 to 28.7 MJ/kg. In contrast, the oxygen content in the residue is reduced. Comparing CHNS values of the char and the bio-crude oil, less oxygen content is measured and the carbon content is above 74.0 wt.% for the starch which is higher to the value obtained in the literature [265].

The formation of char is again a major phase during the conversion of alginic acid. The highest oxygen content is measured at 300 °C. For mannitol, the residue fraction increases with the temperature. The energy recovery is at its highest at 300 °C for glucose. In contrast, the energy recovery decreases with temperature in parallel to the residue yield for starch. Formic acid helps to reduce the oxygen content of the residue from glucose, otherwise the effect of this acid and potassium hydroxide to the residue is unclear.

Titiric et al. [265] studied the formation of char at 180 °C for 24 hours; the elemental composition of the residue from starch at the condition used in their study gave 64.5 wt.% of carbon, 4.6 wt.% of hydrogen and 31 wt.% of oxygen content. It was revealed that 5-HMF was a precursor of the formation of spherical char. The CHNS analysis at 250 °C from glucose is closely matched to this study. The reduction of oxygen content could suggest an aromatisation or cyclisation of the compounds of the char [266]. The formation of char from calcium alginic was studied for producing nanoparticles or beads in order to absorb metals [267, 268]. Previous studies did not report the formation of char as semi-continuous reactors were used [259, 269, 270].

Figure 6-5 (a) and (b) illustrate the analysis of char by thermogravimetry under pyrolysis with the weight loss and the derivative curve for the raw carbohydrates (starch, glucose, alginic acid and mannitol) and the resulting chars at 350 °C.

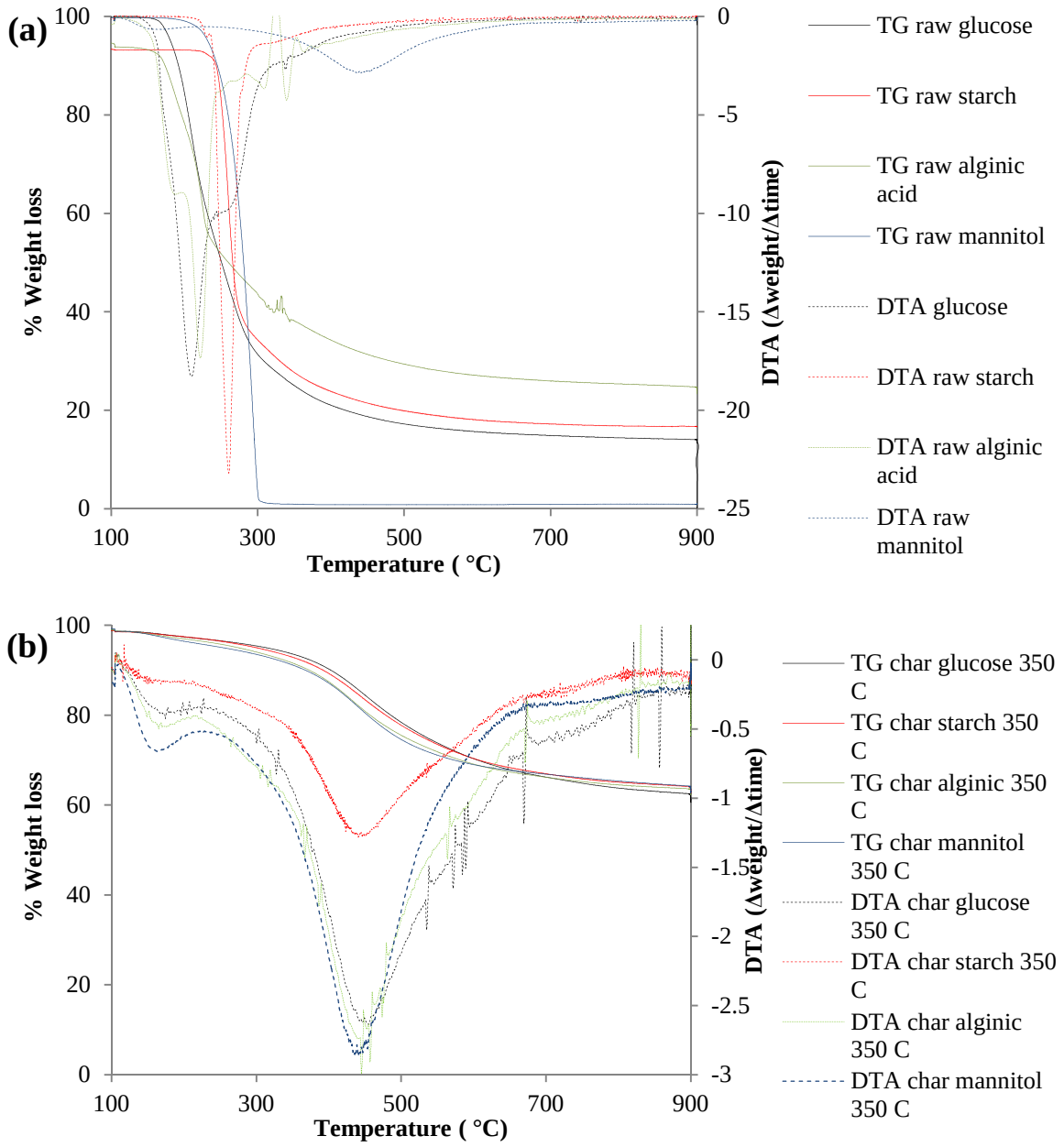

Figure 6-5: Weight loss curve and the its derivative in function of the temperature for (a) the four raw carbohydrates and (b) for the processed char

The weight loss curves (Figure 6-5 (a)) indicate that mannitol is fully degraded between 250 to 300 °C, similar temperatures are measured for the start of degradation with starch except that 20 wt.% of the char is still present at 900 °C. Alginic acid contains more char at this temperature. Glucose, under pyrolysis, is degraded into two steps at 216 °C and the second at 270 °C. The percentage weight loss is more significant with mannitol at 290 °C.

The percentage weight loss curve for chars (Figure 6-5 (b)) produce during hydrothermal liquefaction has a different behaviour compared to the raw materials.

Moreover, among all the carbohydrates, the variation is low and chars are relatively stable under pyrolytic condition as the average weight loss is approximately 40 wt.%. The maximum for the DTA curve is observed at higher temperature 450 °C compared to the unprocessed carbohydrates. These results demonstrate that the char is stable under hydrothermal or pyrolysis condition. The low weight loss indicated that the residue contained low amount of volatiles. These compounds are contained in the bio-crude oil or the aqueous phase.

6.4.4 Analysis of the aqueous phase

Table 6-5 contains the TOC concentration corrected for the dilution. Calculation for the percentage carbon in the aqueous phase, carbon in the bio-crude oil calculated was present in **Chapter 5**.

Table 6-5: TOC concentration and the carbon mass balance for the processing of starch in water, formic acid and KOH

	TOC (ppm)	%C aqueous	% C bio-crude	% C residue	% C gas
			Starch		
250 °C	7136	22.9	2.6	55.7	18.9
300 °C	5011	16.0	2.6	53.7	27.7
350 °C water	4668	14.8	4.0	38.6	42.6
formic acid	5970	17.0	3.9	44.9	59.6
potassium hydroxide	4660	9.8	7.0	24.3	58.9
			Glucose		
250 °C	4447	13.8	5.8	55.6	25.3
300 °C	8332	25.6	1.8	58.0	14.6
350 °C water	4455	12.4	1.3	48.3	37.9
formic acid	6178	16.9	1.9	52.1	29.1
potassium hydroxide	3858	7.9	7.0	31.3	53.8
			Alginic acid		
250 °C	5459	17.0	3.0	49.7	30.2
300 °C	2660	8.5	5.7	55.9	29.8
350 °C water	7128	22.4	4.9	45.6	27.0
formic acid	10274	29.4	4.0	42.9	23.7
potassium hydroxide	2635	7.9	10.4	36.3	45.4
			Mannitol		
250 °C	28574	87.7	4.8	0	7.5
300 °C	12428	38.9	18.4	8.8	33.9
350 °C water	9350	28.7	26.6	14.2	45.4
formic acid	6091	17.0	19.48	12.8	50.8
potassium hydroxide	27749	81.9	3.2	1.7	12.2

Results for starch and mannitol show a decrease of the TOC concentration with the temperature. The TOC concentrations for glucose and alginic acid are not affected by the temperature. Promdej et al. [263] measured an increase of the TOC concentration from the processing of glucose with temperatures ranging from 300 to 400 °C for 10 seconds. Nevertheless, longer residence time reduced the TOC concentration for the same temperatures. It is the reason why the TOC concentration of glucose increases first, and subsequently decreases at 350 °C. Similar behaviour was observed for starch, where the concentration of monosaccharaides increased in relation to the temperature and subsequently decreased after more than 4-5 minutes which explained the reduction of the TOC concentration [256, 257].

With a rise in temperature, for starch and mannitol, the carbon fraction has been converted into gas and more likely into carbon dioxide. This may imply a decarboxylation and reduction of the molecular weight size. The carbon fraction in the bio-crude as well increases with the temperature for the same carbohydrates. The opposite trend is observed with glucose. A clear decrease of the carbon fraction in the residue is measured for starch. The fluctuation of the carbon fraction in the char is minimal implying that the carbon fraction is converted mainly from the aqueous phase to the gaseous phase.

The addition of potassium hydroxide allows an increase of the carbon fraction into the bio-crude oil for starch, glucose and alginic acid. Furthermore, the TOC concentration is reduced for the three carbohydrates. The opposite effect is measured with mannitol correlating with the mass balance yield. Formic acid generally enhances the TOC concentration for starch, glucose and alginic acid.

The general pH from the process water is approximately 3. Nevertheless, the processed water from mannitol and potassium hydroxide, a pH of 6 is measured; it could be explained by higher TOC concentration. No chemical composition of the aqueous phase is carried out, yet several studies indicated that the main compounds from the degraded starch were furfural, 5-HMF, fructose and purivicaldehyde [262]. Major compounds identified in the aqueous phase from the processing of glucose were 5 hydroxymethylfurfural, glycoaldehyde, 1,2,4 benzenetriol, acetic acid, it clarified why the pH value in the aqueous phase were low in the acidic range [261]. Aida et al. [259] and [270] measured a fast decomposition of alginic acid into monosaccharaides which were converted to organic acids at higher temperature such as formic acid,

acetic acid, lactic acid, glycolic acid, 2-hydroxybutyric acid, succinic acid and malic acid. Aida et al. [270] proposed the use of alginic as a green route in order to produce short organic acids. Zhou et al. [271] studied the degradation of mannitol in sodium hydroxide (1.2 M) at 300 °C, where, in the aqueous phase, lactic acid acetic, formic and acrylic acid were detected.

To summarise, the degradation of carbohydrates (polysaccharides or monosaccharides) in hydrothermal water is readily carried out even at low temperatures.

– The formation of bio-crude oil with less than 5 wt.% of yield is negligible compared to other feedstocks such as lipids (80 wt.%).

– More bio-crude yield is produced during the liquefaction of mannitol with a maximum yield of 13 wt.%. The bio-crude is composed in majority of phenolic compounds.

– The other drawback is the high amount of chars, approximately yield of 30 to 40 wt.% which is likely to be caused by the long heating rate or cooling down of the reactor. These char are stable under pyrolysis and hydrothermal condition. Additionally these chars contain the majority of the initial energy from the raw carbohydrates.

– There was an obvious trend showing the increase of the aqueous phase for starch, but also for the oxygen content in the char.

– On the whole, the addition of formic acid has an effect on improving the gaseous formation whereas potassium hydroxide increases the formation of bio-crude (tar) with a molecular weight approximately 500 g/mol and the carbon fraction in the bio-crude oil.

6.5 Catalytic processing of different carbohydrates with HZSM-5 in water and formic acid

Experiments are carried out using HZSM-5 with different carbohydrates in order to investigate whether the catalyst improve the formation of not. The screening of metal doped catalysts was performed with starch, nevertheless, no significant results have been observed.

6.5.1 Mass balance yield

Starch, glucose, alginic acid, and mannitol were processed in water and formic acid with HZSM-5 as catalyst. Figure 6-6 includes the diagram of yields of the different phases (starch, glucose, alginic and mannitol) obtained after processing carbohydrates.

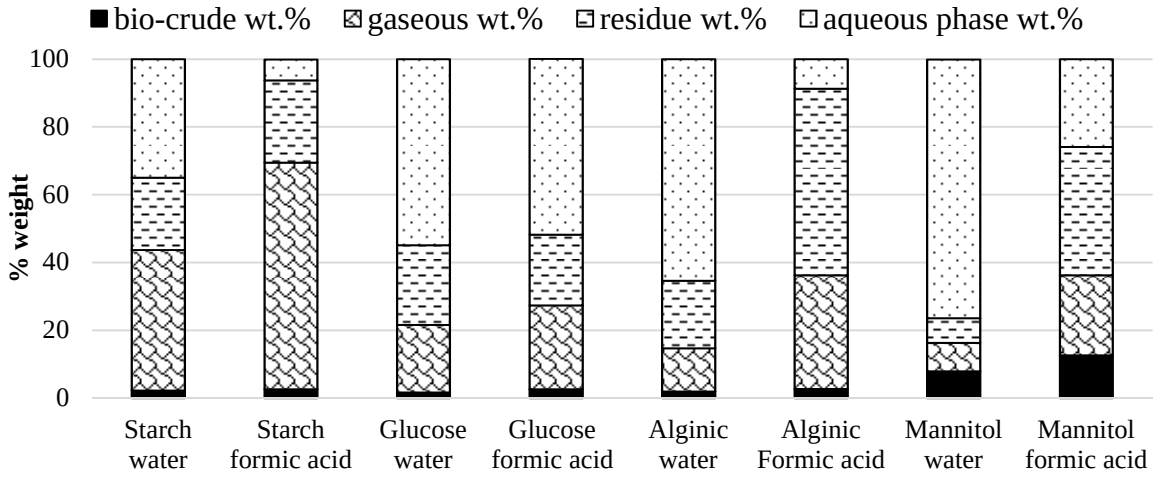

Figure 6-6: Diagram of the mass balance yield for the hydrothermal liquefaction with starch, glucose, alginic, mannitol with HZSM-5 in water and formic acid at 350 °C

The results shown in Figure 6-10 indicate that using formic acid increases the formation of gas, and the highest yield is achieved with starch. Moreover, the residual fraction (chars) with the exception of starch is increased in this solution particularly with alginic acid and mannitol. Thus, formic acid with HZSM-5 enhances the formation of gas and chars which for liquefaction is not the ideal outcome. The bio-crude formation is higher with mannitol in formic acid as with the run without the catalyst.

6.5.2 Analysis of the bio-crude oil

6.5.2.1 GPC analysis

To investigate the effect of HZSM-5 in water and in formic acid on the molecular weight range, GPC analysis is carried out and is displayed in Figure 6-7.

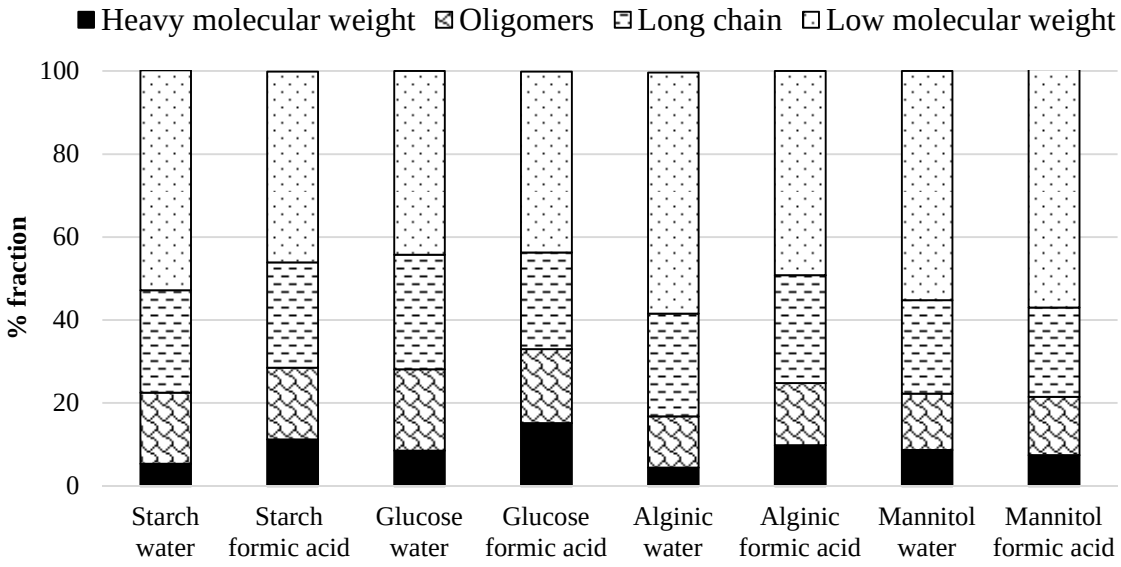

Figure 6-7: Diagram of the different molecular weight fraction measured by GPC in THF as solvent of the HZSM-5 in formic acid and in water for different carbohydrates

The use of formic acid enhances slightly the formation of “heavy molecular weight” materials and oligomers with the exception of mannitol. Low molecular weight materials production (below 200 g/mol) is enhanced with HZSM-5 by alginic acid in water and mannitol in formic acid (58 %).

6.5.2.1.1 GC-MS analysis

Figure 6-8 illustrates one example of chromatograms of the processing bio-crude oils for alginic acid with HZSM-5 and formic acid. The bio-crude oil from alginic acid processed with HZSM-5 contains approximately 60 % of compounds with a molecular weight lower than 200 g/mol. It is different from the run without catalysts. Peaks at 28 minutes and 41 minutes could not be assigned. Table 6-6 lists the main compounds identified in the chromatogram.

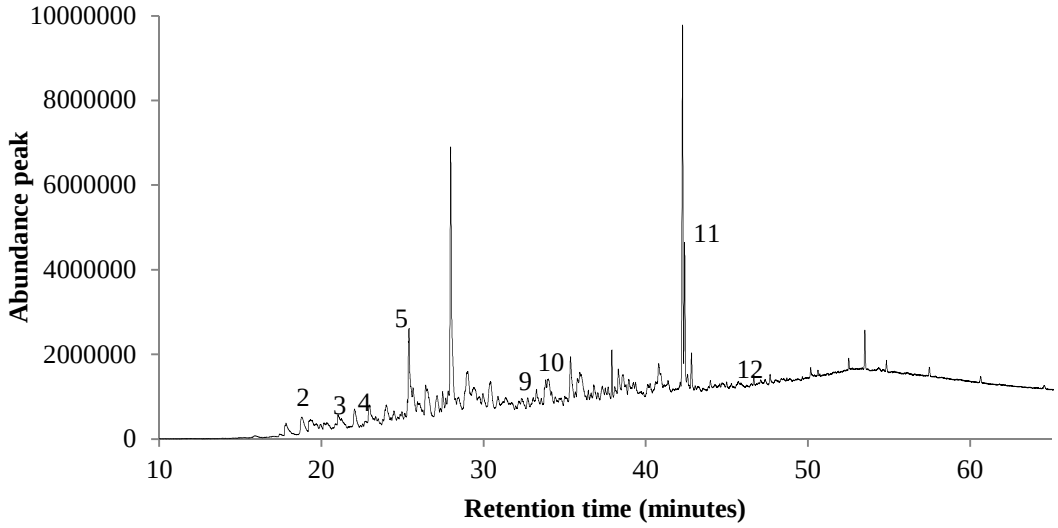

Figure 6-8: Chromatograms alginic acid with HZSM-5 and formic acid

Table 6-6: Peaks identification in the GC-MS in the bio-crude oils from alginic in formic acid HZSM-5

Number	Retention time (minutes)	Compounds
1	18.0	3-methyl-pentan-one
2	19.0	2,3-dimethyl-2-cyclopenten-1-one
3	21.8	oxadispiro-undecen-1-ol
4	22.4	naphathadione
5	26.0	Menthol-2,3-dihydro 1H-inden-1-one
6	27.1	1,2,3,4-tetrahydro-1,5,7-trimethyl-naphthalene
7	28.0	5-methyl-2-(1-methylethyl)-2-cyclohexen-1-one
8	33.8	1-(3-hydroxyphenyl)-ethanone,
9	34.0	7-methylindan-1-one
10	36.0	1,2-diethoxybenzene
11	43.1	7-methyl-1-naphthol
12	46.2	(4-hydroxy-3-methoxyphenyl)-2-propenoic acid

The majority of compounds in the bio-crude oil contains a ketone functional group and were mono or polycyclic. More aromatic compounds such as 1,2,3,4-tetrahydro-1,5,7-trimethyl-naphthalene is observed compared to the run without catalyst. Therefore, HZSM-5 could favour the formation of cycle compounds.

6.5.2.1.2 Elemental analysis

To compare the effect on different carbohydrates on the chemical composition, the CHNS value was calculated as dried basis and is shown in Table 6-7.

Table 6-7: Elemental analysis of the bio-crude oil of starch, glucose, alginic acid and mannitol in water and formic acid with HZSM-5

	C wt.%	H wt.%	O wt.%	HHV (MJ/kg)	H/C	O/C	% Energy recovery
Starch : water	74.2	5.3	20.5	28.9	0.9	0.2	5.1
Starch : formic acid	70.9	4.7	24.3	26.3	0.8	0.3	5.1
Glucose : water	62.4	2.9	34.7	19.0	0.6	0.4	2.4
Glucose : formic acid	65.2	2.9	31.9	20.5	0.5	0.4	3.6
Alginic acid : water	64.8	3.2	32	20.8	0.6	0.4	3.0
Alginic acid : formic acid	67.2	3.4	29.3	22.4	0.6	0.3	4.0
Mannitol : water	64.8	3.2	31.5	21.0	0.6	0.4	10.6
Mannitol : formic acid	79.6	3.3	16.5	28.8	0.5	0.2	22.5

HZSM-5 in formic acid enhances the deoxygenation and the percentage energy recovery of the bio-crude oil. The oxygen content with mannitol in formic acid is 16.5 wt.% whereas in water it was 31.5 wt.%. There is no major change for the other saccharides between the reaction in water and formic acid. It becomes apparent that HZSM-5 is more active with mannitol.

6.5.2.2 Analysis of the aqueous phase

The TOC concentration of the aqueous phase was measured for the different carbohydrates with HZSM-5 in water and formic acid; the results are shown in Table 6-8.

Table 6-8: TOC concentration and the carbon mass balance for experiment in formic acid and water of different carbohydrates

	TOC (ppm)	**%C aqueous**	**%C Bio-crude**	**%C remaining**
Starch : water	5360	16.5	6.0	77.6
Starch : formic acid	6126	17.4	4.4	78.2
Glucose : water	7806	23.5	3.2	73.3
Glucose : formic acid	5497	15.0	3.8	79.2
Alginic acid : water	9360	30.1	3.2	66.7
Alginic acid : formic acid	856	2.5	4.2	81.2
Mannitol : water	15017	46.3	12.9	40.8
Mannitol : formic acid	7366	20.5	22.8	56.7

A low TOC concentration is measured for alginic acid (856 ppm) whereas the others are approximately ten-fold increase since the production of gaseous and residue phases are higher. In contrast, more carbon fraction is present with 46 % in the aqueous phase with mannitol in water coinciding with the high yield of the aqueous phase. As noted previously the percentage of carbon is greater in the bio-crude oils with formic acid.

In conclusion, formic acid with HZSM-5 favours side reaction by increasing the production of gas and residue or chars which is higher than without a catalyst. More aromatic in the bio-crude of alginic acid is observed. The deoxygenation of bio-crude oils from mannitol in formic acid is improved with an important high yield of residue; nevertheless some further investigations would be necessary to explain this result.

6.6 Discussion about the degradation of carbohydrates

Oppositely to the lipids, the hydrolysis of polysaccharides into monosaccharides is almost instantaneous (less than one minute) in subcritical water above 300 °C [257]. Monosaccharides such as glucose or fructose are converted into short carboxylic acids, 5-HMF and aromatic compounds [261]. Their high solubility in water may explain the fast reactivity, although, few products are produced as bio-crude oil. The major fraction is degraded into the water phase. There are different pathways for the degradation of glucose in subcritical water as presented in Figure 6-9:

1) During the first step, starch is hydrolysed into glucose. Afterwards, glucose undergoes tautomerisation (isomers rearrangement) yielding D-fructose which is subsequently converted to 5- hydroxymethylfurfuraldehyde (5-HMF) by hydrolysis [264]. Glucose is interconnected to mannose, fructose and galactose thanks to the Lobry de Bruyn-Alberda van Ekenstein (LBAE) rearrangement, which involves a 1,2-enediol anion interconnection [272].

2) The hydrolysed glucose undergoes a retro-aldol reaction producing different aldehydes such as the glycol aldehydes or the glyceralaldehydes, it was observed that these aldehydes increased with time [261]. Some further hydrolysis occurs to produce acids such as acetic acids, alcohols and lactic acid with further rearrangement. In order to detect these compounds, it is recommended the water phase be analysed by HPLC.

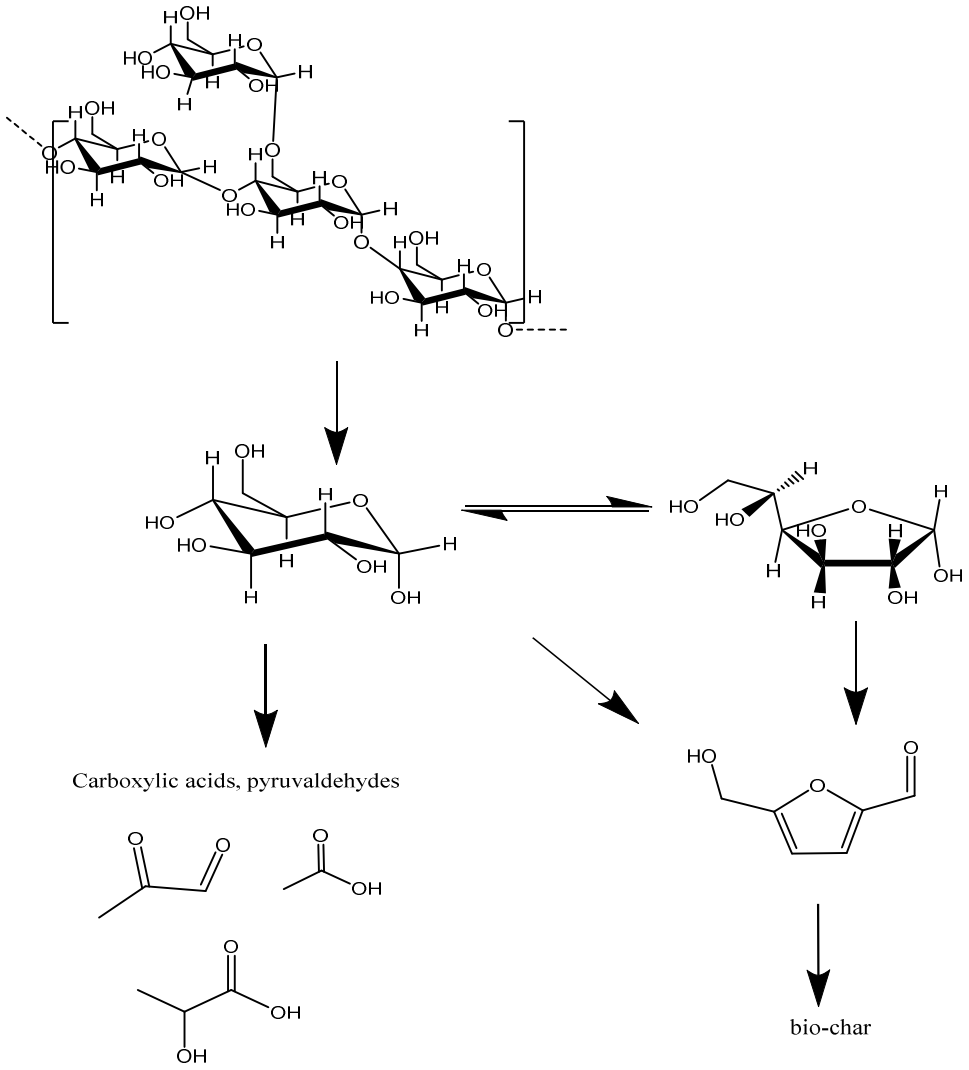

Figure 6-9: Brief degradation route of starch and glucose under hydrothermal liquefaction according to Srokol et al. [261]

The production of char is enhanced over a long heating and cooling rate [273], In the present research, a heating mantle is required to heat the 77 ml reactor because of the high surface area, in order to reach 350 °C. A 40 minutes heating rate is necessary and approximately two hours to cool down to 30 °C. Macromolecules (starch) decompose during the first step of the heating; to recombine later during the cooling step forming high molecular polymers or chars. Chuntanapum et al. [266] studied in detail the formation of char from 5-HMF, there was a relationship with the increase of formation of chars and the concentration of 5-HMF and the residence time (1-50 minutes). 5-HMF could decomposed in the aqueous phase as 1,2,4-benzentriol, benzenzendiol or furfural which later formed chars. The solidification occurred via the polymerisation of the 2,5 substitution functional groups of the previous compounds or by carbonisation.

The effect of HZSM-5 on the hydrothermal liquefaction of carbohydrates

The results found previously that with formic acid and more in particular with HZSM-5 the formation of char is enhanced. Watanabe et al. [260] suggested that sulphuric acid (H_2SO_4) had consequence on increasing the concentration of 5-HMF and subsequently to produce more chars.

The study of 5-HMF is important because the formation of this compound should be inhibited [274]. Srokol et al. [261] suggested that if the reaction were carried out in alkali solution, the production of 5-HMF was suppressed instead the concentration of glyceraldehyde was enhanced. Watanabee et al. [260] found that sodium hydroxide also promoted the formation of fructose from glucose. It could explain why less char is produced in the presence of potassium hydroxide. Mannitol is more selective to produce bio-crude oil as the chemical structure of mannitol is linear, thus the formation of 5-HMF from fructose is reduced. Nevertheless adding formic acid increases the residue fraction.

Furthermore, hydrothermal liquefaction could be the start of a chemical platform to transform them into suitable products [275], for example to produce lactic acid from mannitol and subsequently polylactic polymer (PLA). Organic acids could be produced (formic and acetic acids) from alginate acid instead of using petroleum base [270].

The doped metals from HZSM-5 have a minor impact towards the processing of starch it was the reason it was omitted from this chapter; the plain zeolite is even more active. It is possible that the metal obstructs pore access to the Brønsted site. However, the catalyst emphasises the gas and residue formation especially in presence of formic acid which is not the desired route. It is possible that HZSM-5 enhances the formation of formic acid from glucose and later degraded into gas [270]. The oxygen content in the mannitol bio-crude oil is the lowest yet some char is also formed. In different conditions, during pyrolysis HZSM-5 has been demonstrated to convert cellulose into a green gasoline mixture (short alkanes and aromatics) [276].

6.7 Implications for the hydrothermal liquefaction of microalgae

These results made it clear that microalgae processed under hydrothermal condition should contain fewer carbohydrates. On the whole, the carbohydrate range in microalgae is not significant (within 5-20 wt.%); [251] although, with the high

mixture complexity, the interaction between elements would reduce the production of char, discussed in detail during **Chapter 8**. Carbohydrates (hexoses) reacts with proteins in the Maillard reaction to form complex oil mixture including nitrogen heterogeneous compounds (pyrrole) [277, 278].

Macroalgae such as *L. Saccharina* contained high amount of carbohydrates including mannitol [279], brown seaweed *D. ligulata* contained 27.2 % of sodium alginic acid [280]. Zhou et al. [148] investigated the liquefaction of *E. prolifera* from 220 to 320 °C, the highest yield 28 wt.% was achieved at 300 °C with approximately 10-20 wt.% of residue, it should be added that the drawback was their high ash content with high halogens. Anastasakis et al. [149] obtained an lower bio-crude oils (maximum of 19.5 wt%) yield with *L. Saccharina* and roughly 20-25 wt.% of residue, as the temperature was increasing the amount of ash was also increased.

Recently, there is a high interest regarding growing microalgae under heterotrophic condition using glucose to feed them, so this carbohydrate might reduce the oil production [281]. Miao et al. [138] carried out sequential liquefaction (two steps) of a strain of *Chlorella* grown under heterotrophic condition. In the first step at 175 °C, allowed the carbohydrates to be extracted and the second under normal hydrothermal condition (350 °C). This method could also be used to reduce the formation of chars when a microalgal strain contained high level of carbohydrates.

6.8 Conclusion

In this chapter, it was demonstrated that the hydrothermal processing of carbohydrates (starch, glucose and alginic acids) did not enhance the formation of bio-crude yield with less than 5 wt.%. Slightly more bio-crude was produced with mannitol with approximately 13.1 wt.%. The majority of the carbohydrates were converted to material retained in residue and in aqueous phase. The residue (char) contained the greatest energy content. The high yield of char was caused by a long cooling/heating rate. The major part of the carbon fraction was distributed in the aqueous or the char. Formic acid enhanced the formation of gas phase whereas potassium hydroxide increased slightly the bio-crude yield. The different metal doped HZSM-5 showed no major difference. However, the gas formation increased with the combination of formic acid and HZSM-5 especially with starch and alginic acid. One of the reasons could be that HZSM-5 helps to degrade the carbohydrates into organic acid which later decomposed into gas. Therefore, for microalgae carbohydrates would probably reduce the bio-crude oil content. It is the reason probably why the HTL of seaweed or high carbohydrate microalgae normally produce low bio-crude yield. Therefore, it would be more suitable to remove the carbohydrate content first by fast hydrolysis and produce in-situ organic acids. In the following chapter, proteins and amino acids will be studied in the same conditions.

Chapter 7 Hydrothermal liquefaction of proteins and amino acids with and without HZSM-5

This chapter presents results from the hydrothermal liquefaction of two types of proteins derived from soya and hemp at different conditions (250, 300 and 350 °C) in water for one hour, and at 350 °C in formic acid. Moreover, the same conditions have been run for asparagine, glutamine and a mixture of both amino acids as a comparison. A catalytic screening with different metal doped HZSM-5 (nickel, iron, copper, and molybdenum) using soya proteins at 350 °C in water and in formic acid has also been conducted.

7.1 Introduction

Proteins and nucleotides are macromolecules which have a key role inside living cells. Proteins are composed of different amino acids linked by peptide bonds (amide bonds). The majority of the nitrogen in biomass originates from proteins and nucleotides. The liquefaction of high protein containing feedstocks, typically produces a bio-crude containing nitrogen compounds which will lower the heating value of bio-crude oils and produced NO_x upon combustion [94].

Dote et al. [282] were the first research group to process proteins (albumin eggs) in subcritical water at 300 °C. They concluded that proteins produce less bio-crude than biomass and that the nitrogen content in the bio-crude was relatively high (9 %). Few amino acids were recovered after the reaction implying that they were hydrolysed completely into ammonia.

Several research groups, particularly in Japan, succeeded in extracting amino acids after short reaction times, less than one or two minutes, below 300 °C [283, 284]. Stabilities of amino acids are widely studied as a large part of the scientific communities believe that the proteins had firstly been synthesised by the polymerisation of amino acids in the bottom of the ocean in the hydrothermal vents which have similar conditions to hydrothermal liquefaction [285, 286]. Dote et al. [111] processed 19 amino acids at 300 °C; most of these products such as asparagine or lysine decomposed mainly into ammonium compound and other water soluble products; low bio-crude oils were produced with the exception of tryptophan and

phenylalanine with resulting in yields above 10 %. Sato et al. [287] proposed that under high temperature and pressure conditions, proteins decompose in two steps: firstly a deamination step (ammonia and organics acids), and subsequently a decarboxylation step (CO_2 and amines). Aspartic acid and serine were found to decompose at a faster rate compared to leucine and alanine which decomposed at a slower rate. The reactivity depended on the chemical structure in the R groups of the amino acid. The pH of the solution also had an effect for example, leucine, isoleucine, phenylalanine, serine, threonine, and histidine were all stable in alkali medium while methionine, tyrosine, lysine, and arginine were stable in acidic pH [288].

The aim of this chapter is to develop a better understanding of the hydrothermal liquefaction of proteins and amino acids as well as the fate of nitrogen compounds into the aqueous phase and the bio-crude. In this context, it can improve our comprehension towards the processing of microalgae, a high protein feedstock, which is discussed in the next chapter. Process variables investigated include temperature ranging from 250 to 350 °C and the presence of formic acid. A catalytic screening is performed at 350 °C in water and in formic acid to study the effect on catalytic nitrogen chemistry with soya protein.

7.2 Methodologies

Further techniques are discussed in this chapter; in particular the methods used in the aqueous phase to measure the anions, cations in the aqueous phase are included in **Chapter 3**. The nitrogen balance in the aqueous phase is calculated as followed in the Equation 7-1 where % $N_{ammonium}$ is the % of nitrogen in ammonium molecule (0.77),$[NH_4^+]$ is ammonium compound concentration (ppm), V_{water} is the volume of water added (27 ml) and $m_{raw\ biomass\ (daf)}$ is the mass of the raw biomass on a dried ash free basis and % $N_{raw\ biomass}$ is the % nitrogen of the raw sample measured by the CHNS analyser.

$$\%\ N_{aqueous} = \frac{\left(\left[NH_4^+\right]/1000\right) \times \%\ N_{ammonium} \times V_{water}}{m_{raw\ biomass\ (daf)} \times \%\ N_{raw\ biomass}}$$

Equation 7-1

Bio-crude oils are also characterised by STA-MS and infrared following the methods described by Darvell et al. [289] and Jones et al. [290]. The bio-crude oils were heated in oxidative mode in a Netzsch STA 449C Jupiter coupled to a Netzsch QMS 403C Aeolos quadrupole mass spectrometer and an infrared spectrometer to analyse the emission of evolved gases. Approximately 5 mg of bio-crude was introduced into an alumina crucible. Prior to combustion the sample was dried from room temperature to 105 °C with a heating rate of 10 °C/min. Afterwards, the evolved of gases started from 110 to 900 °C using a heating rate of 10 °C/min. The reagent gas used is composed of 12.5 vol.% oxygen in helium with a flow rate of 50 ml/min. After the measurement, the thermogravimetric curve was corrected with the buoyancy curve. For the infrared spectrometer there was a lag time between STA and the infrared cell which was taken into account during measurements.

The mass spectrometer was set up to monitor ions corresponding to hydrogen cyanide (HCN), nitric oxide (NO), and nitrogen dioxide (NO_2). Hydrogen cyanide has a mass ion of 27 (m/z) and the ion current is adjusted to reduce the interference from tailing of the mass ion carbon monoxide 28 (m/z) as explained by Jones et al. [290]. For nitric oxide, the isotope ratio ($^{12}C^{18}O/^{12}C^{16}O$) is taken in account; the same correction is applied for nitrogen dioxide 46 (m/z). The emission of ammonia could not be measured as the water emission interfered with this mass ion. The experiment is performed to see if it was possible to determine whether the nitrogen in the bio-crude oil is associated with lighter lower molecular weight compounds, or heaver higher boiling points compounds.

7.3 Chemical composition of proteins

Table 7-1 lists the elemental composition of raw materials on the dry ash free basis, the energy content from the Dulong formula and ash content. The protein and the lipid content were taken from supplier information.

Table 7-1: Initial elemental analysis on a dry basis, ash and lipids and proteins content

	N wt.%	C wt.%	H wt.%	S wt.%	O wt.%	Dulong HHV (MJ/kg)	Proteins	Lipids	Ash
Soya protein	14.2	50.6	7.4	0.4	27.4	22.8	90		3.5
Hemp proteins	8.7	50.6	7.7	0.3	32.8	22.2	45	12	10.3
Asparagine	19.5	33.8	7.4	0.0	39.3	15.0	-	-	-
Glutamine	18.3	41.8	7.5	0.0	32.4	19.0	-	-	-
Mixture asn/gnu	18.0	37.0	7.3	0.0	37.7	16.2	-	-	-

Hemp and soya proteins are both food supplements therefore they are sold not as pure proteins and contain some minerals such as iron salts, and phosphates, etc, to improve the health benefits of the product. The ash content of these products is relatively high for hemp proteins (10.3 wt.%) although lower for soya protein (3.5 wt.%). The hemp protein also contains approximately 12 wt.% lipids and some fibrous material whereas the soya protein contained mainly protein (90 wt.%). Despite these impurities, the two products contain high levels proteins and are relatively low cost source of high protein feedstock. In addition, the manufacturer supplied each product with a list of amino acids allowing some basic information on the type of protein in the different feedstock. For the elemental composition, the major difference involved the nitrogen content with 8.7 wt.% for hemp and 14.2 wt.% for soya protein while carbon and hydrogen contents are similar.

Asparagine contains two nitrogen atoms as amides and primary amine for 4 carbon atoms as $C_4H_8N_2O_3$, the nitrogen level is higher than soya proteins at 19.5 wt.%. Glutamine has a very similar chemical structure with one extra carbon atom. The chemical structure is included in Figure 7-1. These two amino acids are part of non-essential amino acids for the diets. These amino acids are selected because of their simple structure and they have two nitrogen groups (an amide and amine).

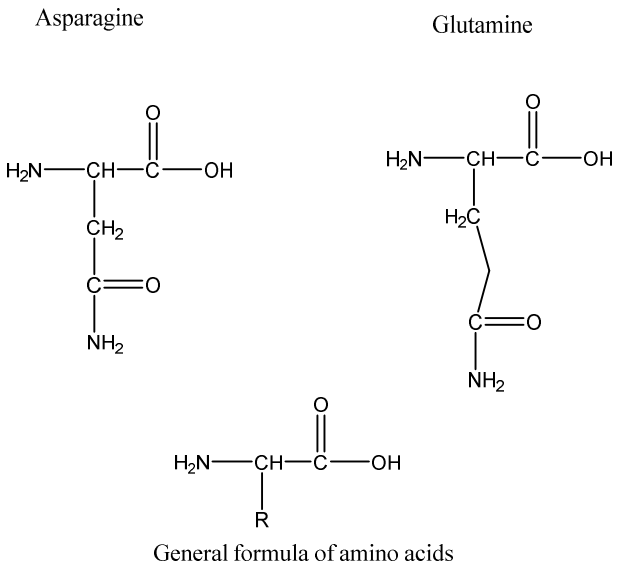

Figure 7-1: Molecular structure of asparagine and glutamine and a general formula for amino acid

7.4 Effect of HTL temperature

7.4.1 Mass balance yield

Figure 7-2 (a), (b) and (c) present the mass balance of the different products (bio-crude, gaseous, residue and mass aqueous phase yields) for the processing of hemp, soya proteins and asparagine respectively. Experiments were carried out at different temperatures and in formic acid. The experiment at 350 °C in water and formic acid were in duplicate for soya and hemp proteins with a coefficient of variance of 3.5 %.

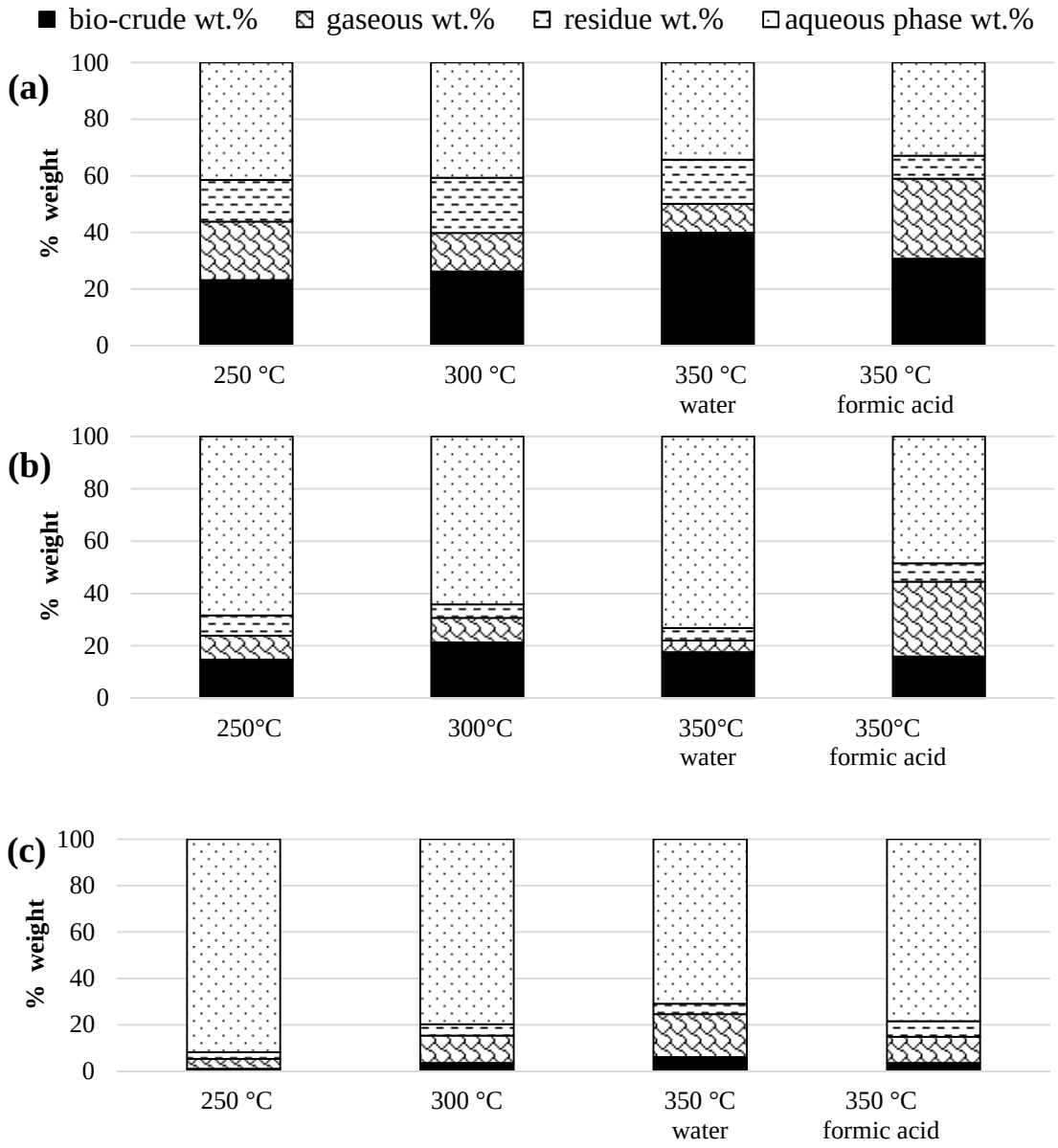

Figure 7-2: Diagram mass balance yield of the different outcome phase for (a) hemp proteins, (b) soya proteins and (c) asparagine at 250, 300 and 350 °C in water, in formic acid

Proteins and amino acids, in general (Figure 9-2), are in majority degraded in the aqueous phase especially for soya proteins (approximately 68.0-73.1 wt.%). Biller et al. [112], at 350 °C, reported a yield of 60 wt.% for the processing of the same proteins. The bio-crude formation is higher for hemp protein in Figure 7-2 (a) as this protein contains other components such as lipids. An increase in bio-crude yield from 23.2 to 39.9 wt.% is observed for this protein as the temperature increases from 250 to 350 °C. The aqueous phase yield here decreases with temperature. These trends suggest that molecules initially in the aqueous phase polymerise as the temperature increases to 350 °C. The results for soya protein (Figure 7-2 (b)) show that less bio-crude is obtained compared to hemp protein and the bio-crude yield does not increase in relation to the temperature; the highest yield (21.3 wt.%) is obtained at 300 °C. The formation of bio-crude is reduced with asparagine (Figure 7-2 (c)) with less than 7 wt.% compared to the proteins. At room temperature, asparagine is not soluble and thus it implies that this amino acid is degraded during liquefaction [291].

Other experiments were performed for glutamine and a mixture of both amino acids (shown in Appendix 2, page 323). This resulted in an increased bio-crude yield compared to asparagine alone agreeing with previous reports [288]. The low levels of bio-crude from the amino acids also agree with previous reports. Dote et al. [282] started to observe the bio-crude formation above 300 °C but with a low yield below 10 wt.% with a majority of the product was degraded in the aqueous phase.

The addition of formic acid reduces the bio-crude yield and increases the gaseous yield. There is more similarity from the study of Biller et al [112] with the run using formic acid (even though a more concentrated formic acid was used) with a rise of gas production. The use of formic acid with asparagine enhances the aqueous phase yield.

7.4.2 Bio-crude analysis of the non-catalytic runs

7.4.2.1 GPC analysis

Figure 7-3 presents the different molecular weight fractions determined in the bio-crude oil from (a) the hemp proteins, (b) soya protein and (c) asparagine measured by the GPC.

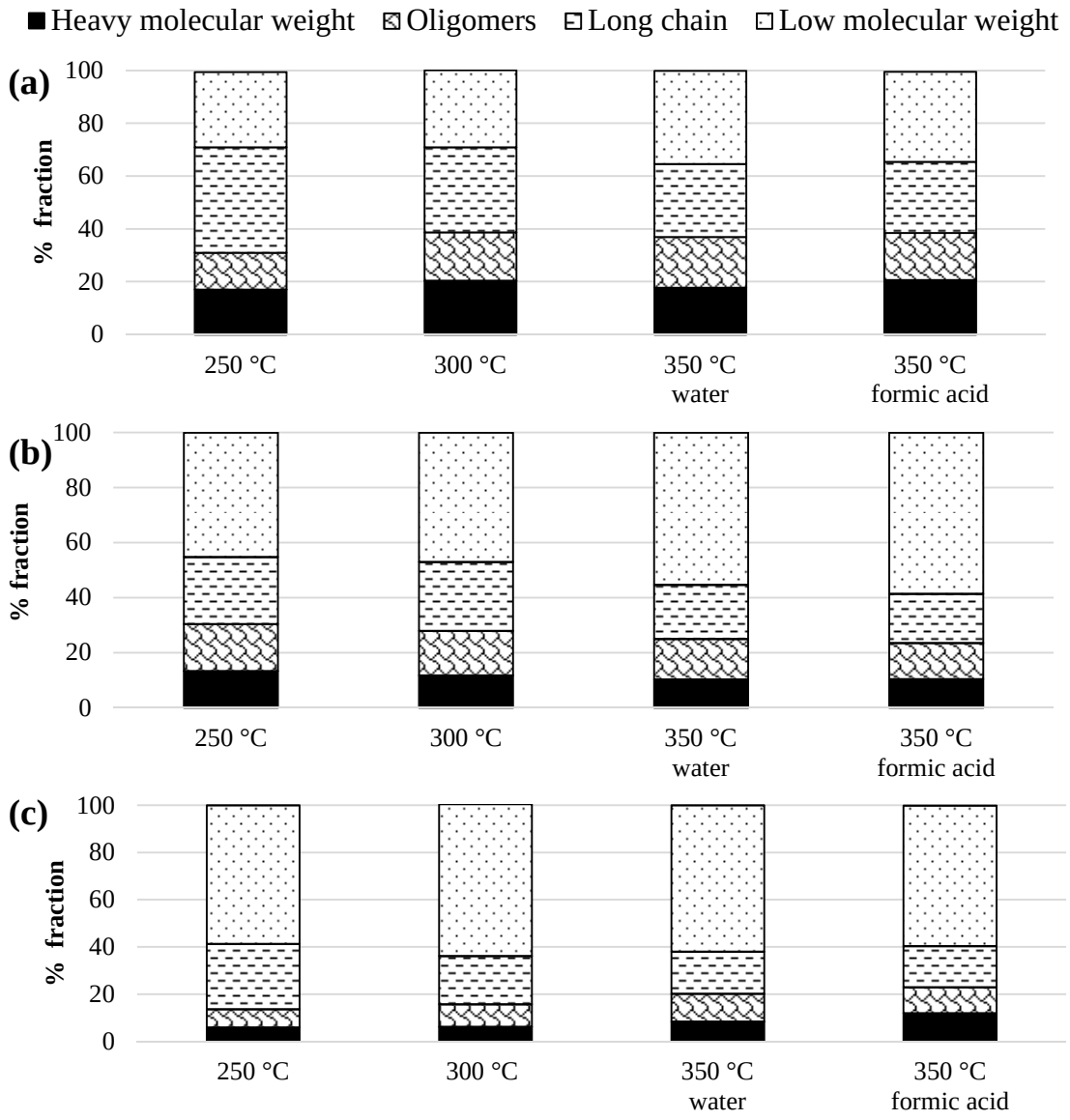

Figure 7-3: Different molecular weight fractions determined by GPC in THF of the bio-crude oils of (a) hemp (b) soya proteins and (c) asparagine at different temperatures and conditions

The bio-crude oils from proteins shown in Figure 7-3 (a) and (b) indicate that there is a relatively uniform distribution of each molecular weight fraction over the whole temperature range. There is some evidence of an increase in lower molecular weight materials as the temperature increases corresponding with a slight reduction in

the “long chain” materials for both proteins. The presence of lipids for the hemp protein (polyunsaturated fatty acids indicated by the supplier particularly linolenic acid) in this protein sample explains the large amount of “long chain” and oligomer materials. The polymerisation of heterocyclic molecules could equally explain the existence of “heavy molecular weight” materials.

In general, there are higher amounts of low molecular weight material present for the results of asparagine (shown in Figure 7-3 (c)). The fraction of “long chain” materials (200-600 g/mol) are reduced as the temperature increases. The reaction for glutamine (shown in Appendix 2, page 323) contains larger fraction of “heavy molecular weight” and “long chain” materials compared to asparagine. This result suggests that glutamine forms more oligomers compared to asparagine. The mixture of both amino acids follows a similar trend with slightly more “heavy molecular weight” materials. Hemp proteins which contain higher levels of glutamine also lead to the formation of high fraction of “heavy molecular weight” materials. Islam et al. [285] observed the polymerisation of glycine between 250 to 350 °C. It suggests thereby that amino acids can form oligomer chains in subcritical water.

The addition of formic acid appears to make very little difference to the molecular weight fractionation. There is also a slight reduction in “heavy molecular weight” material and an increase the lower molecular weight material below 200 g/mol particularly for soya proteins.

7.4.2.2 GC-MS analysis

Figure 7-4 shows the GC-MS chromatograms of the bio-crude from (a) hemp protein at 350 °C and (b) soya protein in water at 350 °C. Table 7-2 lists the main compounds identified in the chromatograms.

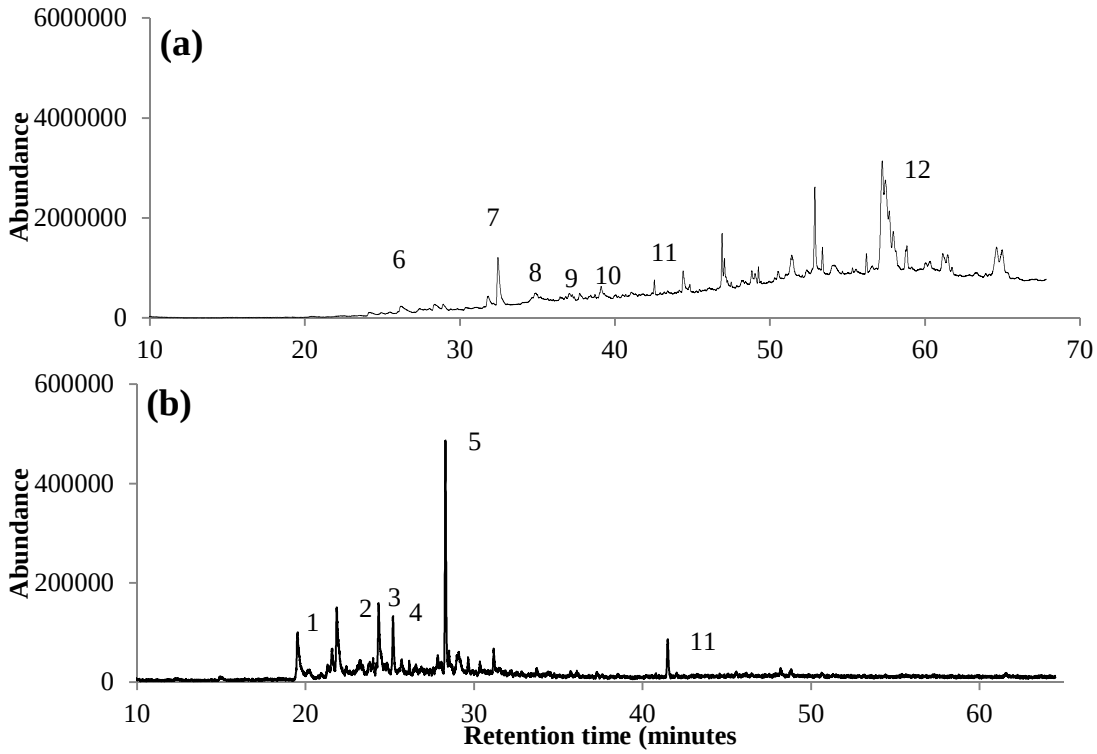

Figure 7-4: GC-MS chromatogram of hydrothermal liquefaction of (a) hemp protein at 350 °C (b) soya protein in water at 350 °C

Table 7-2: Peaks identification in the GC-MS

Number	Retention time (minutes)	Compounds
1	19.4	phenol
2	21.8	4-methyl phenol
3	24.3	4-ethylphenol
4	25.2	methyl-2-oxo-pyrolidine-acetate
5	28.2	2-pyrrolidinone
6	32.4	1-butyl-2-pyrrolidinone
7	34.4	1-(1-oxo-9,12-octadecadienyl)-pyrrolidine
8	38.6	2,5-dimethyl-indolizine
9	39.0	diisopropylpiperazin-2,5-dione
10	39.5	2,4,6-trimethyl-benzonitrile
11	41.4	3-methyl-1-H-indole
12	58.0	9-octadecenamide

The compounds are principally heterocyclic compounds (nitrogen and oxygen), ketones such as 2-decanone, fatty acids and amides such as hexadecanamide

or 9-octadecenamide. Phenol-compounds can be produced by the decomposition of carbohydrates; and is a precursor to coke formation [292]. Pyrrolidinone is a key compound and indicates the degradation of diketopiperazine (DKP) compounds such as diisopropylpiperazin-2,5-dione [293]. This compound originate from the degradation of the protein peptide chain [137]. There is a significant difference between the composition of the hemp and soya protein bio-crude because for the impurities. The soya protein contains higher amounts of phenols and pyrolidinone. On the other hand, hemp protein contains some amides such as 9-octadecanamide and 1-(1-oxo-9,12-octadecadienyl)-pyrrolidine. The formation of these compounds will be developed in the next chapter.

The main compounds observed in the bio-crude oil from asparagine (in appendix 3, section 3-2, 327) include 2-pyrrolidinone, 5,6,7-trimethyl-1H-indole, 2,6-bis-(1-methylethyl)-benzenamine, ethyl-2-amino-3-cyano-5,6-dimethylpyridine-4-carboxylate. A very similar chemical composition with glutamine is observed. Some further compounds are been identified such as (formamide-N-methylpyrrodinyl-butinyl) and cycle including one and two nitrogen atoms including and ergoline. Some examples of molecular structures found during the processing of amino acids are included in Figure 7-5. The bio-crude derived from the mixture of both amino acids contains pyrrolidinone. The majority of the compounds remain unidentified by the MS library as the compounds proposed by the software have a low probability match.

Biller et al. [112] identified mainly piperidine and cyclohexylamine compounds in the bio-crude from asparagine. For soya protein, pyrrols, phenols and piperidine were observed in the bio-crude at 350 °C. Nitrogen cycles such as pyroglutamic acid was identified by Islam et al. [285] to be produced by condensation of glutamic acid.

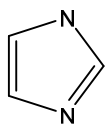

imidazole

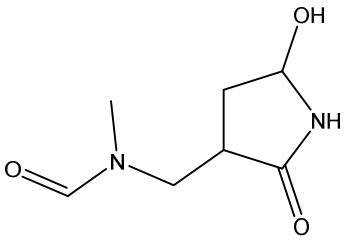

formamide-N-methylpyrrodinyl-butinyl

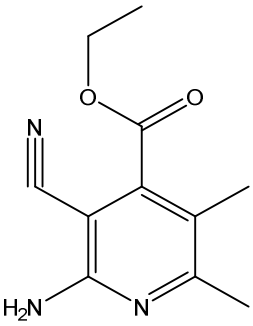

ethyl 2-amino-3-cyano-5,6-dimethylpyridine-4-carboxylate

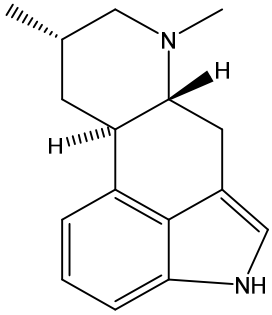

ergoline

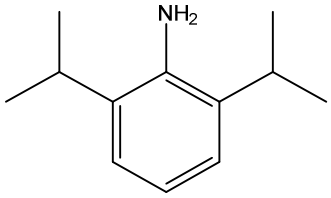

2,6-bis(1-methylethyl)-benzenamine

Figure 7-5: Structure of some molecules found with the processing of amino acids

7.4.2.3 Elemental analysis

The fate of nitrogen is an important aspect of the project and the main source of nitrogen in the feedstock as the protein fraction. Table 7-3 lists the elemental analysis, HHV and energy content. The heating content is determined using two formulas the Dulong and the Milne (MJ/kg) as shown in Equation 7-2. Milne is selected here because the nitrogen is included compared to the Dulong equation [294]. The H/C and O/C ratio and the energy recovery are calculated as in **Chapter 3**. It is assumed that the bio-crude oil do not contain moisture and ash.

$$HHV_{Milne} = 0.341 \times \% C + 1.322 \times \% H - 0.12 \times \% O - 0.12 \times \% N + 0.0686 \times \% S$$

Equation 7-2

Table 7-3: % Elemental analysis in the bio-crude oils, energy content (Dulong and Milne) and % Energy recovery for experiments for different model compounds (hemp, soya and asparagine)at different temperatures and conditions

	N wt.%	C wt.%	H wt.%	S wt.%	O wt.%	Dulong HHV (MJ/kg)	H/C	O/C	Milne HHV (MJ/kg)	% Energy recovery
Hemp proteins										
250 °C	4.2	71.6	10.8	0.3	13.1	37.3	1.8	0.1	36.5	38.9
300 °C	4.6	69.1	9.5	0.2	9.1	35.3	1.7	0.1	34.3	41.8
350 °C water	4.9	70.8	9.6	0.4	7.0	36.5	1.6	0.1	35.3	65.6
formic acid	4.0	72.6	11.9	0.2	11.6	39.4	2.0	0.1	38.5	40.2
Soya proteins										
250 °C	7.8	69.7	9.4	0.0	13.0	34.7	1.6	0.1	33.5	22.4
300 °C	7.2	72.8	9.3	1.1	9.6	36.2	1.5	0.1	35.0	30.7
350 °C water	6.1	72.8	9.2	0.4	11.5	35.7	1.5	0.1	34.7	25.6
formic acid	4.4	67.1	8.9	0.7	18.8	32.1	1.6	0.2	31.7	22.9
Asparagine										
250 °C	5.4	68.1	9.4	0.0	17.1	33.4	1.7	0.2	32.8	2.5
300 °C	8.2	65.1	6.8	0.0	19.9	28.2	1.3	0.2	27.6	6.8
350 °C water	6.7	63.7	6.2	0.0	23.4	26.2	1.2	0.3	26.1	10.7
formic acid	4.5	65.7	7.9	0.0	21.9	29.6	1.4	0.2	29.5	9.6
glutamine	7.3	73.7	6.8	0.0	12.3	32.4	1.1	0.1	31.6	8.5
asn-gnu	8.4	71.3	4.2	0.2	16.0	27.3	0.7	0.2	26.8	14.0

Opposite trends from hemp and soya proteins are obtained for the nitrogen content in relation to the temperature. For hemp proteins, the nitrogen content only increases slightly (4.2 to 4.9 wt.%) whereas for soya protein the nitrogen content falls from 7.8 to 6.1 wt.%. The difference in nitrogen variance with temperature for both of the protein samples may have been due to the presence of contaminants in the raw proteins. The elemental analysis results of bio-crude derived from the soya protein contain a higher nitrogen content since the raw materials has almost the double nitrogen content (14 wt.%) compared to hemp protein. The high nitrogen content for soya protein broadly agrees with the results from GC-MS indicating many of the compounds identified contained nitrogen. Dote et al (1996) remarked that the nitrogen content from the liquefaction of albumin protein was diminished from 9 to 6 wt.% between 200 to 340 °C with a reaction time of 30 minutes [282].

The elemental analysis results of bio-crude derived from the asparagine show a less obvious trend with the nitrogen content in relation to the temperature. The content at 350 °C is 6.7 wt.% [112]. Dote et al. [111] measured a lower content from asparagine at 300 °C (5.2 wt.%). The bio-crude from glutamine contains higher nitrogen content than asparagine with 7.3 wt.% and a higher carbon content of 73.7 wt.%. Mixing the both of the amino acids increases further the nitrogen content to 8.4 wt.%.

The addition of formic acid results in a slight lowering for the two proteins and asparagine. Previous work by Biller et al. [112] who used a higher concentration of formic acid (1.0 M instead of 0.26 M) showed a lower reduction of nitrogen content than the results obtained in this study which is interesting. A higher reduction could be achieved however using sodium carbonate (1 M) rather than formic acid.

The elemental analysis results of bio-crude derived from the hemp protein reveal that the oxygen content reduces as the temperature increases. The energy recovery of asparagine is negligible as the bio-crude yields are small. The energy recovery increases in relation to the temperature for hemp protein and asparagine. On average, the difference between both formulas (by means of Dulong and Milne formulas) is minor with approximately 3 %.

7.4.2.4 Analysis of the bio-crude oil and raw materials by STA-MS

Figure 7-6 (a) illustrates the weight loss curve and derivative of raw asparagine and raw soya protein. Samples were combusted and the evolved gas was analysed with mass spectrometry and infrared detection. Figure 7-6 (b) illustrates the weight loss curve and derivatives for the bio-crude from the soya protein and asparagine processed at 350 °C.

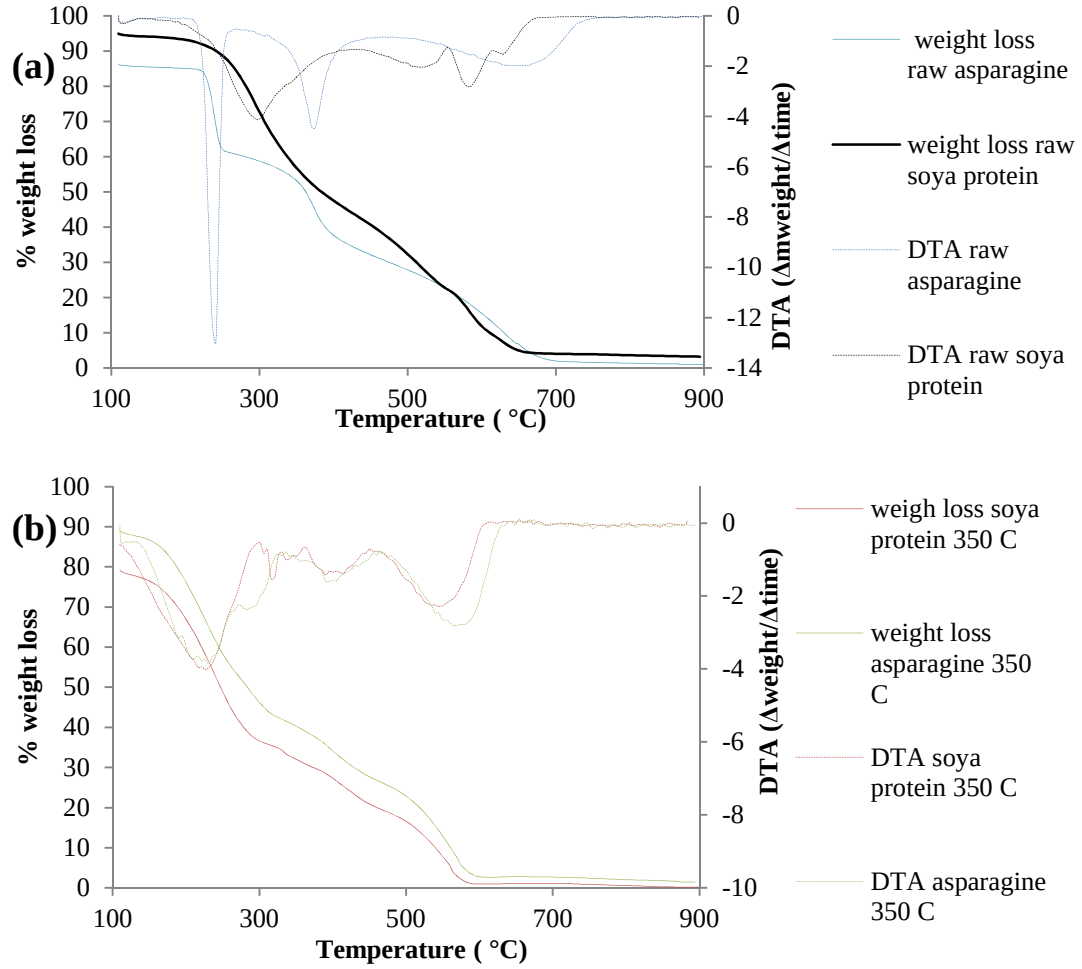

Figure 7-6: Thermogravimetry and derivatives curves (a) raw samples and (b) of the bio-crude oil asparagine and soya protein at 350 °C

The combustion of the raw asparagine can be subdivided into three steps, at first at approximately 240 °C, the second at 380 °C and the third over a broader temperature range starting approximately 600 °C. Similarly, the decomposition of raw soya protein can also be divided into three steps although they are more complicated with first DTA step at 286 °C, the second at 514 °C and the third at 574 °C. The combustion profiles of the bio-crude oils shown Figure 7-6 (b) on the other hand are

much more similar and once again show three main steps. These steps broadly correlate with the release and combustion of volatiles, secondary degradation of larger molecules to smaller molecules and lastly combustion of chars.

The measurement of carbon dioxide and carbon monoxide in relation to the temperature are displayed in Figure 7-7 for the raw feedstocks (a) and bio-crude oils (b). The wavelength measured of carbon dioxide (CO_2) is 2362 cm^{-1} and for carbon monoxide (CO) 2175 cm^{-1}. As expected, production of carbon dioxide and carbon monoxide are spread throughout the combustion profile for all the samples.

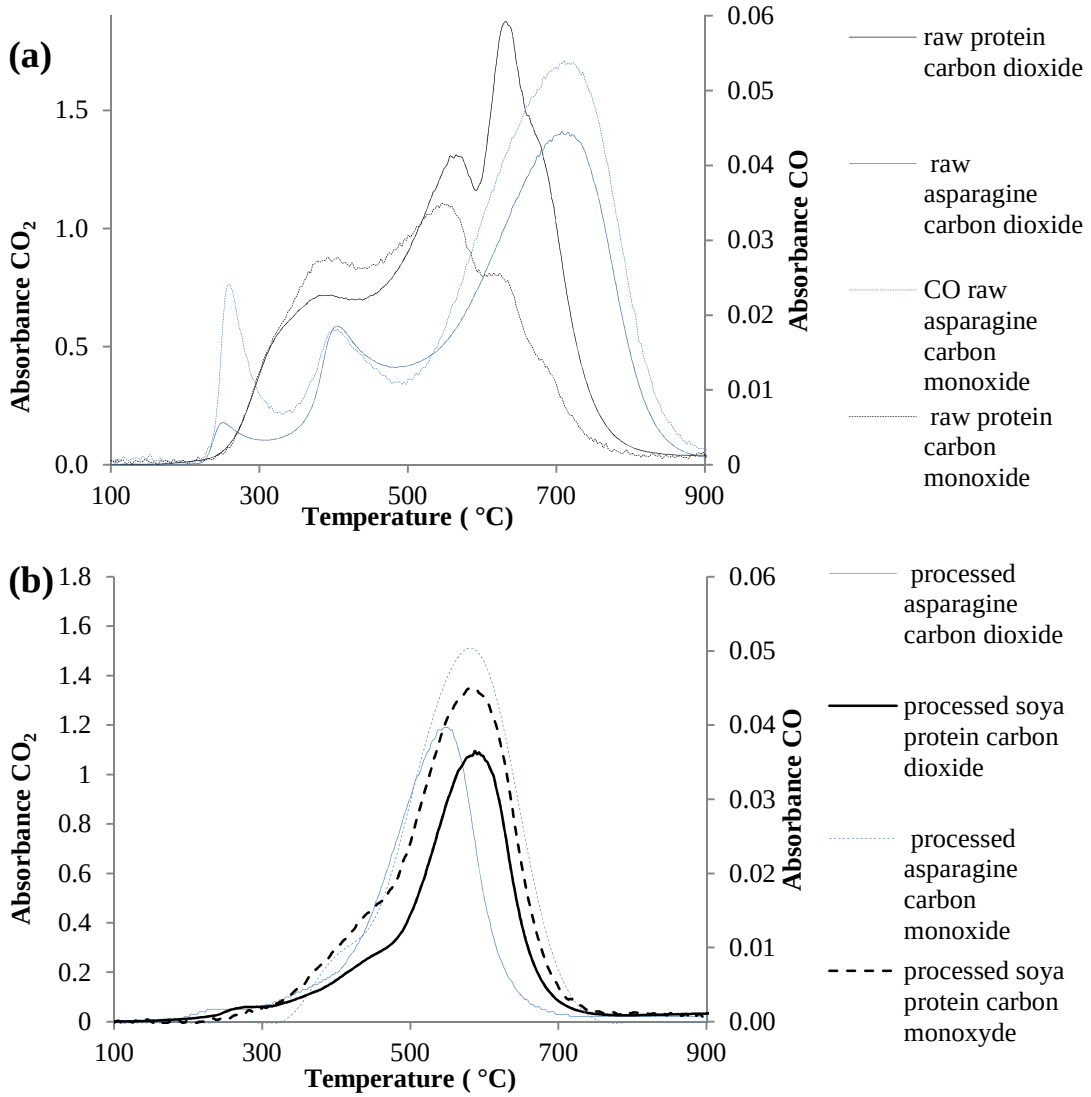

Figure 7-7: Heating profile of CO and CO_2 measured by the FT-IR from 100 to 900 °C for the raw samples (a) and the processed of soya protein and asparagine (b)

The release of carbon monoxide is measured at a lower temperature of 254 °C with the raw asparagine although; the highest temperature is measured at 715 °C for both gases, which is different to soya protein. The carbon dioxide profile for the

processed bio-crude is less spread with a maximum at 530 °C for asparagine and 570 °C for soya protein.

Figure 7-8 (a) and (b) show the evolved gas analysis for nitric oxide (NO), nitrogen dioxide (NO_2) and hydrogen cyanide (HCN) for the raw and the processed soya protein and asparagine. There is emission of nitric oxide associated with each of the steps shown the thermogravimetry at 241, 370 and 644 °C. The production of nitrogen dioxide is negligible. The emission of hydrogen cyanide is low compared to nitric oxide. Two main peaks of the emission of the nitric oxide are detected at approximately 340 and 574 °C, no nitrogen dioxide is produced and the emission of hydrogen cyanide is spread between 300 and 500 °C.

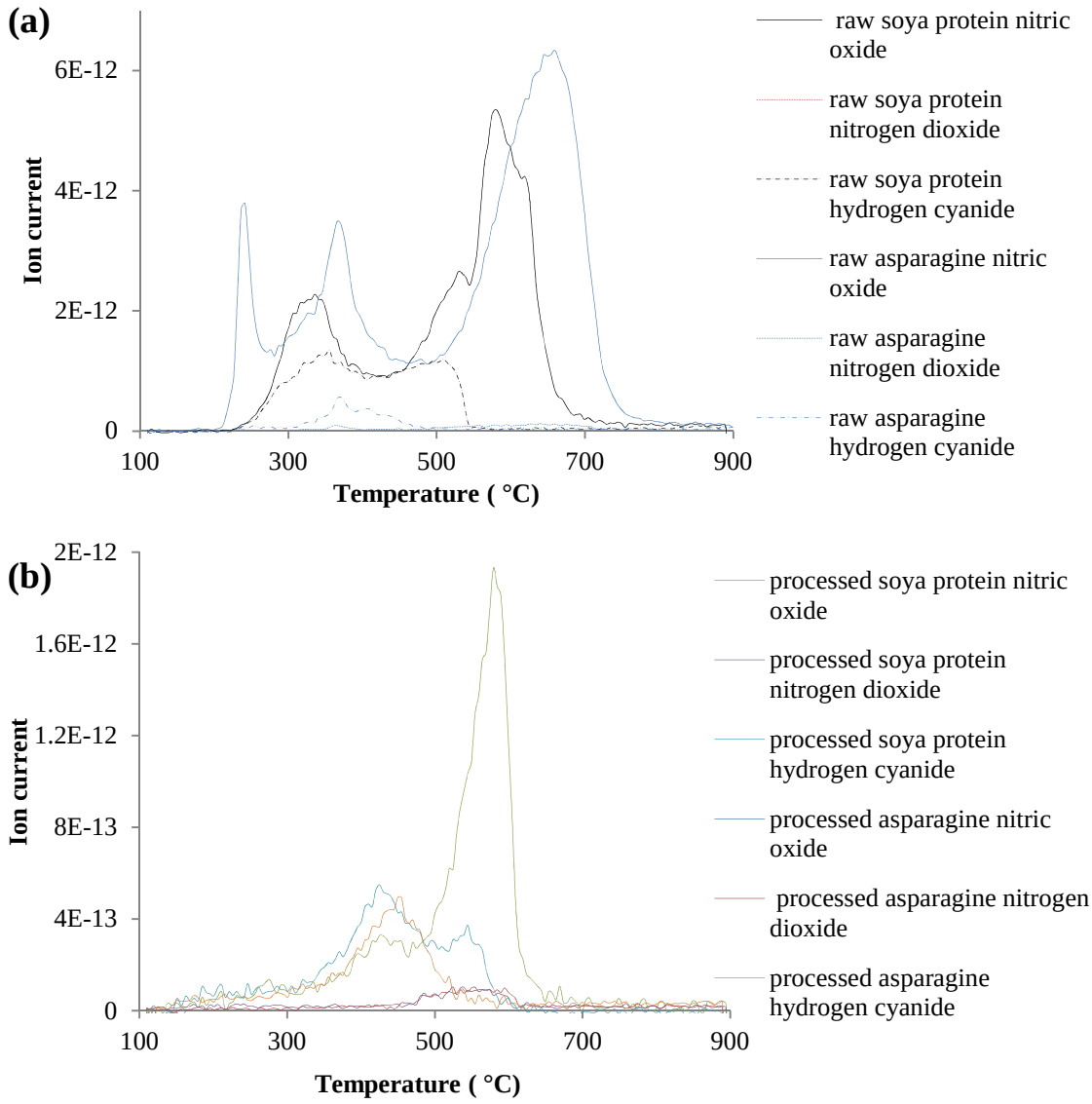

Figure 7-8: Heating profile of NO and NO_2 HCN measured by the MS from 100 to 900 °C for the (a) raw samples and (b) processed bio-crude oil of soya protein and asparagine

The evolved nitrogen gases from the bio-crude are shown in Figure 7-8 (b). The main gas produced with the bio-crude oil of soya protein is nitric oxide with a maximum at 579 °C. Hydrogen cyanide is also detected before within the 400-500 °C regions. Surprisingly, no nitric oxide is detected during the combustion of bio-crude oil from asparagine, an insignificant amount of nitrogen dioxide is produced; more hydrogen cyanide at 440 °C is measured. The highest release of nitrogen is released at 579 °C which could imply that nitrogen in the oils is present in the "heavy molecular weight" materials. Hydrogen cyanide is one precursor to nitric oxide and nitrous oxide (N_2O) explaining why the peak emission for hydrogen cyanide is observed first and subsequently nitric oxide [295]. The gas released profile temperature is similar to chars measured by Darvell et al. [129] with a maximum emission at high temperature to the slow combustion rate (10 °C/min). It is important to note that after 500 °C, over half of the bio-crude has been lost and so it is possible that the nitrogen is largely associated with "heavy molecular weight" materials. Hydrogen cyanide was detected in the gaseous phase from the hydrothermal liquefaction of microalgae. The pyrolysis of 2,5-diketopiperazine originally from protein produces isocyanic acid (HNCO) and hydrogen cyanide at high temperature [296]. Under combustion, a similar pathway could be assumed except that hydrogen cyanide can be further degraded into nitric oxide as a final product. Herrera et al. [297] measured the formation of hydrogen cyanide at 410 °C during the degradation of polyamide polymers in air, nonetheless the formation of nitric oxide was not mentioned.

7.4.3 Residue analysis

Table 7-4 lists the elemental analysis, energy content and the energy recovery from the residue of the different reactions. Not all samples were analysed but the data still provides some useful information. The ash content for the sample of soya protein is 3.5 wt.% and 5.2 wt.% of moisture content. The ash content of hemp protein is 10.5 wt.% and 5.0 wt.% of moisture. The sample from the processing of hemp protein in formic acid contains 20.5 wt.% of ash.

Table 7-4: Nitrogen, carbon, hydrogen, sulphur and oxygen content in the residue energy content (Dulong and Milne) and % energy recovery for experiments for different models (hemp, soya)at different temperatures and conditions on a dried free ash basis

	N wt.%	C wt.%	H wt.%	S wt.%	O wt.%	Dulong HHV (MJ/kg)	H/C	O/C	Milne HHV (MJ/kg)	% Energy recovery
Hemp proteins										
250 °C	4.5	44.6	6.0	0.0	29.4	18.5	1.6	0.5	19.0	19.3
300 °C	3.8	39.9	4.6	0.0	36.2	13.6	1.4	0.7	14.7	9.4
350 °C water	4.2	47.1	5.3	0.0	27.9	18.5	1.3	0.4	19.1	9.5
formic acid	2.1	23.7	1.9	0.0	40.6	2.1	1.0	1.5	4.0	0.9
Soya proteins										
250 °C	7.3	49.7	6.6	0.0	27.6	21.3	1.6	0.4	21.4	7.3
300 °C	6.8	38.0	5.2	0.1	41.3	12.9	1.6	0.8	13.9	2.9
350 °C water	5.4	48.8	3.6	0.0	33.8	15.6	0.9	0.5	16.5	2.9
formic acid	-	-	-	-	-	-	-	-	-	-

Firstly, most of the residue contains low amounts of carbon compared to the bio-crude oils with exception of asparagine at 350 °C with 61.9 wt.% (not shown in the table). For soya and hemp proteins, the carbon and nitrogen contents are reduced indicating that the carbon content is moving towards the aqueous phase and the bio-crude. The nitrogen content in the residues is relatively high suggesting there is indeed "heavy molecular weight" nitrogen materials such as asphaltene being formed.

The presence of formic acid lowers the carbon and the nitrogen contents of the residue further compared to in water alone. Ash is important because it could play a role on catalysing reaction and in the presence of heterogeneous catalysts they could foul or poison them [146].

7.4.4 Aqueous phase analysis

As a major part of products are fractionated into the aqueous phase especially with asparagine and soya proteins, the analysis of the aqueous phase is important in order to have a better knowledge about the fate of nitrogen. Thus, analysis of the process water are performed in details for the pH, the ammonium compound concentration, phosphate, sulphate, potassium, total organic carbon for all the experiments. This data can be found in Appendix 1, section 1.1.1 page 317.

For both proteins, the ammonium compound concentration increases in relation to the temperature. The concentration is more significant with soya protein at 350 °C (18,537 ppm) compared to hemp proteins (4730 ppm), as the first one contain more nitrogen content. The increase of ammonium compound induces a rise of the pH value from 7.1 to 8.9 for soya protein and 6.8 to 7.2 for hemp proteins. In general, the pH is significant factor as it has an influence on the concentration of the ionic and cationic species, the pKa for NH_4^+/NH_3 is approximately 9.2, and it implies that below a pH of 9.2 the concentration of NH_4^+ is more significant compared to NH_3 [298]. Therefore, in alkali pH, the presence of nitrogen species is enhanced and *vice versa*. A lower ammonium compound concentration is observed when using formic acid (4437 ppm) with hemp protein. A lower ammonium compound concentration can be explained by the formation of amides. In contrast, the ammonium compound concentration increases for soya protein. Dote et al. [111] found that the majority of nitrogen in processed water from protein was present as ammonium, (approximately 70 %), and only a small portion of organic nitrogen measured by the Kjeldahl method.

For the processed water from asparagine, the increase of ammonium compound between the temperatures is less obvious than for soya proteins. It is likely that the asparagine is already converted as explained by Abdelmoez et al. [288]; the kinetic of decomposition was high with glutamic acid (similar structure to glutamine with a carboxylic acid instead of an amide group). In the same study, it was deduced that most of amino acids were stable in alkali pH and more reactive in acidic pH. For the processed water from glutamine and the mixture, the ammonium compound concentration is lower, it was demonstrated in the previous study that mixture of two amino acids were more stable [288].

Asparagine contains two nitrogen functional groups, an amide and a primary amine attached to a α-carbon, nitrogen functional group (amides + amines) representing 24 % of the whole molecular weight. The conversion into ammonium compound is calculated thanks to the Equation 7-3 where $\left[NH_4^+\right]$ the ammonium compound concentration is in ppm, V_{water} is the volume of water in litre (27 ml or 0.027 L) and $m_{initial\ asparagine}$ the initial mass in g approximately 3 g.

$$\text{Conversion } NH_4^+ = \frac{m_{\text{initial asparagine}} - \left(\left[NH_4^+\right]/1000\right) \times V_{water}}{m_{\text{initial asparagine}}} \times 100$$

Equation 7-3

Approximately 76.4 wt.% of the initial asparagine is converted into ammonium compound which is close to the value from Dote et al. [111]. The hydrolysis of asparagine could yield several supposed products (Figure 7-9). A more detailed analysis of the aqueous phase should be carried out to find out if these products are present.

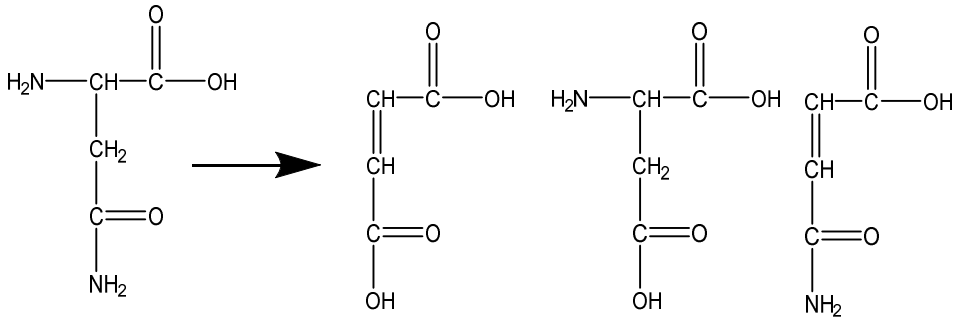

Figure 7-9: Likely product from the hydrolysis of asparagine after hydrothermal liquefaction

In general, the TOC concentration of the processed water for both proteins decreases as the temperature increases. The TOC concentration of glutamine is double (20,220 ppm) compared to asparagine, where the concentration of acetic acid is also significant with 51,000 ppm. The acetate ion is not detected for the other sample as high dilution is prepared to fall within the ammonium compound calibration range. The high concentration in acetate explained why a pH of 7.5 is determined. Rogalinski et al. [284] discovered that amino acids could decompose into carboxylic acids (acetic or propanoic acid), amides (ethanolamide) and other products.

7.4.5 Carbon and nitrogen mass balance

Using the data collected, it is possible to determine the carbon and nitrogen mass balance and this data is listed in Table 7-5. When the CHNS of the residue is not available, the carbon or nitrogen gaseous and residue mass balance is calculated as a single term.

Table 7-5: Carbon and nitrogen mass balance for the aqueous, bio-crude oils and remaining phases for the experiments model compounds (soya, hemp and asparagine) at different temperature and conditions

	% C aqueous	% C bio-crude	% C residue	% C gas	% N aqueous	% N bio-crude	% N residue	% N gas
Hemp proteins								
250 °C	31.6	30.6	20.4	17.3	21.0	12.6	13.6	52.8
300 °C	26.5	36.5	12.1	24.9	45.2	15.7	7.5	31.6
350 °C water	15.5	57.2	10.7	16.6	49.5	25.4	6.2	18.9
formic acid	16.8	28.8	3.3	51.1	42.3	12.9	2.2	42.6
Soya proteins								
250 °C	57.2	20.3	7.6	14.8	63.5	8.2	4.0	24.3
300 °C	42.0	30.7	3.9	23.4	91.0	10.9	2.5	-4.4
350 °C water	36.8	28.1	4.2	30.9	97.8	8.3	1.6	-7.7
formic acid	38.5	21.2	0	40.3	93.3	4.9	0	1.8
Asparagine								
250 °C	60.5	2.3	0	37.2	92.0	0.3	0	7.7
300 °C	25.4	7.7	7.1	59.7	84.7	1.5	0.1	13.7
350 °C water	25.6	10.2	8.1	56.1	95.2	2.1	0.5	2.2
formic acid	37.3	8.2	11.6	42.9	86.4	1.0	0.3	12.4
glutamine	59.8	8.5	0	31.7	49.2	2.0	0.0	48.8
Mix asn-gnu	33.8	14.0	0	52.2	54.1	3.9	0.0	42.1

The nitrogen fraction in the aqueous phase and in the bio-crude generally increases as the temperature increases and is explained by ammonium compound being produced. At 300 °C, Dote et al. [282] detected that 80 % of the nitrogen was in the aqueous phase which was coherent with the result above. The use of formic acid generally reduces the nitrogen content in the bio-crude. Similar trends are observed for each of the feedstock investigated.

There is a reduction in carbon fraction in the process waters as the temperature increases for soya protein. At higher temperatures, the carbon fraction is generally transferred into the bio-crude and into the gaseous phase. For hemp protein, the transfer of the carbon fraction from the aqueous phase and the residue to the gaseous

phase and the bio-crude oils is observed suggesting a polymerisation of the polar molecule to form the bio-crude. There is a slight increase in carbon fraction in the process waters when using formic acid and it is possible this is due to unreacted formic acid.

To summarise this section, during the hydrothermal liquefaction of proteins and amino acids, most of the products are decomposed into the aqueous phase.

- More bio-crude oils were obtained with hemp protein because of the initial presence of lipids.
- The presence of lipids also led to the production of fatty acid amides in the bio-crude.
- As the temperature increases from 250 to 350 °C, the carbon fraction is transferred from the aqueous phase into the bio-crude oils and in the gaseous phase.
- The ammonium compound concentration in the aqueous phase increases in relation to the temperature.
- Most of compounds in the bio-crude oil are identified as heterocyclic compounds which are relatively stable.
- The result from the STA-MS could suggest that most of the nitrogen were present in the “heavy molecular weight” materials.

Finally, comparable to starch and triglycerides the hydrolysis of proteins under subcritical water was rapid and subsequently amino acid decomposed into ammonium or organic nitrogen compounds.

7.5 Influence of metal doped HZSM-5 catalysts on bio-crude composition

In this section, screening undertaken with different metal (molybdenum, iron, copper and nickel) doped HZSM-5 in water and in formic acid solution (1 vol.%) with soya protein is discussed. These metal doped zeolites are investigated whether they have any impact on the fate of nitrogen.

7.5.1 Mass balance yield

Determination of the mass balance allows evaluation of the activity of catalyst for enhancing more bio-crude production from soya proteins. Results in water and formic acids are presented in Figure 7-10. Experiments were carried out in duplicate therefore average values are shown here. The coefficient of variance for the following experiment in water was 9.5 % in water respectively and in formic acid for the same order of catalysts the variance was 6.6 %.

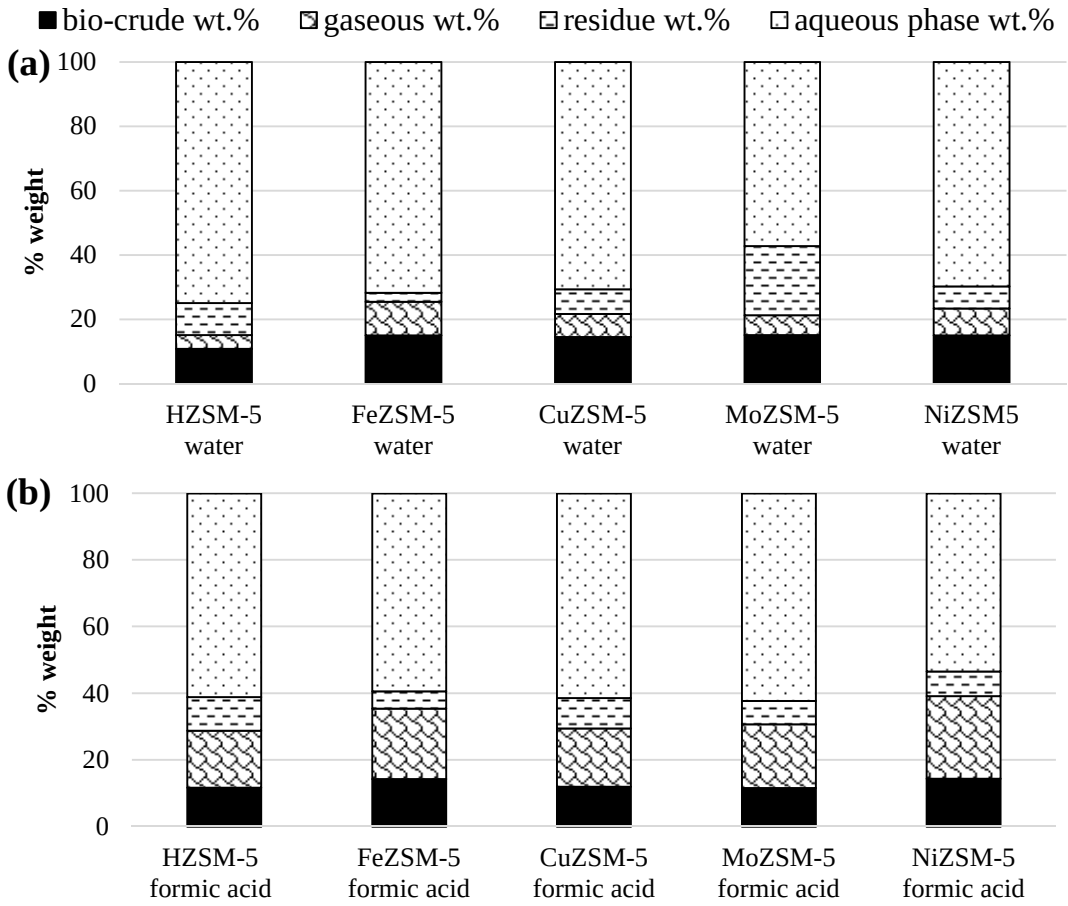

Figure 7-10: Diagrams representing mass balance for the different fractions of bio-crude oils, gaseous, residue and aqueous fractions for the catalytic screening using metal doped HZSM-5 for soya proteins (a) in water and (b) in formic acid.

Using water alone, doped metal HZSM-5 does not enhance the production of bio-crude yield compared to the experiments without catalyst. Similar bio-crude yields are obtained with copper and molybdenum, the bio-crude yield is lower than 15 wt.% for the other catalysts. FeZSM-5 enhances the production of gas compared to the others catalysts and MoZSM-5 enhances the production of residue.

Using formic acid, as with the carbohydrate experiments, the gas fraction is more pronounced than with water alone and particularly with iron and nickel, in contrast the bio-crude production is lower than in water (approximately 12-14 wt.%). On the whole, the difference between each catalyst is subtle. A major part of the products are detected in the aqueous phase.

7.5.2 Bio-crude analysis of the catalytic runs

7.5.2.1 GPC analysis

The bio-crude oils were analysed using the same techniques as previously analysed with GPC, CHNS analyser and GC-MS. Figure 7-11 presents the different molecular weight fraction for the catalytic screening of soya protein in (a) the water and (b) in formic acid.

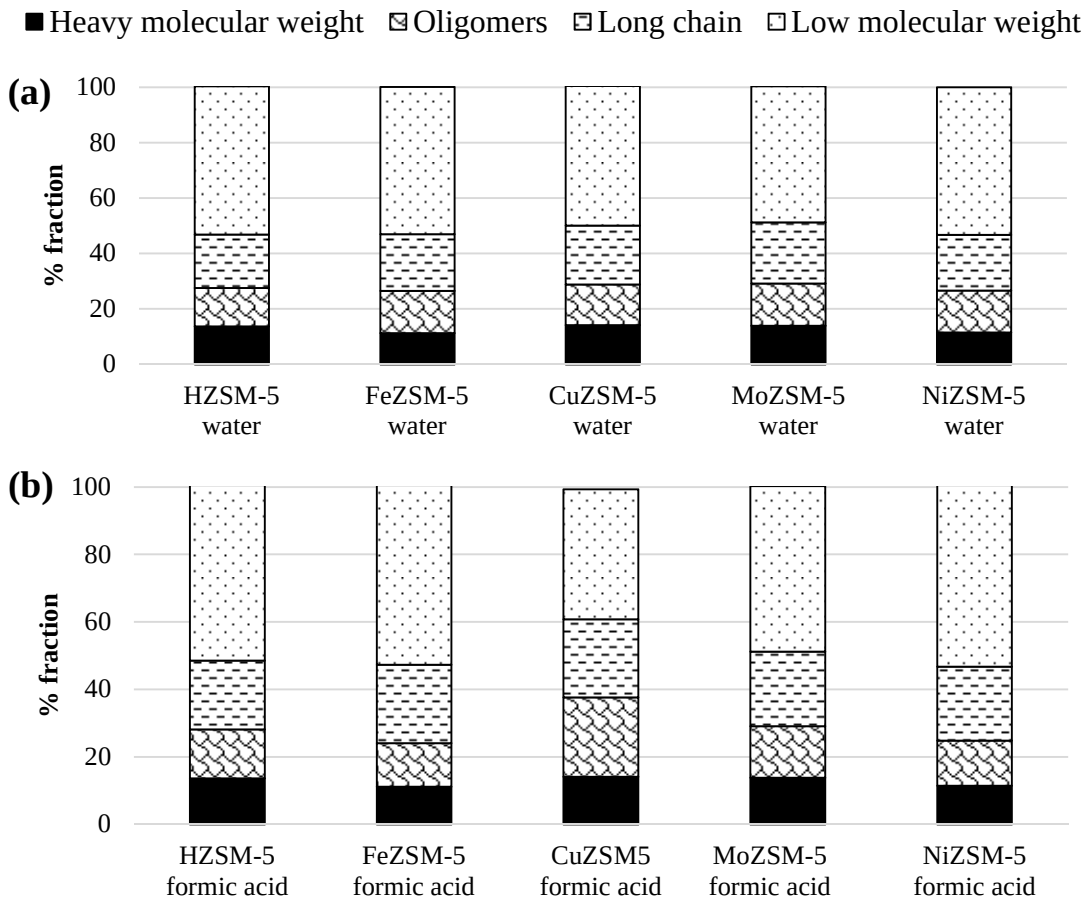

Figure 7-11: Different molecular weight fraction of the bio-crude oils for soya proteins for the catalytic screening (a) in water (b) in formic acid

In water, half of the bio-crude oils are composed of low molecular weight materials (lower than 200 g/mol), materials with a molecular weight above 200 g/mol increase with CuZSM-5 and MoZSM-5.

In formic acid, there are lower impacts with HZSM-5, FeZSM-5 and NiZSM-5. CuZSM-5 is more selective for the production oligomers and "heavy molecular weight" materials. One study from Imai et al. [286] suggested that in hydrothermal vents $CuCl_2$ enhances oligomerisation of glycine where the excess

amino acid formed a chain with diketopiperazine. Obviously, the goal of the catalyst is to obtain low molecular weight materials and here leachate metals seemed to have more effect than the HZSM-5 as the acidic sites enhance slight the fractionation of the proteins into the formation of low molecular weight materials. On the other hand, metal or leachate metal favoured other chemical reaction such as condensation.

7.5.2.2 GC-MS analysis

A typical example of GC-MS chromatograms is shown in Figure 7-12 for the bio-crude formed using CuZSM-5 in water with soya proteins. Figure 7-13 contains some examples of molecule identified in the chromatogram. Table 7-6 lists the main compounds identified in the chromatogram.

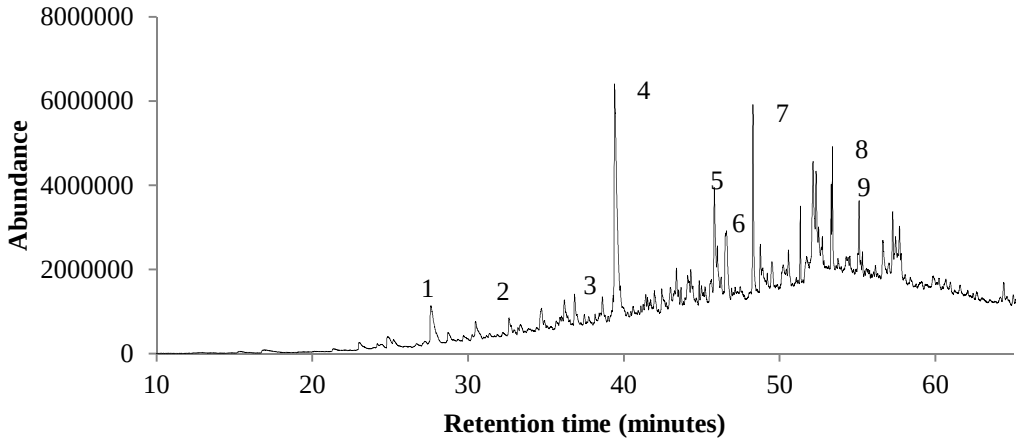

Figure 7-12: Examples of chromatograms for CuZSM-5 in water with soya proteins

Table 7-6: Peaks identification in the GC-MS

Number	Retention time (minutes)	Compounds
1	27.5	1-butyl-2-pyrrolidinone
2	32.6	N-(1-methyl-2-propynyl)-benzenamine
3	36.1	1-(2-phenylethyl)-pyrimidine-2,4,6trione
4	39.6	methyl-2-oxo-pyrolidine-acetate
5	28.2	(1-ethyl-2-pyrrolidinyl)-methylamine
6	45.8	5,10-diethoxy-2,3,7,8-tetrahydro-dipyrrolopyrazine
7	48.3	L-Leucine-N-cyclopropylcarbonyl-methyl ester 9H-pyridoindole
8	53.1	N-(5-methyl-3-isoxazolyl)-2-(4-methyl-4H-1,2,4-triazol-3-ylthio)-acetamide,
9	55.0	hexahydro-3-(phenylmethyl)-pyrrolopyrazine-1,4-dione

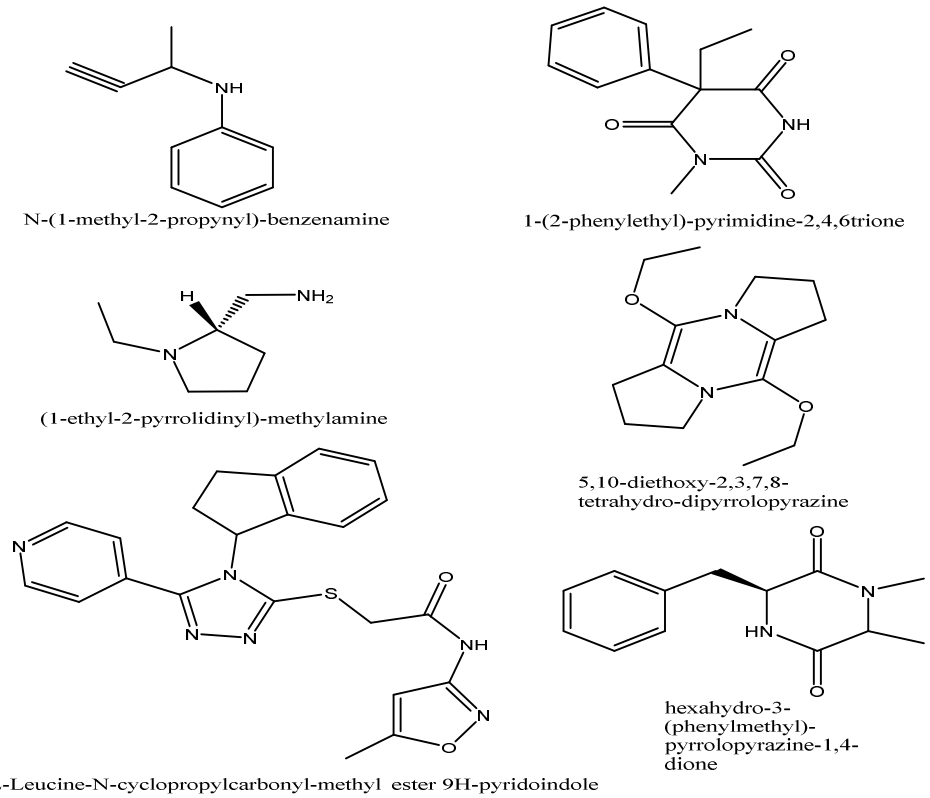

Figure 7-13: Main molecule identified from the bio-crude processed with CuZSM-5 in water

These compounds are mainly nitrogen heterocycles such as pyrazine with two nitrogen atoms formed by the condensation of two amino acids. Compared to the run without catalyst more aromatic nitrogen compounds are identified such as N-(1-methyl-2-propynyl)-benzenamine. Compounds 7 and 8 are an indication of the condensation of several cycles and amino acids to form later oligomers. The compound 9 is a derivative of a diketopiperazine from a phenylalanine and probably a serine. The complexity of the molecules identified with CuZSM-5 could explain why the fraction of “heavy molecular weight” determined by GPC is more significant.

7.5.2.3 Elemental analysis

To investigate the effect of catalysts on the nitrogen content of the bio-crude oils, elemental analysis is lists in Table 7-7.

Table 7-7: % nitrogen, carbon, hydrogen, sulphur and oxygen content in the bio-crude oils, energy content (Dulong and Milne) and % energy recovery for experiments for soya proteins for the screening of metal doped HZSM-5 as dried basis

	N wt.%	C wt.%	H wt.%	S wt.%	O wt.%	Dulong HHV (MJ/kg)	H/C	O/C	Milne HHV (MJ/kg)	% Energy recovery
water										
HZSM-5	7.5	71.5	9.7	0.6	10.7	36.1	1.6	0.1	34.9	28.9
FeZSM-5	6.6	70.5	9.5	0.7	12.8	35.2	1.6	0.1	34.1	19.8
CuZSM-5	7.8	79.1	10.5	0.7	1.9	41.5	1.6	0.0	39.6	30.3
MoZSM-5	5.7	67.6	9.3	0.5	16.9	33.2	1.6	0.2	32.5	15.1
NiZSM-5	7.3	75.7	9.9	0.9	6.3	38.7	1.6	0.1	37.1	30.3
Formic acid										
HZSM-5	5.9	71.3	9.1	0.6	13.1	34.9	1.5	0.1	33.9	17.9
FeZSM-5	6.4	72.2	9.3	0	12.1	35.5	1.5	0.1	34.5	22.4
CuZSM-5	6.3	74.6	9.4	0.2	9.6	36.9	1.5	0.1	35.8	19.4
MoZSM-5	5.8	71.2	9.2	0.3	13.4	34.8	1.5	0.1	34	17.8
NiZSM-5	6.2	75	9.6	0	9.3	37.4	1.5	0.1	36.2	23.7

For the experiment in water, for most of the catalyst, a high carbon and hydrogen contents are determined in the bio-crude resulting in an increase in energy content. Nitrogen content is still high and above the run without any catalysts with 6.5 wt.%, however for MoZSM-5 a reduction of the nitrogen content is measured. CuZSM-5 and NiZSM-5 achieved a good deoxygenation capacity with 1.9 wt.% and 6.3 wt.%. It is confirmed by the GC-MS chromatogram where few compounds with oxygen are identified. The energy content is higher with CuZSM-5, nevertheless; the bio-crude oils contains 8.4 wt.% of nitrogen content.

For the experiment in formic acid, lower amounts of nitrogen and hydrogen content is detected compared to reaction in water. The same conclusion can be drawn that the runs in formic acid alone reduce the nitrogen content. For NiZSM-5 in formic acid a good energy recovery is achieved with 23.7 % even though it is below of the value obtained in water. In general, the impact of the impact of doped metal is negligible.

7.5.3 Aqueous phase analysis

The aqueous phase was analysed to measure TOC, ammonium, phosphate, sulphate, potassium concentrations and the pH value, displayed in the shown in Appendix 1, section 1.1.2 page 318. The trend for the ammonium compound concentration is significant in understanding the impact on the effect of metal doped catalyst.

In water, the highest ammonium concentration is measured with MoZSM-5 (12,415 ppm), the other catalysts have a close concentration (approximately 11,800 ppm). In presence of formic acid, the ammonium compound concentration with NiZSM-5 is enhanced to 9130 ppm compared to 2224 ppm in water. The pH in the alkali region (8-9) could emphasise the high ammonium compound concentration.

HZSM-5 and MoZSM-5 result in TOC concentration above 16,000 ppm. Conversely, NiZSM-5 reduces the fraction of aqueous compounds. There is no link with the mass balance and the TOC concentration for MoZSM-5 (16,343 ppm) since the yield of the aqueous phase is the lowest (57 wt.%). Iron effects by reducing the level of phosphate to 1810 ppm in the solution contrary to MoZSM-5 in water (2447 ppm). In general, phosphate (PO_4^{3-}) concentration is more significant above a pH of 12.7 because of its pKa. The sulphate concentration (SO_4^{2-}) is not affected by the change of catalysts, the concentration is low because of the alkali pH and biomass contains also low sulphur.

7.5.4 Carbon and nitrogen mass balance

Table 7-8 contains the balance for nitrogen and carbon for catalytic screening of metal doped HZSM-5 with soya protein. The carbon and nitrogen fraction in the aqueous phase and in the bio-crude oils are calculated and the nitrogen and carbon in the residue and gaseous phase are determined by difference of the two others.

Table 7-8: Carbon and nitrogen mass balance for the aqueous, bio-crude oils and remaining phases for the experiments using soya protein with metal doped HZSM-5

	% C aqueous	% C bio-crude	% C remaining	% N aqueous	% N bio-crude	% N remaining
			Water			
HZSM-5	45.1	15.7	39.1	89.0	9.0	1.9
FeZSM-5	31.1	24.9	44.0	89.8	12.9	-2.7
CuZSM-5	31.3	23.3	45.4	89.7	14.4	-4.1
MoZSM-5	43.5	18.4	38.1	91.7	8.5	-0.2
NiZSM-5	25.2	21.6	53.2	16.4	13.0	70.5
			Formic acid			
HZSM-5	39.9	16.5	43.6	80.1	7.5	12.4
FeZSM-5	32.6	20.5	46.9	46.9	10.0	43.0
CuZSM-5	26.3	17.7	56.0	62.3	8.2	29.5
MoZSM-5	35.5	16.4	48.0	66.2	7.4	26.4
NiZSM-5	34.1	21.4	44.5	61.7	9.7	28.6

HZSM-5 and MoZSM-5 are selective towards enhancing the carbon fraction in the aqueous phase. FeZSM-5 is more selective towards increasing carbon fraction to the bio-crude. The addition of formic acid increases the amount of nitrogen fraction partitioned in the aqueous phase. The lowest nitrogen fraction is obtained for HZSM-5 and formic acid.

Lastly, the influence of metal doped HZSM-5 is somehow minimal on enhancing the formation of bio-crude of soya proteins. MoZSM-5 reduces slightly the nitrogen fraction in the aqueous phase but on the other hand, copper and iron increase the nitrogen fraction into the bio-crude. Copper in formic acid could enhance the polymerisation of molecules to form oligomers.

To summarise, the following general conclusions can be drawn:

- Compared with the non-catalytic run, no increase of bio-crude yield is observed with the catalyst.
- The addition of metal doped zeolite seems to have an impact on the mass balance in particular with CuZSM-5 to improve the carbon and also reduces the oxygen content to 1.6 wt.% in the oil and likewise result in an increase for the nitrogen in oil and aqueous phase.

– Metal doped catalyst enhances the production of ammonium compound (up to 90 wt.%) in water compared to formic acid.

– FeZSM-5 reduces slightly the nitrogen content in the bio-crude oil.

– There is a question whether the metal leachate had more effect on the conversion than the zeolite alone.

7.6 Discussion about the degradation of proteins

As with polysaccharides, the hydrolysis of protein is rapid and occurs at low temperatures probably 250-275 °C. The study of Pińkowska et al. [299] showed a full hydrolysis of soya protein completing after 15 minutes at 268 °C. Rogalinski et al. [284] showed that the hydrolysis of bovine serum albumin protein (BSA) readily occurred in semi continuous reactor below 300 °C in a few seconds; yielding different amino acids (for example asparagine). Torri et al. [137] suggested that the most likely degradation route under hydrothermal conditions for proteins was by formation of oligopeptide based on the condition observed under pyrolysis by Meetani et al. [293]. Figure 7-14 shows the degradation towards the hydrolysis of proteins for forming nitrogen heterocyclic compounds [293].

1) The both end extremity of the peptide chain (amide and carboxylic group) reacts together to form a cycle. As the temperature increases the cycle size subsequently decreases by losing amino acids. It is possible to observe with the GPC analysis that the fraction of oligomers is reduced in relation to the temperature to form lighter compounds.

2) Released amino acids condense together to form diketopiperazine (DKP). This compounds are found in the bio-crude at low temperature (250 and 300 °C) in the study suggested that the degradation of protein is similar than explained by Meetani et al. [300]. One example of DKP is given where the first one was produced by the cyclisation of two valine amino acids (Figure 7-15). Faisal et al. [301] gave evidence of the formation of the formation of cyclodipeptides from glycine dipeptide between 240 to 300 °C. The reaction of cyclodehydration is reversible in a short time at low temperature.

3) Above 300 °C, diketopiperazine (DKP) could decompose by rearrangement into ammonium compound and 1-butyl-2-pyrrolidinone. This compound is considered as a key compound for the degradation of proteins and amino acids [302].

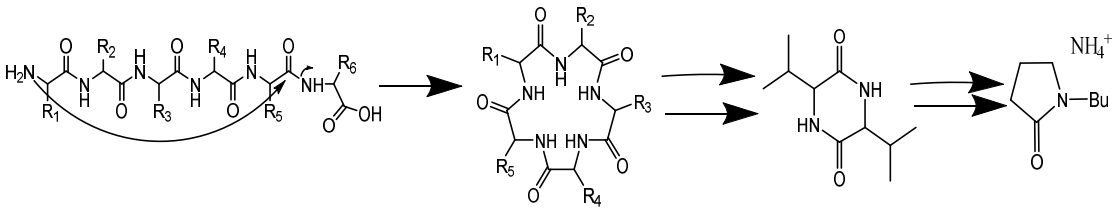

Figure 7-14: Decomposition route of proteins [137]

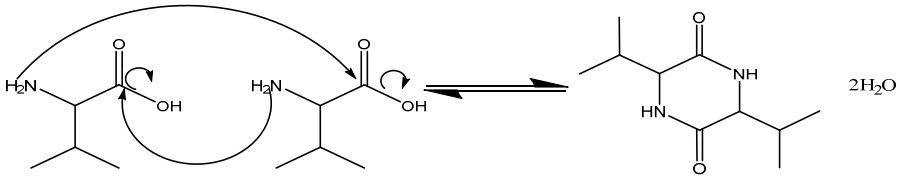

Figure 7-15: Formation of diketopiperazine from condensation of two valine amino acids

The degradation of amino acids is also rapid to occur under subcritical water. Yoshida et al. [283] showed that asparagine was fully degraded in less than five minutes at 270 °C in subcritical water. The decomposition depend on their R functional groups; for example, the decomposition of aspartic acid occurred rapidly whereas glycine and alanine were more thermally stable [285]. As Dote et al. [282] observed, most of the nitrogen in the aqueous phase was present as ammonium. Nevertheless, other compounds were detected by several studies such as ethylamine which was transformed further to ammonium compound [287]. At higher temperature, the formation of "heavy molecular weight" materials could have happened, it is one of the hypotheses advanced by several research groups which was that primitive life was created in the bottom of the ocean in hydrothermal vents [303]. Basically, amino acids polymerise to create oligomer chains [93, 286]. Thus, it could indicate that under hydrothermal liquefaction an equilibrium between depolymerisation and recombination occurs [2].

Figure 7-16 illustrates the different decomposition of asparagine under hydrothermal liquefaction from the compounds identified by the GC-MS in the bio-crude where the dash square represents possible compounds in the aqueous phase and the plain square the compound in the bio-crude oils.

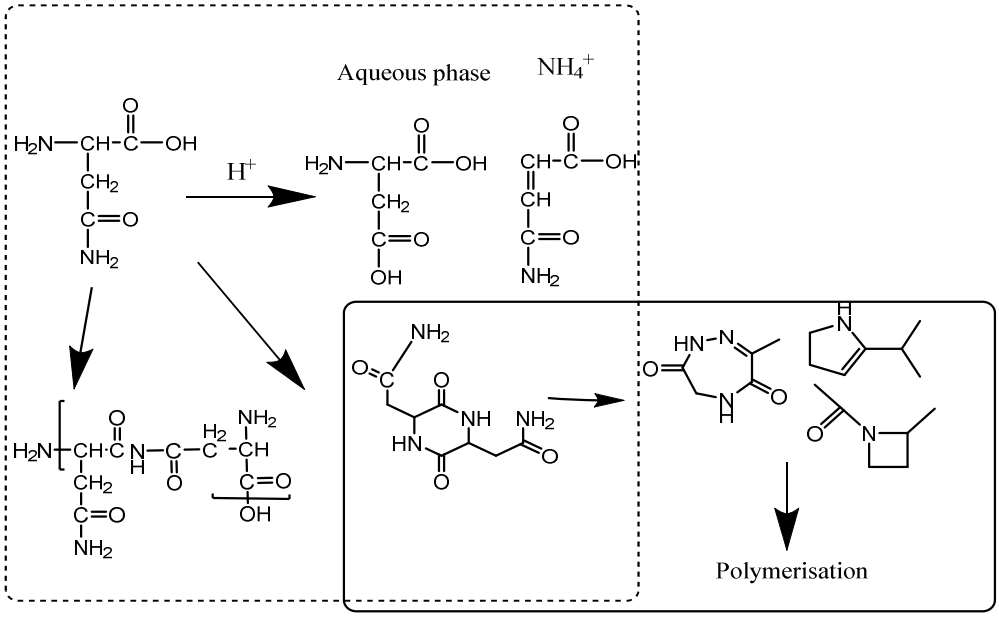

Figure 7-16: Decomposition route of asparagine under hydrothermal liquefaction

The main route involves the formation of acids and amides/amines as the main fraction is the aqueous phase. The bio-crude oil yield is mainly composed of heterocyclic compounds and oligomers probably pyrrole polymers. Obviously some products are not present as they are not stable and degraded into further compounds.

The presence of lipids in the hemp protein leads to the formation of amides in the bio-crude oils. This point will be discussed in more detail in the next chapter. It is important to emphasise that high yield of bio-crude is not necessarily a good effect when the main composition is made of nitrogen heterocyclic compounds resulting in a low energy content and production of NO_x during the combustion. To finish, amino acids forms low bio-crude yields similar to the level of carbohydrates (less than 10 wt.%). Soya and hemp protein yield more bio-crude (approximately 20-30 wt.%). The consistency is dark and very viscous and not suitable for any usage.

CuZSM-5 is more selective to enhance the carbon fraction in the bio-crude oil and the nitrogen fraction in the bio-crude oil and in the aqueous phase. The addition of metal salts such as copper enhance the kinetic reaction and the formation of “heavy molecular weight” materials, that is the reason why the GPC, the fraction of compounds in the processed bio-crude from soya protein with a molecular weight above 600 g/mol is more significant.

The purpose of these catalysts is to improve the production of ammonium compounds, for soya protein this cation is more predominant with HZSM-5 compared

to the run without catalyst. Yet, it should be mentioned that some compounds containing nitrogen and sulphur could poison the catalyst or the metal active site or even block the pore explaining why there could have been no major difference during the screening [163, 304]. Zeolites with larger pore size (mesoporous or macropores) would have been more suitable. HY (a meso porous zeolite) was used by Liu et al. [305] to absorb nitrogen heterogeneous cyclic compounds. In future work, the development of a similar material stable under hydrothermal conditions such as molecular sieves would be one solution to reduce the nitrogen content of the bio-crude oil or even in the aqueous phase by absorbing compounds and afterwards regenerate them for a another run.

7.7 Implications for the hydrothermal liquefaction of microalgae

Proteins are a key component in microalgal cells, the composition depends on the strain and even the growth condition whether the algae was put under nitrogen starvation or not [306]. Cyanobacteria such as *Spirulina* are known to contain high protein between 60-68 wt.% and, *Chlorella* with 55 wt.% [307] whereas *Nannochloropsis o.* contains 35 wt.% protein [251]. The composition of amino acids was different for example with *Chlorella* is as follows: glutamic acid with 11.6 wt.%, aspartic 9 wt.%, leucine 8.8 wt.% and lysine 8.4 wt.% [308].

Essentially, the processing of low lipids algae could cause a similar behaviour than hemp protein where products degraded into the aqueous phase and bio-crude oils. In conclusion, it could be deduced that compounds such as diketopiperazine and pyrrolidone would be identified in the bio-crude oils. Therefore, the most suitable strain would have fewer amounts of proteins. It would be expected to find a high amount of ammonium and phosphate compounds in the aqueous phase in general after the processing of microalgae. Nutrient recycling could subsequently be carried out for the algae culture growth [143].

Fast liquefaction of nitrogen containing biomass such as microalgae could be considered as a pre-treatment. The hydrolysis of proteins and even carbohydrates would be readily carried out. Garcia Moscoso et al. [140] succeeded to extract 60 wt.% of nitrogen from the microalgae (*Scenedesmus sp*) in to the aqueous phase at 240 °C in a couple of seconds. Yet, a solution should be investigated to avoid

recombination of small molecules in the next step to form “heavy molecular weight” materials.

7.8 Conclusion

This chapter gave an insight about the processing of nitrogen model compounds under subcritical conditions. Amino acids were mainly degraded into the aqueous phase as ammonium and organic compounds. Hydrothermal reaction of proteins yielded more bio-crude such as 39.9 wt.% for hemp proteins and 17.5 wt.% for soya proteins at 350 °C in water. The bio-crude oil obtained was composed of nitrogen heterocyclic compounds such as diketopiperazine or pyrrolidinone. Moreover, compounds with a molecular weight above 200 g/mol represented half of the bio-crude oil partition. Ammonium compound concentration was significant in the water in particular with soya proteins. Furthermore, the concentration increased from 250 to 350 °C. As the temperature was increased, the nitrogen content was decreased with soya protein from 7.8 to 6.8 wt.% in the oil whereas an opposite trend was measured by hemp proteins. CuZSM-5 in formic acid had an impact on enhancing the % carbon in the bio-crude but also the nitrogen in the aqueous and bio-crude oils. The deoxygenation of the bio-crude was higher with NiZSM-5 and CuZSM-5. During the next chapter, microalgae with different compositions were processed using the same conditions as in this chapter.

Chapter 8 HTL of microalgae with and without catalysts

Throughout this chapter, four different microalgae (stressed and non-stressed strains of *P. ellipsoidea, Chlorella* and *Spirulina*) have been processed at three different temperatures (250, 300 and 350 °C). At 350 °C, experiments have been carried out in water and formic acid. A catalytic screening with different metal doped HZSM-5 (nickel, iron, copper, and molybdenum) using *Chlorella* and the stressed *P. ellipsoidea* at 350 °C in water and in formic acid has been conducted. The overall purpose is to associate these results with the previous chapters and to evaluate the impact of lipids, carbohydrates and proteins.

8.1 Introduction

Interest in the production of bio-crude from microalgae was prompted by promising results obtained by Dote et al. [119]. In this paper, a bio-crude yield of 64 wt.% is achieved from *Botryococcus b.* at 300 °C (30 minutes). The drawback of this algal strain is its slow growth rate and a poor harvesting yield [309]. Since subsequently, various microalgae strains have been processed under subcritical conditions to obtain bio-crude including *Chlorella v.* [112, 129, 134, 310], *Nannochloropsis sp.* [112, 127, 134, 135, 190, 199], *Dunaliella t.* [48, 124, 134], *Spirulina* [112, 129, 131, 310], *Porphyridium cr.* [112, 134], *Desmodesmus sp.* [133] *Scenedesmus o.* [134], *Phaeodactylum t.* [134]. Indeed, these species are less scarce and obtainable at a reasonable cost. Furthermore, the influence of process variables such as time (5 to 120 minutes) [124, 131, 133, 134], temperature (175 to 450 °C) [124, 129, 131, 133-135] and concentration of initial slurries (10-50 wt.%) [124, 131] on the quality of the bio-crude oil has been investigated in detail.

There is a logical trend that the lipid content in the microalgae will impact the bio-crude yield. Biller et al. [112] proposed that the bio-crude yields are influenced by the biochemical components in the alga and that yield is based on the content of each following the relationship, lipids ≥ proteins ≥ carbohydrates. The nitrogen content in the bio-crude oil is also dependent upon the initial composition of the feedstock and which is evident by the presence of heterocyclic compounds such as pyrrole or indole. The challenge is to produce a high quality fuel; to do so ideally the processed bio-

crude oils should contain hydrocarbon and aromatic compounds with a low fraction of molecules containing hetero-atoms such as nitrogen, oxygen and sulphur.

In order to improve the bio-crude yield and to reduce the level of nitrogen compounds, various heterogeneous catalysts were examined. A broad range of catalysts have been investigated including Pd/C, Pt/C, Ru/C, Ni/SiO_2-Al_2O_3, CoMo/γ -Al_2O_3 (sulfided), and zeolites with and without pressurised hydrogen [190] likewise by Biller et al. [196] with metal impregnated (Co/Mo, Ni, Pt) on alumina. These catalysts have an impact on the deoxygenation of the bio-crude from *Chlorella* and *Nannochloropsis* although only a mild effect is observed on the reduction of nitrogen. In most cases, the use of catalysts often enhances the gas formation and the bio-crude yield is lower. Yang et al. [191] upgraded *Dunaliella s.* at 200 °C with REHY (a HY zeolite doped with rare-earth metal) doped with nickel with and without hydrogen. Lower oxygen content was measured in the bio-crude oils with this catalyst; REHY was robust under this condition with a negligible deactivation of the active site.

Over the last year, some research groups including Savage et al. [147, 189, 199] (Michigan, US) and Duan et al. (Henan, China) focussed their research towards the catalytic upgrading of pre-treated oil. This has demonstrated the reduction in the nitrogen content from 8 % to 1-2 wt.%, although high temperatures were required and the amount of coking and gas formation was significant. HZSM-5 favour the formation of paraffin oil with a yield of 75 wt.% at 400 °C for four hours [189].

In this work, four different strains of microalgae *Chlorella vulgaris*, *Spirulina* and (stressed strain and non-stressed) *Pseudochoricystis ellipsoidea* are processed under subcritical water at different temperatures (250, 300 and 350 °C). At 350 °C, the experiments were carried out in water and formic acid (one hour). The *Chlorella vulgaris* and stressed *Pseudochoricystis ellipsoidea* were also processed at 350 °C for one hour with different metal doped HZSM-5 in water and formic acid. Products were analysed by the same techniques used in **Chapter 7**.

The purpose of this chapter is to improve the understanding of the chemical pathways occurring during processing of different microalgae strains, in particular the fate of nitrogen. Experimental results are compared with results from the literature and a model for the fate of nitrogen is proposed. By combining results obtained from the previous chapter an overall mechanism is elucidated.

8.2 Methodologies

The same techniques were used to investigate the processing of microalgae as were as discussed previously in **Chapter 3**. The lipid from the raw microalgae was extracted using 3:1 chloroform: methanol. The corresponding fatty acids were analysed as the method in **Chapter 5**.

8.3 Chemical composition of the microalgae

Table 8-1 lists the elemental analysis on a dry basis, the energy content (HHV) determined from the Dulong equation and the proximate analysis (ash and the moisture) of the microalgae investigated. The protein and lipid content of the algae and *Spirulina* were measured by Biller et al. [141].

Table 8-1: Proximate and elemental analysis as dried basis of the raw feedstock with the lipids and proteins content.

	Elemental analysis						Composition microalgae (wt.%)				
	N wt.%	C wt.%	H wt.%	S wt.%	O wt.%	HHV (MJ/kg)	Lipids	Proteins	Carbohydrates	Ash	Moisture
Chlorella	10.3	49.4	7.4	0.5	21.5	21.5	25.0	55.0	10.0	10.9	5
Stressed *P. ellipsoidea*	2.9	63.4	9.5	0.0	30.6	30.6	67.0	25.0	7.0	0.8	2.5
Non-stressed *P. ellipsoidea*	8.7	53.5	7.7	0.6	23.9	23.9	23.8	48.0	28.2	4.0	2.5
Spirulina	10.9	48.3	3.7	2.4	15.6	15.6	14.4	73.8	11.8	8.0	5

Table 8-2: FAME of both raw P. ellipsoidea strains in g/kg and in per cent composition

	C16:0 (g/kg)	C18:0 (g/kg)	C18:1 (g/kg)	C18:2 (g/kg)	C18:3 (g/kg)	% C16:0	% C18:0	% C18:1	% C18:2	% C18:3
Stressed *P. ellipsoidea*	17.6	23.4	139.7	60.0	2.5	7.2	9.6	57.4	24.7	1.0
Non-stressed *P. ellipsoidea*	131.6	40.1	7.2	22.9	46.8	52.9	16.1	2.9	9.2	18.8

P. ellipsoidea and *Chlorella* are classified as green algae whereas *Spirulina* is a cyanobacterium. *Spirulina* exhibits the highest nitrogen content with 10.9 wt.%. Cyanobacteria are well known to have high protein content; this partly explains their use as a dietary supplement. The most abundant amino acids in *Spirulina* are glutamic acid with 11.4 wt.%, arginine acid 10.2 wt.% and aspartic acid 8.3 wt.% [307]. *Chlorella* also has a high nitrogen content with 10.3 wt.% correlating with the protein content although it also contains a significant amount of chlorophyll [311]. The two samples of *P. ellipsoidea* were cultivated under different conditions. The lipid content was increased by starving the microalgae of nitrogen nutrients for several days. Furthermore, under these conditions, 9 wt.% hydrocarbons was produced among the lipids [61]; this strain is highly innovative and can replace *Botryococcus b.*in the future. Indeed, *P. ellipsoidea* has a faster growth rate (3.5 g dry weight/day) compared to *Botryococcus* [61, 312]. Based on the result from **Chapter 5** on the processing of lipids, a high yield of bio-crude is expected from the stressed microalgae compared to the non-stressed. The high ash and protein contents from *Spirulina* and *Chlorella* would also reduce the production of bio-crude yield.

As discussed in the last section of **Chapter 5**, microalgae contain mainly C_{18} unsaturated fatty acids (mono or polyunsaturated). Table 8-2 shows the lipids compositions in g/kg from both strains of *P. ellipsoidea*. These strains are selected to show the different lipid profile for the same species. The two different *P. ellipsoidea* strains have different profiles for example the stressed strain contains mainly oleic and linoleic acids. On the other hand, the non-stressed microalga contains mostly linoleic and palmitic acids. The nitrogen composition has an impact on the lipids profile thus oleic acid is common for microalgae grown under nitrogen starvation while with a normal nutrient algae, linoleic, linolenic acids and poly unsaturated C_{16} fatty acids are the main lipids [313].

8.4 Hydrothermal processing of microalgae without catalyst

8.4.1 Mass balance yield

The mass percentage yield of the different phases (bio-crude, residue, the gaseous and aqueous phase) for the different microalgae and cyanobacteria are illustrated in Figure 8-1 (a) for *Chlorella*; (b) stressed *P. ellipsoidea* (stressed); (c) *P. ellipsoidea* (non-stressed); (d) *Spirulina*. The HTL runs with *Chlorella* were performed in duplicate resulting in a coefficient of variance of 5.6 %. The main reason for this variance includes the difficulty in obtaining complete removal of the oil from the reactor and losses due to evaporation. The residue analysis is also difficult due to losses during filtration. The gas composition is assumed based on Biller et al. [112] and therefore this measurement is semi quantitative. In some cases, the alga are difficult to weigh out accurately, for instance *P. ellipsoidea* is quite electrostatic resulting in small errors in transferring the alga during weighing. Despite these problems, the errors associated with the experimental design are minimised as much as possible allowing the trends to be investigated with confidence.

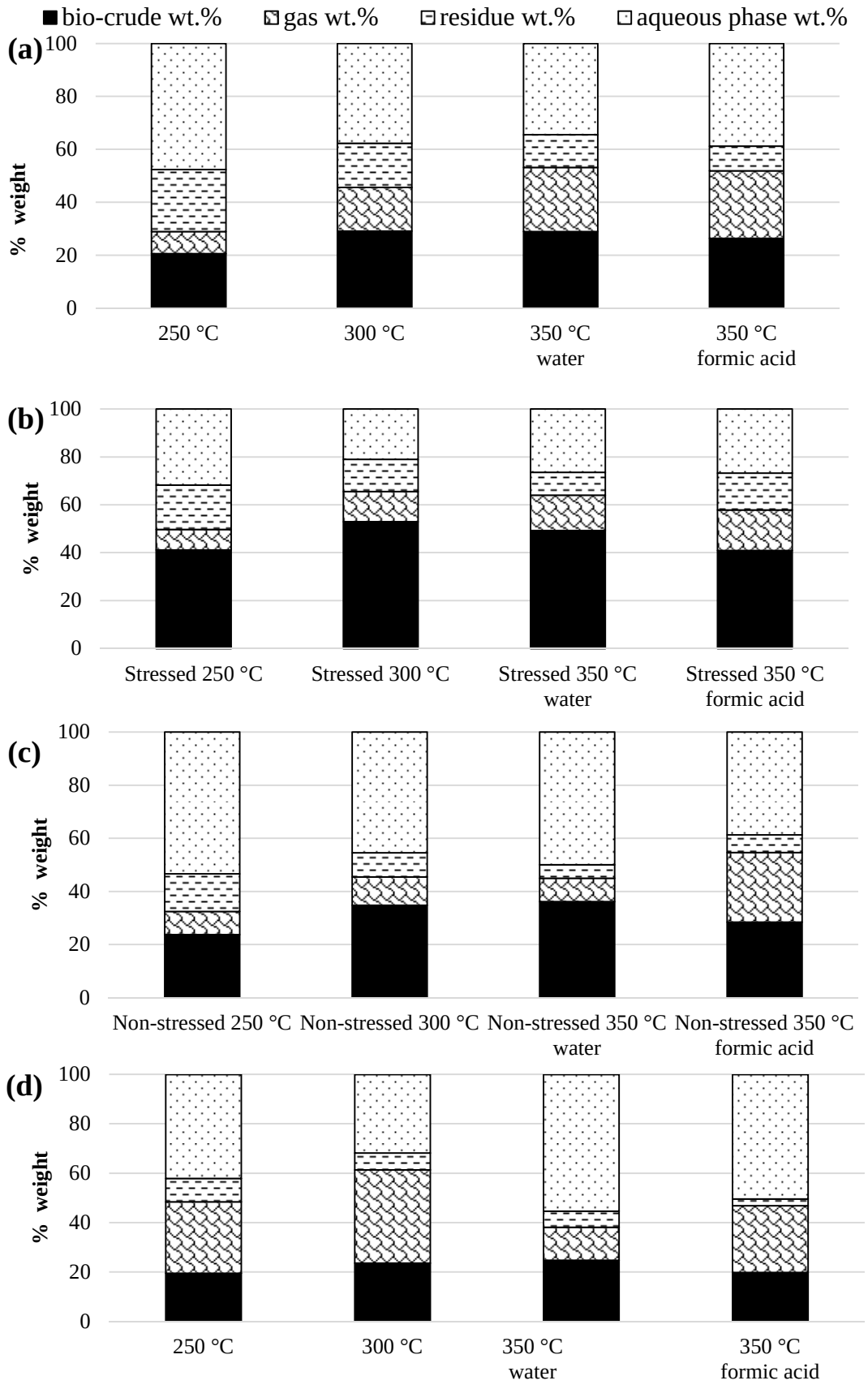

Figure 8-1: Diagrams representing mass balance for the different fractions: bio-crude oils, gaseous, residue and aqueous fractions for the four different microalgae for (a) Chlorella; (b) *P. ellipsoidea* (stressed); (c) *P. ellipsoidea* (non-stressed); (d) *Spirulina*.

During the processing of microalgae, from 250 to 300 °C, a general increase of bio-crude yield is observed. The processing of stressed *P. ellipsoidea* at 300 °C (Figure 8-1 (b)) achieves the maximum bio-crude yield of 52.9 wt.% (with a coefficient of variance of 2.8 %). For the non-stressed *P. ellipsoidea* (Figure 8-2 (c)), a lower bio-crude yield is obtained which emphasises that the bio-crude is related to the initial lipids content as suggested Biller et al. [112]. Nevertheless, the initial lipid content of the stressed *P. ellipsoidea* is approximately 67.0 wt.% [141], thus it would be expected to obtain a high bio-crude yield; in contrast to *Chlorella* (Figure 8-1 (a)), the yield (29.0 wt.%) is above the initial lipid content (25.0 wt.%). It is possible that some free fatty acids are soluble in the aqueous phase reducing the yield of the bio-crude. The lowest bio-crude yield at 350 °C is achieved for *Spirulina* (Figure 8-1 (d)) as it contains the highest amount of proteins. An increase between the bio-crude yield and the temperature was observed by Jena et al. [131] and Zou et al. [124] with the processing *Spirulina* and *Dunaliella*. López Barreiro et al. [134] suggested that the bio-crude yield especially at low temperature (250-300 °C) depended on the cell wall strength. Here, it could be deduced from the bio-crude yield for example that *P. ellipsoidea* has a lower cell wall compared to *Spirulina*.

The residue yield generally decreases in relation of the temperature suggesting the degradation of the microalgae as observed by Garcia Alba et al. [133]. The gaseous yield is the highest for *Spirulina* compared to the other microalgae, the same observation was drawn by Biller et al. [112].

Formic acid enhances the formation of gas, and leads to a slightly lower bio-crude yield. Ross et al. [129] showed with formic acid (1 M) using the same algae, lower bio-crude yield with 14.5 wt.% while Biller et al. [112] obtained a higher bio-crude with 20 wt.%. This acid by decomposing could lead to the hydrolysis of large molecules in the bio-crude oil with the increase of pH [112, 129].

Looking to the previous chapter, the processing of the stressed strain *P. ellipsoidea* shows a similar trend mass balance to vegetable oils. For the case of *Chlorella* and *Spirulina*, most of degraded products are found in the aqueous and in the gaseous phases similar to the experiments carried out with soya protein and asparagine which implies that proteins have a major role on the mass balance. An increase of bio-crude yield in relation to the temperature was observed with hemp

proteins and *Chlorella* whereas the maximum of bio-crude oil produced was obtained at 300 °C with the stressed strain *P. ellipsoidea* and soya protein.

8.4.1 Bio-crude analysis of the non-catalytic runs

8.4.1.1 GPC analysis

Figure 8-2 illustrates the different molecular weight range of the bio-crude oils from the different microalgae (a) *Chlorella*, (b) stressed *P. ellipsoidea* (c) non-stressed *P. ellipsoidea* (d) *Spirulina.*

From Figure 8-2, as observed from the degradation of carbohydrates in **Chapter 6**, the fraction of low molecular weight materials increases in relation to the temperature. This trend is more significant with the bio-crude of *Chlorella* observed in Figure 8-2 (a). It suggests that there is a breakdown of the oligomers and "heavy molecular weight" materials into smaller molecules. The reduction of the molecular weight size is advantageous as low molecular weight materials generally have a low boiling range. The stressed *P. ellipsoidea* (Figure 8-2 (b)) contains the largest fraction of "long chain" materials (up to 50.0 %) as this microalga initially contain up to 67.0 wt.% of lipids. There is a slight reduction of this fraction suggesting a mild cracking. For the other microalgae, this fraction is not affected by the temperature change.

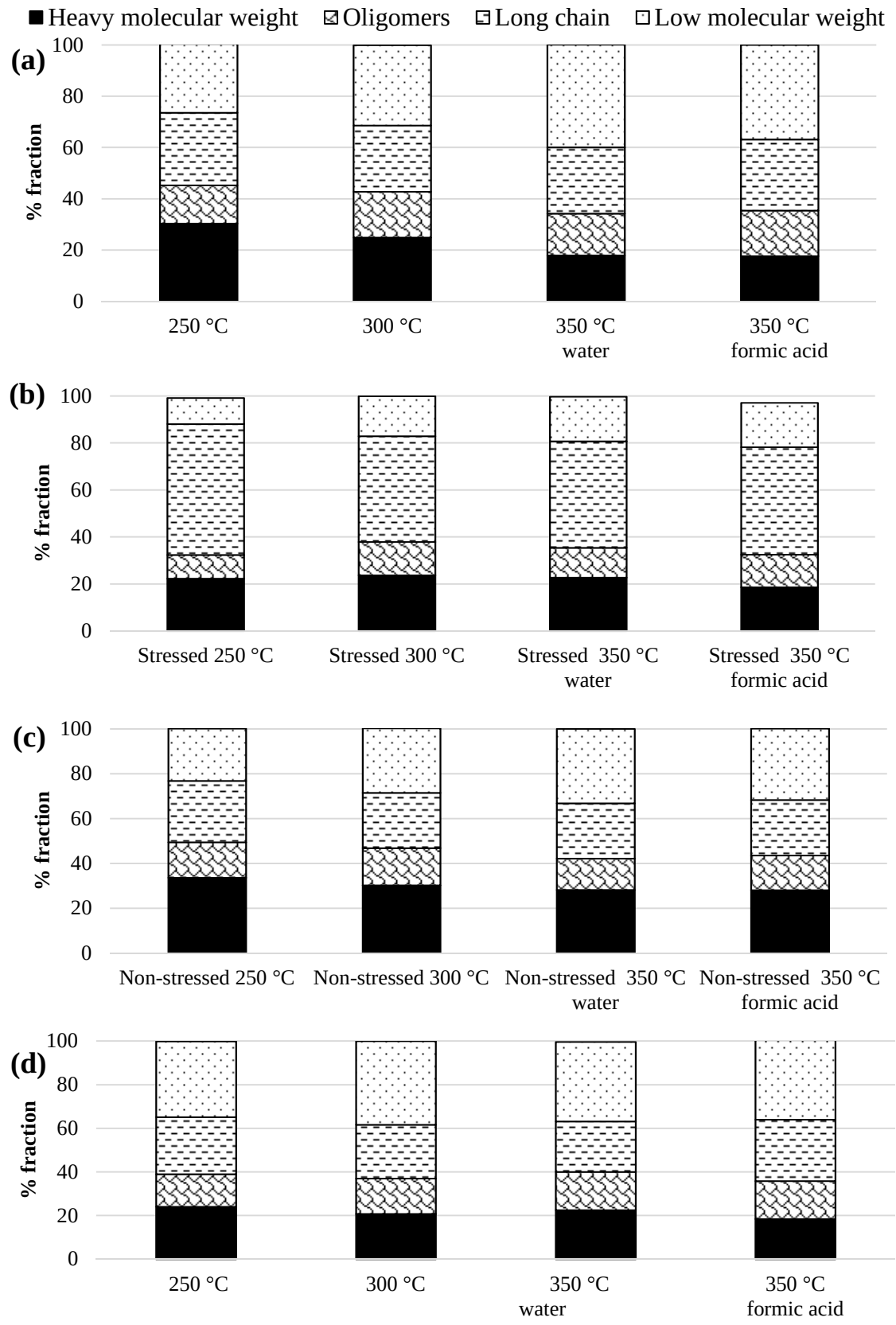

Figure 8-2: Different molecular weight fraction of the bio-crude oils of the different microalgae at different temperatures and conditions for (a) *Chlorella*; (b) stressed *P. ellipsoidea*; (c)non-stressed *P. ellipsoidea*; (d) *Spirulina*.

The addition of formic acid has generally a mild effect on the molecular weight distribution with evidence for reduction in the “heavy molecular weight” materials. Opposite results was found for the processing of carbohydrates in **Chapter 6** where formic acid enhanced the formation the “heavy molecular weight” materials. The difference is caused by different chemical structures. It was demonstrated by Ross et al. [129] and later by Biller et al. [112] using the simulated distillation method that organic acid in particular formic acid (1 M) enhanced the formation of the lighter fraction. There was a high probability that the same observation would have been drawn with the GPC technique. In this study, with other model compounds (sunflower oil, starch, and asparagine acid) there are little differences between runs in water and in formic acid. For future work, it would be interesting to test different concentrations of acid to investigate when the molecular weight would start to diminish.

Figure 8-3 represents the molecular profiles of the different feedstock used in this project such as Chlorella, stressed *P. ellipsoidea*, soya protein, glucose sunflower and asparagine. The molecular weight profile of *P. ellipsoidea* is similar to the sunflower oil in **Chapter 5** with mainly “long chain” materials (200 to 500 g/mol). The molecular weight profiles of *Chlorella* are broader such as those observed for soya protein in **Chapter 7**. Asparagine acid and some carbohydrates for instance glucose (in **Chapter 6**) contained up to 50 % compounds with a molecular weight lower than 200 g/mol.

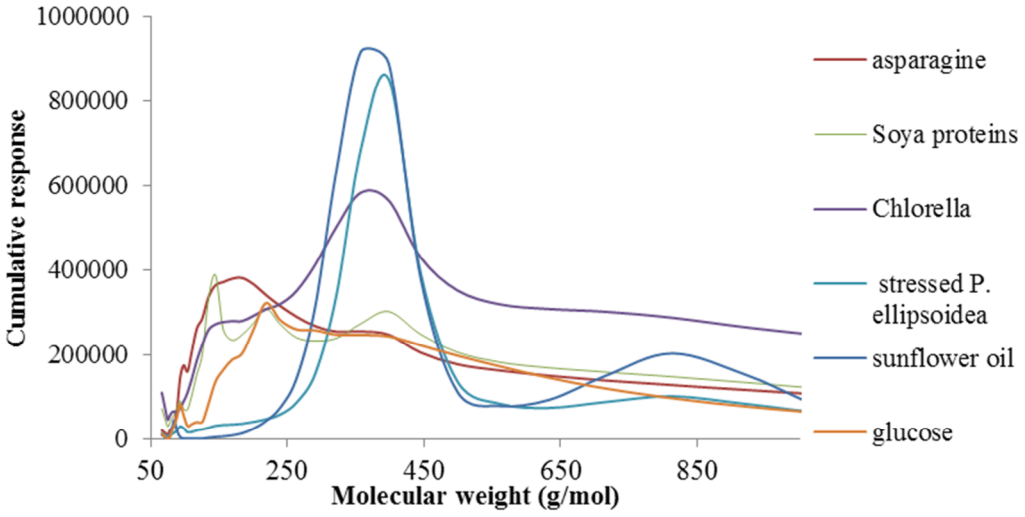

Figure 8-3: GPC chromatogram for different model compounds

López Barreiro et al. [134] noticed that at lower temperatures the molecular size was focused between 400-500 g/mol indicating mainly a lipid extraction whereas

at the higher temperature of 375 °C, there was a broader distribution. Garcia Alba et al. [133] observed the same trend, explaining that the bio-crude oil at high temperature was forming a broader molecular weight range due to the presence of hydrophobic polypeptide or proteins. Vardon et al. [128] obtained a bio-crude oil with high molecular weight with approximately 3260 mol/g with raw *Scenedesmus*; it was lower with *Spirulina* with 1860 mol/g.

8.4.1.2 GC-MS analysis

Figure 8-4 shows the chromatograms obtained from each microalgae processed at 350 °C in water where (a) *Chlorella* (b) *P. ellipsoidea* (stressed) (c) *P. ellipsoidea* (non-stressed) (d) *Spirulina*. The compounds identified are listed in Table 8-3. At 32.2 minutes, butylated-hydroxytoluene could be observed in some chromatograms, this compound was extracted from the caps of the vials where the bio-crude oil was stored. Figure 8-5 shows the chemical structures of some of the nitrogen compounds found in the bio-crude oils.

The processing of high content protein microalgae such as *Chlorella*, *Spirulina* and non-stressed *P. ellipsoidea* (Figure 8-4 (a), (c), (d)) yields a majority complexes compounds containing hetero-atoms (oxygen and nitrogen). These compounds includes nitrogen heterocyclic compounds (1-butyl-2-pyrrolidinone, 1-methyl-piperidine, indole); oxygenated long chain compounds such as alcohols (6-nonen-1-ol); aldehydes (8-hexadecenal); ketones (1-methoxy-3-(2-hydroxyethyl)-nonane), free fatty acids (palmitic acid), amides (hexadecanamide) and some aliphatic compounds such as alkanes (heptadecane), alkenes (hexadecane) and non-aromatic cycles (1,2-dimethyl-cyclooctane).

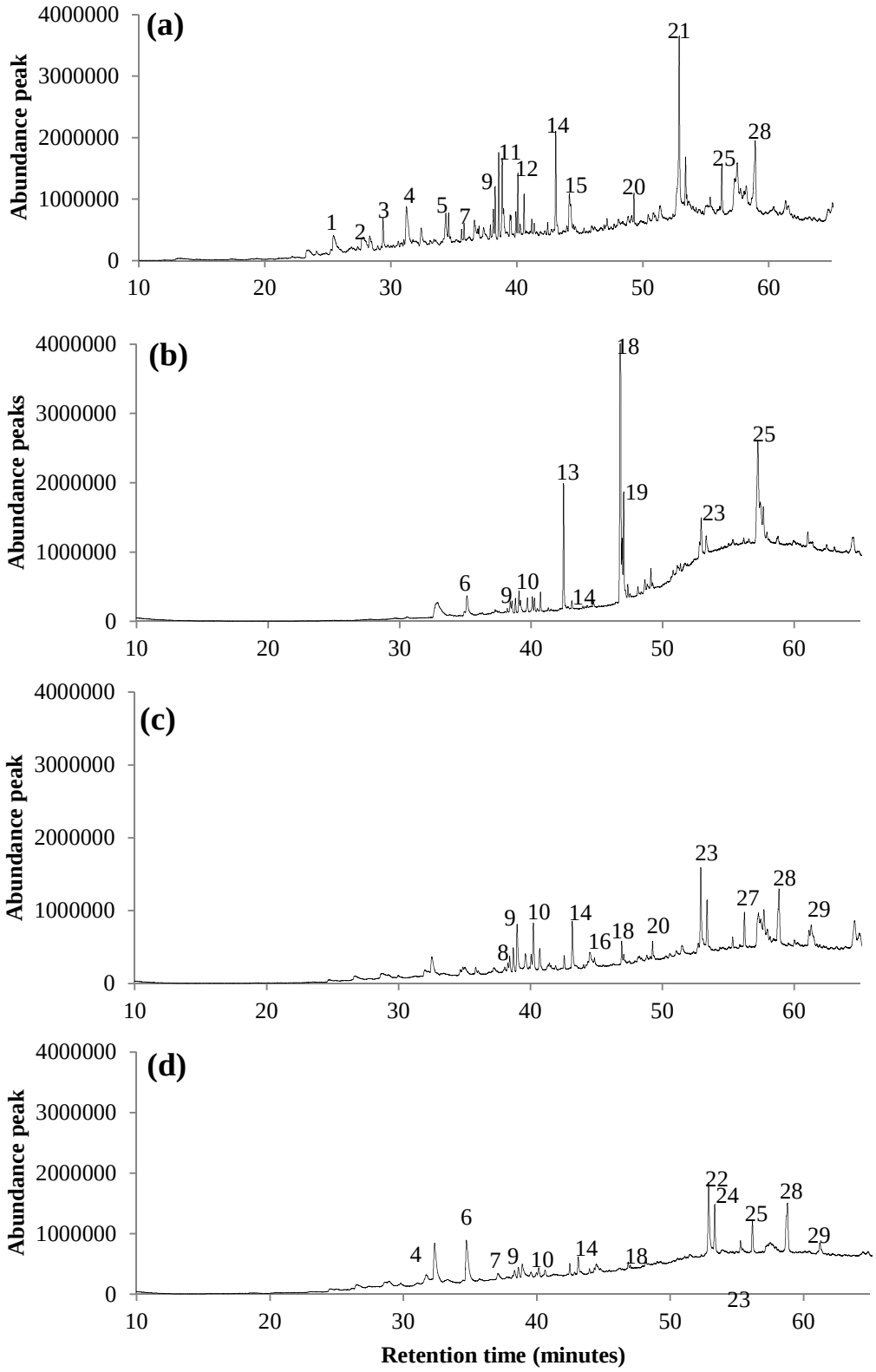

Figure 8-4: GC-MS chromatograms of the bio-crude oils at 350 °C in water where (a) *Chlorella* (b) *P. ellipsoidea* (stressed) (c) *P. ellipsoidea* (non-stressed) (d) *Spirulina*

Table 8-3: Identification of compounds from previous chromatograms

Number	Retention time (minutes)	Compounds
1	25.4	4-methyl-phenol
2	27.8	3-ethyl-phenol
3	29.4	1-pentadecene
4	31.7	1-butyl-2-pyrrolidinone
5	34.3	3-methyl-indole
6	35.1	heptadecane
7	36.6	benzonitrile
8	38.2	1-methoxy-3-(2-hydroxyethyl)-nonane
9	38.3	3,7,11,15-tetramethyl-2-hexadecene
10	39.1	1,4-eicosadiene
11	39.5	7-hexadecyn-1-ol
12	10.1	9-octadecyle
13	42.4	palmitic acid
14	43.1	isophytol
15	44.1	ethyl-phenyl-piperidine
16	44.5	(hydroxypropyl)-piperidine
17	46.7	octadecanoic acid
18	46.9	11-octadecenoic acid
19	47.3	9,12,15-linolenic acid
20	49.3	1-nonadecene
21	52.8	hexadecademide
22	52.9	dodecanamide
23	53	9-octadecenamide
24	53.2	hydroxymethyl-propanone-1-(2-hydroxy-3-indolylazo)
25	56.2	octadecenamide
26	56.3	(5-amino-thiadiazol-2-yl)-propyl-3H-benzooxazol-2-one
27	56.8	N-butyl-octadecanamide
28	59.8	octanoic acid, morpholide
29	61.2	1-(3,6-dimethyl-1-oxopentadecyl)-pyrrolidine

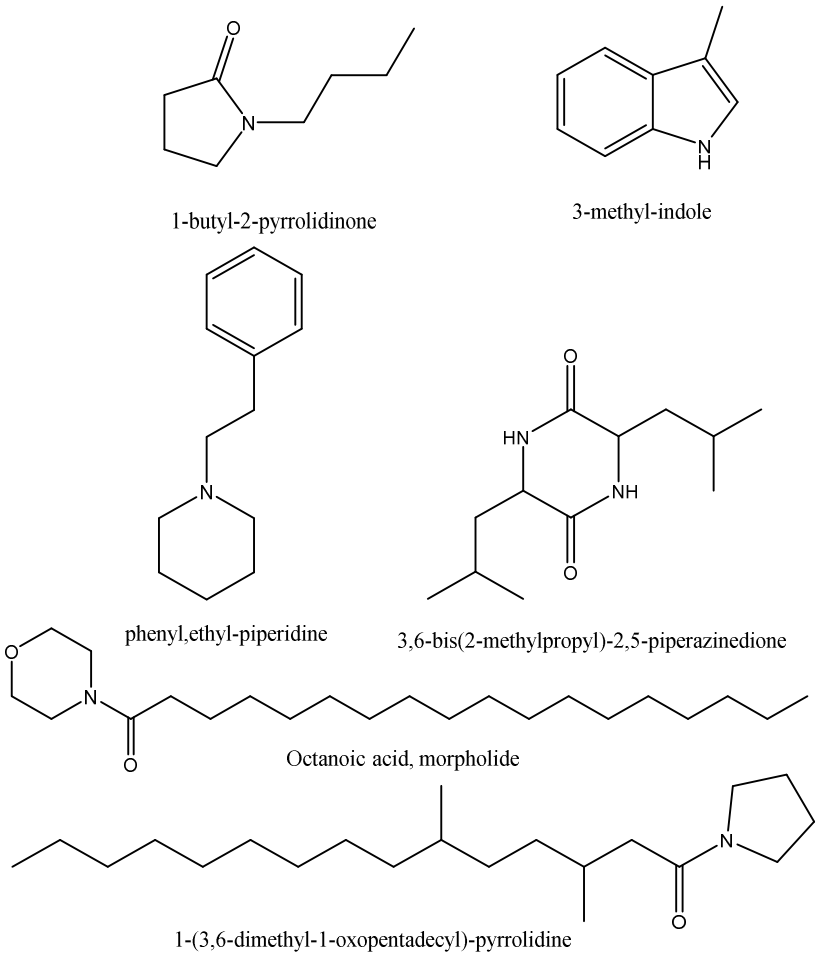

Figure 8-5: Chemical structure of some molecules with nitrogen identified in the bio-crude oil

The processing of high lipid microalgae, such as the stressed *P. ellipsoidea*, (Figure 8-4 (b)) yields a majority of long chain compounds as suggested by the GPC analysis in the previous section. These compounds include oxygenated compounds such as ketone, alcohols. Aldehydes and fatty acids (3,5-dimethyl-cyclohexanone, dodecanol, hexadecanal, nonanoic acid, oleic acid), a lower fraction of nitrogen containing compounds (piperidine, hexadecanamide) and finally aliphatic compounds such as alkenes (8-heptadecene); alkanes and naphsubsequentlyic (tridecane, propyl-cyclohexane).

At lower temperatures (250 and 300 °C), there is evidence of the formation of some piperazinediones (DKP, where the K stand for ketones) which are identified such as 3-benzyl-6-isopropyl-2,5-piperazinedione and 3,6-bis(2-methylpropyl)-2,5-piperazinedione (MS spectrum is present in the appendix 3, section 3.3 page 332) with *Chlorella* and *Spirulina*, and are similarly observed by Torri et al. [137]. As discussed

previously in **Chapter 7**, this group of compounds could be characteristic of the degradation of proteins.

Other nitrogen compounds containing one or two nitrogen atoms such as 5,10-diethoxy-2,3,7,8-tetrahydro-dipyrrolo-pyrazine identified in the bio-crude of *Chlorella* can result from the Maillard reaction [314]. Indole is found principally with *Chlorella*, this compound is likely to originate from the degradation of amino acids (tyrosine and tryptophan). Indole derivatives are known to be stable under hydrothermal liquefaction [315]. Biller et al. [112] observed pyrrolidine and piperidine compounds in the bio-crude from the processed *Spirulina* and *Chlorella*.

For microalgae, the major compounds with the highest peak areas are the amides including hexadecanamide and octadecanamide; pyrrolidine, 1-(1-oxooctadecyl). Morpholide octanoic acid are also identified but with a lower abundance. They are present in the bio-crude for *Chlorella v.*, *P. ellipsoidea* at different temperatures and in formic acid. Chiaberge et al. [316] investigated the reaction between different amino acids and palmitic acid. Most of the hydrothermal reactions with amino acids and fatty acids yielded unsubstituted hexadecanamide for example with arginine, aspartic acid and asparagine acids. Furthermore, secondary and tertiary amides were also observed in the bio-crude oils, produced by β-elimination which is favoured by the conjugation of the double bonds. Reddy et al. [317] identified 8-morpholino-4-cycloocten-1-one oxime and 9-octodecenamide in the bio-crude oil from the processing of *Duanaliella t.*. In order to lower the amount of amide, Cheng et al. [142] first processed the microalga *Nannochloropsis o.* under microwaves to extract the lipids and subsequently the remaining residue was upgraded under hydrothermal liquefaction, 26.7 % of nitrogen removal was achieved in the bio-crude oil using this method.

For all the microalgae strains, hydrocarbons (alkanes or alkenes) such as 1-pentadecene, heptadecane, 3,7,11,15-tetramethyl-2-hexadecene and 1,4 eicosadiene are identified in the bio-crude oils. The presence of 3,7,11,15-tetramethyl-2-hexadecene is a derivative from lipids [133]. Other aliphatic chain compounds could have been produced by decarboxylation of lipids or alcohol chains. Isophytol is commonly identified in the bio-crude from microalgae as described by Biller et al. [112]. This compound could be formed from the reaction of chlorophyll and lipids [166].

FAME analysis is performed with the bio-crude oil of the four different microalgae according to the procedure in **Chapter 5** and the results are included in Figure 8-6.

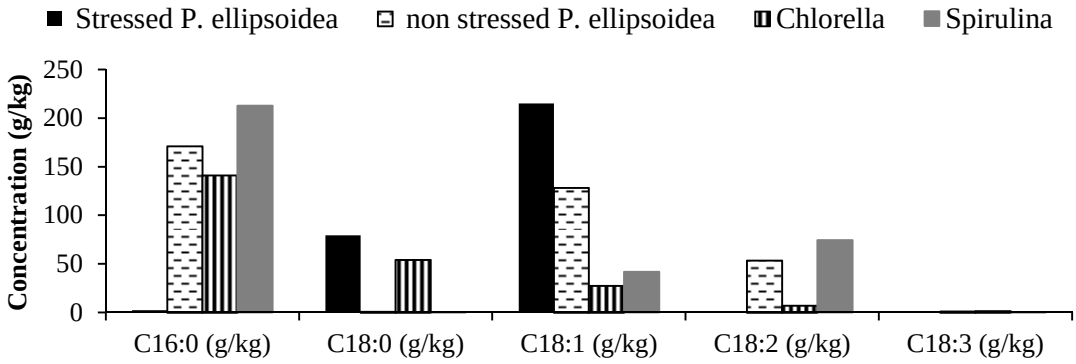

Figure 8-6: FAME profile for the different microalgae at 350 °C in water

For the stressed *P. ellipsoidea*, the main fatty acid in the bio-crude oil is oleic acid, followed by stearic acid; in addition some further fatty acids are identified from the NIST library such as 14-methyl-pentadecanoic acid, heptadecanoic acid, 11-eicosenoic acid. For the non-stressed strain, FAMEs are present in lower concentrations for example with palmitic acid. The delocalisation of the double bond from oleic acid to position 7 or 11 instead of 9 could have occurred making difficult their quantification. For *Chlorella*, oleic, stearic and palmitic acids are the most abundant fatty acid with some 9-hexadecenoic acid. For *Spirulina*, the most abundant FAME is palmitic acid followed by linoleic acids. Related results with the vegetable oils at the same temperature 350 °C are achieved with low concentration of polyunsaturated fatty acids. Torri et al. [137] observed that the recovery of polyunsaturated fatty acid was reduced as the temperature increased.

8.4.1.3 Elemental analysis

The elemental analysis of the bio-crude oils is listed in Table 8-4 and includes the elemental values, HHV Dulong energy content, H/C, O/C, the Milne energy content (formula in **Chapter 7**) and energy recovery (formula in **Chapter 3**).

Table 8-4: Weight % nitrogen, carbon, hydrogen, sulphur and oxygen content in the bio-crude oils as dry basis, energy content (Dulong and Milne) and % energy recovery for experiments for different model and microalgae at different temperatures and conditions

	N wt. %	C wt. %	H wt. %	S wt. %	O wt. %	Dulong HHV (MJ/kg)	H/C	O/C	Milne HHV (MJ/kg)	% Energy recovery
					Chlorella					
250 °C	7.0	73.5	9.9	0.5	9.2	37.4	1.6	0.1	36.1	36.3
300 °C	6.2	69.5	8.9	0.5	14.9	33.6	1.5	0.2	32.8	52.1
350 °C water	5.9	74.9	9.3	0.6	9.4	36.9	1.5	0.1	35.9	50.3
formic acid	5.2	68.6	8.9	0.5	16.8	32.9	1.6	0.2	32.4	41.1
					Stressed *P. ellipsoidea*					
250 °C	1.3	75	11.5	0	12.2	39.6	1.8	0.1	39.0	53.2
300 °C	1.5	71.1	10.6	0	16.8	36.2	1.8	0.2	35.94	62.6
350 °C water	1.0	70.5	10.3	0	18.2	35.3	1.8	0.2	35.23	56.9
formic acid	2.3	84.1	12.3	0	1.3	45.8	1.8	0	44.3	61.4
					Non-stressed *P. ellipsoidea*					
250 °C	6.1	77.7	6.8	-	9.4	34.3	1.1	0.1	33.6	34.4
300 °C	6.4	80.7	7.1	-	5.9	36.3	1.1	0.1	35.4	50.5
350 °C water	4.9	70.4	3.8	-	20.9	25.5	0.6	0.2	25.9	38.8
formic acid	5.2	72.4	4.3	-	18.1	27.4	0.7	0.2	27.5	33.1
					Spirulina					
250 °C	7.7	72.6	7.6	-	12.1	33.2	1.3	0.1	32.4	40.9
300 °C	6.3	66.6	7.4	-	19.6	29.6	1.3	0.2	29.4	44.3
350 °C water	5.6	70.3	8.1	-	15.9	32.5	1.4	0.2	32.2	50.7
formic acid	5.1	63.4	7.2	-	24.3	27.3	1.4	0.3	27.6	34.8

For the bio-crude of *Chlorella* and *Spirulina*, the nitrogen content is reduced as the temperature increases. The same trend is observed for soya proteins with close values (7.8 to 6.1 wt.%). The decrease is less obvious for both strain of *P. ellipsoidea*, as the nitrogen content increases slightly at 300 °C. In general, the nitrogen content in the bio-crude in average is related to the initial protein content, as the high nitrogen content are measure measured for *Chlorella* and *Spirulina* (with relatively close value), followed by the non-stressed (5.0 wt.%) and finally to the stressed *P. ellipsoidea* (1.0 wt.%). It is encouraging to measure less than 1.5 wt.% of nitrogen in the bio-crude of the stressed *P. ellipsoidea*. This result meets the initial target.

In literature such as Alba Garcia et al. [133], Brown et al. [127] and Valdez et al. [135], Jena et al. [131], most of studies observed an increase from low temperature to approximately 300 °C, subsequently levelled out until the supercritical point (375 °C). The increase of the nitrogen could be explained by the recombination of nitrogen monomers to form long chain polymers.

For *Spirulina* and *Chlorella*, the nitrogen content decreases with the addition of formic acid. The opposite trend is been observed with both strain of *P ellipsoidea*. Biller et al. [112] showed that the nitrogen content of the bio-crude increased in the presence of formic acid compared to the run in water at 350 °C for *Nannochloropsis* and *Porphyridium* whereas the nitrogen content was reduced with *Chlorella* and *Spirulina*. The same trends are observed in this case for the previous microalgae although with a lower concentration of formic acid [112, 129]. In **Chapter 7**, formic acid also reduces the nitrogen content during the processing of soya proteins and asparagine. It could imply that this organic acid is more efficient with high protein content.

In general, the highest energy content is measured at 250 °C except for the non-stressed *P ellipsoidea*. The reduction of hydrogen and carbon contents with the temperature is unexpected for the stressed *P. ellipsoidea*, which results in diminishing the energy content and increasing the oxygen content. The addition of formic acid enhance the carbon content for the stressed *P. ellipsoidea* and yield an energy content of 45.0 MJ/kg.

The deoxygenation in relation to the increase of temperature between 250 to 350 °C occurs with soya and hemp proteins. Nevertheless, the opposite trend is observed with microalgae and lipids (**Chapter 5**) especially between 250 and 300 °C. At 250 °C, high hydrogen content is detected generally. The other reason could be that the polymerisation of molecules from the aqueous phase takes place above 250 °C. Yu et al. [318] stated that the removal of hydrogen was maximal at approximately 220 °C in the bio-crude oil processed from *Chlorella sp.*. The energy recovery from the bio-crude oil is at its maximum at 300 °C. Garcia Alba et al. [133] determined that the energy recovery increased constantly between 175 to 300 °C and subsequently levelled out between 300 to 350 °C and finally decreased at higher temperature.

The van Krevelen diagram (Figure 8-7) represents the ratio of molar H/C versus the O/C. For *P. ellipsoidea* (stressed and non-stressed), the ratio O/C is lower at

300 °C, additionally the stressed strain has a better hydrogen/carbon ration compared to petroleum oil of 1.8 [319]. *Spirulina* bio-crude oil contained a lower O/C at 250 °C. The ratio O/C is similar between 250 and 350 °C with a higher H/C with the later temperature. The liquefaction of microalgae overall allows the reduction of the oxygen in the bio-crude oil compared to the unprocessed microalgae. Garcia Alba et al. [133] measured the decrease of the O/C and H/C ratio from the processing of *Desmodesmus sp.* from 175 to 300 °C which levelled out between 300 to 400 °C implying that the major deoxygenation reactions occurred at temperatures below 300 °C. An increase of the H/C ratio and decrease of O/C ratio was measured by Yu et al. [318] from the temperature of 220 °C.

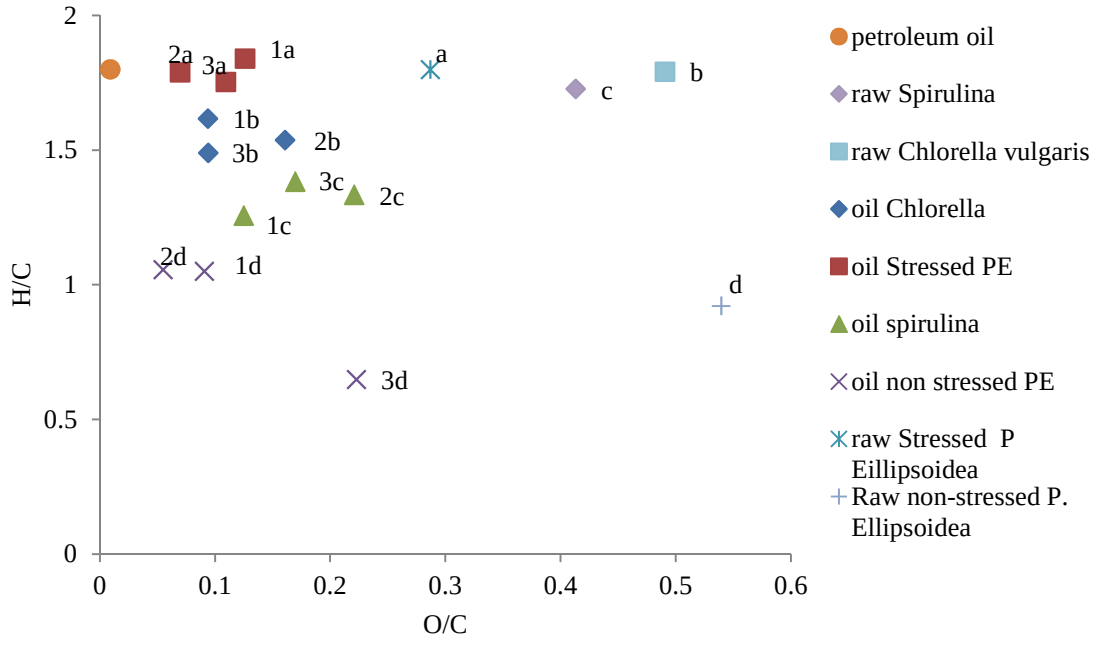

Figure 8-7: Van Krevelen diagram of the raw algae and bio-crude oil at 250, 300 and 350 °C a) represents the stressed *P. ellipsoidea*; b) *Chlorella*; c) *Spirulina*; d) the non-stressed *P. ellipsoidea*, the number 1) is experiment carried out at 250 °C; 2) 300 °C and 3) 350 °C

Consequently, the fate of nitrogen under subcritical conditions in the bio-crude oils is dependent on the temperature and on the initial composition of the microalgal strain.

8.4.1.4 Analysis of the bio-crude oil by STA-MS

Temperature programmed oxidation of the bio-crude oils from three different microalgal strains (*Chlorella*, *P. ellipsoidea* (stressed) and *Spirulina*) has been analysed. Additionally the raw *Chlorella* was analysed by the STA under combustion

conditions; the thermogravimetric curve of the weight loss and the DTA are shown in Figure 8-8. The evolved gases was analysed by a mass spectrometer (MS) and Fourier transformer infrared (FT-IR) detectors. Figure 8-9 represents the absorption values of carbon dioxide and carbon monoxide by FT-IR, Figure 8-10 shows nitric oxide (NO), nitrogen dioxide (NO_2) and hydrogen cyanide (HCN) absorbance for the processed bio-crude.

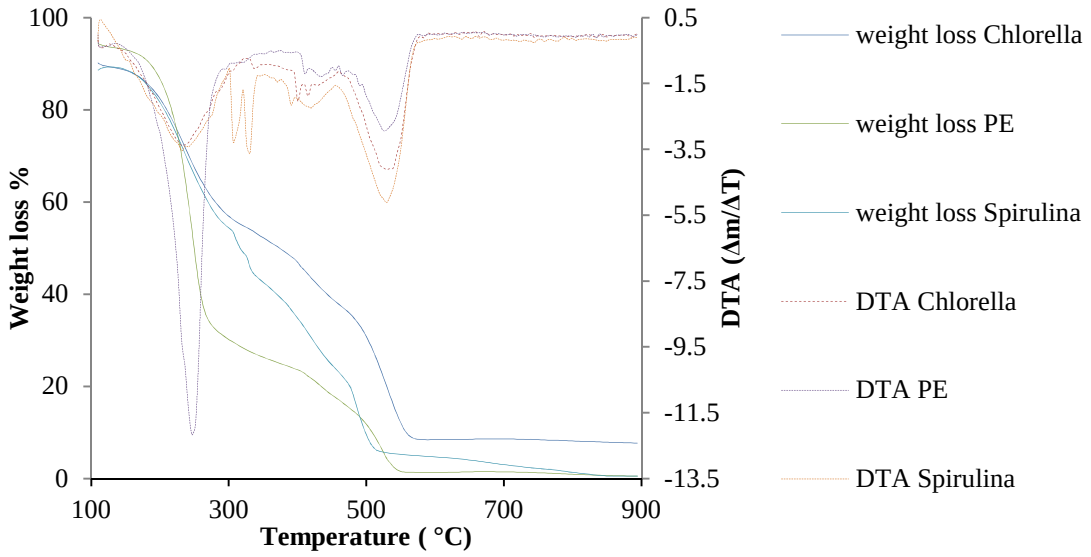

Figure 8-8: Thermogravimetry and derivatives for the combustion of *Chlorella*, *P. ellipsoidea* (PE) and *Spirulina* of the bio-crude oil

The combustion of bio-crude of the stressed *P. ellipsoidea*, *Spirulina* and *Chlorella* can be subdivided into two major steps, the first at 230 °C and 520 °C. The weight loss curve and DTA are relatively alike between the bio-crude oils of *Spirulina* and *Chlorella* as these microalgae have a similar level of protein. The result are similar with Gai et al. [320] who observed that the combustion profile of *Spirulina* contained three stages of mass loss corresponding to the dehydration (from room temperature to 120 °C) (not observed in the TGA), devolatilation (120 to 377 °C) and the char oxidation (from 400 to 900 °C). The bio-crude oil from *P. ellipsoidea* shows a greater weight loss within the 200-300 °C window and corresponded to the combustion of the lipid content and volatile compounds.

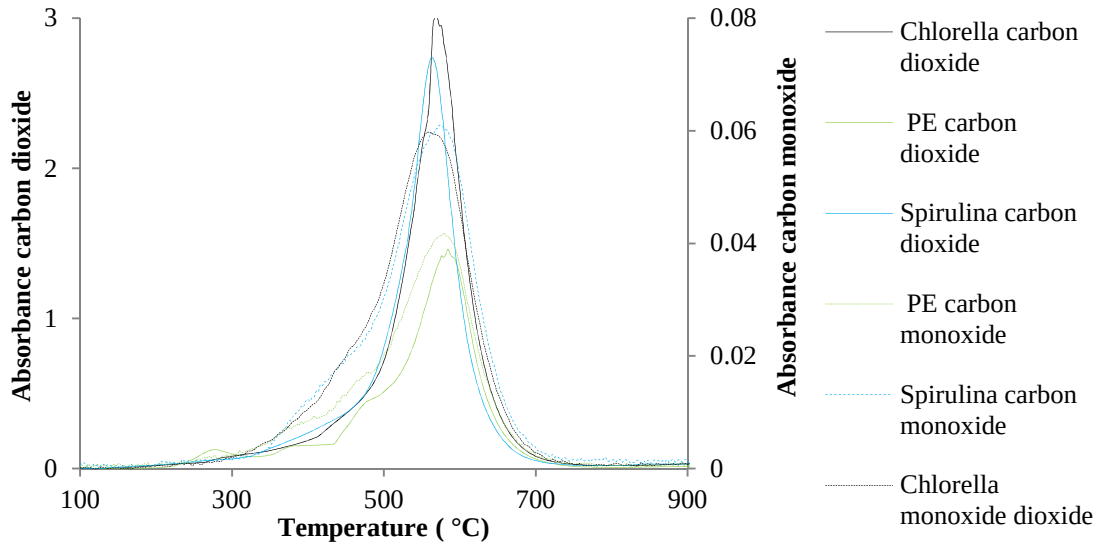

Figure 8-9: Heating profile of carbon monoxide and carbon dioxide measured by the MS from 100 to 900 °C for *Chlorella, P. ellipsoide* (PE), *Spirulina* of the biocrude oil

The production of carbon dioxide is spread throughout the combustion of the bio-crude *Chlorella*. Similar to **Chapter 7**, carbon monoxide is realised at lower temperature and lower intensity. The intensity of carbon dioxide with *P. ellipsoidea* is lower to the other microalgae.

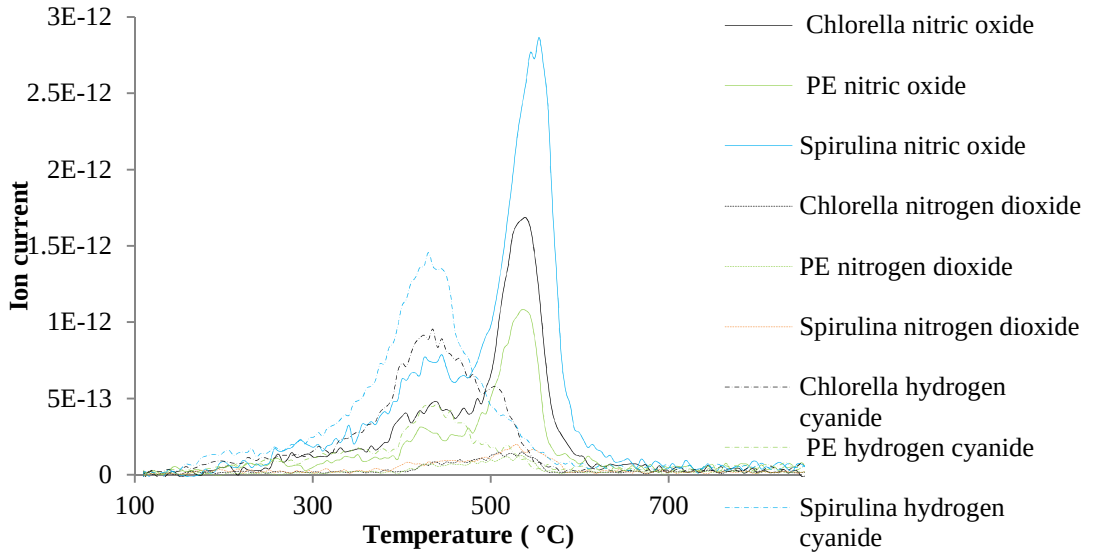

Figure 8-10: Heating profile of nitric oxide and nitrogen dioxide, hydrogen cyanide measured by the MS from 100 to 900 °C for *Chlorella, P. ellipsoidea* (PE), *Spirulina* bio-crude

The formation of nitric oxide (in Figure 8-10) is spread through a large temperature range compared to carbon dioxide. Similarly than in **Chapter 7** with the combustion of protein, hydrogen cyanide is detected before the release of nitric oxide. The highest intensity of nitric oxide is obtained with *Spirulina* while the signal is

lower for *P. ellipsoidea* as the nitrogen content in the bio-crude is lower than the other algae. By comparing the DTA curve and the nitric oxide curve, the peak at approximately 530 °C correspond mainly to the combustion of nitrogen present in "heavy molecular weight" material identically than in **Chapter 7**.

To conclude, this analysis allows predicting that during the processing of microalgae at 350 °C, hydrogen cyanide are the first to be produced during the combustion followed from nitric oxide and carbon dioxide and monoxide. The intensity of the gases is greater with *Spirulina*, *Chlorella* and finally with stressed *P. ellipsoidea*. The evolved gases measured from the MS suggest that the nitrogen fraction is mainly present in the "heavy molecular weight" materials. The intensity depends on the initial nitrogen content of the microalgae.

8.4.2 Residue analysis

The thermogravimetric analysis of the residue included in Figure 8-11 suggests that *Spirulina* contains up to 60 wt.% volatiles, followed by *P. ellipsoidea* (stressed) with approximately 50 wt.%, whereas *Chlorella* has only 10 wt.%, where the remaining microalgae residue is ashes. This is important information as until now, the research community has taken little interest on the effect of ash during hydrothermal liquefaction regarding the mass balance yield, and the degradation route.

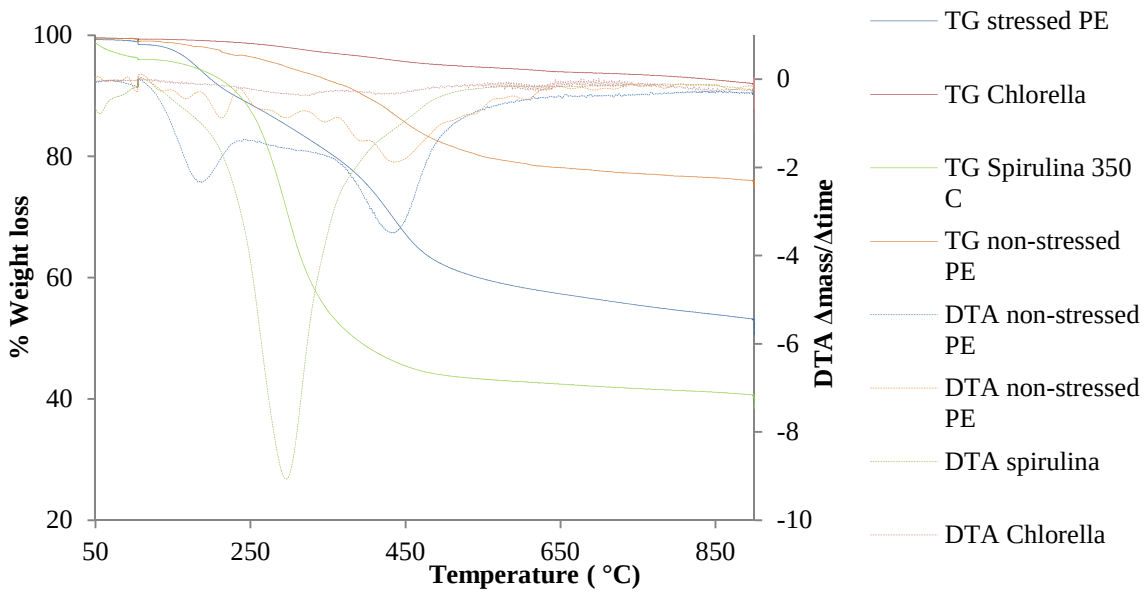

Figure 8-11: TG and DTA of the residue of the processed residue of the four microalgae strains at 350 °C stressed *P. ellipsoidea* (PE), non-stressed *P. ellipsoidea* (PE) and *Spirulina*

The elemental analysis, energy content (Milne and Dulong equations), H/C, O/C and energy recovery are displayed in Table 8-5 for the sample analysed. Unfortunately, the residue of the sample from formic acid and *P. ellipsoidea* was not carried out as there were insufficient samples available.

Table 8-5: Weight % nitrogen, carbon, hydrogen, sulphur and oxygen content as received in the residue, energy content (Dulong and Milne) and % energy recovery for experiments with four microalgae at different temperatures and conditions

	N wt. %	C wt. %	H wt. %	S wt. %	O wt. %	Dulong HHV (MJ/Kg)	H/C	O/C	Milne HHV (MJ/kg)	% Energy recovery
Chlorella										
250 °C	2.0	41.5	2.2	0.1	38.8	10.2	0.6	0.2	12.0	9.6
300 °C	1.3	50.3	1.4	0.1	31.4	13.4	0.3	0.2	14.9	10.2
350 °C water	0.8	44.3	1.2	0.1	38.1	9.8	0.3	0.2	11.8	5.7
formic acid	1.6	37.0	2.1	0.2	43.7	7.7	0.7	0.2	9.8	3.7
Stressed *P. ellipsoidea*										
250 °C	4.3	68.5	6.9	0.1	20.1	29.5	1.2	0.2	29.4	17.8
300 °C	4.2	74.4	7.6	0.2	13.6	33.6	1.2	0.1	33.1	14.7
350 °C water	4.5	77.0	6.8	0.1	11.5	33.8	1.1	0.1	33.2	10.6
formic acid	-	-	-	-	-	-	-	-	-	-
Non-stressed *P. ellipsoidea*										
250 °C	7.3	64.4	3.4	1.3	23.6	22.5	0.6	0.3	22.6	13.4
300 °C	5.9	62.4	3.2	1.3	27.2	21.0	0.6	0.3	21.5	8.0
350 °C water	1.9	55.2	2.1	0.2	40.7	14.3	0.4	0.6	16.3	3.1
formic acid	5.6	53.5	2.9	2.0	36.0	16.1	0.7	0.5	17.1	4.5
Spirulina										
250 °C	7.4	53.0	2.8	1.9	21.9	18.2	0.6	0.3	20.2	10.8
300 °C	6.6	43.4	2.6	1.6	32.8	12.7	0.7	0.6	16.7	5.4
350 °C water	7.7	41.1	2.7	1.8	33.7	11.9	0.8	0.6	15.8	4.8
formic acid	2.5	21.1	2.0	0.0	41.4	2.6	1.1	1.5	5.3	1.8

For *Chlorella* and *Spirulina*, the carbon and hydrogen contents are low compared to the elemental composition of the bio-crude; It is assumed that the major part of the residue (up to 80 wt.%) is composed of ash measured by TGA.

For both strains of *P. ellipsoidea*, higher carbon content is measured compared to the previous biomass and furthermore the nitrogen level is higher than in the bio-crude oil which implies that nitrogen compounds formed chars preferentially at low

temperature. Formic acid, in general, reduces the formation of residue; it is the reason why a low carbon and hydrogen contents are measured. It should be observed that the level is higher in the residue whereas in the bio-crude, it is negligible.

According to Garcia Alba et al. [133], residue represented the undegraded microalgae. As the temperature increases, the microalgae form clusters and decrease in size; this explains why the carbon matter is reduced as carbon compounds are soluble in the bio-crude oils. Finally, the energy recovery decreases as the temperature increases, being recovered preferentially to the bio-crude oils.

Finally, the formation of residue containing a high volatile fraction from *P. ellipsoidea* could be seen as a drawback as it decreases the amount of bio-crude yield. The particle seize used in hydrothermal liquefaction is shown to have impact on the formation of char or residues. Large particles of biomass favour the formation of chars to the detriment of the bio-crude. This could be due to that more energy being required to convert solid residues into oil.

8.4.3 Aqueous phase analysis

Results obtained from the analysis can be found in the Appendix 1, section 1.2.1 page 319. The analysis of this phase is important as it represented up to 50 wt.% of the total mass balance with the exception of *P. ellipsoidea* (stressed).

In all the processed water from microalgae, as the temperature increases from 250 to 350 °C, the ammonium compound concentration increases. Valdez et al. [135] drew a similar conclusion that ammonium compound concentration was influenced by temperature. For *Chlorella*, the concentration is higher (6284 ppm) compared to the stressed *P. ellipsoidea* (397 ppm). It can be deduced that the high proportion of lipids induce the formation of amides which reduce the ammonium compound concentration. It is surprising to observe that the ammonium compound concentration is lower with *Spirulina* compared to *Chlorella*. Because *Spirulina* is a cyanobacteria and have a different compositions, the nitrogen in the aqueous phase could be decomposed in different compounds such as amines instead of ammonium. Further analysis should be performed to know the molecular composition of the aqueous phase.

Ammonium compound is mainly produced generally by the deamidation of the amino acids or the peptide bonds; the increased concentrations with temperature are

explained by the increase of protonation which favours the deamination of amino acids or others nitrogen compounds [119, 282]. There is a linear relationship between the three microalgae (*Chlorella* and the stressed and non-stressed *P. ellipsoidea*) and the protein content given the following equation:

$$y = 197.7x - 4526.9$$ **Equation 8-1**

Formic acid for the case of *Chlorella* and the stressed *P. ellipsoidea* increased the ammonium compound concentration. For the other microalgae, formic acid has the opposite effect.

The pH of the process water increases and becomes more alkali with increasing temperature for each of the four algae. The pH for the processed water from the stressed *P ellipsoidea* with 7 compared to *Chlorella* with 9.2. The difference is caused by a higher ammonium compound concentration. Similar behaviour was observed by Yu et al. [318] from 180 to 300 °C which was explained by the increase of organics from the decomposition of protein dissolved into the aqueous phase. The pH is important as it has some impact on the solubility of some species as explaining in **Chapter 7**.

The TOC concentration generally decreases as the temperature increases for all the processed microalgae. In this study, the identification could be not be performed; nevertheless, Garcia Alba et al. [321] identified in the aqueous phase the following organics: acetone, polyols, amines, amino acids, nitrogen containing aromatics and pyrrolidones (in high concentration) compounds. Sudasinghe et al. [322] analysed the processed water from *Nannochloropsis s.* using the Fourier transform ion cyclotron resonance mass spectrometry (FT-ICR MS) method. It was observed that in the aqueous phase contained complex compounds with an average molecular weight of 400 g/mol, suggesting the presence of long chain amides.

There is no relationship apparent between the phosphate concentration and temperature. For the stressed microalgae, the concentration is low, just above the detection limit. Valdez et al. [135] measured a decrease in total phosphorus concentration from 76 % to 38 % when the temperature increased from 250 °C to 350 °C, whereas Ross et al. [129] observed 20-30 % of phosphorus compounds in the aqueous phase in formic acid, sodium potassium and carbonate ions.

One of the concepts being proposed for hydrothermal liquefaction of microalgae is to have a closed loop by recycling the aqueous phase as a growth media for the microalgae (to be considered as a green process). To generate a greater understanding of the fate of carbon and nitrogen, the following section discusses the elemental mass balance of carbon and nitrogen.

8.4.4 Carbon and nitrogen mass balance

Table 8-6 lists the elemental mass balance of the nitrogen and the carbon calculated according to the formula in the previous chapters.

For *Chlorella* and *Spirulina*, as the temperature increases, the carbon fraction in the aqueous phase and in the residue decreases whereas the carbon fraction in the bio-crude increases. Formic acid increases the carbon fraction in the aqueous phase. As the ammonium compound concentration increases with temperature, the nitrogen fraction in the aqueous phase increases also. The nitrogen fraction, in the bio-crude, decreases from 300 to 350 °C. The results are, for both microalgae, coherent with Biller et al. [112] who found that at 350 °C, the carbon fraction was the highest in the bio-crude, and for the nitrogen fraction in the aqueous and in the gaseous phases.

For both strains of *P. ellipsoidea*, the carbon fraction is in majority present into bio-crude oils with a maximum at 300 °C. The nitrogen fraction, in the aqueous phase, is lower for the stressed *P. ellipsoidea*, compared to the non-stressed. Yet, formic acid enhances the production of this ammonium compound for the stressed algae. The nitrogen fraction is the highest at 300 °C in the bio-crude. The stressed *P. ellipsoidea* contains higher nitrogen fraction in the residue compared to the other microalgae.

A large nitrogen fraction is determined in the gaseous phase for most of the microalgae. Nevertheless, no gas analysis has been performed; Ross et al. [129], observed the formation of nitrogen gaseous compounds such as ammonia, nitric oxide and hydrogen cyanide for Chlorella and for Spirulina in presence of organic acids at 350 °C.

Table 8-6: Carbon and nitrogen mass balance for the aqueous, bio-crude and remaining phases for the experiments using microalgae and model compounds at different temperatures and conditions

	% C aqueous	% C bio-crude	% C residue	% C gas	% N aqueous	% N bio-crude	% N residue	% N gas
				Chlorella				
250 °C	45	30.7	16.9	7.4	20.6	14.0	2.2	63.2
300 °C	38	41.5	16.6	3.9	33.3	17.8	3.1	45.8
350 °C water	37.2	44.2	11.1	7.5	49.7	16.7	1.6	32.0
formic acid	27	41.3	7.1	24.6	61.1	13.5	0.7	24.7
				Stressed *P. ellipsoidea*				
250 °C	6.6	48.6	19.7	25.1	1.5	18.3	27.4	52.8
300 °C	7.3	59.4	15.3	33.4	5.7	28.4	19.4	46.5
350 °C water	15.9	54.8	11.5	29.3	9.7	18.1	23.9	48.2
formic acid	10.2	54.5	0.0	35.4	30.1	33.7	0.0	36.1
				Non-stressed *P. ellipsoidea*				
250 °C	35.9	34.5	17.1	12.6	4.7	16.6	11.9	54.9
300 °C	34.8	52.4	10.5	2.3	31.2	25.6	6.1	30.1
350 °C water	14.9	47.5	5.2	32.3	45.6	20.4	1.1	33.0
formic acid	14.9	41.2	6.6	37.2	11.6	18.1	4.0	41.7
				Spirulina				
250 °C	45.2	29.5	10.3	15.0	9.0	13.8	6.8	70.3
300 °C	35.2	32.7	6.1	26.0	18.3	13.7	4.3	63.6
350 °C water	27.0	36.1	5.5	31.4	23.7	12.8	4.9	58.7
formic acid	38.5	26.4	1.2	33.9	21.2	9.1	0.7	69.0

To summarise, as the temperature increases from 250 to 350 °C, the carbon fraction in the aqueous phase is reduced while the nitrogen fraction in the aqueous phase increases. The nitrogen fraction, in the bio-crude, decreases towards 350 °C.

The processing of *P. ellipsoidea* yields promising results, with a low nitrogen content, and a high bio-crude yield. Moreover, this alga contained mostly monosaturated fatty acids which reduced the formation of cross linked compounds. The low nitrogen content in the processed oil with less than 1.5 wt.% is an encouraging result. Nevertheless, the fraction of amides represents a large part of the bio-crude oil composition.

The type of the reactor was a predominant parameter which could have an influence on the composition of the bio-crude oils. With the batch reactor used, a long heating and subsequently cooling rate was achieved, recombination of small molecules forming high polymers could reduce the quality of the bio-crude oil. Temperatures also have an influence on the yield and bio-crude composition. For the two varieties of *P. ellipsoidea* best conditions is achieved at 300 °C whereas with *Chlorella* and *Spirulina* was found at 350 °C. In terms of energy, it would be more suitable to carry out the experiment at milder temperature (between 200 to 300 °C) in order to save some energy. Long reaction times at temperature below 300 °C are recommended in order to achieve the lowest nitrogen recovery in the bio-crude. One explanation could be that the polymerisation of short nitrogen heterocyclic compounds such as pyrrole were not favoured compared to higher temperatures [323].

To conclude this section:

- The protein and lipid contents have an impact on the bio-crude yield.
- *Chlorella* and *Spirulina* have similar behaviour during hydrothermal liquefaction with temperature in increasing the bio-crude yields and the fraction of low molecular weight compounds.
- The ammonium compound concentration, in the aqueous phase, increases in relation to the temperature for the four microalgae whereas the nitrogen decreases in the bio-crude oils. There is a linear fit between the protein content of the three microalgae and the ammonium compound concentration.
- A large range of nitrogen compounds are identified in the bio-crude oil including piperidine, indole, 1-butyl-2-pyrrolidone and C_{18} amide chains. The most abundant fatty acid in the bio-crude is oleic acid.
- The same conclusion is observed with the STA as for the processing of proteins
- The carbon fraction is transferred from the aqueous phase into the bio-crude oils or the gaseous phases with increasing temperature. The best condition to produce the highest bio-crude with low nitrogen depends on the composition of the strain used.

8.5 Influence of metal doped HZSM-5 catalysts on *Chlorella* and the stressed *P. ellipsoidea*

In the following section, a catalytic screening with metal doped zeolite will be carried out in order investigate the effect on the nitrogen and in the mass balance yield.

8.5.1 Mass balance yield

In order to reduce the work load, the catalytic screening is performed using two different strains, *Chlorella* and *P. ellipsoidea*, using the following metals: iron, copper, molybdenum and nickel doped in HZSM-5. Experiments are performed in water and in formic acid. The mass balances for both microalgae are illustrated in Figure 8-12. Some experiments were carried out in duplicate with HZSM-5 in water and formic acids with the following coefficient of variance for the bio-crude oil production: 4.2 % in water and 6.4 % in formic acid. (a) represents the experiment *Chlorella* in water; (b) the experiments *Chlorella* in formic acid; (c) stressed *P. ellipsoidea* in water; (d) stressed *P. ellipsoidea* in formic acid**.**

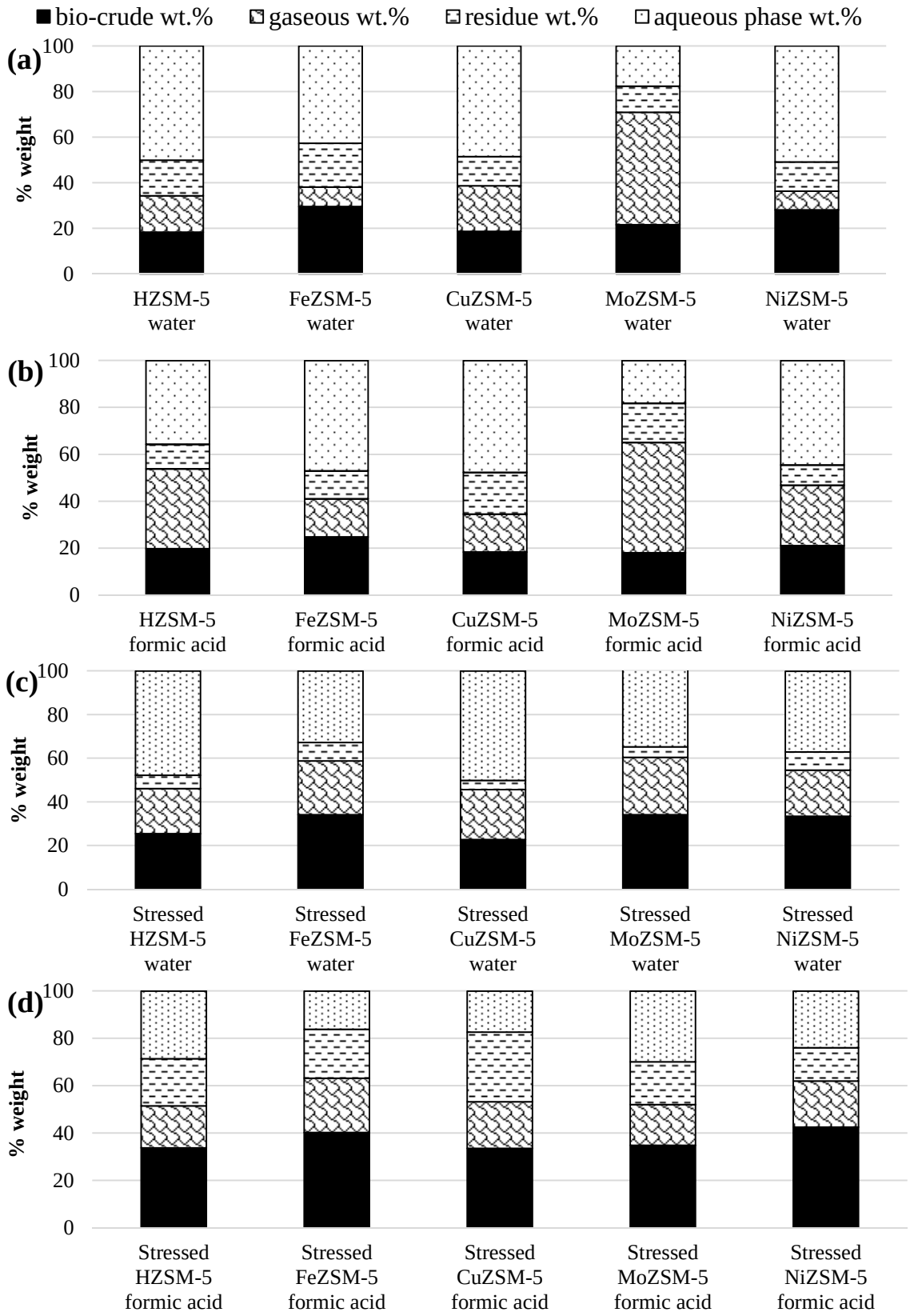

Figure 8-12: Diagrams representing mass balance for the different fractions bio-crude oils, gaseous, residue and aqueous fractions for the catalytic screening using metal doped HZSM-5 with *Chlorella* and stressed *P. ellipsoidea*.

For the catalytic processing with *Chlorella*, FeZSM-5 and NiZSM-5 enhance the yield of the bio-crude compared with the other doped zeolites. MoZSM-5 is selective for the production of gas. Nevertheless, bio-crude yields are reduced compared to the experiments in water especially with FeZSM-5. Copper is more selective to enhance the aqueous phase fraction.

For the catalytic processing with *P. ellipsoidea*, a lower bio-crude yield is observed compared to without catalyst, for example with 33.5 wt.% for NiZSM-5 and 49.3 wt.% without catalyst at 350 °C. Nickel and iron result in the highest yield of bio-crude. As stated, the gaseous fraction is more significant with MoZSM-5 which is unexpected as nickel was known to promote gasification. In contrast to *Chlorella*, a higher bio-crude yield is achieved with formic acid; with NiZSM-5 with a yield of 42.0 wt.%. With this alga, the bio-crude yield differed compared to soya protein where the yield was higher in water.

Overall, FeZSM-5 and NiZSM-5 enhances the formation of bio-crude yield, while MoZSM-5 promotes gasification and CuZSM-5 increases the level of product into the aqueous phase.

8.5.2 Bio-crude analysis of catalytic runs

In order to investigate the impact of metal and HZSM-5 towards the composition of the bio-crude oil, GPC, GC-MS analysis and elemental analysis were carried out.

8.5.2.1 GPC analysis

Figure 8-13 shows the molecular weight fraction in the bio-crude oil using GPC for the catalytic screening of both microalgae. (a) represents the experiment with *Chlorella* in water; (b) the experiments with *Chlorella* in formic acid; (c) stressed *P. ellipsoidea* in water (d) stressed *P. ellipsoidea* in formic acid.

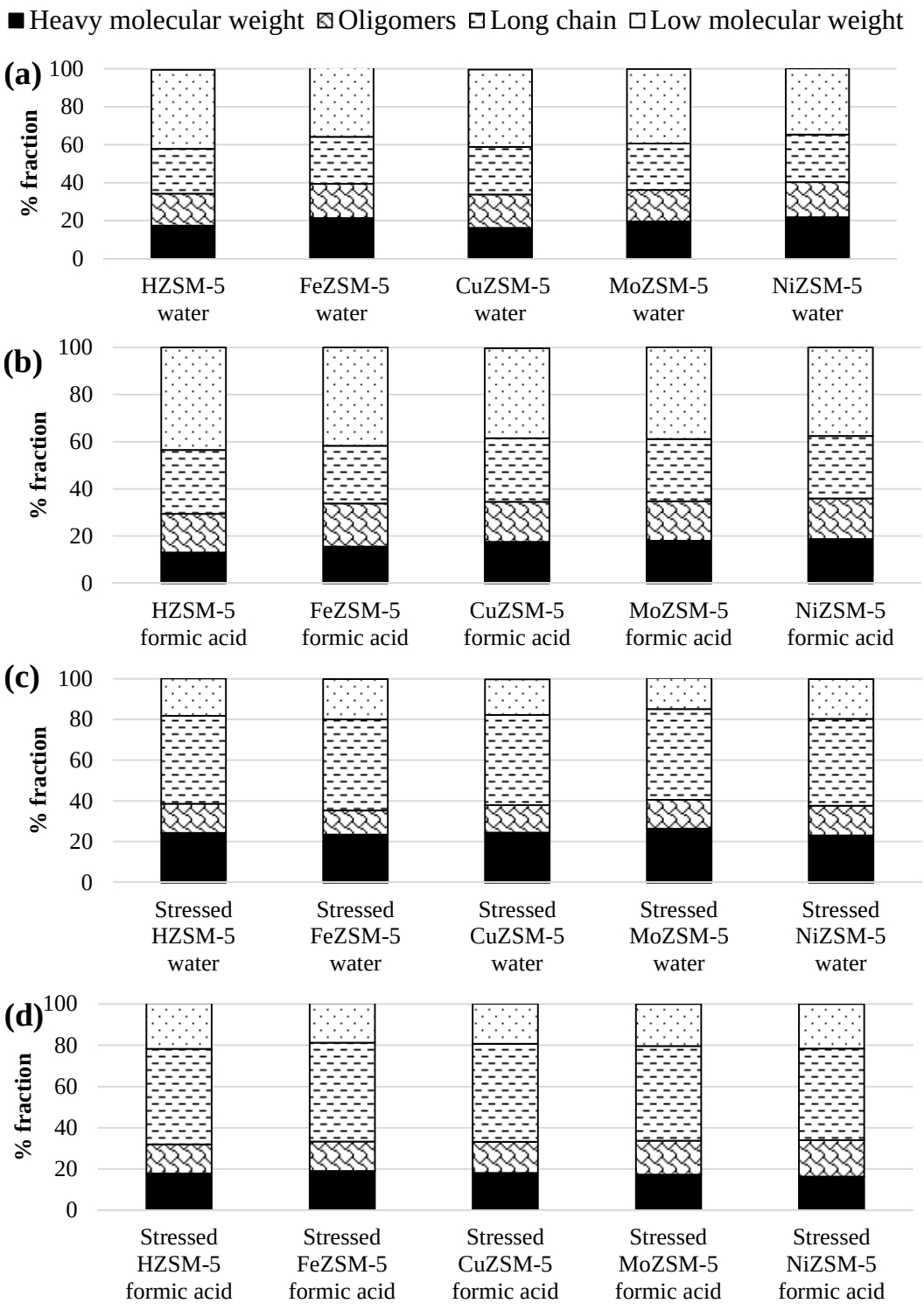

Figure 8-13: Different molecular weight fraction of the bio-crude oils of for *Chlorell*. and stressed *P. ellipsoidea* for the catalytic screening.

For the processing of *Chlorella*, FeZSM-5 and NiZSM-5 exhibit larger fractions of oligomers and "heavy molecular weight" materials. Conversely, CuZSM-5 and HZSM-5 result in increased yields of lower molecular weight materials. The

presence of catalyst did not have a significant impact on level of “long chain” materials which remains constant. Contradictory results are found with soya proteins as discussed in **Chapter 7** which indicated that with CuZSM-5, polymerisation was enhanced. The variation between each experiment with formic acid is insignificant.

For the processing of *P. ellipsoidea*, the “long chain” material is the highest fraction since this alga contains 67 wt.% dry weight lipids. MoZSM-5, in water, enhances the formation of “heavy molecular weight” materials. In general, it is with HZSM-5 and formic acid that the fraction of low molecular weight materials is the largest with low polymerisation with microalgae and proteins (**Chapter 7**).

8.5.2.2 GC-MS analysis

Figure 8-14 represents one example of GC-MS chromatogram for the processing with MoZSM-5 in water of *P. ellipsoidea* (a) and *Chlorella* (b). Table 8-7 lists the main compounds in the chromatograms of the two algae processed with MoZSM-5.

The processing of the stressed *P. ellipsoidea* with the metal doped zeolite for example with MoZSM-5 Figure 8-14 (a) show mainly long chain compounds such as alkenes, amides and fatty acids. Except the formation of amides and pyrrole, less nitrogen compound is identified compared to *Chlorella*. For CuZSM-5, the formation of amide, such as 9-octadecenamide (57.2 minutes), is lower in formic acid compared to water with a ratio of 92 of difference between the two areas. Copper has been demonstrated to promote the hydrolysis of amides [324]. Biller et al. [196] observed that formic acid alone increase the formation of amides, it could suggests that HZSM-5 reduces the formation of amides.

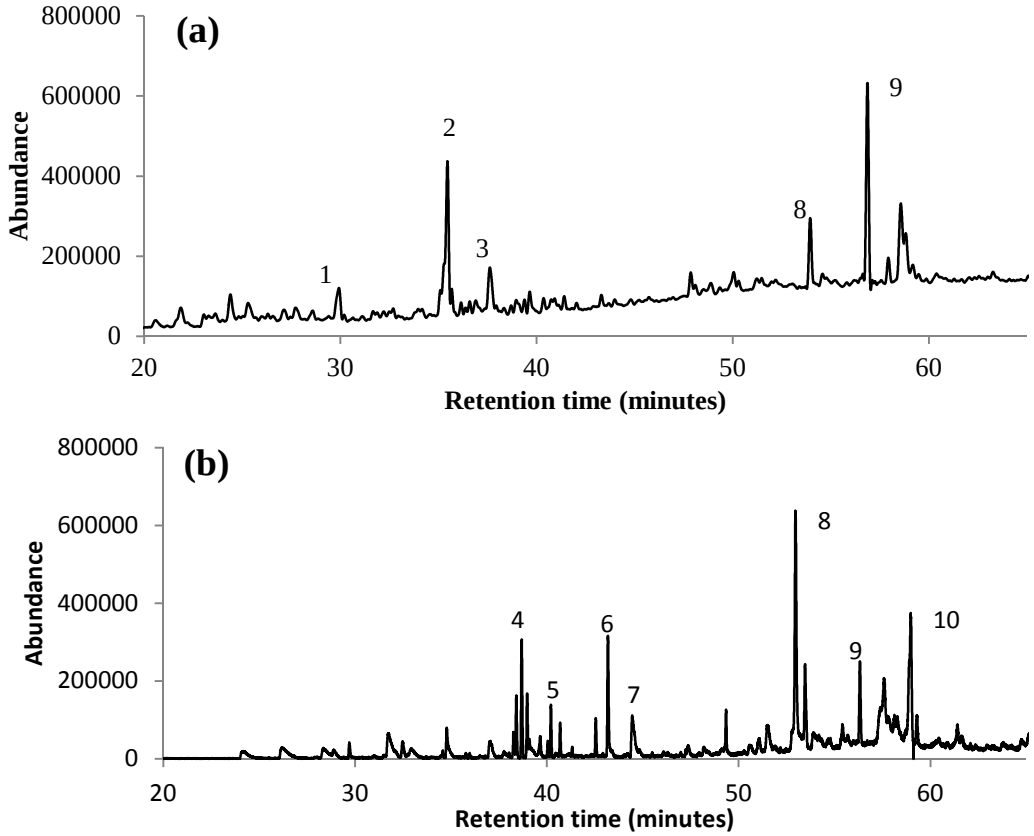

Figure 8-14: GC-MS chromatograms of the bio-crude oils at 350 °C in water where (a) *Chlorella* (b) stressed *P. ellipsoidea* with MoZSM-5

Table 8-7: List of compounds identified in chromatogram using *Chlorella* and stressed *P ellipsoidea* with MoZSM-5

Number	Retention time (minutes)	Compounds
1	29.2	Hexadecane
2	35.3	3-octadecene
3	37.5	2,3-dihydro-1-methyl-1H-pyrrole
4	38.6	3,7,11,15-tetramethyl-2-hexadecene
5	40.2	2-n-octylfuran
6	43.2	isophytol
7	44.5	1-phenyl-5-(1-piperidinyl)-pentan-1-one
8	52.9	hexadecamide
9	56.3	2-butylhexanoic acid, 3-pentyloxycarbonylpropyl ester
10	59.0	triazin-5(2H)-one compounds

The processing of *Chlorella* with the metal doped zeolite for example with MoZSM-5 (Figure 8-14 (b)) produces lower oxygenated compounds included 2-n-

octylfuran with more hydrocarbons such as 3,7,11,15-tetramethyl-2-hexadecene. Complexes nitrogen compounds are identified at 59.0 minutes one molecule containing an atriazin-5-(2H)-one group. A large formation of isophytol (43.2 minutes) is identified in most of the chromatogram from the processed catalyst. As shown previously, 2-pyrrolidinone is only observed in formic acid with CuZSM-5 and HZSM-5, whereas with CuZSM-5 a compounds containing imidazole attached to a long alkane chain is identified. 1-ethyl-2-undecylimidazole is shown in Figure 8-15.

A large range of alkenes are typically observed for the other catalysts. In general, new compounds has been identified performing the catalytic screening which indicates that metal doped zeolite enhance the formation of compounds.

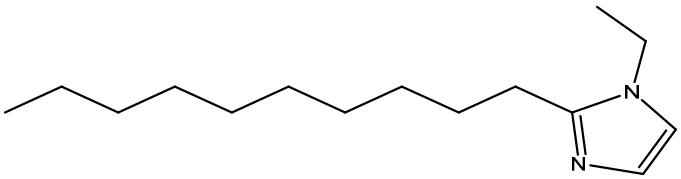

Figure 8-15: Chemical structure of 1-ethyl-2-undecylimidazole

8.5.2.3 Elemental analysis

Table 8-8 lists the elemental analysis of the bio-crude oil from the catalytic experiments from the two microalgae in water and formic acid.

For *Chlorella,* a slight decrease in nitrogen is measured with FeZSM-5 and MoZSM-5 in formic acids, otherwise for the remaining catalysts; there is little effect on the level of nitrogen compared to the runs without the zeolites. MoZSM-5 gives an encouraging result by lowering the oxygen content to 0.5 wt.%.

For *P. ellipsoidea,* the nitrogen content for the catalyst is higher with the catalysts compared to the run without any catalysts. Similar results were observed with soya protein in the previous chapter. Duan and Savage (2010) found that the addition of “zeolite” reduced the nitrogen content from 6.3 to 4.3 wt.% which was slightly higher than with the non-catalytic run [190].

Table 8-8: Weight % nitrogen, carbon, hydrogen, sulphur and oxygen content as received in the bio-crude oils, energy content (Dulong and Milne formula) and % energy recovery for experiments for microalgae during the screening of metal doped HZSM-5

	N wt.%	C wt.%	H wt.%	S wt.%	O wt.%	Dulong HHV (MJ/kg)	H/C	O/C	Milne HHV (MJ/kg)	% Energy recovery
Chlorella										
Water										
HZSM-5	5.5	75	9.3	0.4	9.7	37.0	1.5	0.1	36.0	36.5
FeZSM-5	5.2	73.4	8.8	0.8	11.8	35.4	1.4	0.1	34.5	48.9
CuZSM-5	6.7	80	10.1	0.4	2.8	41.0	1.5	0	39.3	42.4
MoZSM-5	6.2	82.5	10.5	0.4	0.5	42.8	1.5	0	41.0	51.1
NiZSM-5	6.5	75.5	9.7	0.6	7.7	38.0	1.5	0.1	36.7	38.5
Formic acid										
HZSM-5	6.1	67.6	9.5	0.2	16.7	33.4	1.7	0.2	32.7	31.4
FeZSM-5	5.0	74.3	8.9	1.2	10.5	36.1	1.4	0.1	35.2	48.9
CuZSM-5	6.1	73.7	10	0.5	9.7	37.5	1.6	0.1	36.3	32.6
MoZSM-5	5.0	71.5	9.4	0.4	13.8	35.1	1.6	0.1	34.3	30.0
NiZSM-5	5.9	76.4	9.9	0.4	7.5	38.6	1.6	0.1	37.3	38.5
Stressed *P. ellipsoidea*										
water										
HZSM-5	2.1	78	11.7	0	8.1	41.7	1.8	0.1	40.7	35.8
FeZSM-5	1.6	75.2	11.3	0	11.9	39.4	1.8	0.1	38.8	33.9
CuZSM-5	2.2	81.5	11.9	0	4.5	43.7	1.8	0	42.5	33.7
MoZSM-5	2.2	80.4	11.2	0	6.2	42.1	1.7	0.1	41.1	46.2
NiZSM-5	1.5	74.6	11	0	12.9	38.6	1.8	0.1	38.1	47.7
Formic acid										
HZSM-5	1.4	66.5	9.7	0	22.4	32.3	1.8	0.3	32.5	50.9
FeZSM-5	1.9	80.6	11.7	0.4	5.4	43	1.7	0.1	41.9	38.0
CuZSM-5	1.7	74.5	10.9	0	12.9	38.4	1.8	0.1	37.9	44.6
MoZSM-5	1.7	77.8	11	0	9.5	40.3	1.7	0.1	39.6	50.5
NiZSM-5	1.5	77.1	11.3	0	10.1	40.4	1.8	0.1	39.6	35.8

MoZSM-5 and CuZSM-5 enhance the deoxygenation of the bio-crude yielding higher level of carbon (above 80 wt.%) in water. The result is emphasised with the GC-MS composition where lower oxygenated compounds are observed in the bio-crude. The hydrogen content, for the stressed *P. ellipsoidea*, increases to more than 10

wt.% resulting in higher energy content due to the increase of the “long chain” range. For both algae, the most efficient energy recovery is achieved in formic acids with FeZSM-5 and NiZSM-5.

8.5.3 Aqueous phase analysis

The results from the analysis of the aqueous phase are shown Appendix 1, section 1.2.2 page 320. For *Chlorella*, the ammonium compound concentration is at its maximum with MoZSM-5 (5158 ppm) with the aqueous phase being alkali with a pH of 9. On the other hand, the production of ammonium compound is reduced with NiZSM-5 and CuZSM-5 (in water with a pH of 8.5).

For *P. ellipsoidea*, the ammonium compound is 2-5 times lower compared to the other algae. Nevertheless, with formic acid an increase is measured. As explained before, the formation of amide reduces the ammonium compound concentration in the aqueous phase. In formic acid, the formation of amides is lower resulting in an increase in ammonium compound in the aqueous phase. The pH of the processed water phase with this alga is acidic (4-6) possibly due to lower nitrogen content. The Brønsted acidic site of HZSM-5 and formic acid could promote the hydrolysis of the amides and enhances the formation of ammonium compounds. It explained why the abundance of amides in the bio-crude is lowered compared to the run in water. In general, the ammonium compound concentration is lower using the catalysts than the non-catalytic run.

The TOC concentration is enhanced by FeZSM-5 and HZSM-5 with formic acid. From the previous chapter, similar results were obtained using the nickel and the copper catalyst. There is incoherence with CuZSM-5 where with *Chlorella,* the largest aqueous phase mass balance (40.7 wt.%) is deduced while the low TOC concentration is measured (8942 ppm).

The production of phosphate concentration increase with *Chlorella* compared to soya protein particularly with MoZSM-5 in formic acid. The sulphate concentration is enhanced with NiZSM-5 in formic acid.

8.5.4 Carbon and nitrogen mass balance

In order to understand the influence of the addition of catalyst, the carbon and nitrogen mass balance is calculated and the values are lists in Table 8-9.

For the processing of *Chlorella*, the use of CuZSM-5 in water and formic acid enhances the carbon fraction in the bio-crude followed by NiZSM-5. FeZSM-5 favours the distribution of carbon fraction to the aqueous phase and HZSM-5 to the gaseous phase. MoZSM-5 is more selective at increasing the nitrogen fraction in the aqueous phase in water and FeZSM-5 reduces the nitrogen fraction in the bio-crude oil to the lowest value. CuZSM-5, in formic acid, seems the most suitable catalyst to process *Chlorella* as high carbon and a relatively low nitrogen fraction are achieved.

For the processing of *P. ellipsoidea*, MoZSM-5 and FeZSM-5, in water, and NiZSM-5, in formic acid, yield the highest carbon fraction in the bio-crude oil. In **Chapter 5**, the processing of lipids with MoZSM-5 showed the highest propensity towards aromatics. In this case, there is no evidence for the increase of aromatic compounds being produced. In formic acid, the nitrogen fraction in the aqueous phase is increased by a factor of three. Here the most suitable catalyst is NiZSM-5 which produces a bio-crude with a high carbon fraction and low nitrogen fraction.

Table 8-9: Carbon and nitrogen mass balance for the aqueous, bio-crude oils and remaining phases (gaseous and residues) for the experiments using microalgae and model compounds using metal doped HZSM-5

	% C aqueous	% C bio-crude	% C remaining	% N aqueous	% N bio-crude	% N remaining
Chlorella						
Water						
HZSM-5	22.5	25.3	52.2	29.4	8.4	62.2
FeZSM-5	33.4	39.8	26.8	32.8	13.6	53.6
CuZSM-5	28.3	54.7	17.0	21.3	17.7	61.0
MoZSM-5	30.0	38.0	32.0	39	14.5	46.5
NiZSM-5	31.3	53.7	15.0	13.1	21.1	65.8
Formic acid						
HZSM-5	9.1	27.4	63.4	28.5	12.1	59.4
FeZSM-5	3.6	25.8	70.6	28.6	8.8	62.6
CuZSM-5	9.3	36.6	54.2	29.5	12.0	58.5
MoZSM-5	9.5	27.8	62.7	36.0	11.3	52.7
NiZSM-5	10.2	32.6	57.2	22.1	12.3	65.6
Stressed *P. ellipsoidea*						
Water						
HZSM-5	15.5	32.4	52	6.6	19.1	74.3
FeZSM-5	7.8	31.2	61.0	16.5	14.5	68.9
CuZSM-5	8.7	30.3	60.9	13.4	17.9	68.7
MoZSM-5	7.8	44.8	47.4	16.6	26.8	56.6
NiZSM-5	6.5	40.1	53.4	18.8	17.6	63.5
Formic acid						
HZSM-5	12.9	35.5	51.5	32.2	16.3	51.5
FeZSM-5	8.1	45.1	46.8	30.2	23.3	46.5
CuZSM-5	13.1	36.6	50.3	32.0	18.3	49.8
MoZSM-5	9.0	43.0	48.0	31.4	20.5	48.1
NiZSM-5	10.1	46.7	43.3	31.2	19.8	48.9

After the CHNS, GPC and GC-MS, the best bio-crude oil is achieved with CuZSM-5 containing more than 45 % of low molecular weight for *Chlorella* and a high carbon and low oxygen content are achieved. Even though with FeZSM-5 and NiZSM-5 the highest bio-crude yield are obtained.

To summarise, FeZSM-5, MoZSM-5 and NiZSM-5 have an impact on the formation of the bio-crude oil and result in a slight reduction in nitrogen. CuZSM-5 improved the carbon distribution of the bio-crude oil for *Chlorella* and NiZSM-5 and MoZSM-5 for the stressed algae. So far, noble metals such as Pd/C, Ru/C or Pt/C achieved good bio-crude yields and low nitrogen and oxygen content in the oil [156, 190, 196]. The problem is that these catalysts are expensive and when this process is scaled up this system would not be competitive compared to the traditional route without catalyst.

In this section, the following points are observed:

- FeZSM-5 in water increases the bio-crude yield for *Chlorella* even though more "heavy molecular weight" materials are produced.
- MoZSM-5 promotes gasification in water and in formic acid for *Chlorella.*
- CuZSM-5 and MoZSM-5 enhances the reduction of oxygen in the bio-crude of *Chlorella*.
- Compared to HZSM-5, the iron has an effect on reducing the nitrogen content in the bio-crude. The reduction of nitrogen is not improved by the catalysts.
- Formic acid and metal doped HZSM-5 enhances the formation of ammonium concentration compared to the run in water and thus reduces the formation of amides in the bio-crude.

8.6 Discussion about the degradation of microalgae

Reactions occurring during hydrothermal liquefaction of microalgae are complex as a range of interactions and reactions can take place. According to Toor et al. [2], there are three reaction steps occurring during the hydrothermal liquefaction of microalgae as explained in the literature reviews. Figure 8-16 gives a brief insight regarding the different interactions and the degradation of the main component of the microalgae (protein, carbohydrates and lipids). This diagram is drawn in relation with the results obtained from literature [325].

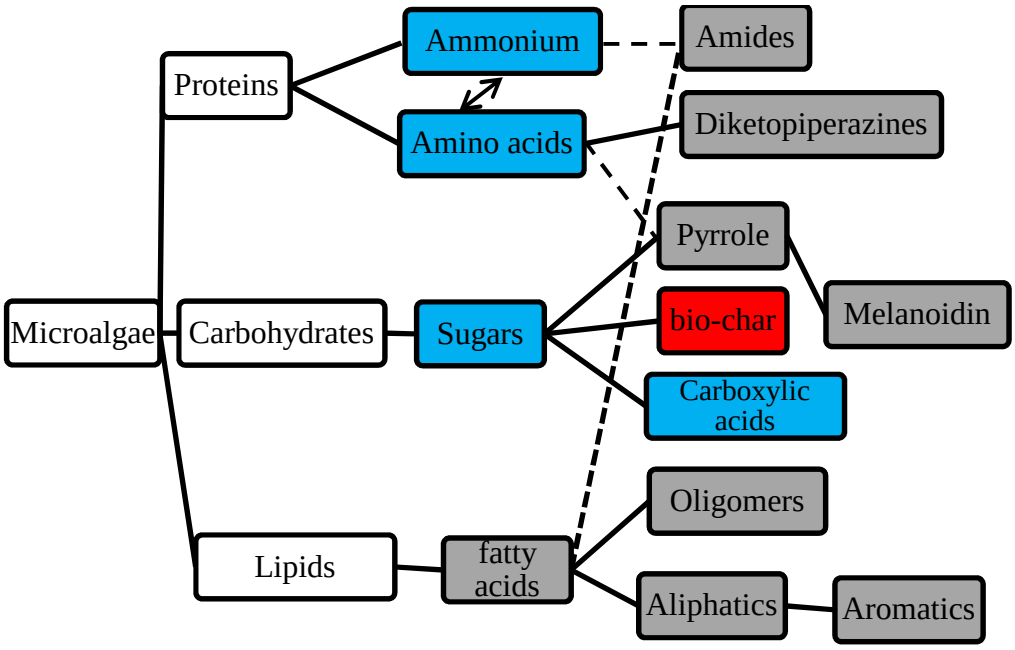

Figure 8-16: Diagram of the main degradation routes during hydrothermal liquefaction of microalgae, the grey represent product soluble in the bio-crude oil, the blue the product soluble in the aqueous phase and red in the residue

1) As explained in the previous chapters, during the first step, the macromolecules (proteins, carbohydrates and lipids) from the microalgae are been depolymerised and hydrolysed. For instance, the degradation of carbohydrates and lipids molecules from microalgae occurs rapidly [326]. The same conclusion was drawn for the proteins by Garcia Moscoso et al. [140]. Using SEM, Garcia Alba et al. [133] observed that the degradation of the cell from the microalgae began at 225 °C by forming a cluster which coagulated together. At 250 °C, most of the cells were broken down producing bio-crude oil.

2) In the second step, the following monomers (for examples glucose, amino acids and fatty acids) produced from the hydrolysis, degrade further and subsequently recombine together. It is at this stage that the bio-crude oil is forming. It is the reason why Valdez et al. [135] achieved high bio-crude yield (50 wt.%) in less than 10 minutes from *Nannochloropsis* at 300 °C. From the HTL processing of *Chlorella py*, Gai et al. [327] found that the bio-crude drastically increased from 260 to 280 °C and subsequently started to decrease between 280 to 300 °C as secondary cracking was more preponderant which followed the result obtained by Li et al. [147]. The same degradation pathway as in **Chapter 7** could be deduced for the proteins of the

microalgae, as diketopiperazine has been identified in the bio-crude of *Chlorella* such as 3-benzyl-6-isopropyl-2,5-piperazinedione and 1-butyl-2-pyrrolidinone. Further interactions can occur between other components even in low proportion such as with ashes, nucleotides, chlorophylls, etc…

3) Cross linking between different molecules creates side reaction for example between carbohydrates and proteins for example [314]. This reaction (explained more in detailed in the next chapter) is known to produce "heavy molecular weight" materials. In order to reduce the nitrogen content into the bio-crude oil, the formation of these compounds should be hindered as these compounds are stable under high temperature [315].

The formation of amides is one example of cross linking reaction. This compound is produced via nucleophilic substitution of fatty acids and ammonia. The mechanism is shown in Figure 8-17 from Clayden et al. [328] between a carboxylic group and the ethylamine. In the first step, the nucleophilic group of the amine attacks the carboxylic group; subsequently there is a proton transfer which leads to the leave of the hydroxyl group. At room temperature, acyl chloride is more reactive compared to a carboxylic acid group. As the polarity of water decreases with an increase in temperature, the long chain fatty acids become soluble into the aqueous phase and react with ammonium cations. At room temperature, a catalyst would be necessary in order to activate the carbonyl groups and allow the condensation to occur. However, at high temperatures, the ion dissociation constant K_w is increased from 250 to 350 °C (close to a pK of 10^{-11}), with higher proton donation characters [94].

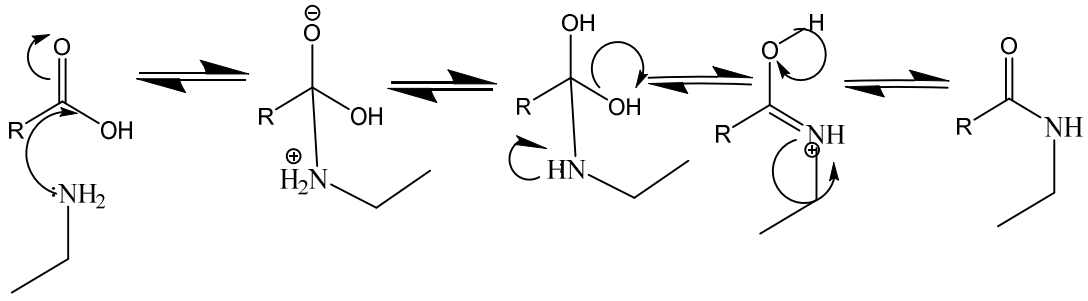

Figure 8-17: Mechanism for the formation of amides [328]

Duan et al. [100] illustrated that the hydrolysis of N-methylacetamide was reversible for a neutral pH (between 3 and 8). Under an acidic pH (below 3) and alkali pH (upper than 9), the hydrolysis of this amide was enhanced followed an SN_2

mechanism. It is why the concentration of ammonium is higher with the addition of formic acid and HZSM-5 as the hydrolysis of amides is more significant. Within the pH range 3-8, amides are more stable.

8.7 Conclusion

The hydrothermal liquefaction of the four different microalgae was investigated at different conditions (temperature, time, in water and formic acid). The maximum bio-crude yield was achieved with *P. ellipsoidea* (stressed) with 52.9 wt.% at 300 °C. The bio-crude oil increased with temperatures for *Chlorella* and *Spirulina*; molecular weight of the bio-crude decreased with temperature as temperature increased. Formic acid enhanced the formation of gas however the bio-crude oil was reduced compared to the experiment in water. Contrary to results in the literature, the nitrogen content decreased from 250 to 350 °C for *Chlorella* and *Spirulina*, while the ammonium compound concentration increased in the aqueous phase. With both *P. ellipsoidea* strains, the nitrogen was reduced from 300 to 350 °C. The high lipid content enhanced the formation of amides in the bio-crude which reduced ammonium compound concentration. Oleic acid was the main fatty acid observed in the bio-crude. There is some evidence that the use of formic acid and zeolites decreased the level of amides formation. Diketopiperazines were observed as a key product derived from the degradation of proteins. NiZSM-5 and MoZSM-5 for the stressed algae increased the carbon content in the bio-crude oil and were more active promoting deoxygenation.

Chapter 9 HTL of model compounds and their mixtures

This chapter includes HTL experiments with various binary mixtures composed of soya proteins, sunflower or linseed oils and starch; they have been processed at different temperatures (250, 300 and 350 °C). Afterwards, proteins, lipids and carbohydrates have been mixed together to obtain synthetic alga compositions. Experiments have been carried out at three temperatures and at 350 °C in formic acid and with HZSM-5.

9.1 Introduction

The formation of Maillard compounds between glycine and glycerol was studied by Peterson et al. [314] and Minowa et al. [329]. Products called melanoidin decompose into chars and subsequently at higher temperature into oils. Kruse et al. [278] determined that the processing of protein and carbohydrates mixtures at high temperature forms some scavengers (eg pyrazine molecules) which reduce the formation of gas. Chiaberge et al. [316] investigated the formation of amide with stearic acid and different amino acids. A wide array of primary and secondary amides were synthesised with 20 amino acids.

A mixture of models containing lipids and carbohydrates has been studied by co-processing sunflower and soya bean stalk with sunflower and with rapeseed meal (high protein and fats) [330, 331]. The outcome of these experiments yielded a high char content and many carbonyl and phenolic compounds in the bio-crude oils. Sinag et al. [192] studied the decomposition of baby food (a blend of proteins, carbohydrates and minerals) below the supercritical point (375 °C). Carbohydrates are mainly degraded into aqueous products such as formic acid or glycolic acid and 20.0 wt.% of solid residue is obtained. Biller et al. [112] mentioned a tertiary mixture with the following composition: 43.0 wt.% protein, 27.6 wt.% carbohydrate and 28.7 wt.% lipid, a similar bio-crude yield is achieved between the synthetic and the real microalgae. Valdez et al. [152] predicted a numerical model from experimental results of different microalgae as a continuity of Biller et al. [112]. It was deduced that the bio-crude formation was more favourable with less carbohydrates and more lipids.

The chapter aims to discuss the processing of different mixtures from feedstocks used in the previous sections. The different interactions between each mixture will be studied depending on the proportion and temperature. Furthermore, synthetic mixtures similar to two microalgae *Chlorella* and *P. ellipsoidea* are processed using hydrothermal liquefaction. These results are compared with real algal biomass.

9.2 Methodologies

Different binary mixtures were prepared with the following proportion of starch-protein, sunflower-protein, linseed-protein, sunflower-starch and linseed-starch (25-75, 50-50 and 75-25). The 50-50 composition of the previous mixtures was used at 250 °C and 300 °C. The synthetic microalga called *Chlorella* or high nitrogen microalga was prepared with the following composition for 3 g: 9.0 wt.% of starch; 34.8 wt.% of sunflower oil and 56.3 wt.% of proteins. The stressed *P. ellipsoidea* was simulated with: 7.3 wt.% starch, 66.3 wt.% sunflower oil, 26.3 wt.% proteins. Experiments were carried out at 250, 300 and 350 °C, in water and in formic acid and HZSM-5 for the highest temperature. Two additional experiments were carried out using a mixture of glucose, different fatty acids (oleic 67.0 wt.% and linoleic acid 33.5 wt.%) and amino acids (50-50 asparagine-glutamine) using the same proportion of the algal mixtures. The resulting products (bio-crude oil and aqueous phase) were analysed using the same procedures as in the previous chapters.

9.3 Binary mixtures

9.3.1 Initial composition

Table 9-1 contains the initial composition of the raw mixture between each element (starch, soya protein, sunflower and linseed oil) and for the model mixture asn-glucose represents the mixture asparagine and glucose with a 50-50 ratio. The mixture of starch and protein is determined by the elemental analyser, and the other value was calculated by doing the average of the initial component.

Table 9-1: Elemental composition as dried basis of the raw mixtures and the exact wt.% composition in proteins, carbohydrate and lipids for the mixtures

	N wt. %	C wt. %	H wt. %	O wt. %	HHV (MJ/kg)	Proteins wt.%	Lipids wt.%	Carbohydrates wt.%
Starch-protein								
75-25	3.3	40.7	6.4	49.6	14.1	23.5	-	76.5
50-50	6.9	43.2	6.6	43.3	16.3	47.4	-	52.6
25 -75	10.2	45.5	6.7	37.6	18.2	66.8	-	33.2
asn-glucose	9.7	35.3	6.6	48.4	12.7	49.3	-	50.7
Sunflower-protein								
75-25	3.6	67.3	10.2	19.0	33.9	28.6	71.4	-
50-50	7.1	61.8	9.3	21.9	30.2	58.1	41.9	-
25-75	10.7	56.2	8.3	24.9	26.4	78.7	21.3	-
Linseed-protein								
75-25	3.6	67.3	10.3	18.9	34.1	23.2	76.8	-
50-50	7.1	61.7	9.4	21.9	30.3	44.5	55.5	-
25-75	10.7	56.2	8.4	24.8	26.5	74.0	26.0	-
Sunflower-starch								
75-25	-	64.3	9.9	25.8	31.3	-	73.3	26.7
50-50	-	55.7	8.8	35.6	25.0	-	49.2	50.8
25-75	-	47.1	7.6	45.3	18.6	-	25.2	74.8
Linseed-starch								
75-25	-	64.2	10.1	25.7	31.5	-	73.8	26.2
50-50	-	55.7	8.9	35.5	25.1	-	51.6	48.4
25-75	-	47.1	7.6	45.3	18.7	-	27.1	72.9

The weight per cent nitrogen against the protein content of the microalgae is included in Figure 9-1 as reference. This plot suggests that the nitrogen content is related to the protein content.

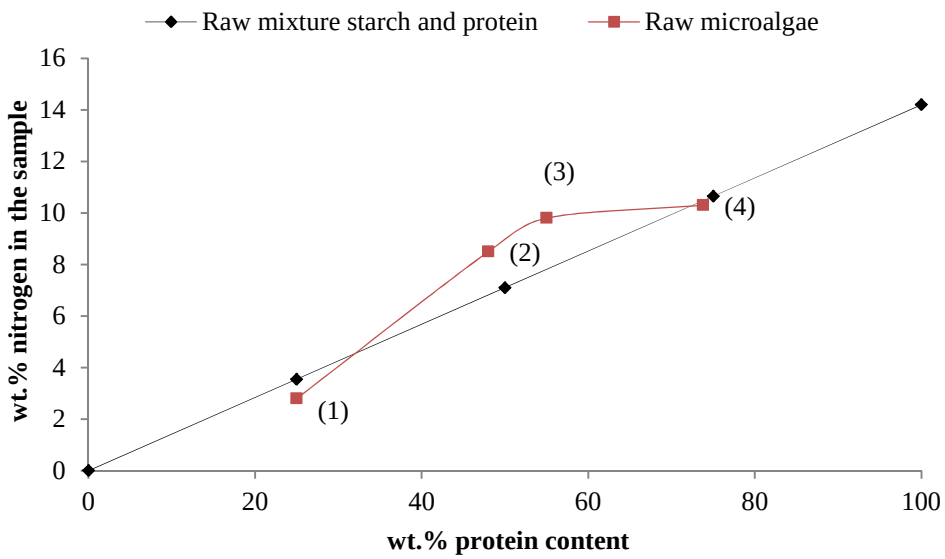

Figure 9-1: Relationship between unprocessed protein and the nitrogen between starch and soya-protein in dark and red was the four microalgae (1) stressed *P. ellipsoidea* (2) non-stressed *P. ellipsoidea* (3) *Chlorella* v. and (4) *Spirulina.*

Between the stressed *P. ellipsoidea* and *Chlorella*, there is a linear relationship with the three microalgae; nevertheless there is no difference with *Chlorella* and *Spirulina*. It suggests that for the raw microalgae after 60 wt.% of proteins the nitrogen content is not proportional to the protein content, although proteins have a major impact with high lipid algae.

9.3.2 Mass balance yield

The effect of different compositions on the mass balance yield of the various phases is investigated. Figure 9-2 shows the mass balance of the experiments with proteins mixed with (a) starch-protein; (b) sunflower-protein; (c) linseed-protein. In the first diagram, an extra run is shown with 50-50 asparagine-glucose (asn-glucose) for comparison and the experiments with starch and sunflower oil in (d) and linseed oil in (e).

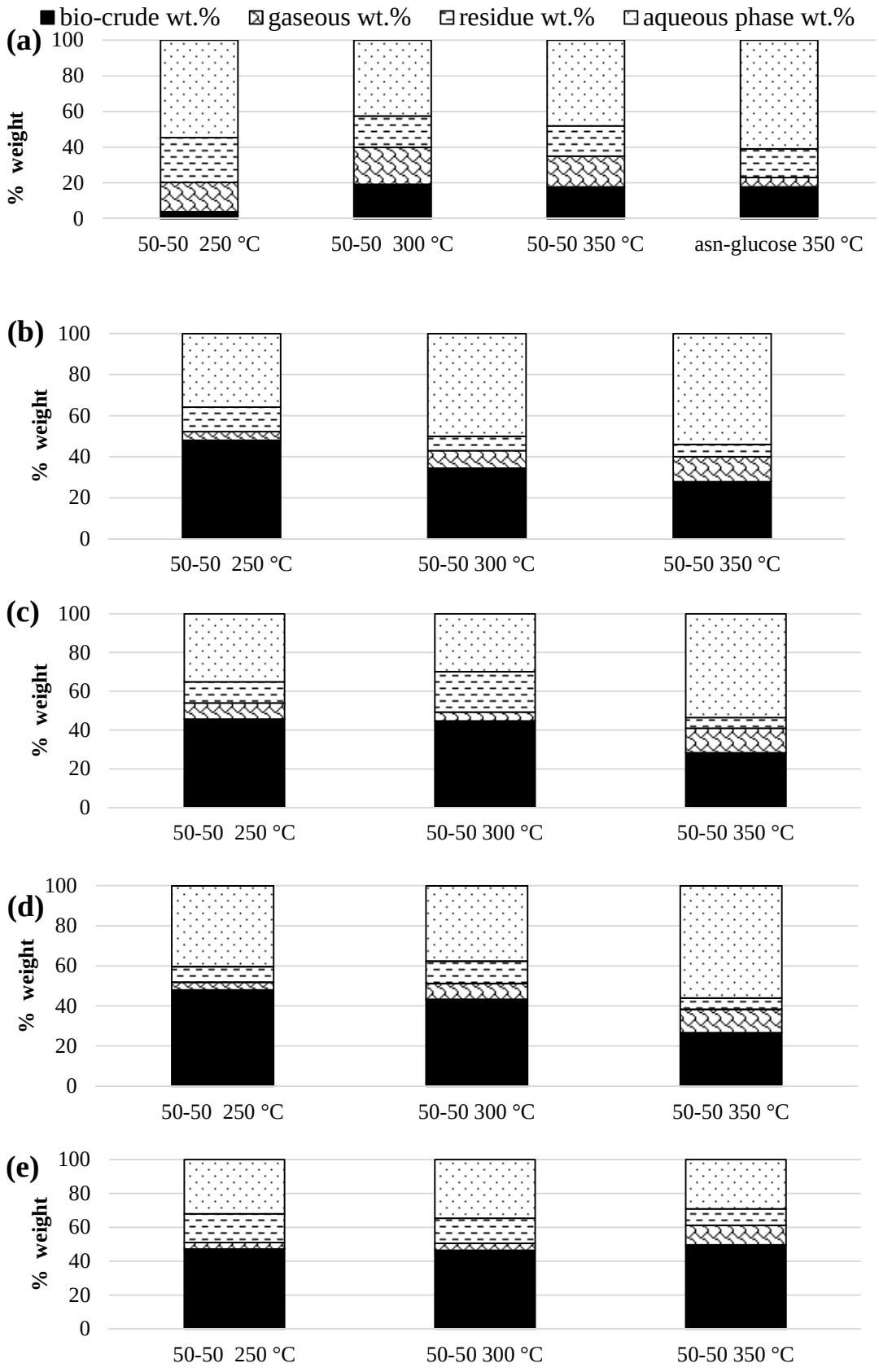

Figure 9-2: Mass balance (oil, gaseous, residue and aqueous phase) of binary mixtures: (a) carbohydrate-protein; (b) sunflower-protein; (c) linseed-protein (d) starch-sunflower; (e) starch-linseed.

For the mixture starch-protein (Figure 9-2 (a)), the residue yield decreases in relation to the temperature. Similar bio-crude yields are obtained between the experiment starch-protein and asparagine and glucose, although the aqueous phase yield is higher for the latter mixture. Minowa et al. [329] measured a constant increase of bio-crude yield with temperature using a combination of 70 % of glucose and 30 % of glycine. The authors explained that low temperatures were more selective for the production of chars which decomposed above 250 °C into bio-crude oil or secondary products in the aqueous phase.

For the mixture sunflower-protein and linseed-protein (Figure 9-2 (b) and (c)), the bio-crude yield reduces as the temperature increases from 250 to 350 °C. This is unexpected, as generally, the opposite trend is measured in the previous experiments for example in **Chapter 5**. Commonly, lipids are fractionated into the bio-crude yield and proteins into the aqueous phase. At 350 °C, the bio-crude yield is approximately 25 wt.% less than the lipids content probably resulting in the solubilisation of them in the aqueous phase either by formation of amides or possible due to saponification reactions. At room temperature, the solubility of stearic acid is negligible (0.4 mg/100 g of water at 25 °C), in contrast sodium stearate is completely soluble in water [332]. The aspect of the aqueous phase is different from the other samples; the water has a “viscous” and turbid appearance supporting the promotion of saponisation reaction which is more likely in alkali pH caused by the degradation of the protein [333]. This result confirms what has been discussed in the previous chapter where some fatty acids are lost with the stressed *P. ellipsoidea*.

For the mixture sunflower-starch (Figure 9-2 (d)), a reduction of the bio-crude yield is also observed. For linseed-starch, the temperature has a minor impact on the bio-crude yield compared to sunflower-starch. The residue yield decreases in relation to the temperature. The result is different suggesting that the unsaturated fatty acids could have an effect on the outcome of the yield.

Figure 9-4 represents the protein content against the different yield (a) bio-crude and aqueous (b) gaseous and residue for the mixture starch-protein, sunflower-protein and linseed-protein.

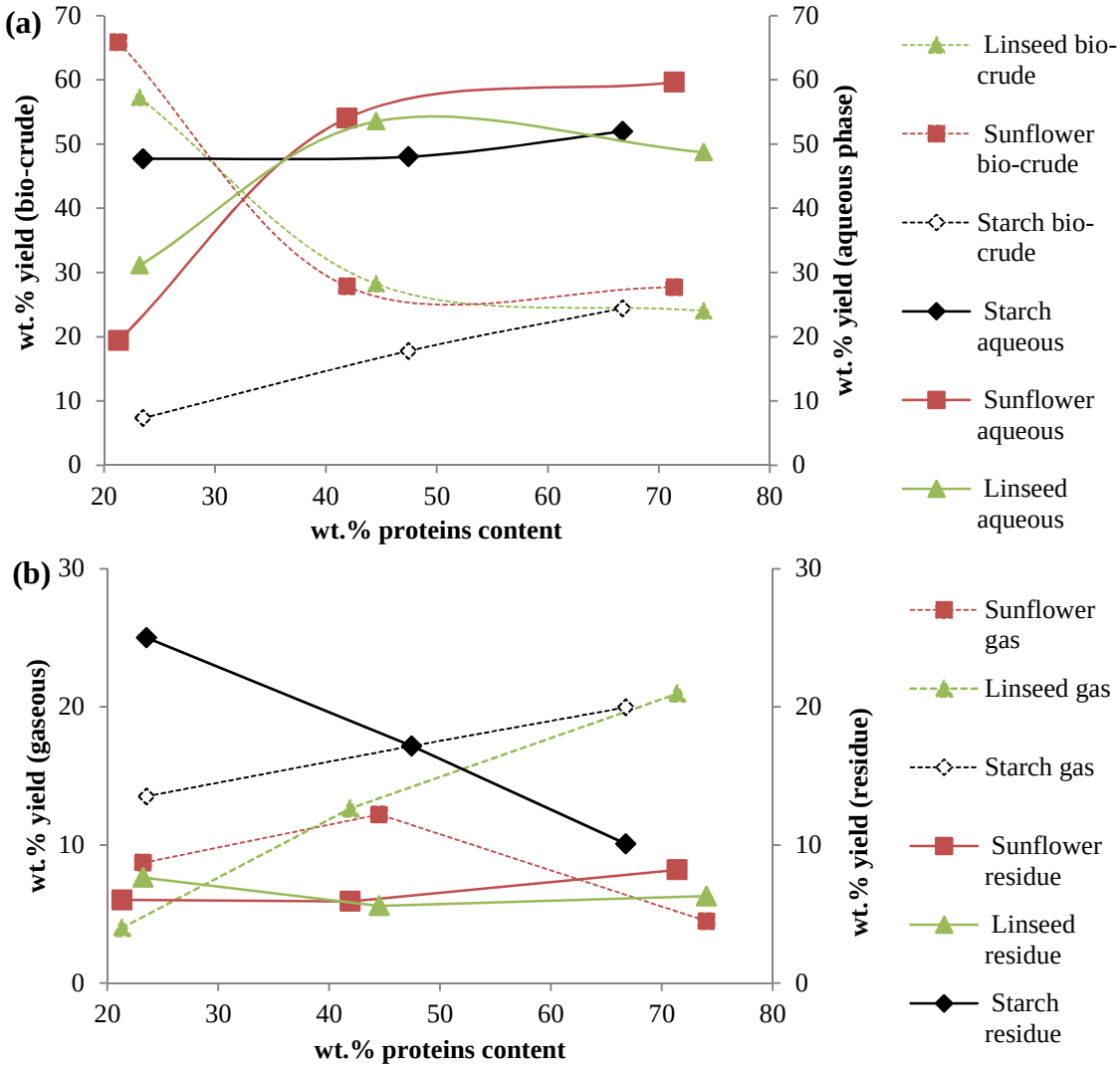

Figure 9-3: Plot of the different phase yield in relation of protein content the mixture starch-protein, sunflower-protein and linseed-protein where (a) is the bio-crude and the aqueous phase; (b) is the gaseous and the residue

For starch-protein, there is a clear pattern indicating that the bio-crude and gaseous yield increase in relation to the protein content. For 75 wt.% of starch at 350 °C, the mass balance is similar during the processing of pure starch and glucose where the degradation of product is enhanced towards the residue and gaseous fraction. The hydrolysis of starch has previously been shown to be faster than protein [2]. On the contrary, proteins favour the formation of bio-crude and aqueous phase fractions, however as explained in **Chapter 7**, the majority of molecules formed in the bio-crude contained nitrogen. Results are in agreement with Inoue et al. [334] where a mixture of cellulose and ammonia with different C/N ratio were processed at 300 °C. There was a relationship between the C/N with an increase of the bio-crude and aqueous phase yield and a decrease of the residue. For linseed-protein and sunflower-protein,

there is an inversion from the bio-crude yield to aqueous phase yield when the protein content increases. It is observed that at high concentration of lipids, the bio-crude yield is lower compared to the initial amount. For example, the per cent loss of the initial lipids for the 75 wt.% sunflower and linseed mixtures are 18.1 and 27.3 wt.% respectively.

Figure 9-4 represents the lipids content against the different yield (a) bio-crude and aqueous (b) gaseous and residue for the mixture sunflower-starch and linseed-starch.

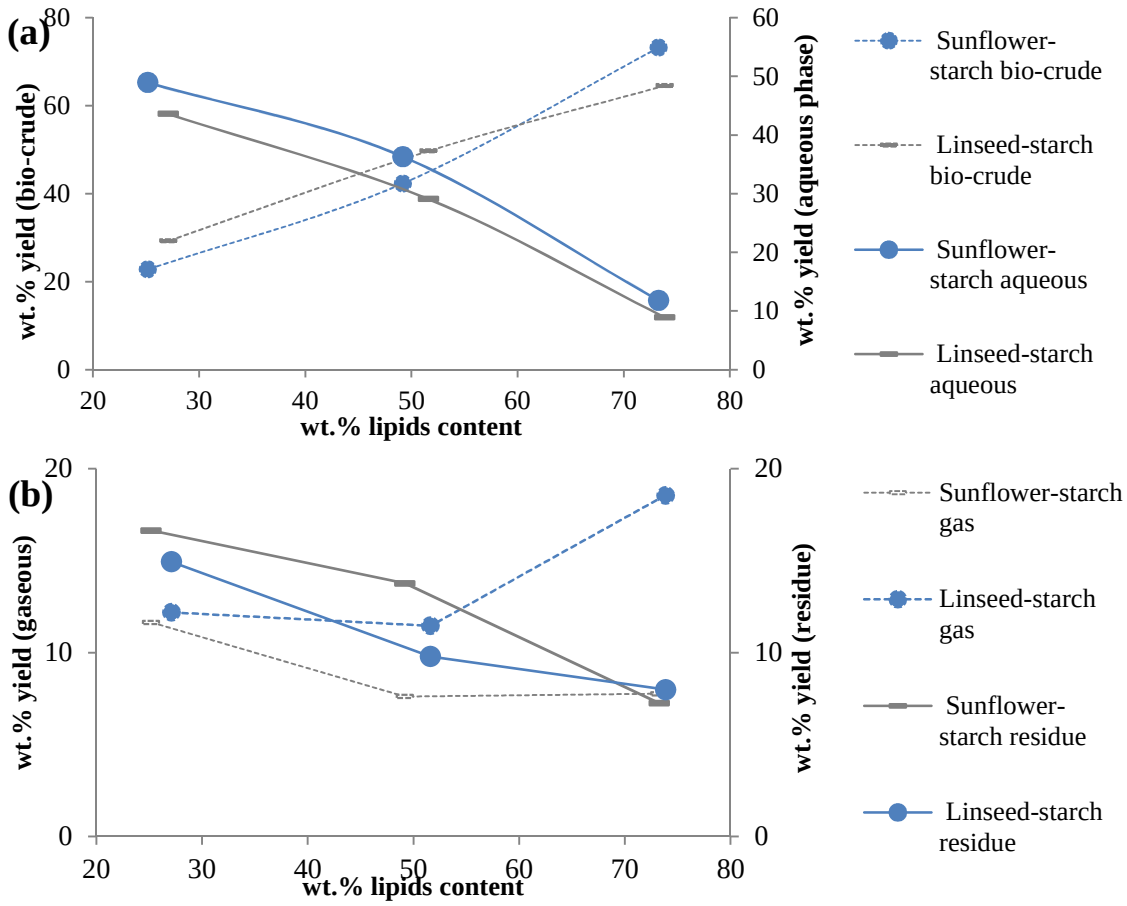

Figure 9-4: Plot of the different phase yield in relation of protein content the mixture sunflower-starch and linseed-starch where (a) is the bio-crude and the aqueous phase; (b) is the gaseous and the residue

For mixture sunflower-starch, linseed-starch and sunflower-proteins, the same trend is observed for the bio-crude and aqueous phase yields. The addition of sunflower oil from 50 wt.% (to 75 wt.%) lowers the formation of chars and increases the bio-crude yield. When 75 wt.% of linseed oil is used, a bio-crude yield of 64 wt.%

is achieved which implies that there are 12 wt.% of lipids lost. When sunflower and linseed oils were processed in **Chapter 5**, the yield of bio-crude was above 80 wt.%.

In conclusion, when carbohydrates are added, the residue yield is greater. As expected, more lipids enhance the bio-crude yield in contrast to proteins and carbohydrates where the opposite trend is observed. Some further investigations are required to explain why a decrease bio-crude yield is measured with temperature using sunflower-linseed and protein but also between sunflower-starch.

9.3.3 Bio-crude analysis

9.3.3.1 GPC analysis

The molecular size range is measured by gel permeable chromatography and is displayed in Figure 9-5 where (a) represents the mixture protein-starch where asp-glucose meant glucose-asparagine; (b) sunflower-proteins and (c) linseed-proteins. (d) sunflower-starch and (e) linseed-starch.

For the experiment starch-proteins (Figure 9-5 (a)), the formation of “heavy molecular weight” materials slightly increases in relation to the temperature. The reaction between glucose asparagine produce lower amount of “heavy molecular weight” materials and higher amount of smaller compounds (200 g/mol).

For the experiment sunflower-proteins and linseed-starch, (Figure 9-5 (b), (c)) an increase of the formation of oligomer materials is observed in relation to the temperature. In **Chapter 5**, especially with linseed oil, the high concentration of linolenic and linoleic acids enhanced the intra-cyclisation and the formation of cross linking compounds. For linseed-protein, the decrease of the fraction of “long chain” materials from 250 to 350 °C could indicate the formation of soap and amides soluble in the aqueous phase as explained previously. For sunflower-protein, the formation of “heavy molecular weight” materials decreases with the temperature contrary to linseed-protein.

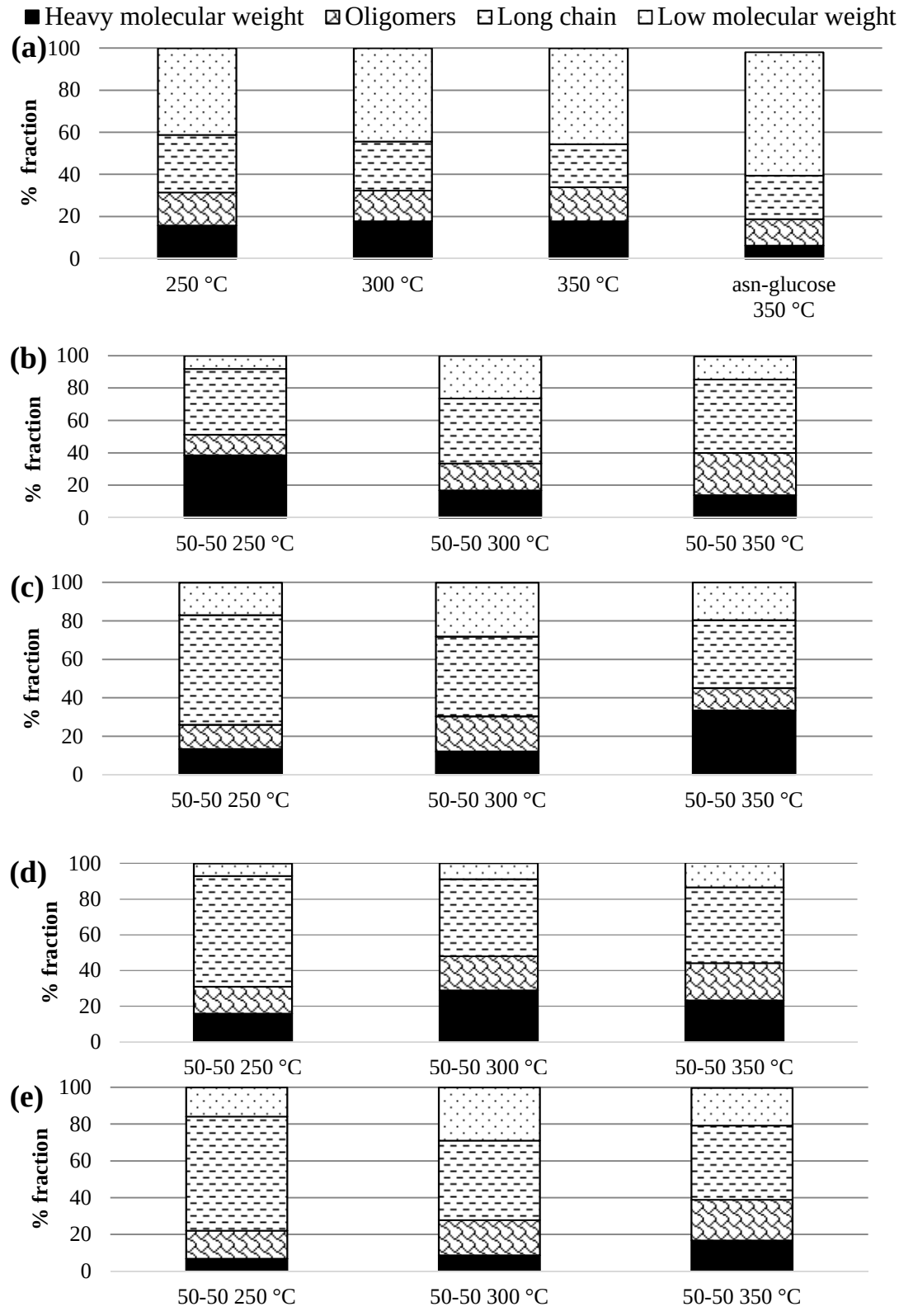

Figure 9-5: Different molecular weight fraction of the bio-crude oils of the different mixtures between (a) starch-protein, (b) sunflower-protein and (c) linseed-protein at different temperatures

Figure 9-6 represents the per cent of the different fraction in function of the protein content (a) “heavy molecular weight” and oligomers and (b) “long chain” and low molecular weight for the mixture starch-protein, sunflower-protein and linseed-protein.

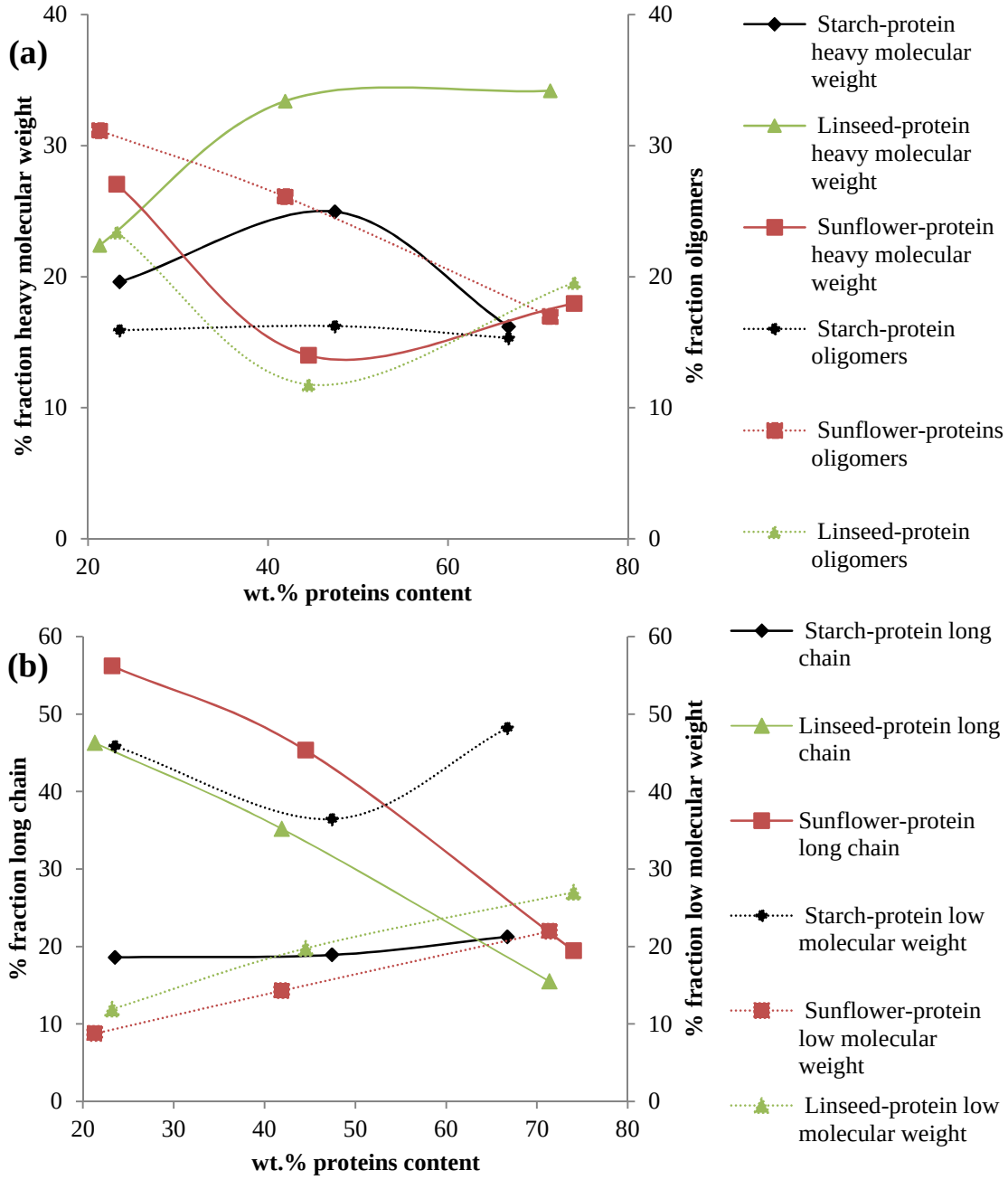

Figure 9-6: Plot of the molecular weight fraction in in relation of protein content the mixture starch-protein, sunflower-protein and linseed-protein where (a) is “heavy molecular weight” and oligomers; (b) is the “long chain” and low molecular weight

For sunflower-protein and linseed-protein, the “long chain” material decreases in relation to the protein content. For linseed-protein, the formation of “heavy molecular weight” materials increases with higher protein content. There is no clear

effect on the molecular weight when starch is mixed with soya protein. Finally, when the lipids proportion is dominant more materials between 200 to 600 g/mol are present whereas for proteins, more materials below 200 g/mol are present.

Figure 9-7 represents the per cent of the different molecular weight fraction in function of the lipids content (a) heavy molecular weight and oligomers and (b) long chain and low molecular weight for the mixture sunflower-starch and linseed-starch.

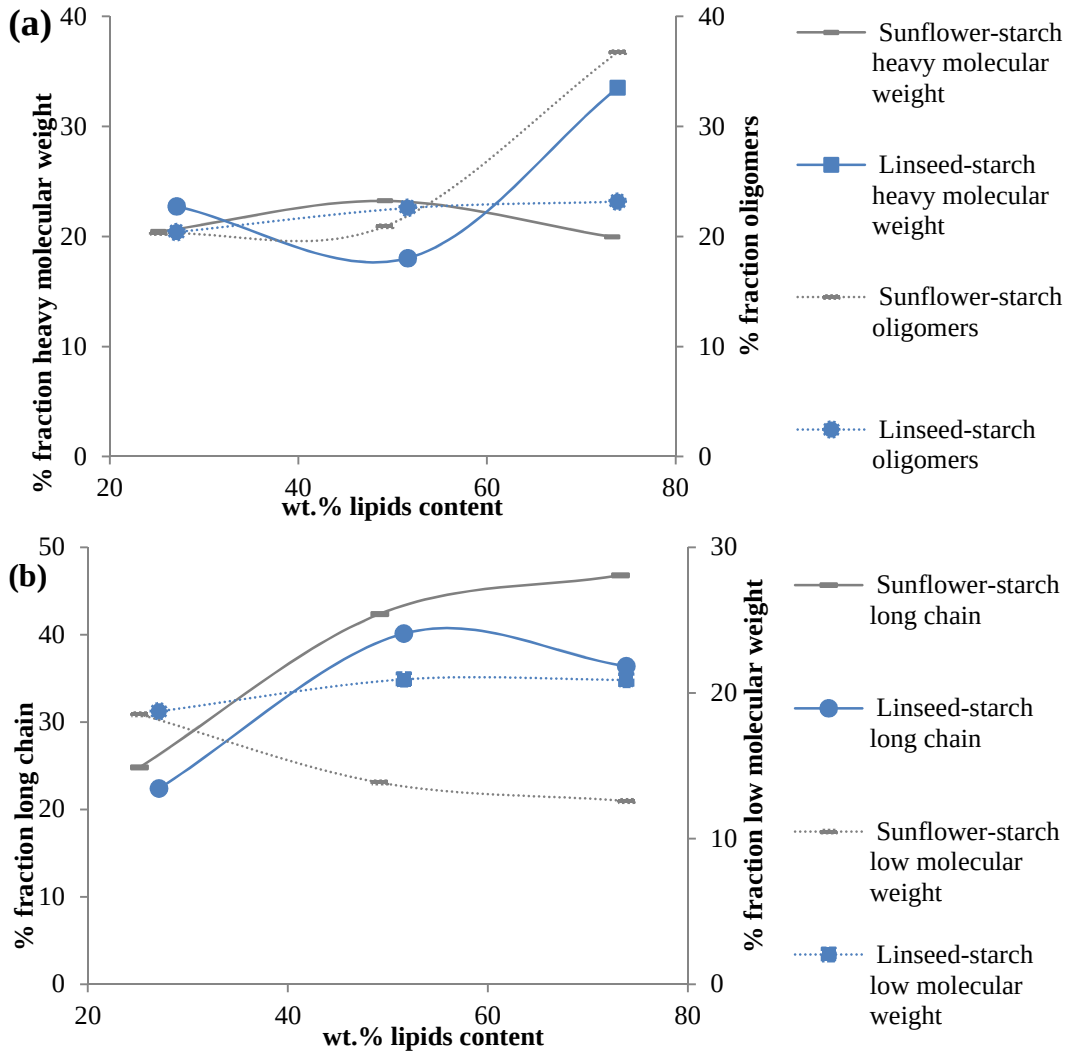

Figure 9-7: Plot of the molecular weight fraction in in relation of the lipids content the mixture sunflower-starch and linseed-starch where (a) is "heavy molecular weight" and oligomers; (b) is the "long chain" and low molecular weight

For the experiment sunflower-starch, similar to the protein mixture, the fraction of the "long chain" and the oligomers materials increases in relation of the lipids content. For the experiments in **Chapter 6,** starch and glucose mainly contained low molecular weight materials. Thus, oligomers production is mainly induced by lipids.

To summarise, the analysis of the bio-crude oils allows us to deduce that linseed oil enhances the formation of "heavy molecular weight" materials with higher protein content. It again emphasises that biomasses containing high level of polyunsaturated fatty acids is not suitable for hydrothermal liquefaction. In order to have more detailed chemical composition of the bio-crude oils, results obtained by GC-MS analysis will be shown in the following section.

9.3.3.2 GC-MS analysis

In this section, some example chromatograms will be presented with peak identification. The first chromatogram (Figure 9-8) represents the bio-crude oil of 75 % soya protein with starch. Identified molecules are listed in Table 9-2.

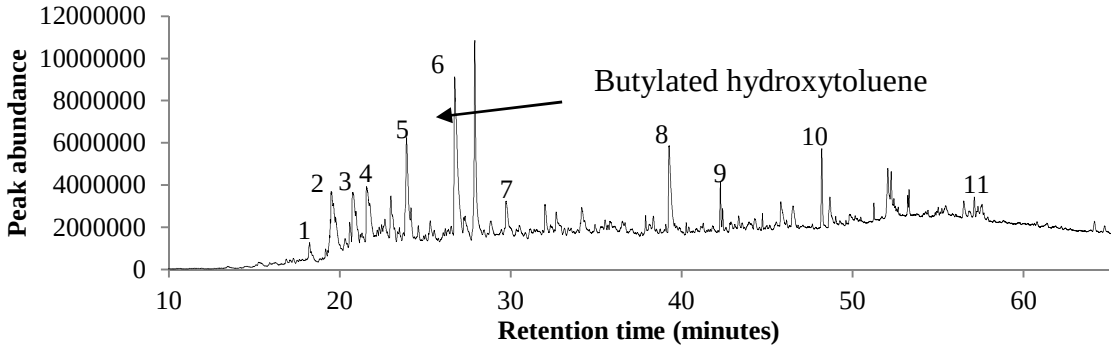

Figure 9-8: GC-MS chromatogram of the sample 75-25 protein-starch in DCM

Table 9-2: Peaks identification in the GC-MS the sample 75-25 protein-starch

Number	Retention time (minutes)	Compounds
1	19.4	2-pyrrolidinone
2	19.5	phenol
3	20.7	1-ethyl-2-pyrrolidinone
4	21.5	4-methyl-phenol
5	23.8	1-ethyl-6-methyl-piperidinone
6	26.7	butyl-2-pyrrolidinone
7	29.7	6-methyl-indole
8	39.2	(1-ethyl-2 pyrrolidinyl)-methanol
9	42.2	cyclopropaneoctanoic acid
10	48.2	1-methyl-9H-pyridoindole
11	57.0	4,5,6,7-tetramethyl-2H-isoindole

Figure 9-9 contains some chemical structures of molecules identified during the processing of the mixture of starch and proteins.

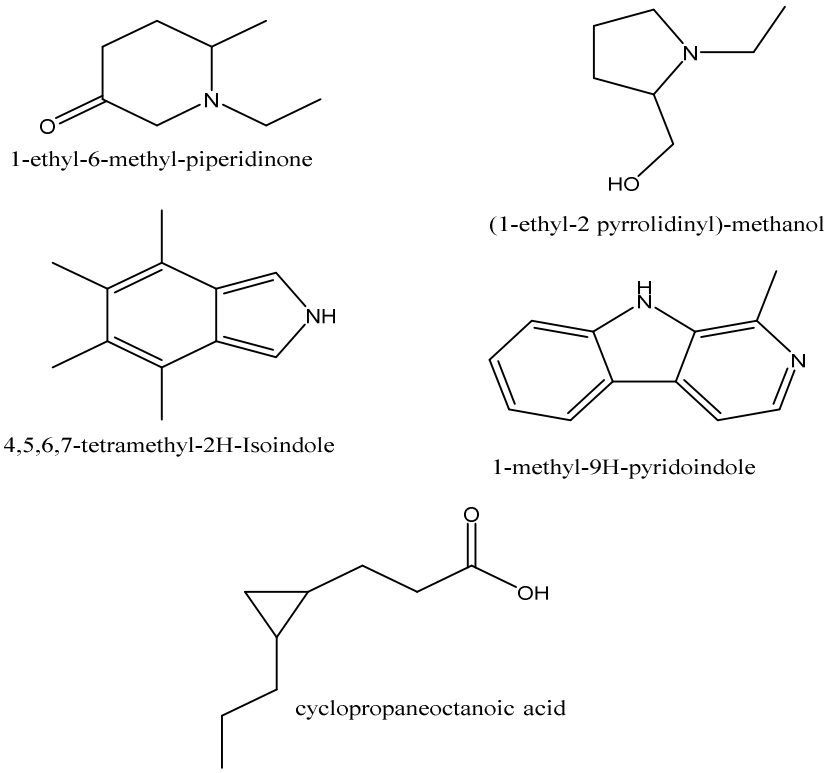

Figure 9-9: Chemical structures of some compounds found in the bio-crude during the processing of starch and proteins

In the bio-crude from these experiments, heterocyclic compounds mainly are identified, for instance methyl-phenol, pyrrolidinone, piperidinone, indole etc. DKP molecules such as cyclo-(L-leucyl-L-phenylalanyl), pyrrolo-pyrazine-1,4-dione, hexahydro-3-(phenylmethyl) are identified at 250 °C. These compounds are characteristic of the degradation of proteins explained in **Chapter 7**.

3,3-diethoxy-2,3-dihydro-1H-pyrrole-4-carboxylic acid observed at 250 and 300 °C could be an indicator of the Maillard reaction [277]. These molecules containing pyrrole can form polymers with a molecular weight higher to 1000 g/mol called melanoidins. More complex oxygenated molecules, compared to the run with starch are detected, for example 2,4,6-cycloheptatriene-1-one, oxahomoadamantan-5-one (two cyclohexanes link together), some similar to the group of sterols and one derivative of cholesterol. For the reaction between glucose and asparagine, the most abundant compound is 2,3,5-trimethyl-indole. Overall, compounds produced between carbohydrates and proteins are complex and relatively stable.

Figure 9-10 shows on example of the chromatogram from the reaction of linseed and soya protein at 250 °C, molecules identified are listed in Table 9-3. The

following compounds are found during the processing of sunflower and protein at different temperatures: ketones (undecanone), carboxylic acid (non-7-enoic acid), and amides (oleic diethanolamide). The majority of the compounds contained a long chain. The majority of amides identified in this study are formed between oleic and stearic acid chains. Nevertheless, (1-oxo-9,12,15-octadecatrienyl)-pyrrolidine is also identified which is produced between a linolenic acid and a pyrrolidine.

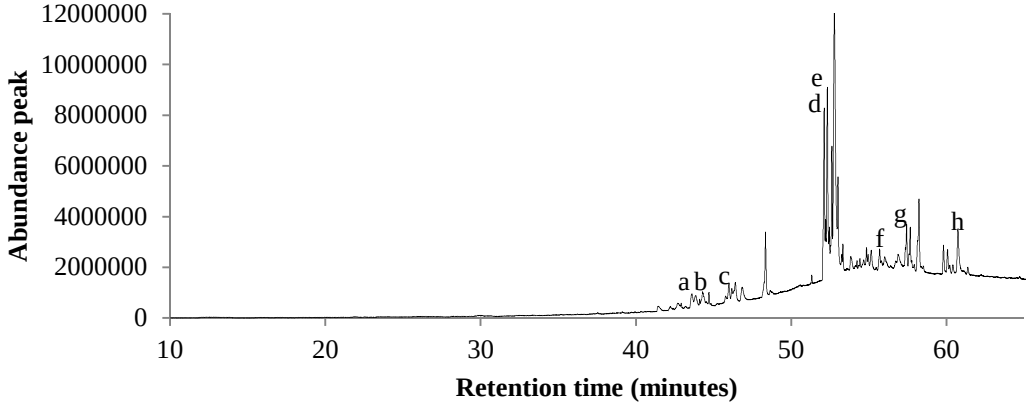

Figure 9-10: GC-MS chromatogram of linseed-protein at 250 °C

Table 9-3: Peaks identification in the GC-MS linseed-protein at 250 °C

Number	Retention time (minutes)	Compounds
a	43.6	3,6-diisopropylpiperazin-2,5-dione
b	44.3	3,3-diethoxy-2,3-dihydro-1H-pyrrole-4-carboxylic acid
c	46.0	3,6-bis(2-methylpropyl)-2,5-piperazinedione
d	52.2	9-octadecenamide
e	52.5	N,N-dimethyl-9-octadecenamide
f	55.1	1-(1-oxo-9-octadecynyl)-pyrrolidine
g	57.6	oleic diethanolamide
h	60.7	1-(1-oxo-9,12,15-octadecatrienyl)-pyrrolidine

Figure 9-11 shows the different concentration of FAME at different proportions with sunflower and linseed oil at 350 °C.

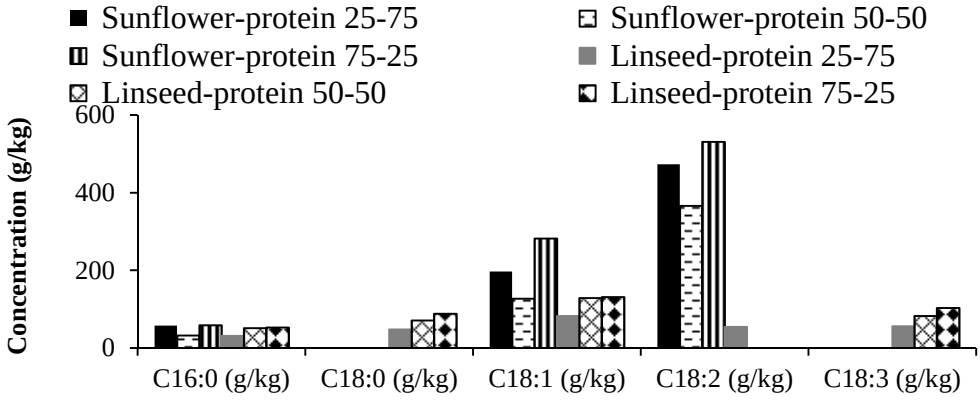

Figure 9-11: FAME of the different mixture composition between sunflower and linseed with soya protein

For sunflower-protein, the FAME profile indicates that linoleic acid is the most abundant fatty acid, contradicting the result in **Chapter 5** where linoleic acid from sunflower oil was completely degraded at 350 °C. For linseed-protein, lower linoleic and linolenic acids is observed in the bio-crude. For linseed-protein, the ratio between the oleic acid (9-octadecenoic acid) and the amide form (using the area) increases from 4 to 13.5 between the 25 % and the 75 wt.% mixtures. For sunflower-protein, the ratio is greater, from 15 to 18, suggesting that fatty acids are in larger proportion than the corresponding amides as the concentration of oleic acid is higher in sunflower oil. Yet, this is a semi-quantitative measurement only judged using the peak areas.

Table 9-4 lists the main compounds identified. Most of the compounds with the mixture of vegetable oils (linseed and sunflower) and starch are long chain compounds or fatty acids.

The compounds are similar to those from processing lipids alone; compounds from starch are limited and are primarily soluble in the aqueous phase. Surprisingly, some FAMEs are detected whereas no esterification is performed in the bio-crude oil, as protonation is more likely to occur under hydrothermal liquefaction, the formation of the ester is possible under this condition [94]. 9-(o-propylphenyl)-nonanoic acid is an example of the internal cyclisation of linolenic acid. Dihydro-5-tetradecyl-2-(3H)-furanone is a common molecule produced from formic acid and a fatty acid. Formic acid could originate from the degradation of starch. This compound was also identified in **Chapter 5** with the experiment of formic acid and sunflower oil.

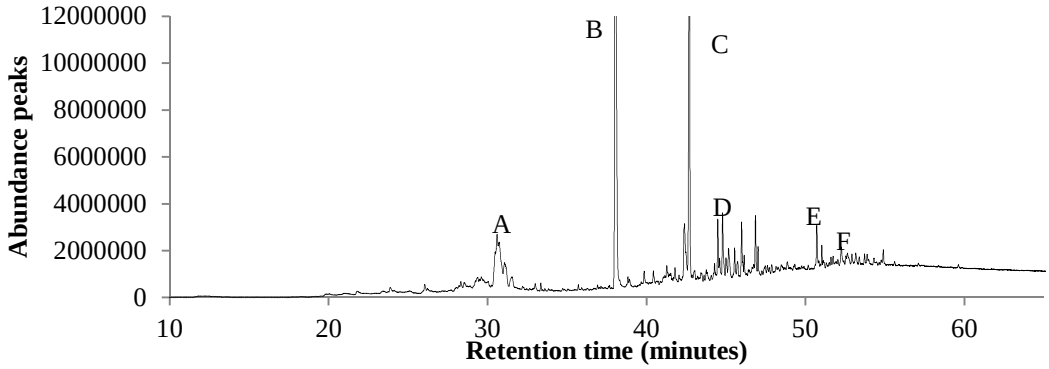

Figure 9-12: GC-MS chromatogram of the HTL experiment between linseed-starch (75-25) at 350 °C

Table 9-4: Peaks identification in the GC-MS linseed-starch at 350 °C

Number	Retention time (minutes)	Compounds
A	30.6	8-heptadecene
B	33.0	hexadecanoic acid, methyl ester acid
C	42.7	octadecanoic acid, methyl ester
D	44.8	9-(o-propylphenyl)-nonanoic acid
E	50.7	dihydro-5-tetradecyl-2(3H)-furanone
F	52	1-(1-methyl-2-propenyl)-4-(2-methylpropyl)-benzene

Moreover, for sunflower-starch, less aliphatic compounds are found, instead aldehydes such as E-14-hexadecenal and Z,Z-10,12-hexadecadienal and other compounds such as 2-pentyl-phenol and phthalic acid. Cyclohexylmethyl-2-phenylethyl ester (observed with the run 50-50 sunflower-starch at 350 °C) could be produced between carbohydrate and lipids. The effect of carbohydrate on lipids is low compared to protein.

To conclude, the majority of identified compounds are produced by condensation reaction and some of these compounds are similar from the molecules produced from the processing of microalgae.

9.3.3.3 Elemental analysis

Table 9-5 includes the elemental value, the energy content and energy recovery. For the energy recovery it should be pointed out that for starch and proteins the initial energy content is calculated according to mixture of unprocessed sample otherwise the other mixture samples are determined by doing the average value in function of the raw energy content of mixtures.

For the mixture of starch-protein, the nitrogen content is constant for all the conditions used (for the three temperatures). Minowa et al. [329] observed a slight increase of the nitrogen content from 250 to 350 °C for short reaction time. Nevertheless, for glucose-asparagine, the nitrogen content in the bio-crude oils is lower, suggesting this element is decomposing to a different phase. In the case for linseed-protein, there is a reduction of the nitrogen content with temperature from 3.4 to 2.4 wt.%. For the mixture sunflower-protein, the nitrogen content is doubled with 75 wt.% of protein compared to 50 wt.%.

For the mixture of sunflower-protein, the carbon content decreases in relation to the temperature; it explains why the highest energy content is achieved at 250 °C. For the mixture linseed-protein, the carbon content is highest at 300 °C yielding a good energy recovery. The presence or not of double bonds in fatty acids could have an impact on the carbon and nitrogen contents in the bio-crude. For the mixture sunflower-starch and linseed-starch, vegetable oils enhance the carbon and hydrogen contents and yield a better energy content and energy recovery. As for in **Chapter 5** for linseed oil, the hydrogen content decreases for linseed-starch in relation to the temperature and the carbon content is at its highest at 300 °C for sunflower-starch similar to the experiment with sunflower oil at the same temperature. For the processing carbohydrates in **Chapter 6**, for example of glucose, the carbon content increased with temperature.

Table 9-5: Nitrogen, carbon, hydrogen, sulphur and oxygen content in the bio-crude oils as received, energy content (Dulong and Milne) and % energy recovery for experiments for different mixtures at different temperatures and proportions

	N wt. %	C wt. %	H wt. %	O wt. %	Dulong HHV (MJ/kg)	H/C	O/C	Milne HHV (MJ/kg)	% Energy recovery
Starch-protein									
250 °C	6.3	76.2	8.5	9.0	36.4	1.3	0.1	35.3	8.6
300 °C	6.3	66.5	7.3	19.8	29.4	1.3	0.2	29.0	34.5
350 °C 50-50	6.0	74.0	7.9	12.1	34.1	1.3	0.1	33.3	37.0
25-75	6.3	76.2	8.5	9.0	36.4	1.3	0.1	35.3	48.9
75-25	7.1	81.0	9.0	2.9	39.7	1.3	0.0	38.1	20.6
asn-glucose	1.0	67.4	9.5	22.1	32.4	1.7	0.2	32.6	45.1
Sunflower-protein									
250 °C	3.0	83.0	12.4	1.7	45.5	1.8	0.0	44.0	72.2
300 °C	3.6	78.3	11.6	6.5	41.9	1.8	0.1	40.7	47.7
350 °C 50-50	2.0	74.6	11.4	11.9	39.4	1.8	0.1	38.7	36.3
25-75	4.1	72.3	10.6	12.9	37.3	1.8	0.1	36.5	35.4
75-25	1.7	73.7	11.5	13.1	39.0	1.9	0.1	38.4	75.9
Linseed-protein									
250 °C	3.4	62.5	10.1	24.0	31.3	1.9	0.3	31.2	47.1
300 °C	3.1	81.1	11.7	4.2	43.3	1.7	0.0	42.0	63.8
350 °C 50-50	2.4	78.5	5.5	13.6	32.0	0.8	0.1	32.0	29.7
25-75	3.7	71.0	9.9	15.4	35.3	1.7	0.2	34.8	31.9
75-25	1.7	75.5	5.6	17.1	30.5	0.9	0.2	30.8	51.2
Sunflower-starch									
250 °C	0.0	67.6	11.2	21.2	35.1	2.0	0.2	35.2	67.6
300 °C	0.0	70.7	11.4	17.9	36.9	1.9	0.2	36.8	64.1
350 °C 50-50	0.3	62.3	8.8	28.6	28.6	1.7	0.3	29.3	48.5
25-75	0.0	69.8	9.4	20.8	33.3	1.6	0.2	33.6	40.7
75-25	0.0	72.0	11.7	16.3	38.1	1.9	0.2	37.8	89.1
Linseed-starch									
250 °C	0.0	72.4	11.5	16.1	38.0	1.9	0.2	37.8	71.5
300 °C	0.0	67.9	10.6	21.6	34.2	1.9	0.2	34.4	63.2
350 °C 50-50	0.0	68.7	10.0	21.3	33.7	1.7	0.2	33.9	66.7
25-75	0.0	61.6	8.9	29.4	28.3	1.7	0.4	29.1	44.4
75-25	0.0	67.9	9.2	22.9	32.1	1.6	0.3	32.5	84.0

9.3.4 Analysis of the residues

Table 9-6 lists the elemental analysis, heating content and energy recovery of the residues (when available).

Table 9-6: Nitrogen, carbon, hydrogen, sulphur and oxygen content in the residue, energy content (Dulong and Milne) and % energy recovery for experiments for different mixtures at different temperatures and proportions as dried basis

	N wt. %	C wt. %	H wt. %	O wt. %	Dulong HHV (MJ/kg)	H/C	O/C	Milne HHV (MJ/kg)	% Energy recovery
Starch-protein									
250 °C	7.0	71.6	6.1	15.3	30.2	1.0	0.2	29.7	22.2
300 °C	5.9	69.5	5.8	18.8	28.5	1.0	0.2	28.3	18.9
350 °C 50-50	7.2	74.9	6.0	11.8	31.8	1.0	0.1	31.0	11.6
25-75	5.0	65.0	5.2	24.8	25.0	1.0	0.3	25.4	13.6
75-25	6.0	69.8	5.7	18.5	28.4	1.0	0.2	28.2	29.0
asn-glucose	8.2	69.5	4.7	17.6	27.1	0.8	0.2	26.7	6.8
Sunflower-starch									
250 °C	-	69.5	4.9	25.7	25.8	0.8	0.3	26.9	17.4
300 °C	-	73.9	5.7	20.4	29.5	0.9	0.2	30.1	17.4
350 °C 50-50	-	75.0	5.5	19.4	29.8	0.9	0.2	30.4	11.6
25-75	-	84.8	5.0	10.1	34.0	0.7	0.1	34.2	27.2
75-25	-	-	-	-	-	-	-	-	-
Linseed-starch									
250 °C	-	65.4	4.5	30.0	23.2	0.8	0.3	24.5	7.2
300 °C	-	71.4	5.2	23.4	27.4	0.9	0.2	28.3	12.3
350 °C 50-50	-	62.3	8.8	28.6	28.6	1.7	0.3	29.3	15.8
25-75	-	76.3	6.2	17.5	31.4	1.0	0.2	31.9	28.1
75-25	-	72.5	4.6	22.9	26.9	0.8	0.2	27.8	6.2

For the char of glucose and asparagine, higher nitrogen content is measured compared to the mixture starch-protein explaining why the nitrogen content in the bio-crude is low for the first mixture. Lower nitrogen content is measured for the char from starch-protein at 300 °C compared to the other temperatures. Minowa et al. [329] observed that temperature had a minor impact on the nitrogen content in the char.

For the char produced from the processing of sunflower-starch and linseed-starch, the energy content (HHV) increases with the temperature. For sunflower-starch, more specifically, the carbon content increases in relation of the temperature in opposition to the oxygen content. For linseed-starch, higher hydrogen content is measured compared to sunflower-starch. The difference could be caused by a higher saturation for linseed oil. The energy recovery is reduced with temperature for sunflower-starch similar to the residues from carbohydrates in **Chapter 6**.

Figure 9-13 shows the three curves of the weight loss and the DTA for starch-protein; sunflower-starch and glucose asparagine chars. The thermogravimetric analysis indicates that starch-protein and glucose-asparagine contains 47 wt.% of volatiles whereas sunflower-starch contains a lower level with 38 wt.%. The other part of the char is combusted (up to 60 %) above 900 °C. The results imply that residues (chars) are stable under hydrothermal conditions. For starch-protein, the DTA shows a shoulder at 280 °C and a main peak around 410 °C.

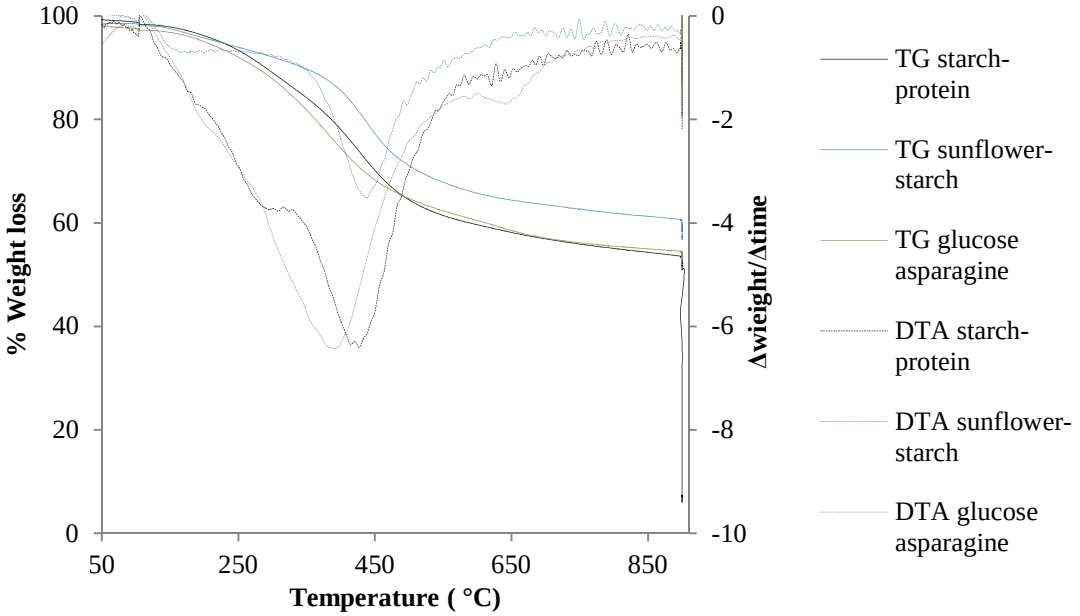

Figure 9-13: TG and DTA of the residue of the processed residue of the mixture: protein-starch; sunflower-starch; glucose-asparagine

To summarise, for protein-starch, the elemental analysis is similar between the bio-crude and the residue. The experiment using glucose and asparagine yields more nitrogen in the char which is probably due to the Maillard reaction. Compared to the elemental analysis of the starch in **Chapter 6**, chars from the sunflower-starch, higher hydrogen content is achieved. Finally, the formation of residue is a drawback in

particular when experiments will be carried out in continuous reactor as plugging could occur.

9.3.5 Aqueous phase analysis

The concentrations are listed in the Appendix 1, section 321. page A-5. For the sample mixed with soya protein (starch, sunflower and linseed oil), in general, when the protein content increases from 25 to 75 wt.%, the ammonium compound concentration increases in the aqueous phase. For the processing of starch-protein, an increase of ammonium compound concentration is measured from 250 to 350 °C. Minowa et al. [329] also mentioned an increase of ammonium with temperature. For the glucose-asparagine mixture, less ammonium compound concentration is detected compared to the starch mixture as probably different compounds are produced such as nitrogen heterocyclic compounds. For linseed-protein mixture, the highest concentration is measured at 250 °C.

There is a linear relationship between the protein content and the ammonium compound in particular with starch-protein with R^2 of 0.97 and with linseed-protein a good coefficient R^2 of 0.99; the curve is shown in Figure 9-14. The equations for starch-protein are found in equation 9-1 and sunflower-protein in Equation 9-2. Yet, these curves are linear from 25 to 75.

$$y = 225.2x - 5320.7$$ **Equation 9-1**

$$y = 107.1x - 214.2$$ **Equation 9-2**

When, the first equation is used for *Chlorella*, a concentration of 6370 ppm is calculated using the average value from the both formulas, which is close to the experimental concentration 6284 ppm. Close value are also found for the non-stressed *P. ellipsoidea* with 5208 ppm compared to 5051 ppm. For the stressed *P. ellipsoidea*, only the first formula from starch-protein give a close value 309.3ppm compared to the experimental concentration. The formation of amides could suggest why a lower concentration was measured. However, these models do not work to predict the ammonium concentration of *Spirulina*. It implies that for these algae the formation of ammonium compound is caused by other factors than proteins, carbohydrates and lipids such as chlorophyll, nucleotides, but also the cell wall strength as described D. López Barreiro et al. [134]. In **Chapter 8**, it was deduced that the stressed *P.*

ellipsoidea had lower cell wall compared to *Spirulina*, this could explain the difference.

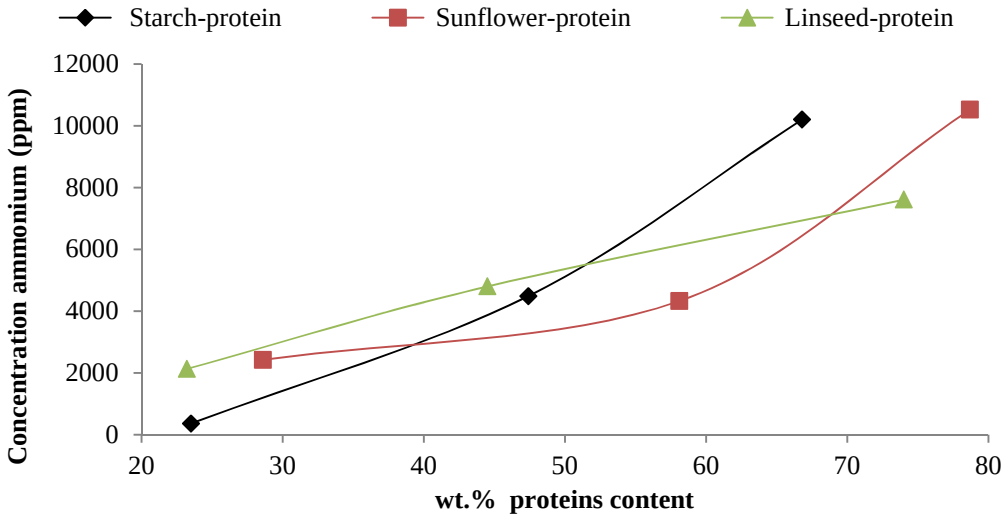

Figure 9-14: Concentration of ammonium versus the protein content

For the samples mixed with starch (proteins, sunflower and linseed), the TOC concentration decreases in relation to the temperature. A pH value of 3 from sunflower-starch and linseed-starch is determined suggesting that the processed water contains a majority of acidic species. For the mixtures sunflower-protein and linseed-protein, the TOC concentration is higher at 300 °C where the pH of aqueous phase is in the mild acid (pH 6-7) region.

Peterson et al. [314] indicated that the main product in the aqueous phase produced by the Maillard reaction was pyruvic aldehyde and ethanolamine. Kruse et al. [278] mentioned that the concentration of phenol increased with temperature. Sinag et al. [192] measured more acetic acid and acetaldehyde during the decomposition of baby food close to the supercritical water. To summarise, a relationship is observed with the protein content and ammonium compound concentration yet this model does not match the results obtained from some microalgae.

9.3.6 Carbon and nitrogen mass balance

In order to have a clear picture of the degradation of the products, the mass balance is calculated for carbon and the nitrogen. The results are listed in Table 9-7. An average carbon and nitrogen value was calculated from the percentage of the pure raw materials for sunflower, linseed with starch and proteins.

Table 9-7: Carbon and nitrogen mass balance for the aqueous, bio-crude and remaining phases for the experiments using mixtures at different temperatures and conditions

	% C aqueous	% C bio-crude	% C residue	% C gas	% N aqueous	% N bio-crude	% N residue	% N gas
Starch-protein								
250 °C	31.7	6.8	41.8	19.7	30.1	3.5	25.7	40.7
300 °C	25.4	29.4	28.1	17.1	41.3	17.7	15.0	26.0
350 °C 50-50	8.6	30.3	29.4	31.8	47.4	15.5	17.9	19.2
25-75	23.1	43.1	14.4	19.4	73.5	15.0	4.9	6.6
75-25	8.4	13.7	42.9	34.9	7.8	15.9	3.7	72.6
asn-glucose	18.6	27.6	10.4	43.4	6.9	1.8	1.2	90.1
Sunflower-protein								
250 °C	33.4	64.4	-	2.2	28.7	13.8	-	57.5
300 °C	42.8	43.6	-	13.6	35.5	17.4	-	47.0
350 °C 50-50	32.5	33.6	-	33.8	43.5	9.7	-	46.7
25-75	30.3	32.4	-	37.3	73.5	13.7	-	12.8
75-25	7.4	72.1	-	20.5	48.5	16.1	-	35.4
Linseed-protein								
250 °C	29.0	46.2	-	24.8	55.5	14.6	-	29.9
300 °C	34.6	58.8	-	6.7	30.7	17.5	-	51.7
350 °C 50-50	33.4	35.9	-	30.7	48.1	9.7	-	42.2
25-75	28.1	30.4	-	41.5	50.7	13.1	-	36.2
75-25	8.5	64.3	-	27.2	41.1	15.5	-	43.5
Sunflower-starch								
250 °C	9.9	58.3	9.1	22.7	-	-	-	-
300 °C	8.7	55.0	14.3	22.0	-	-	-	-
350 °C 50-50	6.3	47.4	18.2	28.1	-	-	-	-
25-75	6.2	33.8	19.7	40.3	-	-	-	-
75-25	3.0	82.0	8.2	6.9	-	-	-	-
Linseed-starch								
250 °C	13.2	53.0	21.1	12.6	-	-	-	-
300 °C	9.9	67.6	19.6	2.9	-	-	-	-
350 °C 50-50	6.8	70.1	13.2	10.0	-	-	-	-
25-75	5.1	44.2	26.9	23.8	-	-	-	-
75-25	5.9	97.0	0.0	-2.9	-	-	-	-

For the experiments of starch-protein and sunflower-protein, the nitrogen fraction in the aqueous phase increases in relation to the temperature. Contrary to the experiment for linseed-protein, where there is no clear trend with the nitrogen fraction and the temperature. When the mixture contains 75 wt.% of protein, the majority of the nitrogen fraction is contained in the aqueous phase. This observation was the same for protein and microalgae with low lipid content in **Chapter 7** and **8**. The opposite is observed with 75 wt.% starch, the nitrogen fraction is more prominent in the gaseous phase. Interestingly, the nitrogen fraction in the bio-crude is higher with 75 wt.% of sunflower oil compared to the mixture with 50 wt.% confirming the formation of amides.

For experiments with starch (starch-protein, sunflower-starch and linseed-starch), the carbon fraction is reduced in the aqueous phase with temperature. Meanwhile, the carbon fraction at 350 °C is more prevalent in the bio-crude oils and in the residue. For sunflower-starch, a decrease of the carbon fraction is noticed in bio-crude. For the processing of starch in **Chapter 6**, lower carbon fraction is observed in the residue as the temperature increased. Increasing the amount of lipid from 25 to 75 wt.% enhances the fractionation of carbon toward the bio-crude oil to around 80 wt.%. There is no obvious explanation for the variation among the two vegetable oils. When starch is added to other components the bio-crude yield is higher than alone. For the sunflower-protein experiments, with larger protein content, the carbon fraction is more predominant in the aqueous phase. The carbon fraction using glucose and asparagine is largest in the bio-crude oil and in the aqueous phase compared to the mixture starch-protein. Minowa et al. [329] observed a transfer of carbon fraction from the solid residue to the bio-crude oil and the aqueous phase during the processing of glucose and glycine; here it was unclear whether this trend occurred.

It is deduced from the results of the binary mixture experiment that lipids played a major role in the formation of bio-crude.

- Proteins and carbohydrates favour the formation of aqueous compounds and residue phase. The protein increases slightly the formation of “heavy molecular weight” materials when linseed oil is mixed with soya protein. Interestingly for sunflower-protein, the fraction of oligomers decreases with higher proteins content, furthermore more linoleic acid is observed compared to the run alone.
- The mixture of carbohydrate and protein form melanoidin compounds which enhance the complexity and the viscosity of the oil. The bio-crude from the experiment between glucose and asparagine contains more nitrogen content in the char compared to the bio-crude oil.
- A linear relationship was elucidated between the formation of ammonium compound and the amount of protein and carbohydrates.
- On the whole, results with mixtures are coherent with the experimental results for starch, sunflower and soya proteins. It implied similar trends with the mass balance and elemental analysis.

9.4 Synthetic of *Chlorella* and *P. ellipsoidea* mixture

9.4.1 Mass balance yield

In this section, two ternary mixtures were prepared similar to *Chlorella* and *P. ellipsoidea.* The elemental composition is included in Table 9-8. Figure 9-15 represents the diagram of the mass balance yield of the different phases with corresponding (a) mixture stressed *P. ellipsoidea* and (b) mixture *Chlorella*. The last diagram included results regarding the simple model compounds mixture. In this section, the metal doped zeolites were not use as only the interactions between the three components were studied. HZSM-5 was only used as comparison with the run in water.

Table 9-8: Elemental composition of the raw mixtures and % composition in proteins, carbohydrate and lipids as dried basis

	N wt. %	**C wt. %**	**H wt. %**	**O wt. %**	**HHV (MJ/kg)**	**Proteins wt.%**	**Lipids wt.%**	**Carbohydrates wt.%**
Stressed *P. ellipsoidea* mixture	3.6	64.5	9.8	22.1	31.9	24.4	68.1	7.5
Chlorella mixture	7.8	56.4	8.5	27.3	26.3	53.8	36.8	9.5
Chlorella model	9.9	50.0	7.6	32.5	22.0	25.5	67.7	6.8
Stressed *P. ellipsoidea* model	4.5	64.1	10.2	21.2	32.5	56.8	32.9	10.3

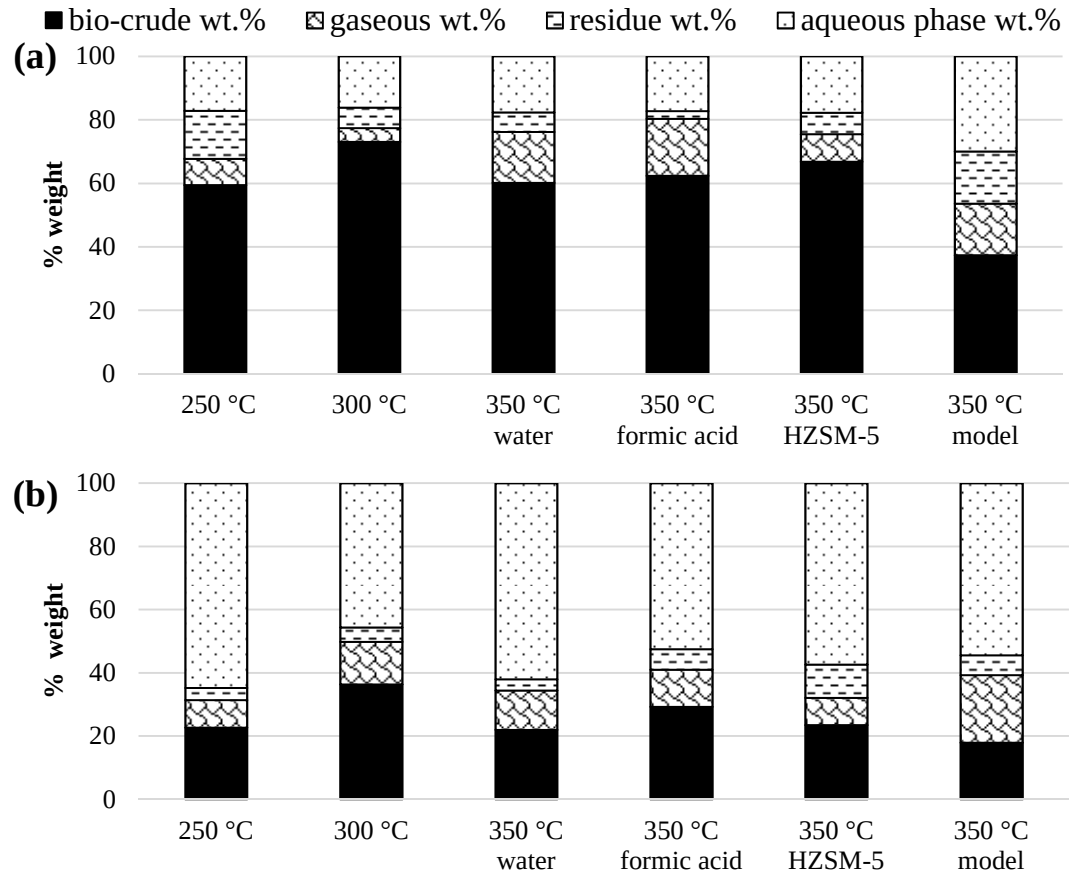

Figure 9-15: Diagrams representing mass balance for the different fractions bio-crude, gaseous, residue and aqueous fractions for (a) the of stressed *P. ellipsoidea* synthetic mixture and (b) *Chlorella* synthetic mixture

For both synthetic mixtures (Figure 9-12 (a), (b)), the highest bio-crude yield is achieved at 300 °C. For the stressed *P. ellipsoidea* in **Chapter 8**, the highest bio-crude yield is also achieved at this temperature with 52.9 wt.%. For the *Chlorella* mixture, higher bio-crude yield is obtained compared to the real microalgae with approximately 28.9 wt.%. Lower bio-crude yield is achieved at 250 and 350 °C. The run in formic acid enhances the formation of bio-crude oils compared to the experiment with water. For the stressed *P. ellipsoidea* mixture with HZSM-5, the bio-crude yield is greater to the yield obtained in **Chapter 8** (25.4 wt.%) suggesting that here more lipids is recovered.

Using model fatty acids compounds yields, less bio-crude yield is achieved compared to the experiment with sunflower oil. Emulsification could have occurred as during the filtration of the aqueous phase bubbles were observed. The presence of glucose enhances the formation of chars.

Biller et al. [112] prepared a synthetic microalgae with the same compounds at 350 °C with 1/3 proportions, a bio-crude oil of 30.4 wt.% was obtained. The following equation was generated (Equation 9-3):

Bio-crude yield % = (protein yield wt.% x protein content %) + (carbohydrate yield wt.% x carbohydrate content %) + (lipid yield wt.% x lipid content yield %)

Equation 9-3

Via this formula, a yield of 62.0 wt.% is calculated for *P. ellipsoidea* which is close to the yield obtained with the synthetic mixture (58.0 wt.%), while with *Chlorella* a value of 31.0 wt.% is determined. The difference for the yield between the synthetic mixture and the real microalgae implies that the other elements (such as the ash, chlorophyll, etc.) in the biomass have an influence on the formation of bio-crude oils. Furthermore, conditions such as reactor size, stirring and heating rate, in which the experiment is carried out played a role as well. The other factor which explains the alteration is complexity and the linkage of each element together in the real biomass. Therefore, some techniques such as microwaves or the pre-treatment which break “these connections” should be investigated in order to improve yields.

9.4.2 Synthetic mixture bio-crude oils analysis

9.4.2.1 GPC analysis

The different molecular weight fraction calculated from the GPC was shown in Figure 9-16 for the experiments using ternary mixture.

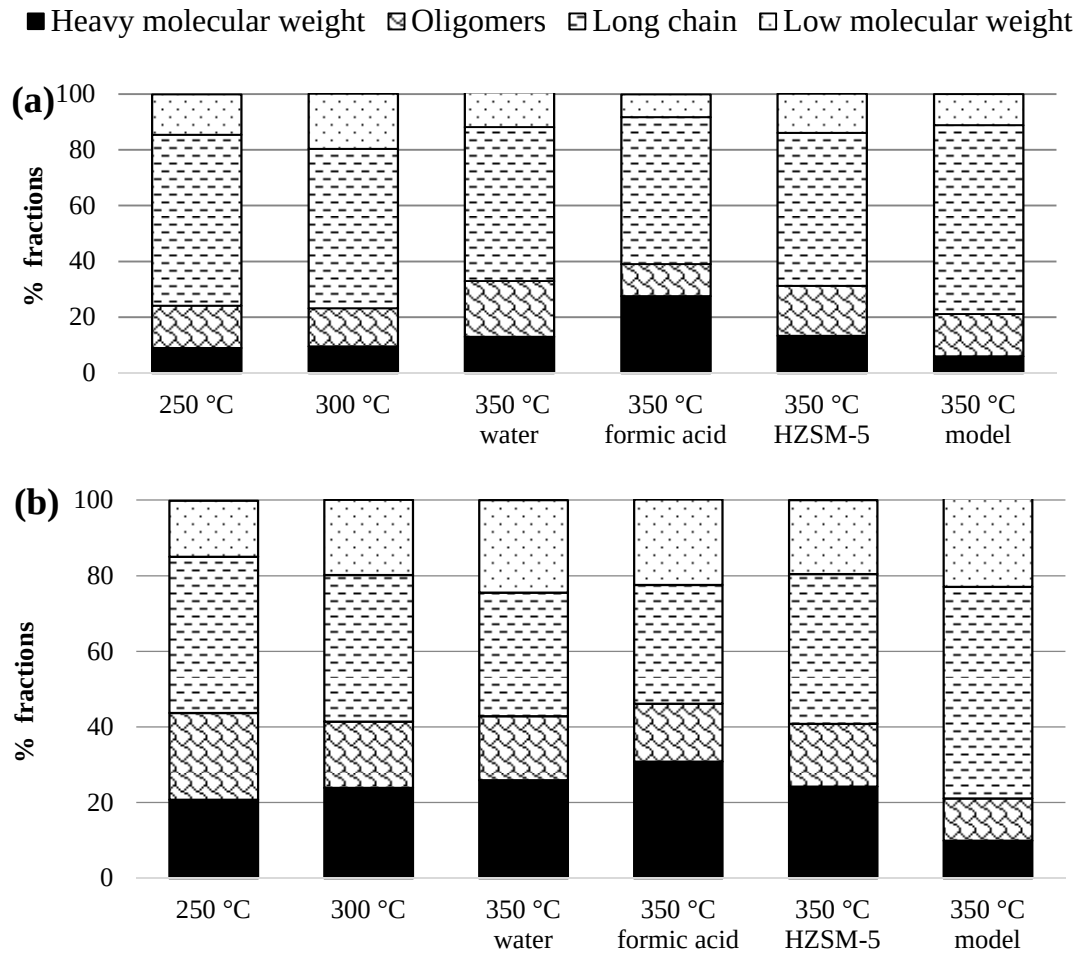

Figure 9-16: Different molecular weight fraction of the bio-crude oils of the different mixture microalgae (a) *P. ellipsoidea* stressed (b) *Chlorella* at different temperatures and conditions

For the processing of both synthetic, a reduction of the "long chain" materials is observed with the increase of temperature*;* indicating that some saponification also takes place as the previous section. The oligomers and "heavy molecular weight" materials increases, here Maillard reaction is most likely responsible. Formic acid enhances the formation of compounds of "heavy molecular weight" materials which is the opposite effect observed in **Chapter 8** for the processing of microalgae. For the

processing of synthetic *Chlorella*, the fraction of lipids is 17.5 % higher with HZSM-5 compared to the run in water.

Runs with the model fatty acids achieves higher fraction of “long chain” materials in the bio-crude oils compared to the results when sunflower oil is used. It could suggest that the saponification process is lower. The “heavy molecular weight” materials are composed of reaction between the two amino acids and glucose.

Both mixtures shows nearly identical pattern under hydrothermal liquefaction concerning the mass balance. GC-MS, CHNS is carried out in order to obtain more information about the composition of the bio-crude oils.

9.4.2.2 GC-MS analysis

Figure 9-17 (a) represents an example of the chromatogram with the synthetic mixture of *P ellipsoidea* at 350 °C in water and (b) synthetic mixture of *Chlorella*. Table 9-9 includes the list of compounds identified within the chromatograms

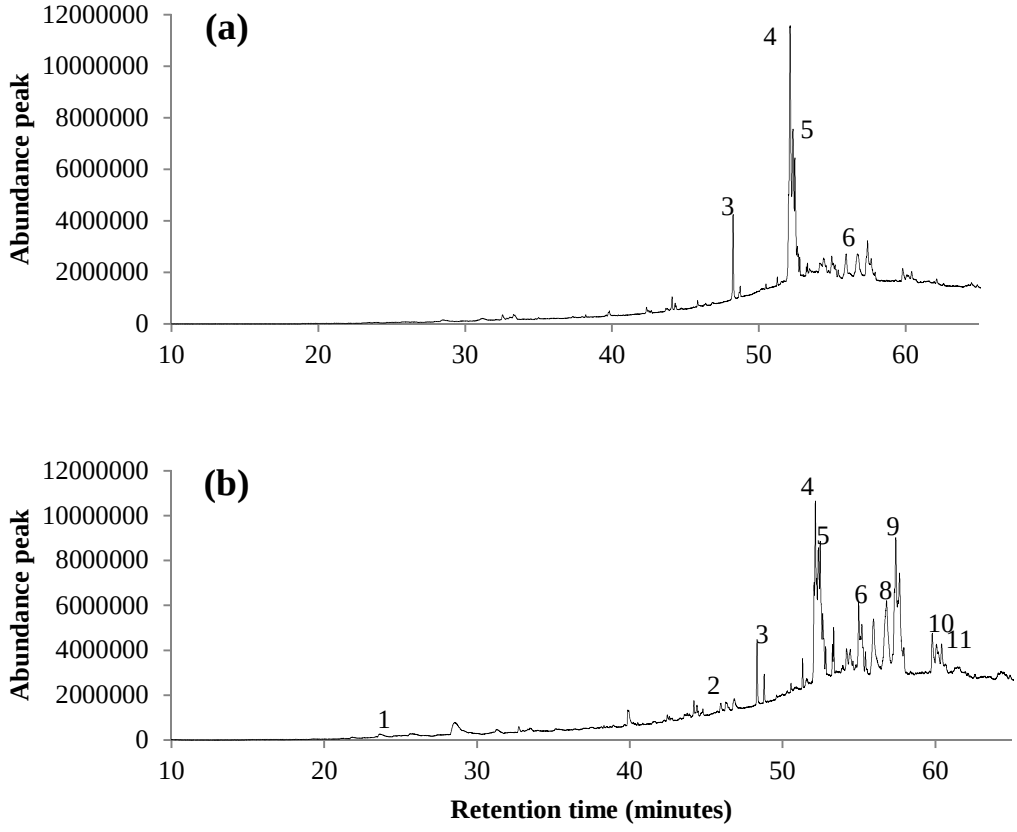

Figure 9-17: GC-MS chromatogram for the (a) stressed *P. ellipsoidea* (b) mixture *Chlorella* at 350 °C in water

Table 9-9: Peaks identification in the GC-MS

Number	Retention time (minutes)	Compounds
1	24.7	1-butyl-2-pyrrolidinone
2	45.8	4-butyl-phenol
3	48.2	hexadecanamide
4	52.0	9-octadecenamide
5	52.4	N,N-dimethyl-9-octadecenamide
6	54.9	n-butyl-9-octadecenamide
7	55.1	N,N-diethyl-9-octadecenamide
8	56.6	N-(2-phenylethyl)-acetamide
9	57.6	oleic diethanolamide
10	59.7	1-(1-oxo-9-octadecenyl)-pyrrolidine
11	60.3	1-(1-oxo-9-octadecenyl)-piperidine

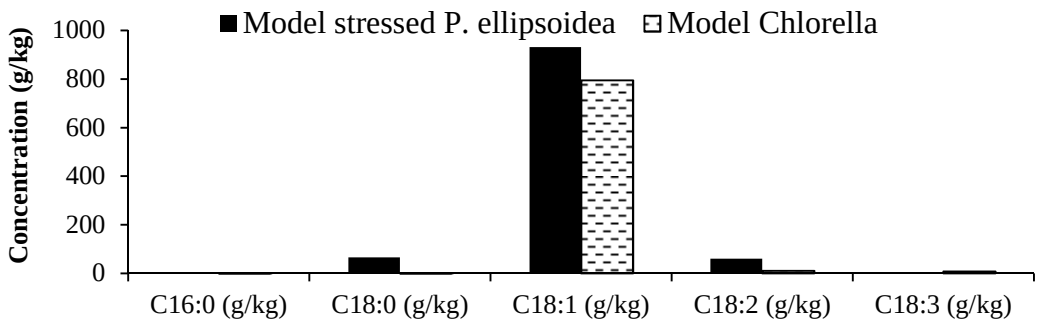

Figure 9-18: FAME profile for both model mixtures of synthetic microalgae.

The main compounds from the GC-MS of the synthetic *P ellipsoidea* are amides, some compounds have not been identified previously such as 4,4-dimethyl-2-(1-hydroxy-heptadec-8-enyl)-2-oxazoline and 2-heptadec-10-enyl-4,4-dimethyloxazoline.

The main compounds from the GC-MS of the synthetic *Chlorella* (Figure 9-17 (b)) are amides such as N-propyl-9-octadecenamide, and N,N-dimethyl-9-octadecenamide. Some fraction of stearic acid with the high lipid mixtures is observed which is not present originally suggesting that a small amount of oleic acid could be hydrogenated.

Figure 9-18 includes the main FAME in the bio-crude oil of the prepared microalgae mixture with oleic and linoleic acids. Both mixtures show that the main fatty acid presents in the oil is oleic acid as for the real stressed *P. ellipsoidea.* The concentration of linoleic acid is reduced however it is possible that delocalisation of the double bonds occurred to 7,10 or 9,12 position explaining the reduction of this compound.

9.4.2.3 Elemental analysis

Table 9-10 lists the elemental values of the bio-crude oil obtained during the hydrothermal processing of two synthetic microalgae using three components. For the energy recovery, the initial energy content is determined using the percentage composition of the different elements (proteins 22.8 MJ/kg, and 37.6 MJ/kg for sunflower oil). Thus the heating content for the synthetic mixture of *P. ellipsoidea* was 31.9 and 23.2 MJ/kg for *Chlorella* in contrast to the real algae with 36.9 and 35.3 MJ/kg respectively.

For the stressed *P. ellipsoidea* mixtures, an increase of the nitrogen content is noticed between 250 to 350 °C compared to the bio-crude oils from the real microalgae. For the *Chlorella* mixtures, the nitrogen content decreases this time from 4.2 to 3.8 wt.% which was coherent with the real *Chlorella* with lower values.

Opposite trends are also found for the carbon content between the stressed *P. ellipsoidea* and *Chlorella* mixtures. For the stressed *P. ellipsoidea* mixtures with formic acid and HZSM-5, the hydrogen content is lower compared to the other samples; a problem of measurement could be the reason as samples are liquids and molecular sieves are used for this sample. Interestingly, HZSM-5 enhances the nitrogen content in the bio-crude oil with both sets of experiments.

The HTL run using fatty acid and amino acids yields similar figures to the bio-crude oil of the real stressed *P. ellipsoidea* at 350 °C. The maximum energy recovery, for both mixtures, is measured at 300 °C.

Table 9-10: Nitrogen, carbon, hydrogen, sulphur and oxygen content in the bio-crude oils, energy content (Dulong and Milne) and energy recovery for experiments for the ternary mixtures of the two algae as dried basis

	N wt.%	C wt.%	H wt.%	O wt.%	Dulong HHV (MJ/kg)	H/C	O/C	Milne HHV (MJ/kg)	% Energy recovery
stressed *P. ellipsoidea* mixtures									
250 °C	1.8	76.1	11.8	10.3	40.7	1.9	0.1	39.9	75.9
300 °C	2.3	76.3	11.5	10.0	40.4	1.8	0.1	39.6	92.6
350 °C	3.7	79.2	12.0	5.1	43.0	1.8	0.0	41.6	81.1
formic acid	3.0	69.9	5.3	21.8	27.3	0.9	0.2	27.7	53.4
HZSM-5	3.7	67.8	5.7	22.9	26.9	1.0	0.3	27.3	56.5
model	1.4	72.3	11.2	15.0	37.8	1.9	0.2	37.4	43.7
***Chlorella* mixtures**									
250 °C	4.2	76.3	8.7	10.8	36.3	1.4	0.1	35.6	75.9
300 °C	4.0	69.5	10.2	16.2	35.2	1.8	0.2	34.7	92.6
350 °C	3.8	62.8	9.0	24.4	29.7	1.7	0.3	29.7	81.1
formic acid	3.2	56.5	8.0	32.3	24.8	1.7	0.4	25.4	53.4
HZSM-5	5.8	69.6	9.3	33.3	30.9	1.6	0.4	31.2	56.5
model	3.2	71.0	10.6	15.2	36.4	1.8	0.2	35.8	43.7

9.4.3 Aqueous phases analysis

The concentrations are listed in Appendix 1, section 1.3.2 page 322. The ammonium compound concentration of *P ellipsoidea* mixture increases with the temperature, from 1250 to 2040 ppm; these values are larger than with the real microalgae. There is no clear trend for the *Chlorella* mixture where the highest concentration is achieved at 300 °C. For the real *Chlorella*, a constant rise from 2576 to 6284 ppm is measured from 250 to 350 °C.

The concentration of cations or anions might be less accurate as the viscosity of the sample is greater compared to other processed water samples which caused a slight lag in the retention time and causes a co-elution of some species. The concentration of ammonium is relatively close between the model experiment (with a mixture of amino acids) and the synthetic mixture with soya protein. By themselves, soya proteins and asparagine acid yields different concentrations of ammonium.

For the *P ellipsoidea* mixture, the maximum TOC concentration (4065 ppm) is measured at 350 °C in water; with a neutral pH (7.3). In contrast, the maximum TOC concentration is achieved with formic acid for the *Chlorella* mixture with an alkali pH of 8.8.

9.4.4 Carbon and nitrogen mass balance

Table 9-11 includes the mass balance of nitrogen and carbon for the synthetic mixture of two microalgae. No residues are available to calculate the mass balance of the carbon and nitrogen.

Table 9-11: Carbon and nitrogen mass balance for the aqueous, bio-crude oils and remaining phases for the experiments using mixtures at different temperature and conditions

	% C aqueous	% C bio-crude	% C remaining	% N aqueous	% N bio-crude	% N remaining
stressed *P. ellipsoidea* mixtures						
250 °C	5.2	70.1	24.8	24.7	17.1	58.1
300 °C	3.0	86.4	10.6	29.2	21.8	49.0
350 °C	5.8	73.9	20.3	40.9	35.7	23.4
formic acid	1.8	67.6	30.7	54.3	25.8	19.9
HZSM-5	3.9	70.2	25.9	49.4	35.2	15.5
model	10.6	42.2	47.1	32.0	10.0	58.0
***Chlorella* mixtures**						
250 °C	33.4	30.8	35.8	60.5	18.8	20.6
300 °C	35.3	44.9	19.8	63.1	17.9	18.9
350 °C	26.7	24.6	48.8	41.7	17.0	41.2
formic acid	40.6	29.4	30.0	83.9	12.8	3.3
HZSM-5	27.3	29.0	43.6	32.9	26.0	41.2
model	44.2	25.5	30.4	25.4	10.7	63.8

For the processing of *P. ellipsoidea* mixtures, the carbon fraction is in majority present in the bio-crude with a maximum (86.4 wt.%) at 300 °C and less in the aqueous phase. The highest fraction is found in the gaseous phase with the model mixture. Overall, the nitrogen fraction is more predominant in the aqueous phase and in the gaseous phase compared to the bio-crude.

For the processing of *Chlorella* mixtures, different results are achieved particularly with the carbon fraction. Contrary to the previous experiment, the carbon fraction is higher in the aqueous phase with the exception of the experiment of the model compound. The nitrogen fraction is higher in the aqueous phase at 300 °C and in formic acid at 350 °C. Likewise for real *Chlorella*, formic acid enhances the formation of ammonium compounds.

To summarise this section:

- Similar patterns were found between the two synthetic mixtures of microalgae especially with the mass balance yields and fraction of molecular weight.
- The yield depended on the lipid content. Yet, the value was below the yield obtained with the true algae because of the simplicity of the mixture.
- When amino acids with glucose were used together, the formation of bio-crude is hindered. It can be deduced that the proportion of protein is higher the nitrogen content is reduced in the bio-crude oil with temperature while when the content of lipids is higher than 50 %, the opposite trend was observed. Thus, the *P. ellipsoidea* mixture is most suitable at 300 °C whereas *Chlorella* it is at 350 °C.

9.5 Discussion of mechanism of reactions

When proteins are added with carbohydrate compounds, a tangle of reaction networks takes place leading to the formation of “heavy molecular weight” materials compared to the processing of soya protein or amino acids alone. Peterson et al. [314] and Kruse et al. [278, 335] remarked that amino acids such as glycine or alanine enhanced the fractionation of glucose. The Maillard reaction is illustrated in Figure 9-19 with the reaction of asparagine and glucose; with this example it was slightly more complex as the amino acids contained two nitrogen groups [336].

The first and second steps involve a condensation between the amine group (proteins or amino acids) with a carbonyl group (from a carbohydrate) to form N-substituted glycosylamine. The following step from 3 to 4 leads to the rearrangement to an Amadori compound by the delocalisation of the double bonds. The compound in step 4 is enediol, from there, lot possible pathways can lead to cyclisation via a retro-aldol obtaining pyrrole or furans [277]. Furan and pyrrole with an aldehyde group can condensate with alcohol molecules etc. Subsequently, there are various possibilities as different monomers can be formed and moreover, polymers could even react together

via cross linking [323, 336]. In the bio-crude from the processing of *Nannochloropsis*, Sudasinghe et al. [337] identified imidazole-like molecules (compounds with two nitrogen atoms) as the most abundant compounds. This class of compounds were produced during the Maillard reaction.

All these reactions are developed for pyrolytic conditions and low temperatures; yet Peterson et al. [314] assumed that under hydrothermal liquefaction similar reactions happen. In order to have a clearer idea of the "heavy molecular weight" materials, the different fractions should be separated using a technique similar to the size exclusion chromatography where the different fractions are analysed by proton NMR.

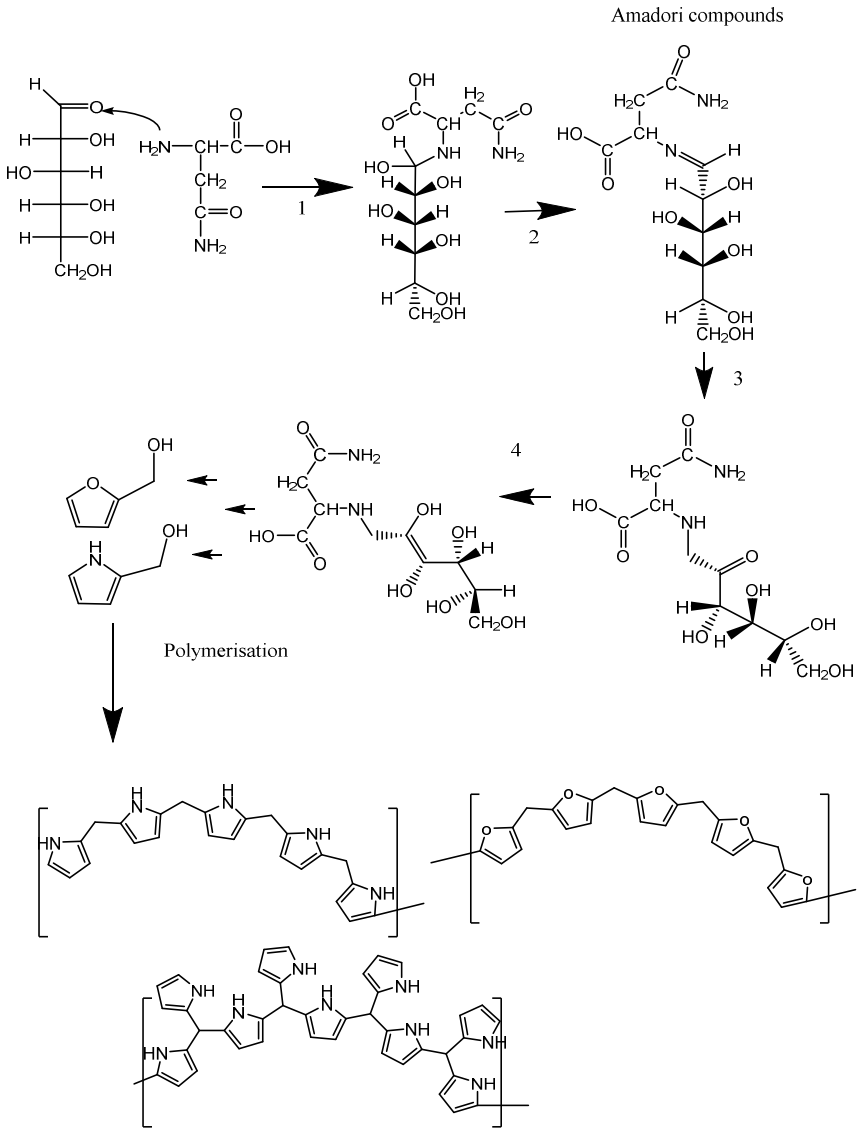

Figure 9-19: Main steps for the Maillard reaction between the asparagine and glucose according to Peterson et al. [94] or Tressl et al. [277]

The reaction between vegetable oils and soya proteins produces mainly long chain compounds with fatty acids, primary amides for example 9-octadecenamide or tertiary amide with oleic diethanolamide (shown in Figure 9-20). This molecule is produced from the condensation of two ethanolamides. This compound is more stable than C_{18} amide chains. The second molecule represents the 2-heptadec-10-enyl-4,4-dimethyloxazoline; it is a long chain with an oxazoline group, they were used as protecting groups for carboxylic acid [338].

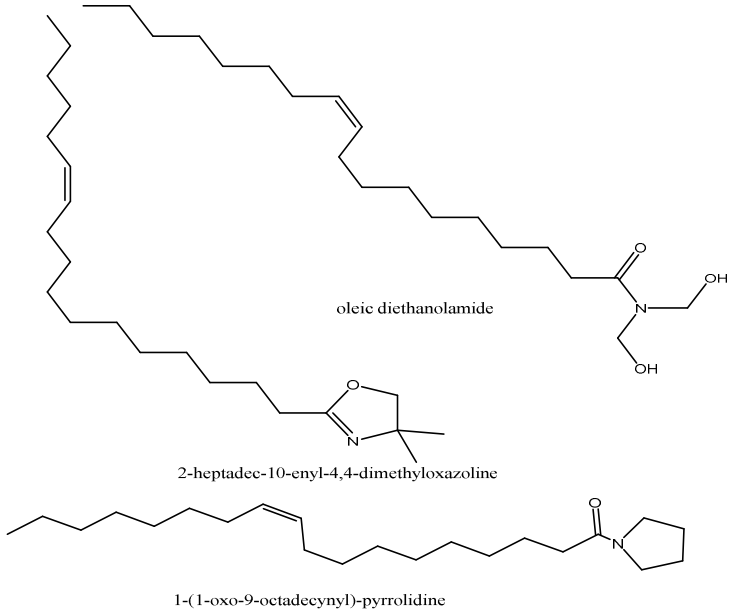

Figure 9-20: Structure of oleic diethanolamide and 2-heptadec-10-enyl-4,4-Dimethyloxazoline 1-(1-oxo-9-octadecynyl)-pyrrolidine

9.6 Implications for the hydrothermal liquefaction of microalgae

For the binary mixture, the yield is plotted in function of the protein content for the experiment performed between the mixture sunflower-protein, linseed-protein and starch-protein and displayed in Figure 9-21. A polynomial fit is applied for the curve with the lipids with a second order.

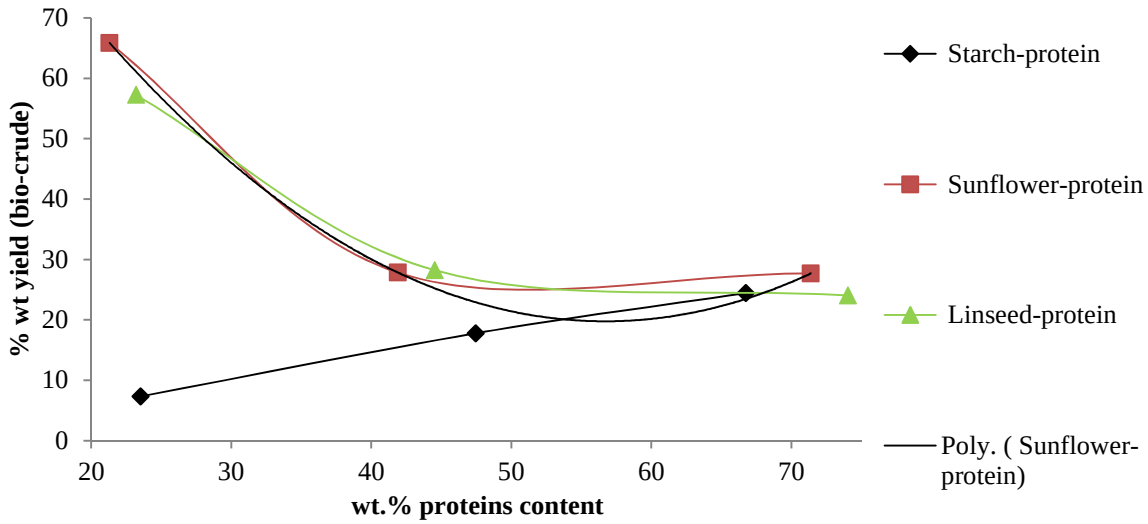

Figure 9-21: Relationship between yield and the protein content for the different mixture of proteins

The equation for the sunflower is shown below in Equation 9-4 and for linseed in Equation 9-5

$$y = 0.0368x^2 - 4.1737x + 138.1$$ **Equation 9-4**

$$y = 0.024x^2 - 2.9872x + 113.6$$ **Equation 9-5**

The curve which is closest to the bio-crude oil mass yield obtained is with linseed as for 55 wt.% of protein for *Chlorella* a theoretical yield of 21 wt.% instead of 28.9 wt.% and 56 wt.% for *P. ellipsoidea* instead of 49 wt.% at 350 °C. Above 60 wt.% of protein, the bio-crude yield seems to level out before 50 wt.% with both sunflower and linseed oil, a linear trend suggesting that proteins do not have an impact on the yield. Therefore, a microalga strain with protein content lower than 40-45 wt.% would be recommended to obtain a yield higher than 40 wt.%.

Interestingly, with the mixture starch-protein a linear curve is obtained when the per cent of protein increased from 25 to 75 wt.% with the following equation (Equation 9-6).

$$y = 0.3975x - 1.73 \ (R^2 = 0.9957)$$ **Equation 9-6**

The yield decreases to 17.5 wt.% for “100 wt.% of protein” (bear in mind that the soya protein used was 90 wt.% pure). On the whole, carbohydrates with lipids or proteins are not beneficial to obtain a good yield, contrary to lipids. On one hand, in the case of low lipid and high protein, the carbohydrate could slightly improve the bio-crude yield; on the other hand, the bio-crude oil would contain high pyrrole and furans

polymers. Cyanobacteria, such as *Spirulina pl.* and *Arthrospira m.* (with high protein content above 60 wt.%), are not suitable for use during hydrothermal liquefaction but better as nutritional purpose or to extract high value chemicals [308].

Figure 9-22 represents the bio-crude oil wt.% yield of model compounds (glucose, starch, soya protein, asparagine acids and sunflower oil) and microalgae (*Spirulina*, Chlorella, stressed and non-stressed *P. ellipsoidea*) against the temperature. Between 250 to 300 °C, the majority of bio-crude yield increases whereas after 300 °C, a decrease of the yield for the stressed *P. ellipsoidea*, soya protein and glucose. It could suggest the largest portion of the formation of the oil occurred before 300 °C. Subsequently, the high nitrogen compounds (soya protein, *Chlorella* and *Spirulina* have a relatively similar behaviour to the bio-crude oil production.

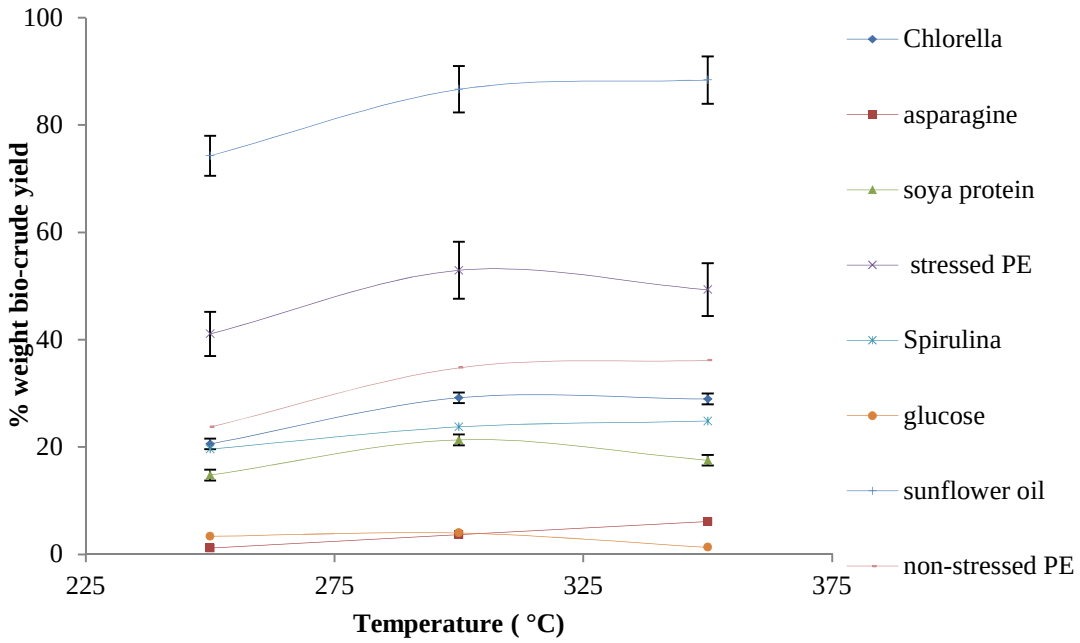

Figure 9-22: Graphic showing the bio-crude oil yield against the temperatures for the model compounds and the microalgae where PE is *P. ellipsoidea*.

Moreover, the result for the ternary mixture suggests that it would be more suitable to process high lipids content at lower temperatures such as at 300 °C whereas for high protein microalgae at a temperature of 350 °C.

9.7 Conclusion

Binary and tertiary synthetic mixtures were prepared in order to have a better understanding of the hydrothermal liquefaction of microalgae. Similarities were found in the bio-crude yields for example *P. ellipsoidea* had a maximum bio-crude yield at 300 °C. The yield in general depended on the amount of lipids but also on the protein content of the microalgae. Carbohydrates enhanced the formation of residue when mixed with vegetable oils. Because of the Maillard reaction, the mixture of starch-protein gave a different behaviour with an increase of the bio-crude oil using 75 wt.% protein mixture. The fraction of “heavy molecular weight” materials using the starch-protein mixture increases with the temperature. During the reaction of sunflower, starch and protein the energy recovery is highest at 250 °C. The nitrogen content is higher in the char compared to the oil for starch-protein. There is a linear relationship between the amount of protein and the concentration of ammonium for the mixture starch-protein. At large proportion of lipids in mixtures, the carbon fraction is located mainly in the bio-crude. Different amides are produced with fatty acids and primary and secondary amides and pyrrole as well. A linear relationship between the amount of ammonium and the % protein within the mixture of linseed and protein is obtained. It was deduced in order to obtain a good quality bio-crude yield of 40-45 wt.% , a microalga should contain less 40 wt.% of protein.

Chapter 10 Conclusion and future works

10.1 General conclusion

More research groups and commercial companies are today considering hydrothermal liquefaction of microalgae as an alternative to produce bio-crude oil (green crude). This technique is more efficient compared to the first and the second generations of biodiesel. The life cycle assessment indicates that this technology would be more economically viable whether the processing is carried out in the surroundings of a coal power station to supply the carbon dioxide and a waste water treatment plant for the supply of nutrient to grow the microalgae. Ideally, a closed loop could be achieved; the aqueous phase could be diluted and fed as nitrogen sources for the microalgae. In theory, all the nitrogen should be fractionated into the aqueous phase however in reality approximately 5 to 10 % is usually lost in the bio-crude.

The challenges of this project are to:

- Have a better understanding of the formation of the bio-crude and in particular the formation of nitrogen compounds. For this purpose, different model compounds were processed separately and in combination such as proteins, carbohydrates and lipids. Afterwards these results were compared with real microalgae.

Instead of using expensive catalysts with noble metals, it would reduce the cost of the process if low cost materials or catalysts such as zeolites (HZSM-5) could be selected. Different metals have been incorporated into HZSM-5 in order to change the physiochemical proprieties to this zeolite. The stability of this catalyst under hydrothermal condition was therefore investigated. The supply of hydrogen for upgrading of biomass requires large amounts of molecular hydrogen. One proposal suggested was to use organic acids to supply hydrogen and promote water gas shift reactions. The project also investigated the effect of the formation of hydrogen donors such as formic acid.

In **Chapter 4**, one of the first goals of this project was to investigate the stability and the robustness of HZSM-5. In contrast to steaming conditions, during

hydrothermal treatment, the de-alumination was less significant compared to the loss of silica. Some metals such as molybdenum reduce the loss of crystallinity and copper lowered the loss of surface area. It was observed that zeolite incorporated via the metal ion-exchanged technique was more robust compared with using wet impregnation. HZSM-5 was recycled four times with sunflower oil. The bio-crude yield was constant even though the amount of coke increased after each test. It was observed that after the third test the coke contained more carbon compared to hydrogen content.

In **Chapter 5**, different vegetable oils (sunflower, soya bean, linseed, jatropha and palm oils) were processed at different temperatures (250, 300 and 350 °C). Triglycerides were readily hydrolysed into free fatty acids at low temperatures. Experiments performed with model polyunsaturated fatty acids (linolenic acid) and linseed oil suggested that the cross linking reaction producing “heavy molecular weight” materials were significant. Fatty acids produced high energy content bio-crude oil. Palmitic and stearic acids were more stable during hydrothermal liquefaction. Therefore, it is more suitable to process microalgae containing higher concentration of monounsaturated fatty acids.

In **Chapter 6,** the processing of carbohydrates (glucose, starch, and alginic acid) demonstrated a propensity towards higher residues and lower bio-crude yields. Nevertheless, for mannitol the formation of bio-crude is slightly enhanced. The char residues were stable under hydrothermal conditions and contained the highest energy recovery amongst all the phases. The long cooling rate probably enhanced the formation of chars. As temperature increased, the fraction of “heavy molecular weight” materials decreased. Therefore, carbohydrates favour side reactions and should be removed in order to favour the formation of high quality bio-crude.

In **Chapter 7**, the processing of soya hemp proteins and asparagine was carried out. Hemp protein produced a higher yield of bio-crude compared to soya proteins. Amino acids principally degraded in to aqueous phase, glutamine produced slightly more bio-crude than asparagine. Soya proteins produced more ammonium compared to hemp proteins. The side reaction from the degradation of protein was the production of heterocyclic compounds which contributed to the high nitrogen content in the bio-crude. Finally, the STA suggested that the nitrogen content was mostly containing in the “heavy molecular weight” materials.

In **Chapter 8**, the maximum bio-crude yield was achieved with *P. ellipsoidea* (stressed) with 52.9 wt.%. For *Chlorella* and *Spirulina*, *P. ellipsoidea* (non-stressed) containing a high protein content, the bio-crude yield increased with temperature. The GPC analysis indicated that the "heavy molecular weight" materials in the bio-crude were reduced with the temperature. The result from the yield of stressed *P.* ellipsoidea was coherent with the bio-crude yield of vegetable oils in **Chapter 5** and *Chlorella* with the yield of protein in **Chapter 7**. Most of the compounds identified in the processed bio-crude from stressed *P. ellipsoidea* contained long chain compounds and amides. The ammonium compound concentration in the aqueous phase increased with temperature. In general, it was demonstrated that the same microalgae grown under different condition yielded different bio-crude compositions. The stressed *P. ellipsoidea* is a strong candidate for the hydrothermal liquefaction as the nitrogen content in the bio-crude is low.

In **Chapter 9**, different mixtures were prepared using different model compounds (vegetable oils, proteins and starch). There was a proportional relationship between the protein content mixed with starch for the bio-crude yield. In contrast, the bio-crude yield decreased when the amount of proteins increased with the lipids. The bio-crude yield was lower than the initial amount of vegetable oils added suggesting the formation of amides and saponification process. The high fraction of carbohydrates enhanced the formation of residues. Two mixtures were prepared according to the composition of the *Chlorella and P. ellipsoidea* microalgae. The maximum bio-crude yield was achieved at 300 °C for both microalgae mixtures.

10.1.1 General trends

- Formic acid, in this study, enhances the formation of the gaseous phase with most of the model compounds and algae at 350 °C compared to experiments performed in water. The gas formation is more significant in the presence of formic acid and HZSM-5. However, bio-crude yield is reduced slightly compared with in water. For high protein content materials, formic acid reduces the nitrogen content in the bio-crude with *Chlorella*, *Spirulina* and soya proteins compared to in the water. Ross et al. [129] observed that formic acid lowers the boiling point of the simulated distillation range and thereby improves the bio-crude viscosity. Using formic acid and oleic acid, the delocalisation of the double bonds is observed with no major hydrolysis

of the unsaturation. Formic acid increases the nitrogen content in the bio-crude with high lipid materials by forming more amides. Formic acid enhanced the deoxygenation for stressed *P. ellipsoidea* compared to the other microalgae. A low concentration of formic acid lowers the formation of gas and avoids the loss of some bio-crude oil.

- Compared to the reactivity in pyrolytic condition, the effect of HZSM-5 is less efficient in subcritical condition. HZSM-5 is more efficient upgrading vegetable oils compared to the other components (carbohydrates, proteins) and for microalgae. Doping with molybdenum increases the fraction of aromatics whereas iron enhances the fraction of heavy molecular weight. Lipids are more reactive with these catalysts as they have a simpler structure. It is likely that some fatty acids could diffuse inside the pores whereas carbohydrates yielded more complex molecules. Furthermore, HZSM-5 because of high acidity in combination of formic acid enhances the hydrolysis of amides. Copper and iron have an effect on the molecular weight for processing of proteins and amino acids by enhancing the polymerisation. Metal doped zeolites have no effect on the upgrading of starch as most of degrading molecules were soluble in water. For the microalgae experiment, NiZSM-5 enhances the deoxygenation in general. For the *Chlorella* bio-crude MoZSM-5 gives good result which is an encouraging result.

- The general trend in the aqueous phase, the carbon fraction decreases whereas the ammonium concentrations increase with the temperature. The carbon fraction is mostly transferred to the bio-crude and the gaseous phase. For the nitrogen fraction, an opposite trend is observed between in the aqueous phase and the nitrogen in the bio-crude oil which decreases with temperature. In general, protein and carbohydrate favours the formation of compounds soluble in the aqueous phase. However, when these are combined together, the production of bio-crude and residue increases.

10.1.2 General mechanism

At the first stage, the macromolecules are hydrolysed. Carbohydrates have the fastest hydrolysis rate into monomers (sugar units) below 200 °C, subsequently to proteins into amino acids and finally triglycerides into fatty acids above 250 °C [261, 299, 339]. With the exception of lipids, at the beginning, the majority of monomers are located in the aqueous phase. Nevertheless, because of the complex structure of

the membranes, Garcia Alba et al. [133] observed no degradation of the cell until 200 °C. In the second step, monomer molecules decompose further either the degraded product are found in the aqueous phase or into the bio-crude. In the third step, molecules undergo condensation or recombination to form oligomers and higher molecular weight polymers. The most likely step is that the polymers could cross-link together.

The hydrolysis of starch or other carbohydrates such as cellulose and alginic acid into monomers is rapid [261]. Subsequently, the sugars cycles such as glucose and xylose are hydrolysed to form linear molecules and carboxylic acids. A small amount of bio-crude is formed compared to the other model compounds as molecules were hydrophilic. 5-HMF is one known precursor for the formation of char [266]. One of the drawbacks of using carbohydrates is the large amount of residue. Alginic acids favour the formation of gas especially with the addition of formic acid and HZSM-5. It is possible that HZSM-5 enhances the formation of small organic acids including formic acid which subsequently decomposes into hydrogen and carbon monoxide [270]. Therefore, if the formation of chars could be reduced, alginic acid could be used to form *in-situ* hydrogen. Furthermore, the batch reactor was not suitable for carbohydrate as there was no possibility to quench the reaction and to have a faster heating rate as in this way, the char amount could be reduced.

One of the initial aims was to convert most of the nitrogen function of the proteins into ammonium or other water soluble compounds such as amines. However, in reality, it is more complicated and side reactions occur. The identification of various diketopiperazine compounds in the bio-crude oil indicates that the proteins have the same degradation route as during pyrolysis as Torri et al. [22] had suggested [137, 293]. At low temperatures, proteins form macrocycles. As the temperature increases, the cycles decrease in size releasing amino acids. At the end, diketopiperazines and pyrrolidinones are found in the bio-crude. Amino acids decompose further into either ammonium or different compounds in the water phase or in the bio-crude oil. One of the solutions would be to pre-treat the microalgae with fast liquefaction as with carbohydrates. It is also investigated that the aqueous phase could be gasified to produce hydrogen to upgrade the bio-crude in the second processing bio-crude to obtain a ready-to-use fuel.

The hydrolysis of triglycerides is slower than proteins and carbohydrates. Fatty acids are relatively stable under hydrothermal conditions. Therefore, catalysts need to be added to enhance the decarboxylation [339].

There were more complex reactions during the decomposition of microalgae as different elements react together. The most known is the Maillard reaction between carbohydrates and proteins. This reaction enhances the formation of "heavy molecular weight" materials. It reduces the quality of the bio-crude and increases the viscosity [314]. Thus, this reaction should be hindered. The formation of amides is observed in addition, not only does the ammonium react with fatty acids but primary and secondary amines and pyrrole could react as well. Nitrogen chemical functions, such as amines and amides, are problematic as they are reactive; at the first stage of the liquefaction, hydrolysis occurs whereas during the cooling stage, the hydrolysed molecules recombine by condensation. In the future, a reagent should be added in order to avoid these chemical groups reacting after the HTL reaction.

To summarise, hydrothermal liquefaction is the stage of complex chemical reaction which explains the extreme complexity of the bio-crude oil with a succession of hydrolysis and recombination of molecules. Therefore, the elucidation of the accurate chemical degradation route of the microalgae is challenging.

10.1.3 Concluding remarks

In 2018, Sapphire Energy one of the companies claiming to produce green bio-crude, expects to produce 5,000 barrels/day. It would represent approximately 681,000 litres of oil and 653,710 kg (with a specific gravity from bio-crude of 960 kg/m^3) [153, 340]. For the highest yield with *P. ellipsoidea* of 52.9 wt.% (daf), it would require 1,257.2 tonnes of dried algae which is a tremendous amount of algae counting that this specie has a slow growth rate of 3.5 g/L/day. If there was still 1 wt.% of nitrogen it would represent 6.5 tons of nitrogen lost in the bio-crude. For the moment, it seems difficult to realise this with a high lipid microalgae. In the case of *Chlorella*, a bio-crude of 28.9 wt.% (daf), 2,334.7 tons of microalgae would be necessary and 37.3 tons of nitrogen would be lost in the system. Davis et al. [340] determined that in order to produce 19 billion of bio-crude from the HTL of *Chlorella*/year, it would require 1671 sites measuring 485 hectares each. For several years, the production fluctuated particularly between the winter and summer. The authors suggested shutting down the

process during the winter as the emissions were greater than fossil fuel production. Furthermore, the increase of productivity of the microalgae lowered the price of the fuel.

Chisti et al. [55] emphasised that in order to have a competitive algal fuel, the processing should be carried out near a carbon dioxide source facility (a coal power plant). It is estimated that 1.5 billion tons of carbon dioxide could help to produce 82 million tons of microalgae. Furthermore, to replace 1 % of the annual US consumption of fuel, microalgae would require the amount of wastewater produced by a city of 10 million inhabitants. To lower the cost, it would be more efficient to mix different strains of microalgae with sludge produced by waste water and swine manure [145, 146].

The development of this technology will depend on the price of crude oil as investment money is required to finance spin off companies. Today, with the high interest in fracking shale gas and the low price of crude oil (the price was close to $50 (£33.5) in end of March 2015 [341]), these companies struggle to develop. It is the reason why a company such as Solazyme sells high value compounds extracted from microalgae in order to gain money. The scale up and increase of investment could lower the production cost of the overall system and make the algal bio-crude more competitive compared to petroleum oil.

In order that the upgraded algal bio-crude should be used as jet fuel, the oil should be good quality. The level of heteroatoms should be the lowest possible to improve the stability of the fuel. The fuel Jet A contained 20 vol.% by volume of aromatics and less than 3 wt.% of naphtha fraction [342]. Until now, there is no complete study of the physical analysis of the bio-crude from microalgae. Bai et al. [147] identified 43.9 % (of total peak area) of saturated hydrocarbons and 21 % (of total peak area) for aromatics upgrading bio-crude oil from *Chlorella py*. with Raney Ni catalysts. The per cent of aromatic should be measured in per cent volume to know whether this fuel meets the regulation, in addition, 4.6 wt.% of nitrogen compounds was identified.

10.2 Future works

In order to improve the quality of the bio-crude oil and therefore meet the expectation and producing a ready-to-use fuel, some further works need to be performed.

- The SAPO-type zeolites should be investigated in more details. SAPO would be interesting as they have larger pore sizes (in the mesopores region) compared with HZSM-5 (micropores) and their hydrothermal stabilities have been demonstrated. A low cost alternative to Pt/C should be investigated, SAPO could be designed in order to produce selected products [343].
- The development of absorbent for nitrogen heterocyclic compounds (pyrrole for example) with molecular sieves and traps deserves further investigation in order to remove the refractory nitrogen materials during the upgrading stage [305].
- The effect of different parameters such as the heating rate should investigate. It will help the development of the continuous reactor. In fact, research about processing of microalgae should be more focussed on the continuous processing of microalgae instead of doing batch reaction.
- In order to reduce further the nitrogen content, the bio-crude oil should be upgraded with two steps. The first step consists of pre-treating the microalgae using flash liquefaction for a short times as performed by Garcia-Moscoso et al. and Faeth et al. [140, 152]. In the second step, the upgraded microalgae should be processed at a temperature below 350 °C with the help of SAPO catalyst for example. The hydrogen should be produced from the gasification of the aqueous phase produced during the first step or by organic acids (formic acids). Figure 10-1 illustrates the overall process of the hydrothermal upgrading of the microalgae using two steps.

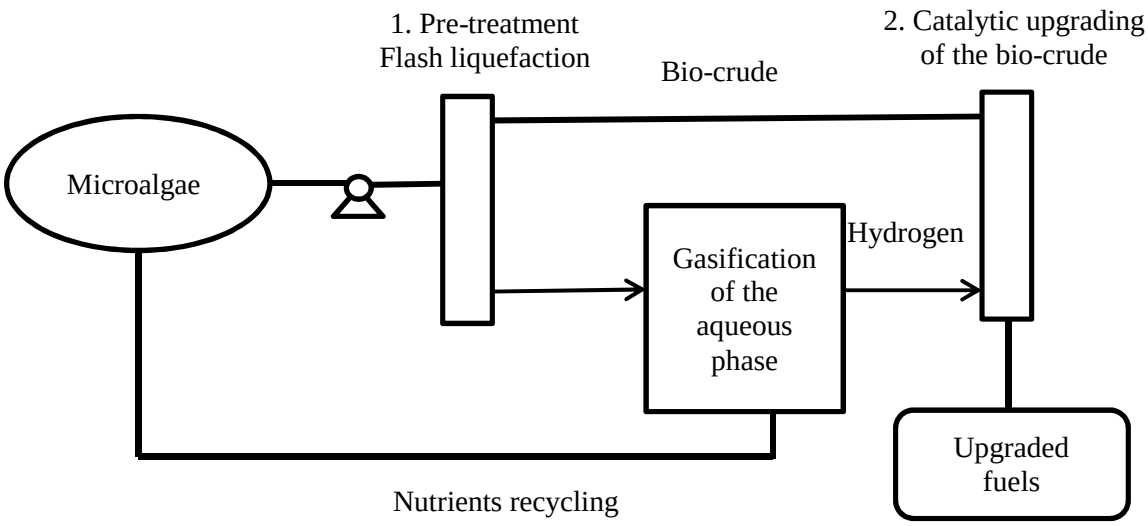

Figure 10-1: Diagram of hydrothermal liquefaction of microalgae using two steps

- The variation of the per cent loading or concentration of formic acid should be studied in more details. Some other hydrogen donors should be investigated such as oxalic acid. As this organic compound decomposes into formic acid more hydrogen should be supplied.
- The kinetic of degradation of microalgae using the technique of TGA-DSC should be investigated in more details. A pressurised cap should be used in order to recreate the hydrothermal condition.
- Some new methods need to be developed in order to have a better identification of organic compounds soluble in the aqueous phase and especially with nitrogen functions. Samples could be analysed through HPLC-MS liquid mass spectrometer. C_{18} absorbent cartridge (reverse phase) could be used to absorb the organic compounds. The development of these methods deserves further investigations.
- The other area which requires more research is to increase knowledge of the chemical structures of the heavy molecular compounds. It would improve knowledge of how “heavy molecular weight” materials form and therefore how they can be reduced. The characterisation of the molecular weight compounds is carried out by proton NMR. Figure 10-22 includes the setting up for the method of fractionation of the bio-crude oil. Proton and carbon NMR should identify “heavy molecular weight” materials [327].

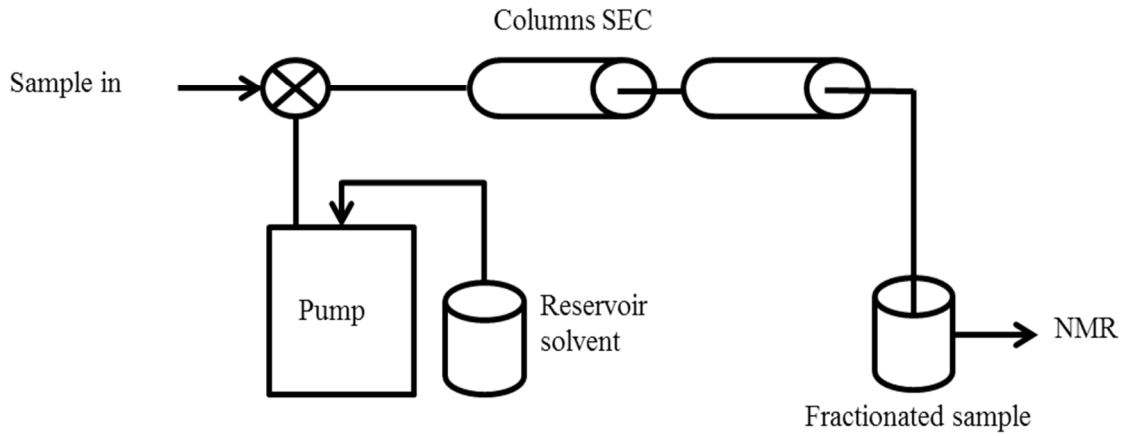

Figure 10-2: Schematics of the set up for the fractionation of the different molecular weight compounds in the bio-crude oil

Chapter 11 Reference

1. Chisti, Y., *Biodiesel from microalgae.* Biotechnology Advances, 2007. **25**(3): p. 294-306.
2. Toor, S.S., L. Rosendahl, and A. Rudolf, *Hydrothermal liquefaction of biomass: A review of subcritical water technologies.* Energy, 2011. **36**(5): p. 2328-2342.
3. Sheehan, J., et al., *A look back at the US Department of Energy's aquatic species program: biodiesel from algae*. Vol. 328. 1998: National Renewable Energy Laboratory Golden.
4. Lackner, K.S., et al., *The urgency of the development of CO2 capture from ambient air*. Proceedings of the National Academy of Sciences, 2012. **109**(33): p. 13156-13162.
5. Cox, P.M., et al., *Acceleration of global warming due to carbon-cycle feedbacks in a coupled climate model.* Nature, 2000. **408**(6809): p. 184-187.
6. IEA, I.E.A. *Energy Technology Perspectives*. 2014; Available from: http://www.iea.org/etp/explore/.
7. Lund, H. and B.V. Mathiesen, *Energy system analysis of 100% renewable energy systems—The case of Denmark in years 2030 and 2050.* Energy, 2009. **34**(5): p. 524-531.
8. Notter, D.A., et al., *Contribution of Li-ion batteries to the environmental impact of electric vehicles.* Environmental Science & Technology, 2010. **44**(17): p. 6550-6556.
9. Franco, J., et al., *Assumptions in the European union biofuels policy: Frictions with experiences in Germany, Brazil and Mozambique.* Journal of Peasant Studies, 2010. **37**(4): p. 661-698.
10. Hammond, G.P., S. Kallu, and M.C. McManus, *Development of biofuels for the UK automotive market.* Applied Energy, 2008. **85**(6): p. 506-515.
11. trnasport, D.o. *Renewable Transport Fuels Obligation*. 2011; Available from: https://www.gov.uk/renewable-transport-fuels-obligation.
12. Agarwal, A.K. and L.M. Das, *Biodiesel Development and Characterization for Use as a Fuel in Compression Ignition Engines.* Journal of Engineering for Gas Turbines and Power, 2001. **123**(2): p. 440-447.
13. Thomas, A., *Fats and fatty oils.* Ullmann's Encyclopedia of Industrial Chemistry, 2007.
14. Yusuf, N.N.A.N., S.K. Kamarudin, and Z. Yaakub, *Overview on the current trends in biodiesel production.* Energy Conversion and Management, 2011. **52**(7): p. 2741-2751.

15. Demirbas, A., *Progress and recent trends in biodiesel fuels.* Energy Conversion and Management, 2009. **50**(1): p. 14-34.
16. Jayed, M.H., et al., *Environmental aspects and challenges of oilseed produced biodiesel in Southeast Asia.* Renewable and Sustainable Energy Reviews, 2009. **13**(9): p. 2452-2462.
17. Kumari, V., S. Shah, and M.N. Gupta, *Preparation of biodiesel by lipase-catalyzed transesterification of high free fatty acid containing oil from Madhuca indica.* Energy & Fuels, 2007. **21**(1): p. 368-372.
18. Kafuku, G., et al., *Heterogeneous catalyzed biodiesel production from Moringa oleifera oil.* Fuel Processing Technology, 2010. **91**(11): p. 1525-1529.
19. Patil, P., et al., *Transesterification kinetics of Camelina sativa oil on metal oxide catalysts under conventional and microwave heating conditions.* Chemical Engineering Journal, 2011. **168**(3): p. 1296-1300.
20. Samniang, A., C. Tipachan, and S. Kajorncheappun-ngam, *Comparison of biodiesel production from crude Jatropha oil and Krating oil by supercritical methanol transesterification.* Renewable Energy, 2014. **68**: p. 351-355.
21. Avinash, A., D. Subramaniam, and A. Murugesan, *Bio-diesel—A global scenario.* Renewable and Sustainable Energy Reviews, 2014. **29**(0): p. 517-527.
22. Ogawa, T., et al., *Analysis of Oxidative Deterioration of Biodiesel Fuel.* SAE Int. J. Fuels Lubr., 2008. **1**(1): p. 1571-1583.
23. Smeets, E.M.W., et al., *Contribution of N2O to the greenhouse gas balance of first-generation biofuels.* Global Change Biology, 2009. **15**(1): p. 1-23.
24. Sanz Requena, J.F., et al., *Life Cycle Assessment (LCA) of the biofuel production process from sunflower oil, rapeseed oil and soybean oil.* Fuel Processing Technology, 2011. **92**(2): p. 190-199.
25. Nanaki, E.A. and C.J. Koroneos, *Comparative LCA of the use of biodiesel, diesel and gasoline for transportation.* Journal of Cleaner Production, 2012. **20**(1): p. 14-19.
26. Chakravorty, U., M.-H. Hubert, and L. Nøstbakken, *Fuel versus food.* Resource, 2009. **1**.
27. Balat, M., H. Balat, and C. Öz, *Progress in bioethanol processing.* Progress in Energy and Combustion Science, 2008. **34**(5): p. 551-573.
28. Gray, K.A., L. Zhao, and M. Emptage, *Bioethanol.* Current Opinion in Chemical Biology, 2006. **10**(2): p. 141-146.
29. Balat, M. and H. Balat, *Recent trends in global production and utilization of bio-ethanol fuel.* Applied Energy, 2009. **86**(11): p. 2273-2282.

30. Luo, L., et al., *Allocation issues in LCA methodology: a case study of corn stover-based fuel ethanol.* The International Journal of Life Cycle Assessment, 2009. **14**(6): p. 529-539.
31. MacLean, H.L. and L.B. Lave, *Evaluating automobile fuel/propulsion system technologies.* Progress in Energy and Combustion Science, 2003. **29**(1): p. 1-69.
32. Kim, S. and B.E. Dale, *Global potential bioethanol production from wasted crops and crop residues.* Biomass and Bioenergy, 2004. **26**(4): p. 361-375.
33. Sims, R.E.H., et al., *An overview of second generation biofuel technologies.* Bioresource Technology, 2010. **101**(6): p. 1570-1580.
34. Parajó, J.C., et al., *Prehydrolysis ofEucalyptus wood with dilute sulphuric acid: operation at atmospheric pressure.* Holz als Roh- und Werkstoff, 1993. **51**(5): p. 357-363.
35. Brownell, H.H. and J.N. Saddler, *Steam pretreatment of lignocellulosic material for enhanced enzymatic hydrolysis.* Biotechnology and Bioengineering, 1987. **29**(2): p. 228-235.
36. Sánchez, Ó.J. and C.A. Cardona, *Trends in biotechnological production of fuel ethanol from different feedstocks.* Bioresource Technology, 2008. **99**(13): p. 5270-5295.
37. Alizadeh, H., et al., *Pretreatment of Switchgrass by Ammonia Fiber Explosion (AFEX)*, in *Twenty-Sixth Symposium on Biotechnology for Fuels and Chemicals*, B. Davison, et al., Editors. 2005, Humana Press. p. 1133-1141.
38. Kim, K.H. and J. Hong, *Supercritical CO2 pretreatment of lignocellulose enhances enzymatic cellulose hydrolysis.* Bioresource Technology, 2001. **77**(2): p. 139-144.
39. Borrion, A.L., M.C. McManus, and G.P. Hammond, *Environmental life cycle assessment of lignocellulosic conversion to ethanol: A review.* Renewable and Sustainable Energy Reviews, 2012. **16**(7): p. 4638-4650.
40. Hoogers, G., *Fuel cell technology handbook*. 2002: CRC press.
41. van Steen, E. and M. Claeys, *Fischer-Tropsch Catalysts for the Biomass-to-Liquid (BTL)-Process.* Chemical Engineering & Technology, 2008. **31**(5): p. 655-666.
42. Tijmensen, M.J.A., et al., *Exploration of the possibilities for production of Fischer Tropsch liquids and power via biomass gasification.* Biomass and Bioenergy, 2002. **23**(2): p. 129-152.
43. Aigner, I., C. Pfeifer, and H. Hofbauer, *Co-gasification of coal and wood in a dual fluidized bed gasifier.* Fuel, 2011. **90**(7): p. 2404-2412.
44. Shafizadeh, F., *Introduction to pyrolysis of biomass.* Journal of Analytical and Applied Pyrolysis, 1982. **3**(4): p. 283-305.

45. Bezergianni, S., A. Dimitriadis, and L.P. Chrysikou, *Quality and sustainability comparison of one- vs. two-step catalytic hydroprocessing of waste cooking oil.* Fuel, 2014. **118**(0): p. 300-307.
46. Whitehurst, D.D., T.O. Mitchell, and M. Farcasiu, *Coal liquefaction: the chemistry and technology of thermal processes.* New York, Academic Press, Inc., 1980. 390 p., 1980. **1**.
47. Singh, A., S.I. Olsen, and P.S. Nigam, *A viable technology to generate third-generation biofuel.* Journal of Chemical Technology & Biotechnology, 2011. **86**(11): p. 1349-1353.
48. Minowa, T., et al., *Oil production from algal cells of Dunaliella tertiolecta by direct thermochemical liquefaction.* Fuel, 1995. **74**(12): p. 1735-1738.
49. Li, Y., et al., *Thermal and hydrothermal stabilities of the alkali-treated HZSM-5 zeolites.* Journal of Natural Gas Chemistry, 2008. **17**(1): p. 69-74.
50. Benziger, J.B. and R.J. Madix, *The decomposition of formic acid on Ni(100).* Surface Science, 1979. **79**(2): p. 394-412.
51. Li, Y., et al., *Biofuels from Microalgae.* Biotechnology Progress, 2008. **24**(4): p. 815-820.
52. Zhu, X.-G., S.P. Long, and D.R. Ort, *Improving photosynthetic efficiency for greater yield.* Annual review of plant biology, 2010. **61**: p. 235-261.
53. Stephens, E., et al., *Future prospects of microalgal biofuel production systems.* Trends in Plant Science, 2010. **15**(10): p. 554-564.
54. Sawayama, S., T. Minowa, and S.Y. Yokoyama, *Possibility of renewable energy production and CO2 mitigation by thermochemical liquefaction of microalgae.* Biomass and Bioenergy, 1999. **17**(1): p. 33-39.
55. Chisti, Y., *Constraints to commercialization of algal fuels.* Journal of Biotechnology, 2013. **167**(3): p. 201-214.
56. Perez-Garcia, O., et al., *Heterotrophic cultures of microalgae: Metabolism and potential products.* Water Research, 2011. **45**(1): p. 11-36.
57. Espinosa-Gonzalez, I., A. Parashar, and D.C. Bressler, *Heterotrophic growth and lipid accumulation of Chlorella protothecoides in whey permeate, a dairy by-product stream, for biofuel production.* Bioresource Technology, 2014. **155**(0): p. 170-176.
58. Grobbelaar, J.U., Algal Nutrition. Teoksessa Handbook of Microalgal Culture: Biotechnology and Applied Phycology. A., 2004: p. 97-115.
59. Woertz, I., et al., *Algae Grown on Dairy and Municipal Wastewater for Simultaneous Nutrient Removal and Lipid Production for Biofuel Feedstock.* Journal of Environmental Engineering, 2009. **135**(11): p. 1115-1122.

60. Markou, G. and D. Georgakakis, *Cultivation of filamentous cyanobacteria (blue-green algae) in agro-industrial wastes and wastewaters: a review.* Applied Energy, 2011. **88**(10): p. 3389-3401.

61. Satoh, A., et al., *Characterization of the lipid accumulation in a new microalgal species, Pseudochoricystis ellipsoidea (Trebouxiophyceae).* 日本エネルギー学会誌, 2010. **89**(9): p. 909-913.

62. Bayramoğlu, G., et al., *Biosorption of mercury(II), cadmium(II) and lead(II) ions from aqueous system by microalgae Chlamydomonas reinhardtii immobilized in alginate beads.* International Journal of Mineral Processing, 2006. **81**(1): p. 35-43.

63. Haiduc, A., et al., *SunCHem: an integrated process for the hydrothermal production of methane from microalgae and CO₂ mitigation.* Journal of Applied Phycology, 2009. **21**(5): p. 529-541.

64. Yusuf, C., *Biodiesel from microalgae.* Biotechnology Advances, 2007. **25**(3): p. 294-306.

65. Sánchez Mirón, A., et al., *Comparative evaluation of compact photobioreactors for large-scale monoculture of microalgae.* Journal of Biotechnology, 1999. **70**(1–3): p. 249-270.

66. Maity, J.P., et al., *Microalgae for third generation biofuel production, mitigation of greenhouse gas emissions and wastewater treatment: Present and future perspectives – A mini review.* Energy, (0).

67. Chisti, Y., *Raceways-based production of algal crude oil.* Green, 2013. **3**(3-4): p. 195-216.

68. Li, Y.-G., et al., *Microalgal biodiesel in China: opportunities and challenges.* Applied Energy, 2011. **88**(10): p. 3432-3437.

69. Pragya, N., K.K. Pandey, and P.K. Sahoo, *A review on harvesting, oil extraction and biofuels production technologies from microalgae.* Renewable and Sustainable Energy Reviews, 2013. **24**(0): p. 159-171.

70. Bligh, E.G. and W.J. Dyer, *A rapid method of total lipid extraction and purification.* Canadian Journal of Biochemistry and Physiology, 1959. **37**(8): p. 911-917.

71. Kim, Y.-H., et al., *Ionic liquid-mediated extraction of lipids from algal biomass.* Bioresource Technology, 2012. **109**(0): p. 312-315.

72. Demirbas, A. and M. Fatih Demirbas, *Importance of algae oil as a source of biodiesel.* Energy Conversion and Management, 2011. **52**(1): p. 163-170.

73. Ehimen, E., Z. Sun, and C. Carrington, *Variables affecting the in situ transesterification of microalgae lipids.* Fuel, 2010. **89**(3): p. 677-684.

74. Ehimen, E.A., Z. Sun, and G.C. Carrington, *Use of Ultrasound and Co-Solvents to Improve the In-Situ Transesterification of Microalgae Biomass.* Procedia Environmental Sciences, 2012. **15**(0): p. 47-55.
75. Martinez-Guerra, E., et al., *Extractive-transesterification of algal lipids under microwave irradiation with hexane as solvent.* Bioresource Technology, 2014. **156**(0): p. 240-247.
76. Levine, R.B., T. Pinnarat, and P.E. Savage, *Biodiesel Production from Wet Algal Biomass through in Situ Lipid Hydrolysis and Supercritical Transesterification.* Energy & Fuels, 2010. **24**(9): p. 5235-5243.
77. Ward, O.P. and A. Singh, *Omega-3/6 fatty acids: alternative sources of production.* Process Biochemistry, 2005. **40**(12): p. 3627-3652.
78. Singh, J. and S. Gu, *Commercialization potential of microalgae for biofuels production.* Renewable and Sustainable Energy Reviews, 2010. **14**(9): p. 2596-2610.
79. Guedes, A.C., H.M. Amaro, and F.X. Malcata, *Microalgae as sources of carotenoids.* Marine drugs, 2011. **9**(4): p. 625-644.
80. Tran, M., et al., *Production of unique immunotoxin cancer therapeutics in algal chloroplasts.* Proceedings of the National Academy of Sciences, 2013. **110**(1): p. E15-E22.
81. French, R. and S. Czernik, *Catalytic pyrolysis of biomass for biofuels production.* Fuel Processing Technology, 2010. **91**(1): p. 25-32.
82. Otsuka, K. and A. Yoshino. *A fundamental study on anaerobic digestion of sea lettuce*. in *OCEANS'04. MTTS/IEEE TECHNO-OCEAN'04*. 2004. IEEE.
83. Long, R.Q. and R.T. Yang, *Superior ion-exchanged ZSM-5 catalysts for selective catalytic oxidation of ammonia to nitrogen.* Chemical Communications, 2000(17): p. 1651-1652.
84. Wojciechowski, B.W., *The Reaction Mechanism of Catalytic Cracking: Quantifying Activity, Selectivity, and Catalyst Decay.* Catalysis Reviews, 1998. **40**(3): p. 209-328.
85. Milne, T.A., R.J. Evans, and N. Nagle, *Catalytic conversion of microalgae and vegetable oils to premium gasoline, with shape-selective zeolites.* Biomass, 1990. **21**(3): p. 219-232.
86. Miao, X., Q. Wu, and C. Yang, *Fast pyrolysis of microalgae to produce renewable fuels.* Journal of Analytical and Applied Pyrolysis, 2004. **71**(2): p. 855-863.
87. Miao, X. and Q. Wu, *High yield bio-oil production from fast pyrolysis by metabolic controlling of Chlorella protothecoides.* Journal of Biotechnology, 2004. **110**(1): p. 85-93.

88. Rawat, I., et al., *Dual role of microalgae: Phycoremediation of domestic wastewater and biomass production for sustainable biofuels production.* Applied Energy, 2011. **88**(10): p. 3411-3424.

89. Modell, M., *Processing methods for the oxidation of organics in supercritical water*. 1982, Google Patents.

90. Brunner, G., *Near critical and supercritical water. Part I. Hydrolytic and hydrothermal processes.* The Journal of Supercritical Fluids, 2009. **47**(3): p. 373-381.

91. Chornet, E. and R.P. Overend, *Biomass liquefaction: an overview*, in *Fundamentals of thermochemical biomass conversion*. 1985, Springer. p. 967-1002.

92. Tissot, B., et al., *Influence of nature and diagenesis of organic matter in formation of petroleum.* AAPG Bulletin, 1974. **58**(3): p. 499-506.

93. Kohara, M., et al., *Stability of amino acids in simulated hydrothermal vent environments.* Chemistry Letters, 1997(10): p. 1053-1054.

94. Peterson, A.A., et al., *Thermochemical biofuel production in hydrothermal media: A review of sub- and supercritical water technologies.* Energy & Environmental Science, 2008. **1**(1): p. 32-65.

95. Heger, K., M. Uematsu, and E.U. Franck, *The Static Dielectric Constant of Water at High Pressures and Temperatures to 500 MPa and 550°C.* Berichte der Bunsengesellschaft für physikalische Chemie, 1980. **84**(8): p. 758-762.

96. Khuwijitjaru, P., S. Adachi, and R. Matsuno, *Solubility of saturated fatty acids in water at elevated temperatures.* Bioscience, biotechnology, and biochemistry, 2002. **66**(8): p. 1723-1726.

97. Akiya, N. and P.E. Savage, *Roles of Water for Chemical Reactions in High-Temperature Water.* Chemical Reviews, 2002. **102**(8): p. 2725-2750.

98. Marrone, P.A., et al., *Salt precipitation and scale control in supercritical water oxidation—part B: commercial/full-scale applications.* The Journal of Supercritical Fluids, 2004. **29**(3): p. 289-312.

99. Krammer, P. and H. Vogel, *Hydrolysis of esters in subcritical and supercritical water.* The Journal of Supercritical Fluids, 2000. **16**(3): p. 189-206.

100. Duan, P., L. Dai, and P.E. Savage, *Kinetics and mechanism of N-substituted amide hydrolysis in high-temperature water.* The Journal of Supercritical Fluids, 2010. **51**(3): p. 362-368.

101. Xu, X., M.J. Antal, and D.G.M. Anderson, *Mechanism and Temperature-Dependent Kinetics of the Dehydration of tert-Butyl Alcohol in Hot Compressed Liquid Water.* Industrial & Engineering Chemistry Research, 1997. **36**(1): p. 23-41.

102. Chandler, K., et al., *Tuning alkylation reactions with temperature in near-critical water.* AIChE journal, 1998. **44**(9): p. 2080-2087.

103. Nolen, S.A., et al., *The catalytic opportunities of near-critical water: a benign medium for conventionally acid and base catalyzed condensations for organic synthesis.* Green Chemistry, 2003. **5**(5): p. 663-669.

104. Kabyemela, B.M., et al., *Glucose and fructose decomposition in subcritical and supercritical water: detailed reaction pathway, mechanisms, and kinetics.* Industrial & Engineering Chemistry Research, 1999. **38**(8): p. 2888-2895.

105. Kruse, A. and E. Dinjus, *Hot compressed water as reaction medium and reactant: properties and synthesis reactions.* The Journal of Supercritical Fluids, 2007. **39**(3): p. 362-380.

106. Ikushima, Y., et al., *Acceleration of Synthetic Organic Reactions Using Supercritical Water: Noncatalytic Beckmann and Pinacol Rearrangements.* Journal of the American Chemical Society, 2000. **122**(9): p. 1908-1918.

107. Mosteiro-Romero, M., F. Vogel, and A. Wokaun, *Liquefaction of wood in hot compressed water: Part 1 — Experimental results.* Chemical Engineering Science, 2014. **109**(0): p. 111-122.

108. Meier, D., D.R. Larimer, and O. Faix, *Direct liquefaction of different lignocellulosics and their constituents: 1. Fractionation, elemental composition.* Fuel, 1986. **65**(7): p. 910-915.

109. Holliday, R.L., J.W. King, and G.R. List, *Hydrolysis of Vegetable Oils in Sub- and Supercritical Water.* Industrial & Engineering Chemistry Research, 1997. **36**(3): p. 932-935.

110. W. King, J., R. L. Holliday, and G. R. List, *Hydrolysis of soybean oil . in a subcritical water flow reactor.* Green Chemistry, 1999. **1**(6): p. 261-264.

111. Dote, Y., et al., *Distribution of nitrogen to oil products from liquefaction of amino acids.* Bioresource Technology, 1998. **64**(2): p. 157-160.

112. Biller, P. and A.B. Ross, *Potential yields and properties of oil from the hydrothermal liquefaction of microalgae with different biochemical content.* Bioresource Technology, 2011. **102**(1): p. 215-225.

113. Titirici, M.-M. and M. Antonietti, *Chemistry and materials options of sustainable carbon materials made by hydrothermal carbonization.* Chemical Society Reviews, 2010. **39**(1): p. 103-116.

114. Heilmann, S.M., et al., *Hydrothermal carbonization of microalgae.* Biomass and Bioenergy, 2010. **34**(6): p. 875-882.

115. Broch, A., et al., *Analysis of Solid and Aqueous Phase Products from Hydrothermal Carbonization of Whole and Lipid-Extracted Algae.* Energies, 2013. **7**(1): p. 62-79.

116. Heilmann, S.M., et al., *Hydrothermal carbonization of microalgae II. Fatty acid, char, and algal nutrient products.* Applied Energy, 2011. **88**(10): p. 3286-3290.

117. Du, Z., et al., *Cultivation of a microalga Chlorella vulgaris using recycled aqueous phase nutrients from hydrothermal carbonization process.* Bioresource Technology, 2012. **126**(0): p. 354-357.

118. Falco, C., et al., *Renewable Nitrogen-Doped Hydrothermal Carbons Derived from Microalgae*. ChemSusChem, 2012. **5**(9): p. 1834-1840.

119. Dote, Y., et al., *Recovery of liquid fuel from hydrocarbon-rich microalgae by thermochemical liquefaction.* Fuel, 1994. **73**(12): p. 1855-1857.

120. Inoue, S., et al., *Analysis of oil derived from liquefaction of< i> Botryococcus Braunii</i>*. Biomass and Bioenergy, 1994. **6**(4): p. 269-274.

121. Metzger, P. and C. Largeau, *<i>Botryococcus braunii</i>: a rich source for hydrocarbons and related ether lipids.* Applied Microbiology and Biotechnology, 2005. **66**(5): p. 486-496.

122. Sawayama, S., et al., *CO2 fixation and oil production through microalga.* Energy Conversion and Management, 1995. **36**(6–9): p. 729-731.

123. Yang, Y.F., et al., *Analysis of energy conversion characteristics in liquefaction of algae.* Resources, Conservation and Recycling, 2004. **43**(1): p. 21-33.

124. Zou, S., et al., *Bio-oil production from sub- and supercritical water liquefaction of microalgae Dunaliella tertiolecta and related properties.* Energy & Environmental Science, 2010. **3**(8): p. 1073-1078.

125. Shuping, Z., et al., *Production and characterization of bio-oil from hydrothermal liquefaction of microalgae Dunaliella tertiolecta cake.* Energy, 2010. **35**(12): p. 5406-5411.

126. Yu, G., et al., *Hydrothermal liquefaction of low lipid content microalgae into bio-crude oil.* Trans. ASABE, 2011. **54**(1): p. 239-246.

127. Brown, T.M., P. Duan, and P.E. Savage, *Hydrothermal Liquefaction and Gasification of Nannochloropsis sp.* Energy & Fuels, 2010. **24**(6): p. 3639-3646.

128. Vardon, D.R., et al., *Thermochemical conversion of raw and defatted algal biomass via hydrothermal liquefaction and slow pyrolysis.* Bioresource Technology, 2012. **109**: p. 178-187.

129. Ross, A.B., et al., *Hydrothermal processing of microalgae using alkali and organic acids.* Fuel, 2010. **89**(9): p. 2234-2243.

130. Vardon, D.R., et al., *Chemical properties of biocrude oil from the hydrothermal liquefaction of< i> Spirulina</i> algae, swine manure, and digested anaerobic sludge.* Bioresource Technology, 2011. **102**(17): p. 8295-8303.

131. Jena, U., K.C. Das, and J.R. Kastner, *Effect of operating conditions of thermochemical liquefaction on biocrude production from Spirulina platensis.* Bioresource Technology, 2011. **102**(10): p. 6221-6229.

132. Toor, S.S., et al., *Hydrothermal liquefaction of Spirulina and Nannochloropsis salina under subcritical and supercritical water conditions.* Bioresource Technology, 2013. **131**(0): p. 413-419.

133. Garcia Alba, L., et al., *Hydrothermal Treatment (HTT) of Microalgae: Evaluation of the Process As Conversion Method in an Algae Biorefinery Concept.* Energy & Fuels, 2011. **26**(1): p. 642-657.

134. López Barreiro, D., et al., *Influence of strain-specific parameters on hydrothermal liquefaction of microalgae.* Bioresource Technology, 2013. **146**(0): p. 463-471.

135. Valdez, P.J., J.G. Dickinson, and P.E. Savage, *Characterization of Product Fractions from Hydrothermal Liquefaction of Nannochloropsis sp. and the Influence of Solvents.* Energy & Fuels, 2011. **25**(7): p. 3235-3243.

136. Valdez, P.J. and P.E. Savage, *A reaction network for the hydrothermal liquefaction of< i> Nannochloropsis</i> sp.* Algal Research, 2013. **2**(4): p. 416-425.

137. Torri, C., et al., *Hydrothermal Treatment (HTT) of Microalgae: Detailed Molecular Characterization of HTT Oil in View of HTT Mechanism Elucidation.* Energy & Fuels, 2011. **26**(1): p. 658-671.

138. Miao, C., M. Chakraborty, and S. Chen, *Impact of reaction conditions on the simultaneous production of polysaccharides and bio-oil from heterotrophically grown< i> Chlorella sorokiniana</i> by a unique sequential hydrothermal liquefaction process.* Bioresource Technology, 2012. **110**: p. 617-627.

139. Chakraborty, M., et al., *Concomitant extraction of bio-oil and value added polysaccharides from< i> Chlorella sorokiniana</i> using a unique sequential hydrothermal extraction technology.* Fuel, 2012. **95**: p. 63-70.

140. Garcia-Moscoso, J.L., et al., *Flash hydrolysis of microalgae (Scenedesmus sp.) for protein extraction and production of biofuels intermediates.* The Journal of Supercritical Fluids, 2013. **82**(0): p. 183-190.

141. Biller, P., C. Friedman, and A.B. Ross, *Hydrothermal microwave processing of microalgae as a pre-treatment and extraction technique for bio-fuels and bio-products.* Bioresource Technology, 2013. **136**(0): p. 188-195.

142. Cheng, J., et al., *Biodiesel production from lipids in wet microalgae with microwave irradiation and bio-crude production from algal residue through hydrothermal liquefaction.* Bioresource Technology, 2014. **151**(0): p. 415-418.

143. Biller, P., et al., *Nutrient recycling of aqueous phase for microalgae cultivation from the hydrothermal liquefaction process.* Algal Research, 2012. **1**(1): p. 70-76.

144. Garcia Alba, L., et al., *Microalgae growth on the aqueous phase from Hydrothermal Liquefaction of the same microalgae.* Chemical Engineering Journal, 2013. **228**(0): p. 214-223.

145. Chen, W.-T., et al., *Hydrothermal liquefaction of mixed-culture algal biomass from wastewater treatment system into bio-crude oil.* Bioresource Technology, 2014. **152**: p. 130-139.

146. Chen, W.-T., et al., *Co-liquefaction of swine manure and mixed-culture algal biomass from a wastewater treatment system to produce bio-crude oil.* Applied Energy, 2014. **128**: p. 209-216.

147. Bai, X., et al., *Hydrothermal catalytic processing of pretreated algal oil: A catalyst screening study*. Fuel, 2014. **120**: p. 141-149.

148. Zhou, D., et al., *Hydrothermal Liquefaction of Macroalgae Enteromorpha prolifera to Bio-oil*. Energy & Fuels, 2010. **24**(7): p. 4054-4061.

149. Anastasakis, K. and A.B. Ross, *Hydrothermal liquefaction of the brown macro-alga Laminaria Saccharina: Effect of reaction conditions on product distribution and composition.* Bioresource Technology, 2011. **102**(7): p. 4876-4883.

150. Li, D., et al., *Preparation and characteristics of bio-oil from the marine brown alga Sargassum patens C. Agardh.* Bioresource Technology, 2012. **104**(0): p. 737-742.

151. Neveux, N., et al., *Biocrude yield and productivity from the hydrothermal liquefaction of marine and freshwater green macroalgae.* Bioresource Technology, 2014. **155**(0): p. 334-341.

152. Faeth, J.L., P.J. Valdez, and P.E. Savage, *Fast Hydrothermal Liquefaction of Nannochloropsis sp. To Produce Biocrude.* Energy & Fuels, 2013. **27**(3): p. 1391-1398.

153. Elliott, D.C., et al., *Process development for hydrothermal liquefaction of algae feedstocks in a continuous-flow reactor*. Algal Research, 2013. **2**(4): p. 445-454.

154. Jena, U., K. Das, and J. Kastner, *Comparison of the effects of Na2CO3, Ca3 (PO4) 2, and NiO catalysts on the thermochemical liquefaction of microalga Spirulina platensis.* Applied Energy, 2012. **98**(C): p. 368-375.

155. Yu, J. and P.E. Savage, *Decomposition of Formic Acid under Hydrothermal Conditions*. Industrial & Engineering Chemistry Research, 1998. **37**(1): p. 2-10.

156. Duan, P., et al., *Catalytic upgrading of crude algal oil using platinum/gamma alumina in supercritical water.* Fuel, 2013. **109**(0): p. 225-233.

157. Salak Asghari, F. and H. Yoshida, *Acid-catalyzed production of 5-hydroxymethyl furfural from D-fructose in subcritical water.* Industrial & Engineering Chemistry Research, 2006. **45**(7): p. 2163-2173.

158. Crossey, L.J., *Thermal degradation of aqueous oxalate species.* Geochimica et Cosmochimica Acta, 1991. **55**(6): p. 1515-1527.

159. Jin, F., et al., *Hydrothermal conversion of carbohydrate biomass into formic acid at mild temperatures*. Green Chemistry, 2008. **10**(6): p. 612-615.

160. Izhar, S., et al., *Hydrodenitrogenation of fast pyrolysis bio-oil derived from sewage sludge on NiMo/Al< sub> 2</sub> O< sub> 3</sub> sulfide catalyst.* Fuel Processing Technology, 2012. **101**: p. 10-15.

161. Elliott, D. and L. Sealock Jr, *Chemical processing in high-pressure aqueous environments: low-temperature catalytic gasification.* Trans IChemE, 1996. **74**(Part A).

162. Minowa, T. and S. Sawayama, *A novel microalgal system for energy production with nitrogen cycling.* Fuel, 1999. **78**(10): p. 1213-1215.

163. Stucki, S., et al., *Catalytic gasification of algae in supercritical water for biofuel production and carbon capture.* Energy & Environmental Science, 2009. **2**(5): p. 535-541.

164. Chakinala, A.G., et al., *Catalytic and Non-catalytic Supercritical Water Gasification of Microalgae and Glycerol.* Industrial & Engineering Chemistry Research, 2009. **49**(3): p. 1113-1122.

165. Guan, Q., P.E. Savage, and C. Wei, *Gasification of alga Nannochloropsis sp. in supercritical water.* The Journal of Supercritical Fluids, 2012. **61**(0): p. 139-145.

166. Onwudili, J.A., et al., *Catalytic hydrothermal gasification of algae for hydrogen production: Composition of reaction products and potential for nutrient recycling.* Bioresource Technology, 2013. **127**(0): p. 72-80.

167. Schumacher, M., et al., *Hydrothermal conversion of seaweeds in a batch autoclave.* The Journal of Supercritical Fluids, 2011. **58**(1): p. 131-135.

168. Cherad, R., et al., *Macroalgae supercritical water gasification combined with nutrient recycling for microalgae cultivation.* Environmental Progress & Sustainable Energy, 2013. **32**(4): p. 902-909.

169. Azadi, P. and R. Farnood, *Review of heterogeneous catalysts for sub- and supercritical water gasification of biomass and wastes.* International Journal of Hydrogen Energy, 2011. **36**(16): p. 9529-9541.

170. E.M. Flanigen, J.C.J., Herman van Bekkum, *Introduction to Zeolite Science and Practice (Studies in Surface Science and Catalysis*. 1991: Elsevier Science (5 Feb 1991) 754.

171. Weitkamp, J., *Zeolites and catalysis.* Solid State Ionics, 2000. **131**(1–2): p. 175-188.

172. Csicsery, S.M., *Shape-selective catalysis in zeolites.* Zeolites, 1984. **4**(3): p. 202-213.

173. Davis, M.E., et al., *VPI-5: The first molecular sieve with pores larger than 10 Ångstroms.* Zeolites, 1988. **8**(5): p. 362-366.

174. Wilson, S.T., et al., *Aluminophosphate molecular sieves: a new class of microporous crystalline inorganic solids.* Journal of the American Chemical Society, 1982. **104**(4): p. 1146-1147.

175. Jhung, S.H., et al., *Selective formation of SAPO-5 and SAPO-34 molecular sieves with microwave irradiation and hydrothermal heating.* Microporous and Mesoporous Materials, 2003. **64**(1): p. 33-39.

176. Venuto, P.B. and E.T. Habib Jr, *Fluid catalytic cracking with zeolite catalysts.* 1979.

177. López, D.E., et al., *Transesterification of triacetin with methanol on solid acid and base catalysts.* Applied Catalysis A: General, 2005. **295**(2): p. 97-105.

178. Shu, Q., et al., *Synthesis of biodiesel from soybean oil and methanol catalyzed by zeolite beta modified with La3+.* Catalysis Communications, 2007. **8**(12): p. 2159-2165.

179. Idem, R.O., S.P.R. Katikaneni, and N.N. Bakhshi, *Catalytic conversion of canola oil to fuels and chemicals: roles of catalyst acidity, basicity and shape selectivity on product distribution.* Fuel Processing Technology, 1997. **51**(1-2): p. 101-125.

180. Kubička, D., M. Bejblová, and J. Vlk, *Conversion of Vegetable Oils into Hydrocarbons over CoMo/MCM-41 Catalysts.* Topics in Catalysis, 2010. **53**(3): p. 168-178.

181. Twaiq, F.A., N.A.M. Zabidi, and S. Bhatia, *Catalytic Conversion of Palm Oil to Hydrocarbons: Performance of Various Zeolite Catalysts.* Industrial & Engineering Chemistry Research, 1999. **38**(9): p. 3230-3237.

182. Perego, C. and A. Bosetti, *Biomass to fuels: The role of zeolite and mesoporous materials.* Microporous and Mesoporous Materials, 2011. **144**(1-3): p. 28-39.

183. Yakovlev, V.A., et al., *Development of new catalytic systems for upgraded bio-fuels production from bio-crude-oil and biodiesel.* Catalysis Today, 2009. **144**(3-4): p. 362-366.

184. Fukuoka, A. and P.L. Dhepe, *Catalytic Conversion of Cellulose into Sugar Alcohols.* Angewandte Chemie International Edition, 2006. **45**(31): p. 5161-5163.

185. Peng, B., et al., *Towards Quantitative Conversion of Microalgae Oil to Diesel-Range Alkanes with Bifunctional Catalysts.* Angewandte Chemie, 2012. **124**(9): p. 2114-2117.

186. Du, Z., et al., *Catalytic pyrolysis of microalgae and their three major components: Carbohydrates, proteins, and lipids.* Bioresource Technology, 2013. **130**(0): p. 777-782.

187. Thangalazhy-Gopakumar, S., et al., *Catalytic pyrolysis of green algae for hydrocarbon production using H< sup>+</sup> ZSM-5 catalyst.* Bioresource Technology, 2012. **118**: p. 150-157.

188. Ravenelle, R.M., et al., *Stability of zeolites in hot liquid water.* The Journal of Physical Chemistry C, 2010. **114**(46): p. 19582-19595.

189. Mo, N. and P.E. Savage, *Hydrothermal Catalytic Cracking of Fatty Acids with HZSM-5.* ACS Sustainable Chemistry & Engineering, 2013.

190. Duan, P. and P.E. Savage, *Hydrothermal Liquefaction of a Microalga with Heterogeneous Catalysts.* Industrial & Engineering Chemistry Research, 2010. **50**(1): p. 52-61.

191. Yang, C., et al., *Bio-oil from hydro-liquefaction of Dunaliella salina over Ni/REHY catalyst.* Bioresource Technology, 2011. **102**(6): p. 4580-4584.

192. Sınağ, A., et al., *Biomass decomposition in near critical water.* Energy Conversion and Management, 2010. **51**(3): p. 612-620.

193. Xian, X., et al., *Catalytic cracking of n-dodecane over HZSM-5 zeolite under supercritical conditions: Experiments and kinetics.* Chemical Engineering Science, 2010. **65**(20): p. 5588-5604.

194. Hillen, L.W., et al., *Hydrocracking of the oils of Botryococcus braunii to transport fuels.* Biotechnology and Bioengineering, 1982. **24**(1): p. 193-205.

195. Matsui, T.-o., et al., *Liquefaction of micro-algae with iron catalyst.* Fuel, 1997. **76**(11): p. 1043-1048.

196. Biller, P., R. Riley, and A.B. Ross, *Catalytic hydrothermal processing of microalgae: Decomposition and upgrading of lipids.* Bioresource Technology, 2011. **102**(7): p. 4841-4848.

197. Zhang, J., et al., *Hydrothermal liquefaction of Chlorella pyrenoidosa in sub- and supercritical ethanol with heterogeneous catalysts.* Bioresource Technology, 2013. **133**(0): p. 389-397.

198. Duan, P. and P.E. Savage, *Upgrading of crude algal bio-oil in supercritical water.* Bioresource Technology, 2011. **102**(2): p. 1899-1906.

199. Duan, P. and P.E. Savage, *Catalytic treatment of crude algal bio-oil in supercritical water: optimization studies.* Energy & Environmental Science, 2011. **4**(4): p. 1447-1456.

200. Duan, P. and P.E. Savage, *Catalytic hydrotreatment of crude algal bio-oil in supercritical water.* Applied Catalysis B: Environmental, 2011. **104**(1): p. 136-143.

201. Duan, J., et al., *Hydrothermally stable regenerable catalytic supports for aqueous-phase conversion of biomass.* Catalysis Today, 2014. **234**(0): p. 66-74.

202. Delrue, F., et al., *Comparison of various microalgae liquid biofuel production pathways based on energetic, economic and environmental criteria.* Bioresource Technology, 2013. **136**(0): p. 205-212.

203. Frank, E., et al., *Life cycle comparison of hydrothermal liquefaction and lipid extraction pathways to renewable diesel from algae.* Mitigation and Adaptation Strategies for Global Change, 2013. **18**(1): p. 137-158.

204. Ou, L., et al., *Techno-economic analysis of transportation fuels from defatted microalgae via hydrothermal liquefaction and hydroprocessing.* Biomass and Bioenergy, 2015. **72**(0): p. 45-54.
205. Liu, X., et al., *Pilot-scale data provide enhanced estimates of the life cycle energy and emissions profile of algae biofuels produced via hydrothermal liquefaction.* Bioresource Technology, 2013. **148**: p. 163-171.
206. Fortier, M.-O.P., et al., *Life cycle assessment of bio-jet fuel from hydrothermal liquefaction of microalgae.* Applied Energy, 2014. **122**(0): p. 73-82.
207. Skoog, D., et al., *Fundamentals of analytical chemistry*. 2013: Cengage Learning.
208. Strobel, H.A., *Chemical Instrumentation: A Systematic Approach*. 1973: Addison-Wesley Pub. Co.
209. Instrument, S. *Size Exclusion Chromatography*. December 2011 [cited 2012 26.03.2012]; Available from: http://www.shimadzu.com/an/hplc/support/lib/lctalk/55/55intro.html.
210. Dugan, G., *Automatic Carbon, Hydrogen, Nitrogen, Sulfur Analyzer Ciiemistry of Sulfur Reactions.* Analytical Letters, 1977. **10**(7-8): p. 639-657.
211. Corbitt, R.A., *Standard handbook of environmental engineering*, ed. T. Engineering. 1999: McGraw-Hill.
212. Vogel, A.I., *Vogel's textbook of quantitative chemical analysis*. 1989: Harlow : Longman Scientific & Technical.
213. Pratt, J.R.A.K.C., *Introduction to Characterisation and Testing of Catalysts*. 1985, Melbourne: Academic Press (Harcourt Brace Jovanovich).
214. Namba, S., et al., *Novel purification method of commercial< i> o</i>-and< i> m</i>-xylenes by shape selective adsorption on HZSM-5.* Microporous materials, 1997. **8**(1): p. 39-42.
215. Corma, A., et al., *Processing biomass-derived oxygenates in the oil refinery: Catalytic cracking (FCC) reaction pathways and role of catalyst.* Journal of Catalysis, 2007. **247**(2): p. 307-327.
216. Gayubo, A.G., et al., *Deactivation of a HZSM-5 Zeolite Catalyst in the Transformation of the Aqueous Fraction of Biomass Pyrolysis Oil into Hydrocarbons.* Energy & Fuels, 2004. **18**(6): p. 1640-1647.
217. de Lucas, A., et al., *Dealumination of HZSM-5 zeolites: Effect of steaming on acidity and aromatization activity*. Applied Catalysis A: General, 1997. **154**(1-2): p. 221-240.
218. Gayubo, A.G., et al., *Role of reaction-medium water on the acidity deterioration of a HZSM-5 zeolite.* Industrial & Engineering Chemistry Research, 2004. **43**(17): p. 5042-5048.

219. Sano, T., et al., *Erratum to: Realumination of dealuminated HZSM-5 zeolites by acid treatment and their catalytic properties [Microporous and Mesoporous Materials 31 (1999) 89–95]*. Microporous and Mesoporous Materials, 2000. **34**(3): p. 348.

220. Gayubo, A.G., et al., *Hydrothermal stability of HZSM-5 catalysts modified with Ni for the transformation of bioethanol into hydrocarbons.* Fuel, 2010. **89**(11): p. 3365-3372.

221. Song, Y., et al., *Hydrothermal post-synthesis of HZSM-5 zeolite to enhance the coke-resistance of Mo/HZSM-5 catalyst for methane dehydroaromatization reaction: Reconstruction of pore structure and modification of acidity.* Applied Catalysis A: General, 2007. **317**(2): p. 266-274.

222. Song, Y., et al., *Hydrothermal Post-synthesis of HZSM-5 Zeolite to Enhance the Coke-resistance of Mo/HZSM-5 Catalyst for Methane Dehydroaromatization.* Catalysis Letters, 2006. **109**(1): p. 21-24.

223. Sato, S., et al., *Cu-ZSM-5 zeolite as highly active catalyst for removal of nitrogen monoxide from emission of diesel engines.* Applied Catalysis, 1991. **70**(1): p. L1-L5.

224. Ortega, J.M., et al., *Role of coke characteristics in the regeneration of a catalyst for the MTG process.* Industrial & Engineering Chemistry Research, 1997. **36**(1): p. 60-66.

225. Xue, N., et al., *Understanding the enhancement of catalytic performance for olefin cracking: Hydrothermally stable acids in P/HZSM-5.* Journal of Catalysis, 2007. **248**(1): p. 20-28.

226. Pieterse, J.A.Z., et al., *Hydrothermal stability of Fe-ZSM-5 and Fe-BEA prepared by wet ion-exchange for N2O decomposition.* Applied Catalysis B: Environmental, 2007. **71**(1-2): p. 16-22.

227. Pollack, S., et al., *SiO2Al2O3 ratios of ZSM—5 crystals measured by electron microprobe and X-ray diffraction.* Zeolites, 1984. **4**(2): p. 181-187.

228. De Lucas, A., et al., *Coke formation, location, nature and regeneration on dealuminated HZSM-5 type zeolites.* Applied Catalysis A: General, 1997. **156**(2): p. 299-317.

229. Ma, F. and M.A. Hanna, *Biodiesel production: a review.* Bioresource Technology, 1999. **70**(1): p. 1-15.

230. Watanabe, M., T. Iida, and H. Inomata, *Decomposition of a long chain saturated fatty acid with some additives in hot compressed water.* Energy Conversion and Management, 2006. **47**(18-19): p. 3344-3350.

231. Shin, H.-Y., et al., *Thermal stability of fatty acids in subcritical water.* Journal of Analytical and Applied Pyrolysis, 2012. **98**(0): p. 250-253.

232. Benson, T.J., et al., *Elucidation of the catalytic cracking pathway for unsaturated mono-, di-, and triacylglycerides on solid acid catalysts.* Journal of Molecular Catalysis A: Chemical, 2009. **303**(1–2): p. 117-123.

233. Harris, H.C., J. McWilliam, and W. Mason, *Influence of temperature on oil content and composition of sunflower seed.* Crop and Pasture Science, 1978. **29**(6): p. 1203-1212.

234. Pinto, J.S.S. and F.M. Lanças, *Hydrolysis of corn oil using subcritical water*. Journal of the Brazilian Chemical Society, 2006. **17**: p. 85-89.

235. Alenezi, R., et al., *Continuous Flow Hydrolysis of Sunflower Oil Using Sub-critical Water*.

236. Li, L., et al., *Catalytic Hydrothermal Conversion of Triglycerides to Non-ester Biofuels.* Energy & Fuels, 2010. **24**(2): p. 1305-1315.

237. Mounts, T.L., et al., *Effect of altered fatty acid composition on soybean oil stability.* Journal of the American Oil Chemists' Society, 1988. **65**(4): p. 624-628.

238. Bannister, C.D., et al., *Oxidative Stability of Biodiesel Fuel.* Proceedings of the Institution of Mechanical Engineers, Part D: Journal of Automobile Engineering, 2011. **225**(1): p. 99-114.

239. Dobson, G. and J.L. Sebedio, *Monocyclic dienoic fatty acids formed from γ-linolenic acid in heated evening primrose oil.* Chemistry and Physics of Lipids, 1999. **97**(2): p. 105-118.

240. Scatchard, G., W. Hamer, and S. Wood, *Isotonic Solutions. I. The Chemical Potential of Water in Aqueous Solutions of Sodium Chloride, Potassium Chloride, Sulfuric Acid, Sucrose, Urea and Glycerol at 25° 1.* Journal of the American Chemical Society, 1938. **60**(12): p. 3061-3070.

241. Gonçalves, M.L.A., et al., *Investigation of petroleum medium fractions and distillation residues from Brazilian crude oils by thermogravimetry.* Fuel, 2006. **85**(7–8): p. 1151-1155.

242. Fu, J., X. Lu, and P.E. Savage, *Catalytic hydrothermal deoxygenation of palmitic acid.* Energy & Environmental Science, 2010. **3**(3): p. 311-317.

243. Demirbaş, A., *Fuel properties and calculation of higher heating values of vegetable oils.* Fuel, 1998. **77**(9): p. 1117-1120.

244. Sturzenegger, A. and H. Sturm, *Hydrolysis of Fats at High Temperatures.* Industrial & Engineering Chemistry, 1951. **43**(2): p. 510-515.

245. Dobson, G., W.W. Christie, and J.L. Sébédio, *The nature of cyclic fatty acids formed in heated vegetable oils.* Grasas y Aceites, 1996.

246. Sato, M., et al., *Highly-selective and high-speed Claisen rearrangement induced with subcritical water microreaction in the absence of catalyst.* Green Chemistry, 2009. **11**(6): p. 763-766.

247. Wu, N., et al., *Interaction of Fatty Acid Monolayers with Cobalt Nanoparticles.* Nano Letters, 2004. **4**(2): p. 383-386.

248. Vardon, D.R., et al., *Hydrothermal catalytic processing of saturated and unsaturated fatty acids to hydrocarbons with glycerol for in situ hydrogen production.* Green Chemistry, 2014.

249. Volkman, J.K., et al., *Fatty acid and lipid composition of 10 species of microalgae used in mariculture.* Journal of Experimental Marine Biology and Ecology, 1989. **128**(3): p. 219-240.

250. Changi, S., A.J. Matzger, and P.E. Savage, *Kinetics and pathways for an algal phospholipid (1, 2-dioleoyl-sn-glycero-3-phosphocholine) in high-temperature (175–350° C) water.* Green Chemistry, 2012. **14**(10): p. 2856-2867.

251. Brown, M.R., *The amino-acid and sugar composition of 16 species of microalgae used in mariculture.* Journal of Experimental Marine Biology and Ecology, 1991. **145**(1): p. 79-99.

252. Renaud, S. and D. Parry, *Microalgae for use in tropical aquaculture II: effect of salinity on growth, gross chemical composition and fatty acid composition of three species of marine microalgae.* Journal of Applied Phycology, 1994. **6**(3): p. 347-356.

253. Haug, A., et al., *Correlation between chemical structure and physical properties of alginates.* Acta Chem Scand, 1967. **21**(3): p. 768-78.

254. Ghoreishi, S. and R.G. Shahrestani, *Subcritical water extraction of mannitol from olive leaves.* Journal of food engineering, 2009. **93**(4): p. 474-481.

255. Bobleter, O., *Hydrothermal degradation of polymers derived from plants.* Progress in Polymer Science, 1994. **19**(5): p. 797-841.

256. Nagamori, M. and T. Funazukuri, *Glucose production by hydrolysis of starch under hydrothermal conditions.* Journal of chemical technology and biotechnology, 2004. **79**(3): p. 229-233.

257. Miyazawa, T., S. Ohtsu, and T. Funazukuri, *Hydrothermal degradation of polysaccharides in a semi-batch reactor: product distribution as a function of severity parameter.* Journal of Materials Science, 2008. **43**(7): p. 2447-2451.

258. Kabyemela, B.M., et al., *Glucose and Fructose Decomposition in Subcritical and Supercritical Water: Detailed Reaction Pathway, Mechanisms, and Kinetics.* Industrial & Engineering Chemistry Research, 1999. **38**(8): p. 2888-2895.

259. Aida, T.M., et al., *Depolymerization of sodium alginate under hydrothermal conditions.* Carbohydrate Polymers, 2010. **80**(1): p. 296-302.

260. Watanabe, M., et al., *Glucose reactions with acid and base catalysts in hot compressed water at 473 K.* Carbohydrate Research, 2005. **340**(12): p. 1925-1930.

261. Srokol, Z., et al., *Hydrothermal upgrading of biomass to biofuel; studies on some monosaccharide model compounds.* Carbohydrate Research, 2004. **339**(10): p. 1717-1726.

262. Williams, P.T. and J. Onwudili, *Subcritical and Supercritical Water Gasification of Cellulose, Starch, Glucose, and Biomass Waste.* Energy & Fuels, 2006. **20**(3): p. 1259-1265.

263. Promdej, C. and Y. Matsumura, *Temperature Effect on Hydrothermal Decomposition of Glucose in Sub- And Supercritical Water.* Industrial & Engineering Chemistry Research, 2011. **50**(14): p. 8492-8497.

264. Aida, T.M., et al., *Dehydration of d-glucose in high temperature water at pressures up to 80 MPa.* The Journal of Supercritical Fluids, 2007. **40**(3): p. 381-388.

265. Titirici, M.-M., M. Antonietti, and N. Baccile, *Hydrothermal carbon from biomass: a comparison of the local structure from poly-to monosaccharides and pentoses/hexoses.* Green Chemistry, 2008. **10**(11): p. 1204-1212.

266. Chuntanapum, A. and Y. Matsumura, *Formation of tarry material from 5-HMF in subcritical and supercritical water.* Industrial & Engineering Chemistry Research, 2009. **48**(22): p. 9837-9846.

267. Rowbotham, J., et al., *Copper (II)-mediated thermolysis of alginates: a model kinetic study on the influence of metal ions in the thermochemical processing of macroalgae.* Interface focus, 2013. **3**(1): p. 20120046.

268. Gao, S., et al., *Biopolymer-Assisted Synthesis of Single Crystalline Gold Disks by a Hydrothermal Route.* Current Nanoscience, 2008. **4**(2): p. 145-150.

269. Matsushima, K., et al., *Decomposition Reaction of Alginic Acid Using Subcritical and Supercritical Water.* Industrial & Engineering Chemistry Research, 2005. **44**(25): p. 9626-9630.

270. Aida, T.M., et al., *Production of organic acids from alginate in high temperature water.* The Journal of Supercritical Fluids, 2012. **65**: p. 39-44.

271. Zhou, H., et al. *Production of lactic acid from C6-polyols by alkaline hydrothermal reactions*. in *Journal of Physics: Conference Series*. 2010. IOP Publishing.

272. Angyal, S.J., *The Lobry de Bruyn-Alberda van Ekenstein transformation and related reactions*, in *Glycoscience*. 2001, Springer. p. 1-14.

273. Brand, S., et al., *Effect of heating rate on biomass liquefaction: Differences between subcritical water and supercritical ethanol.* Energy, 2014. **68**: p. 420-427.

274. Antal Jr, M.J., W.S.L. Mok, and G.N. Richards, *Mechanism of formation of 5-(hydroxymethyl)-2-furaldehyde from d-fructose and sucrose.* Carbohydrate Research, 1990. **199**(1): p. 91-109.

275. Serrano-Ruiz, J.C., R. Luque, and A. Sepulveda-Escribanoa, *Chem Soc Rev Dynamic Article Links.*

276. Carlson, T.R., T.P. Vispute, and G.W. Huber, *Green gasoline by catalytic fast pyrolysis of solid biomass derived compounds.* ChemSusChem, 2008. **1**(5): p. 397-400.

277. Tressl, R., et al., *Pentoses and Hexoses as Sources of New Melanoidin-like Maillard Polymers.* Journal of Agricultural and Food Chemistry, 1998. **46**(5): p. 1765-1776.

278. Kruse, A., P. Maniam, and F. Spieler, *Influence of Proteins on the Hydrothermal Gasification and Liquefaction of Biomass. 2. Model Compounds.* Industrial & Engineering Chemistry Research, 2006. **46**(1): p. 87-96.

279. H, C., N. KM, and F. S, *Macrophytes as habitat for fauna.* Marine Ecology Progress Series, 2009. **396**: p. 221-233.

280. Leal, D., et al., *FT-IR spectra of alginic acid block fractions in three species of brown seaweeds.* Carbohydrate research, 2008. **343**(2): p. 308-316.

281. Liang, Y., *Producing liquid transportation fuels from heterotrophic microalgae.* Applied Energy, 2013. **104**(0): p. 860-868.

282. Dote, Y., et al., *Studies on the direct liquefaction of protein-contained biomass: The distribution of nitrogen in the products.* Biomass and Bioenergy, 1996. **11**(6): p. 491-498.

283. Yoshida, H., M. Terashima, and Y. Takahashi, *Production of Organic Acids and Amino Acids from Fish Meat by Sub-Critical Water Hydrolysis.* Biotechnology Progress, 1999. **15**(6): p. 1090-1094.

284. Rogalinski, T., S. Herrmann, and G. Brunner, *Production of amino acids from bovine serum albumin by continuous sub-critical water hydrolysis.* The Journal of Supercritical Fluids, 2005. **36**(1): p. 49-58.

285. Islam, M.N., T. Kaneko, and K. Kobayashi, *Reaction of Amino Acids in a Supercritical Water-Flow Reactor Simulating Submarine Hydrothermal Systems.* Bulletin of the Chemical Society of Japan, 2003. **76**(6): p. 1171-1178.

286. Imai, E.-i., et al., *Elongation of oligopeptides in a simulated submarine hydrothermal system.* Science, 1999. **283**(5403): p. 831-833.

287. Sato, N., et al., *Reaction Kinetics of Amino Acid Decomposition in High-Temperature and High-Pressure Water.* Industrial & Engineering Chemistry Research, 2004. **43**(13): p. 3217-3222.

288. Abdelmoez, W., T. Nakahasi, and H. Yoshida, *Amino Acid Transformation and Decomposition in Saturated Subcritical Water Conditions.* Industrial & Engineering Chemistry Research, 2007. **46**(16): p. 5286-5294.

289. Darvell, L.I., et al., *Nitrogen in biomass char and its fate during combustion: A model compound approach.* Energy & Fuels, 2012. **26**(11): p. 6482-6491.

290. Jones, J.M., et al., *Detection of reactive intermediate nitrogen and sulfur species in the combustion of carbons that are models for coal chars.* Carbon, 1995. **33**(6): p. 833-843.

291. Trevino, S.R., J.M. Scholtz, and C.N. Pace, *Amino Acid Contribution to Protein Solubility: Asp, Glu, and Ser Contribute more Favorably than the other Hydrophilic Amino Acids in RNase Sa.* Journal of Molecular Biology, 2007. **366**(2): p. 449-460.

292. Kruse, A., et al., *Influence of proteins on the hydrothermal gasification and liquefaction of biomass. 1. Comparison of different feedstocks.* Industrial & Engineering Chemistry Research, 2005. **44**(9): p. 3013-3020.

293. Meetani, M.A., O.K. Zahid, and J. Michael Conlon, *Investigation of the pyrolysis products of methionine-enkephalin-Arg-Gly-Leu using liquid chromatography–tandem mass spectrometry.* Journal of Mass Spectrometry, 2010. **45**(11): p. 1320-1331.

294. Milne, T., A. Brennan, and B.H. Glenn, *Sourcebook of methods of analysis for biomass and biomass conversion processes*. 1990: Springer.

295. Darvell, L.I., et al., *Combustion properties of some power station biomass fuels.* Fuel, 2010. **89**(10): p. 2881-2890.

296. Hansson, K.-M., et al., *The temperature's influence on the selectivity between HNCO and HCN from pyrolysis of 2,5-diketopiperazine and 2-pyridone.* Fuel, 2003. **82**(18): p. 2163-2172.

297. Herrera, M., G. Matuschek, and A. Kettrup, *Main products and kinetics of the thermal degradation of polyamides.* Chemosphere, 2001. **42**(5–7): p. 601-607.

298. Whitfield, M., *The hydrolysis of ammonium ions in sea water-a theoretical study.* Journal of the Marine Biological Association of the United Kingdom, 1974. **54**(03): p. 565-580.

299. Pińkowska, H. and E. Oliveros, *Application of the Doehlert Matrix for the Determination of the Optimal Conditions of Hydrolysis of Soybean Protein in Subcritical Water*. Industrial & Engineering Chemistry Research, 2014. **53**(4): p. 1320-1326.

300. Fabbri, D., et al., *Analytical pyrolysis of dipeptides containing proline and amino acids with polar side chains. Novel 2,5-diketopiperazine markers in the pyrolysates of proteins.* Journal of Analytical and Applied Pyrolysis, 2012. **95**(0): p. 145-155.

301. Faisal, M., et al., *Hydrolysis and cyclodehydration of dipeptide under hydrothermal conditions.* Industrial & Engineering Chemistry Research, 2005. **44**(15): p. 5472-5477.

302. Basiuk, V.A. and J. Douda, *Pyrolysis of poly-glycine and poly-l-alanine: analysis of less-volatile products by gas chromatography/Fourier transform infrared spectroscopy/mass spectrometry.* Journal of Analytical and Applied Pyrolysis, 2000. **55**(2): p. 235-246.

303. Snider, M.J. and R. Wolfenden, *The rate of spontaneous decarboxylation of amino acids.* Journal of the American Chemical Society, 2000. **122**(46): p. 11507-11508.

304. Bartholomew, C.H. and J.B. Butt, *Catalyst Deactivation 1991*. 1991: Elsevier.

305. Liu, D., J. Gui, and Z. Sun, *Adsorption structures of heterocyclic nitrogen compounds over Cu (I) Y zeolite: A first principle study on mechanism of the denitrogenation and the effect of nitrogen compounds on adsorptive desulfurization.* Journal of Molecular Catalysis A: Chemical, 2008. **291**(1): p. 17-21.

306. Griffiths, M.J. and S.T. Harrison, *Lipid productivity as a key characteristic for choosing algal species for biodiesel production.* Journal of Applied Phycology, 2009. **21**(5): p. 493-507.

307. Ortega-Calvo, J., et al., *Chemical composition ofSpirulina and eukaryotic algae food products marketed in Spain.* Journal of Applied Phycology, 1993. **5**(4): p. 425-435.

308. Becker, E., *Micro-algae as a source of protein.* Biotechnology Advances, 2007. **25**(2): p. 207-210.

309. Lee, S., et al., *Effects of harvesting method and growth stage on the flocculation of the green alga Botryococcus braunii.* Letters in Applied Microbiology, 1998. **27**(1): p. 14-18.

310. Jazrawi, C., et al., *Pilot plant testing of continuous hydrothermal liquefaction of microalgae.* Algal Research, 2013.

311. Fowden, L., *The composition of the bulk proteins of Chlorella.* Biochemical Journal, 1952. **50**(3): p. 355.

312. Lupi, F.M., et al., *Temperature profiles of cellular growth and exopolysaccharide synthesis by Botryococus braunii Kütz. UC 58.* Journal of Applied Phycology, 1991. **3**(1): p. 35-42.

313. Ben-Amotz, A., T.G. Tornabene, and W.H. Thomas, *CHEMICAL PROFILE OF SELECTED SPECIES OF MICROALGAE WITH EMPHASIS ON LIPIDS1*. Journal of Phycology, 1985. **21**(1): p. 72-81.

314. Peterson, A.A., R.P. Lachance, and J.W. Tester, *Kinetic Evidence of the Maillard Reaction in Hydrothermal Biomass Processing: Glucose−Glycine Interactions in*

High-Temperature, High-Pressure Water. Industrial & Engineering Chemistry Research, 2010. **49**(5): p. 2107-2117.

315. Guo, Y., et al., *Products, pathways, and kinetics for reactions of indole under supercritical water gasification conditions.* The Journal of Supercritical Fluids, 2012.
316. Chiaberge, S., et al., *Amides in Bio-oil by Hydrothermal Liquefaction of Organic Wastes: A Mass Spectrometric Study of the Thermochemical Reaction Products of Binary Mixtures of Amino Acids and Fatty Acids.* Energy & Fuels, 2013. **27**(9): p. 5287-5297.
317. Reddy, H.K., et al., *ASI: Hydrothermal extraction and characterization of bio‐crude oils from wet chlorella sorokiniana and dunaliella tertiolecta.* Environmental Progress & Sustainable Energy, 2013. **32**(4): p. 910-915.
318. Yu, G., et al., *Distributions of carbon and nitrogen in the products from hydrothermal liquefaction of low-lipid microalgae.* Energy & Environmental Science, 2011. **4**(11): p. 4587-4595.
319. Hunt, J.M., *Petroleum geochemistry and geology.* 1996.
320. Gai, C., et al., *Combustion behavior and kinetics of low-lipid microalgae via thermogravimetric analysis.* Bioresource Technology, 2015.
321. Garcia Alba, L., et al., *Microalgae growth on the aqueous phase from hydrothermal liquefaction of the same microalgae.* Chemical Engineering Journal, 2013. **228**: p. 214-223.
322. Sudasinghe, N., et al., *Hydrothermal liquefaction oil and hydrotreated product from pine feedstock characterized by heteronuclear two-dimensional NMR spectroscopy and FT-ICR mass spectrometry.* Fuel, 2014. **137**(0): p. 60-69.
323. Yaylayan, V.A. and E. Kaminsky, *Isolation and structural analysis of maillard polymers: caramel and melanoidin formation in glycine/glucose model system.* Food Chemistry, 1998. **63**(1): p. 25-31.
324. Dzumakaev, K.K., A. Kagarlitskii, and G. Fedolyak, *Kinetics of benzonitrile hydration on a skeletal copper catalyst.* Reaction Kinetics and Catalysis Letters, 1986. **30**(2): p. 289-295.
325. Tian, C., et al., *Hydrothermal liquefaction for algal biorefinery: A critical review.* Renewable and Sustainable Energy Reviews, 2014. **38**(0): p. 933-950.
326. Patel, B. and K. Hellgardt, *Hydrothermal upgrading of algae paste: Application of 31P-NMR.* Environmental Progress & Sustainable Energy, 2013. **32**(4): p. 1002-1012.
327. Gai, C., et al., *Energy and nutrient recovery efficiencies in biocrude oil produced via hydrothermal liquefaction of Chlorella pyrenoidosa.* RSC Advances, 2014. **4**(33): p. 16958-16967.

328. Clayden, G. and N. Greeves, *Warren: Organic Chemistry*. OUP, Oxford, UK, 2012: p. 542-543.

329. Minowa, T., et al., *Hydrothermal Reaction of Glucose and Glycine as Model Compounds of Biomass*. Journal of the Japan Institute of Energy, 2004. **83**(10): p. 794-798.

330. Chen, Y., et al., *Study of the co-deoxy-liquefaction of biomass and vegetable oil for hydrocarbon oil production.* Bioresource Technology, 2010. **101**(12): p. 4600-4607.

331. Pińkowska, H., P. Wolak, and E. Oliveros, *Hydrothermolysis of rapeseed cake in subcritical water. Effect of reaction temperature and holding time on product composition.* Biomass and Bioenergy, 2014. **64**: p. 50-61.

332. Ralston, A. and C. Hoerr, *The solubilities of the normal saturated fatty acids.* The Journal of Organic Chemistry, 1942. **7**(6): p. 546-555.

333. Rahman, M.A., A.K. Ghosh, and R.N. Bose, *Dissociation constants of long chain fatty acids in methanol-water and ethanol-water mixtures.* Journal of Chemical Technology and Biotechnology, 1979. **29**(3): p. 158-162.

334. Inoue, S., et al., *Liquefaction of ammonia and cellulose: effect of nitrogen/carbon ratio in the feedstock.* Biomass and Bioenergy, 1999. **16**(5): p. 377-383.

335. Kruse, A., P. Maniam, and F. Spieler, *Influence of proteins on the hydrothermal gasification and liquefaction of biomass. 2. Model compounds.* Industrial & Engineering Chemistry Research, 2007. **46**(1): p. 87-96.

336. Tressl, R., et al., *Formation of pyrroles and tetrahydroindolizin-6-ones as hydroxyproline-specific Maillard products from glucose and rhamnose.* Journal of Agricultural and Food Chemistry, 1985. **33**(6): p. 1137-1142.

337. Sudasinghe, N., et al., *High resolution FT-ICR mass spectral analysis of bio-oil and residual water soluble organics produced by hydrothermal liquefaction of the marine microalga Nannochloropsis salina.* Fuel, 2014. **119**(0): p. 47-56.

338. Braunstein, P. and F. Naud, *Hemilability of hybrid ligands and the coordination chemistry of oxazoline-based systems.* Angewandte Chemie International Edition, 2001. **40**(4): p. 680-699.

339. Khuwijitjaru, P., et al., *Kinetics on the hydrolysis of fatty acid esters in subcritical water.* Chemical Engineering Journal, 2004. **99**(1): p. 1-4.

340. Davis, R.E., et al., *Integrated Evaluation of Cost, Emissions, and Resource Potential for Algal Biofuels at the National Scale.* Environmental Science & Technology, 2014. **48**(10): p. 6035-6042.

341. Nasdaq. *Crude Oil WTI (NYMEX) Price*. 2015 28/02/2015]; Available from: http://www.nasdaq.com/markets/crude-oil.aspx.

342. Cookson, D.J., C.P. Lloyd, and B.E. Smith, *Investigation of the chemical basis of kerosene (jet fuel) specification properties.* Energy & Fuels, 1987. **1**(5): p. 438-447.

343. Mees, F., et al., *Improvement of the hydrothermal stability of SAPO-34.* Chemical Communications, 2003(1): p. 44-45.

Appendix 1. **Appendix about the aqueous phase**

Appendix 1 gives further information concerning the concentration of ammonium, TOC concentration, sulphate, phosphate and potassium concentrations for the different chapter.

1.1 Chapter7

1.1.1 The analysis of the processed water of soya protein, hemp protein and asparagine without catalyst

Table A1-1 lists the concentration of ammonium, phosphate, sulphate and potassium in ppm, the TOC concentration in ppm and the pH water for the processed water from the experiment with soya protein, hemp protein and asparagine. Mix gua/asp represents the mixture asparagine and glutamine.

Table A1-1: Including the main anion (sulphate, phosphate) and cation (ammonium, potassium) in the water phase in ppm, TOC (ppm), pH and total nitrogen concentration

	pH	TOC (ppm)	Ammonium (ppm)	Phosphate (ppm)	Sulphate (ppm)	Potassium (ppm)
			Soya proteins			
250°C	7.1	21176	11748	2042	184	303
300°C	7.3	15590	16902	1754		555
350 °C	8.9	13948	18537	1366	103	386
formic acid	8.1	16049	19425	1076	60	183
			Hemp proteins			
250°C	6.8	10600	2029	1387		8278
300°C	7.2	8751	4306	1629		7820
350 °C	7.2	5127	4730	1824		5300
formic acid	7.5	6105	4437	1728		6439
			Asparagine			
250°C	8.5	16721	26119			26119
300°C	8.7	6899	23687			23687
350°C	9.0	7166	27389			35192
formic acid	8.6	5786	26101			32436
glutamine	7.5	20220	13024			
mix gnu/asn	7.7	10162	14090			

1.1.2 The analysis of the processed water of soya protein with the catalytic screening

Table A1-2 lists the concentration of ammonium, phosphate, sulphate and potassium in ppm, the TOC concentration in ppm and the pH water for the processed water from the experiment for soya protein with the different catalyst in water and formic acid.

Table A1-2: Including the main anion (sulphate, phosphate) and cation (ammonium, potassium) in the water phase in ppm, TOC (ppm), pH for soya protein for the screening of metal doped HZSM-5

	pH	TOC (ppm)	Ammonium (ppm)	Phosphate (ppm)	Sulphate (ppm)	Potassium (ppm)
			water			
HZSM-5	9.2	16745	11865	2434	103	377
FeZSM-5	8.8	11975	11843	1810	106	373
CuZSM-5	8.9	11764	12100	2150	94	370
MoZSM-5	8.9	16343	12415	2447	94	389
NiZSM-5	8.5	9485	2224	2357	94	318
			Formic acid			
HZSM-5	8.7	16610	11972	1480	94	303
FeZSM-5	8.9	13527	7001	1428	104	287
CuZSM-5	8.6	10976	9342	1613	106	276
MoZSM-5	8.5	14912	9980	1561	95	963
NiZSM-5	8.8	14035	9130	1876	115	1074

1.2 Chapter 8

1.2.1 The analysis of the processed water of microalgae without catalyst

Table A1-3 lists the concentration of ammonium, phosphate, sulphate and potassium in ppm, the TOC concentration in ppm and the pH water for the processed water from the experiment with the microalgae *Chlorella*, stressed and non-stressed *P. ellipsoidea* and *Spirulina* without catalyst.

Table A1-3: Including the main anion (sulphate, phosphate) and cation (ammonium, potassium) in the water phase in ppm, TOC (ppm), pH

	pH	TOC (ppm)	Ammonium (ppm)	Phosphate (ppm)	Sulphate (ppm)	Potassium (ppm)
			Chlorella			
250°C	7.3	15069	2576	3207	815	1482
300°C	8.1	11197	4175	3282	770	1178
350°C	9.2	12617	6284	3038	282	924
formic acid	8.9	10190	8599	2811	305	1015
			Stressed *P ellipsoidea*			
250°C	6.0	3583	61	121		500
300°C	5.9	3262	229			450
350°C	6.0	7943	397	111	29	165
formic acid	6.5	5646	1366	502	94	234
			Non-stressed *P ellipsoidea*			
250°C	6.5	14629	518			
300°C	6.7	14224	3541	762		
350°C	7.1	5956	5051	137		577
formic acid	7.3	6791	1462	1025		1376
			Spirulina			
250°C	6.6	15628	1258	2316		1743
300°C	6.9	12164	2546	2882		2205
350°C	6.9	9218	3260	2905		2412
formic acid	7.6	14629	2683	2557		2150

1.2.2 The analysis of the processed water of the microalgae catalytic screening

Table A1-4 lists the concentration of ammonium, phosphate, sulphate and potassium in ppm, the TOC concentration in ppm and the pH water for the processed water from the experiment with *Chlorella* and the stressed *P. ellipsoidea* with the different catalysts.

Table A1-4: Including the main anion (sulphate, phosphate) and cation (ammonium, potassium) in the water phase in mg/L, TOC (mg/L), pH

	pH	TOC (ppm)	Ammonium (ppm)	Phosphate (ppm)	Sulphate (ppm)	Potassium (ppm)
			Chlorella			
			water			
HZSM-5	8.1	7133	3710	2307	537	1026
FeZSM-5	7.9	10765	4211	2715	659	1541
CuZSM-5	8.9	8942	2685	2852	604	796
MoZSM-5	9.2	9669	5011	3041	656	1022
NiZSM-5	8.8	9925	1659	3178	774	963
			Formic acid			
HZSM-5	8.2	9604	4011	3230	678	956
FeZSM-5	9.1	7214	4063	2570	704	885
CuZSM-5	8.5	7474	4228	3307	759	1467
MoZSM-5	8.6	9909	5049	3211	796	1037
NiZSM-5	8.8	7487	3131	2648	707	1074
			Stressed *P ellipsoidea*			
			water			
HZSM-5	6.0	7846	272	125	65	184
FeZSM-5	5.6	3937	680	177	62	?
CuZSM-5	5.9	4398	548	273	96	227
MoZSM-5	5.6	3950	683	255	77	239
NiZSM-5	5.5	3267	777	300	75	349
			Formic acid			
HZSM-5	6.4	7142	1448	541	117	260
FeZSM-5	5.5	4455	1359	446	115	264
CuZSM-5	5.6	7077	1409	562	114	276
MoZSM-5	5.6	5009	1427	535	107	204
NiZSM-5	4.5	5549	1402	639	120	276

1.3 Chapter 9

1.3.1 The analysis of the processed water for binary mixtures

Table A1-5 lists the concentration of ammonium, phosphate, sulphate and potassium in ppm, the TOC concentration in ppm and the pH water for the processed water from the experiment with the binary mixtures.

Table A1-5: Including the main anion (sulphate, phosphate) and cation (ammonium, potassium) in the water phase in ppm, TOC (ppm), pH concentration for the mixture solution

	pH	TOC (ppm)	Ammonium (ppm)	Phosphate (ppm)	Sulphate (ppm)	Potassium (ppm)
			Starch-protein			
250°C	6.4	14521	2842	752	113.7	4975
300°C	6.4	11570	3894	1104	109.9	4285
350°C 50-50	7.1	3925	4486	647		117
25-75	6.7	9830	10203	1327		139
75-25	6.1	4198	361	155		16
asn-glucose	7.1	7428	966	0	0	0
			Sunflower-protein			
250°C	5.9	23079	2964	800.5		920
300°C	6.1	28226	3506	684.2		100
350°C 50-50	6.7	21635	4325	425.9		108
25-75	7.2	17633	10521	845.4		164
75-25	6.4	5373	2421	226.4		50
			Linseed-protein			
250°C	6.3	18909	5418	793		104
300°C	5.9	22635	3006	762		75
350°C 50-50	6.7	22276	4798	454		108
25-75	6.8	17085	7609	669		124
75-25	6.2	6403	2128	192		57
			Sunflower-starch			
250°C	3.5	6161				
300°C	3.7	5478				
350°C 50-50	3.6	4017				
25-75	3.6	3248				
75-25	3.5	2140				
			Linseed-starch			
250°C	3.4	8303				
300°C	3.2	6233				
350°C 50-50	3.6	4343				
25-75	3.2	2689				
75-25	2.0	4340				

1.3.2 The analysis of the processed water for ternary mixtures

Table A1-6 lists the concentration of ammonium, phosphate, sulphate and potassium in ppm, the TOC concentration in ppm and the pH water for the processed water from the experiment with the ternary mixtures with different additifs.

Table A1-6: Including the main anion (sulphate, phosphate) and cation (ammonium, potassium) in the water phase in ppm, TOC (ppm), pH and total nitrogen concentration for the mixture solution

	pH	TOC (ppm)	Ammonium (ppm)	Phosphate (ppm)	Sulphate (ppm)	Potassium (ppm)
Mixture stressed *P. ellipsoidea*						
250°C	7.8	3648	1251	248	37	
300°C	7.8	2142	1479	283	37	
350°C	7.3	4065	2043	322	50	
formic acid	6.7	1384	3030			
HZSM-5	6.5	2725	2497			
model	6.9	7817	2146			
Mixture *Chlorella*						
250°C	6.6	19927	6495	669		
300°C	7.8	21034	26337	2433		
350°C	6.5	15900	4477	653		
formic acid	8.8	27189	10113	843		
HZSM-5	6.5	16314	3529	642		
model	8.6	24584	3644			

Appendix 2. Mass balance and molecular weight fraction of glutamine and the mixture

Appendix 2 includes some extra data for the mass balance of glutamine and the mixture glutamine-asparagine in the **Chapter 7.** Figure A2-1 represents the mass balance (bio-crude, residue, gaseous and aqueous phase) for the glutamine and the mixture asparagine-glutamine. Figure A2-2 represents the molecular weight fraction measured by the GPC for the sample samples.

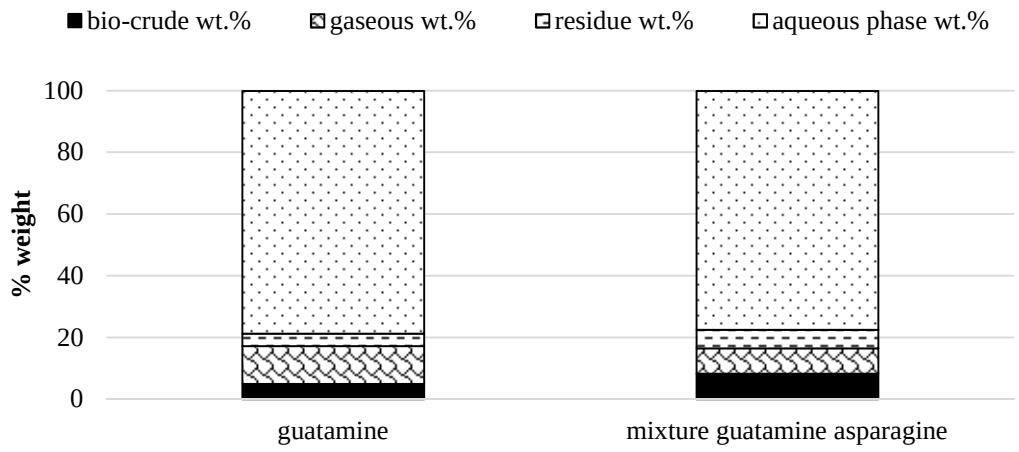

Figure A2-1: Mass balance for glutamine and the mixture glutamine and asparagine in Chapter 7

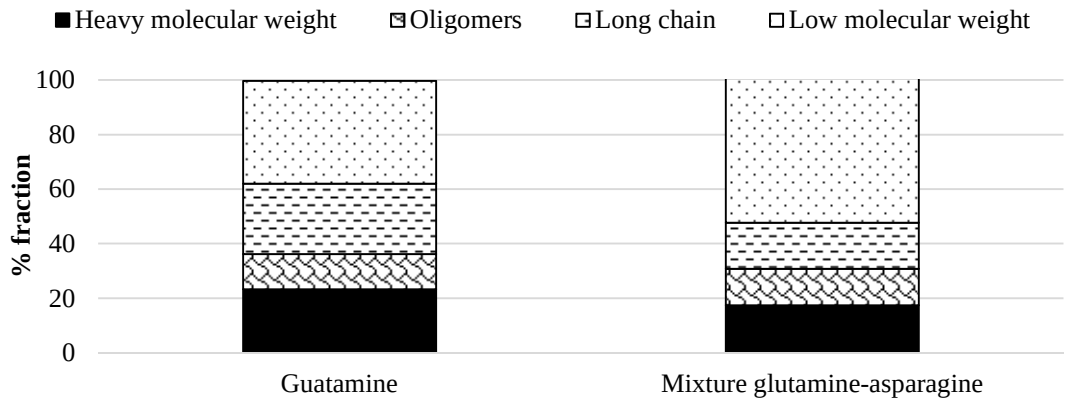

Figure A2-2: Molecular weight fraction balance for glutamine and the mixture glutamine and asparagine in Chapter 7

Appendix 3. GC-MS Chromatograms

3.1 Chapter 6

This section contains extra chromatograms which are not shown in the main thesis. Figure A3-1 shows the chromatogram of (a) starch, (b) glucose, (c) alginic acid and (d) mannitol at 350 °C in formic acid. Table A3-1 lists some examples of compounds identified.

Table A3-1: Peaks identification in the GC-MS

Number	Retention time (minutes)	Compounds
1	18.0	3-methyl-pentan-one
2	19.0	3,4-dimethyl-pentan-one
3	21.8	phenyl-undecen-1-ol
4	22.4	naphathalendione
5	26.0	2,3-dihydro 1H-inden-1-one
6	27.1	1,2,3,4-tetrahydro-1,5,7-trimethyl-naphthalene
7	28.0	5-methyl-2-(1-methylethyl)-2-cyclohexen-1-one
8	33.8	1-(3-hydroxyphenyl)-ethanone

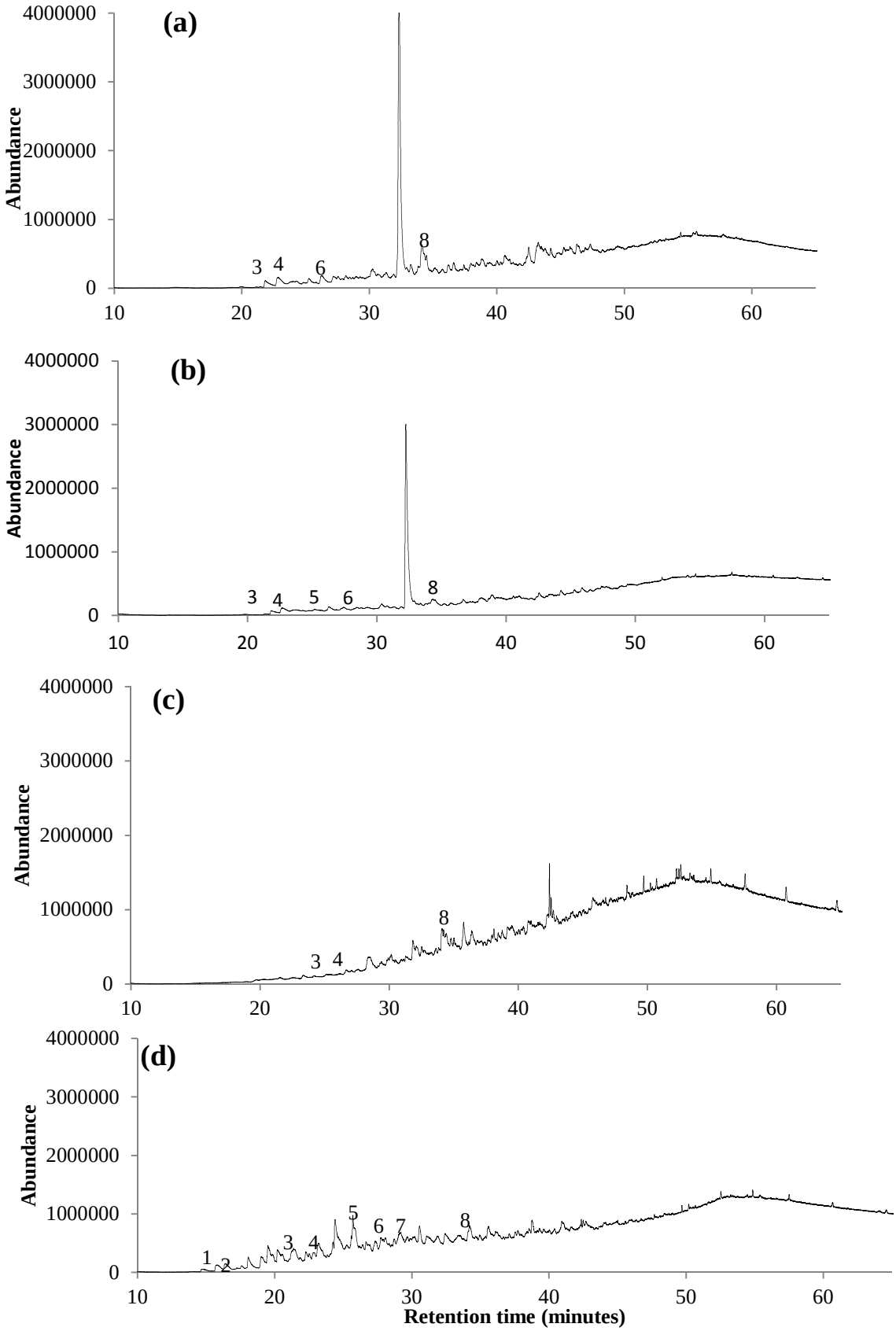

Figure A3-1: Spectrums of the 4 carbohydrates where (a) represents starch in formic acid, (b) glucose in formic acid, (c) alginate in formic acid (d) mannitol in formic acid

3.2 Chapter 7

This section, the chromatograms (Figure A3-2) are included of the processed bio-crude oil from the amino acids, (a) asparagine, (b) glutamine and (c) mixture glutamine-asparagine at 350 °C. Table A3-2 lists the main molecules identified within the chromatograms.

Table A3-2: Peaks identification in the GC-MS

Number	Retention time (minutes)	Compounds
1	22.5	2-pyrrolidinone
2	32.4	2,3-dimethyl-1H-Indole
3	34.4	5,6,7-trimethyl-1H-indole
4	35.7	1H-Indole, 2,3-dihydro-1,3,3-trimethyl-2-methylene-
5	38.5	ergoline
6	41.2	2,6-bis(1-methylethyl)-benzenamine,
7	42.3	2-(2,4-dichlorophenoxy)-N-(2,6-diethylphenyl)-propanamide
8	43.9	Pyridine-4-carboxylic acid, 2-amino-3-cyano-5,6-dimethyl-, ethyl ester
9	48.3	formamide-N-methylpyrrodinyl-butinyl)

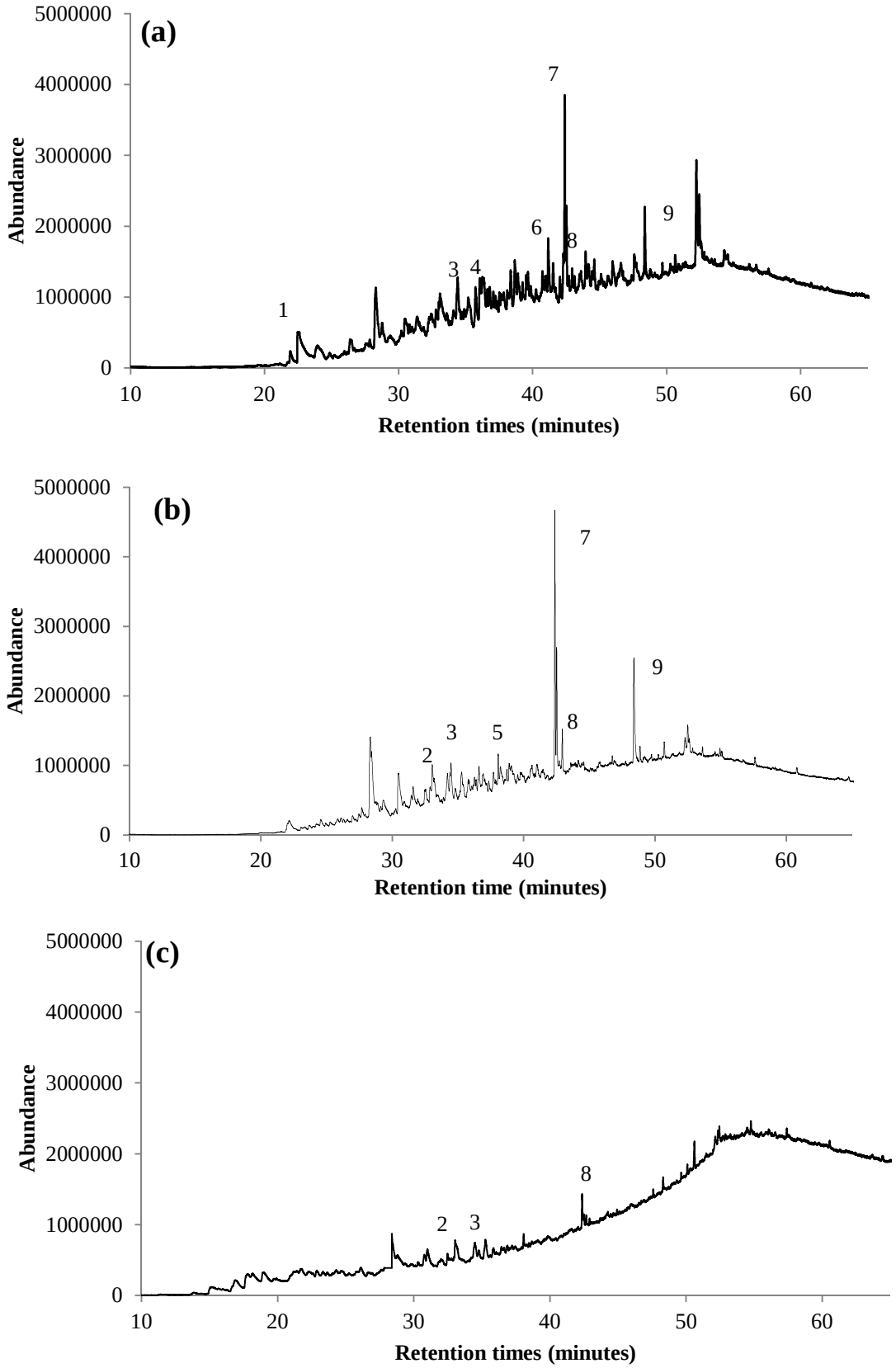

Figure A3-2: GC-MS chromatogram of (a) asparagine, (b) glutamine and (c) mixture asparagine-glutamine processed at 350 °C

3.3 Mass spectrum

Figure A3-3 represents the mass spectrum of the 3,6-diisopropylpiperazin-2,5-dione comparing the mass spectrum (a) of the compounds at a retention time of 48.0 minutes the library (b) and the compounds identified in the bio-crude for the processing of *Chlorella* at 300 °C

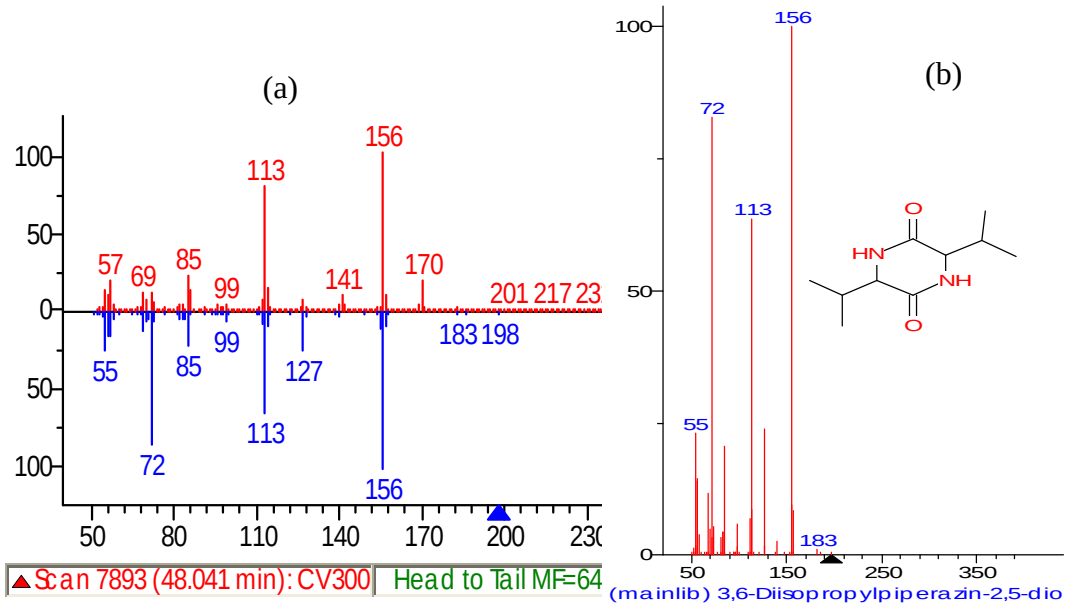

Figure A3-3: Mass spectrum of 3,6-diisopropylpiperazin-2,5-dione, compared the mass spectrum at 48 minutes and the library